UNIVERSITY OF
LIVERPOOL

SCHOOL OF ENGINEERING
Centre for Engineering Sustainability

Characterisation of Warm Asphalt Mixtures with Addition of Reclaimed Asphalt Pavement Materials

Thesis submitted in accordance with the requirements of The University of Liverpool for the degree of Doctor in Philosophy

by

Duraid Muayed Abd
BSc (Eng), MSc (Eng)

March 2017

Dedication

This thesis is dedicated to her pure soul (my mother)

Mom, I will never forget in my life how many sacrifices you made and how much support you gave me to help me obtain a PhD degree

Today, I hope I achieved your desire…

May Allah make your dignity in the highest place of paradise

Duraid 2017

Abstract

Pavement researchers have increasingly focused on reducing production and compaction temperatures in order to improve the environmental and economic impacts of hot mix asphalt, without adversely affecting the workability, durability and performance of asphalt pavements. The introduction of innovations and technologies in the form of warm mix asphalt will lead to substantial environmental improvements and economic prosperity. Moreover, in order to maximise the benefits of such technology, the inclusion of higher percentages of reclaimed asphalt pavement materials in warm mix asphalt allows the development of a more sustainable and cost-effective pavement structure.

This thesis studies the characterisation of warm asphalt mixtures with the addition of reclaimed asphalt pavement materials. The effect of warm additives Sasobit, Rediset WMX and Rediset LQ on the viscosity of bitumen was investigated in detail. Furthermore, the effect of these additives on the rheological properties of bitumen was also identified using a dynamic Shear Rheometer. In fact, there is a point of controversy among pavement engineers about the performance of warm mix asphalt in terms of fatigue; therefore, firstly, the fatigue performance of warm-modified bituminous binder was investigated in detail. Fatigue test were conducted in dynamic Shear Rheometer using a time Sweep method and data were modelled using the viscoelastic continuum damage approach.

After proving that warm additives such as Sasobit and Rediset WMX improved the fatigue life of asphalt binder, emphasises were paid to investigate nano-mechanical properties of warm modified bituminous binders and mix. Therefore this study also presents an investigation into the impact of warm additives on topography, modulus, deformation and adhesion of warm-modified bituminous binders using atomic force microscopy with the peakForce quantitative nano-mechanical mapping modality.

The effect of production temperatures on the performance of warm mix asphalt was further investigated. Nanoindentation, which is an advanced technique, was used to study the effect of warm additives on the nano-mechanical properties of asphalt mixture phases, aggregate, interfacial transition zone (between aggregate and binder) and mastic. The nanoindentation results were used: firstly, to evaluate

the effect of production temperatures and warm additives on the mixture phases; of warm mix asphalt; secondly, the nano-mechanical properties of interfacial transition zone were used to propose a new method to evaluate the degree of bonding between aggregate and binder in the mixture and, thirdly to evaluate the effect of each phase on the overall fatigue performance of warm mix asphalt.

The aggregate-binder bond is one of the main factors that affect the durability of asphalt mixtures. This can be investigated based on the energy required to fracture the adhesive bond between binder and aggregate. In this thesis, the effect of warm additives on the adhesive bond strength of an aggregate-binder system was investigated using the pull-off test. Furthermore, the contribution of warm additives in improving the work of fracture has been linked to the adhesion force determined using atomic force microscopy and work of indentation approach.

The fatigue life of WMAs was further investigated using a dynamic Shear Rheometer to study the effect of warm additives, production temperatures and binder grade. It was found that the level of reduction in the production temperatures and binder grade highly affect the fatigue performance of warm mix asphalt. Moreover, as Nanoindentation has shown to have the potential to characterise the properties of mixture phases, those properties can help in understanding the overall fatigue behaviour of warm asphalt mixture and show how improving nano-mechanical properties of interfacial transition zone and mastic can reflect the significant improvement in the fatigue life of asphalt mixtures. It is therefore recommended that highway agencies should specify a minimum production temperature for warm mix asphalt to reach acceptable mixture stability in terms of fatigue performance, taking into account the binder source and grade.

Two issues regarding the inclusion of reclaimed asphalt pavement materials in asphalt mixtures need to be further investigated: the fatigue behaviour of reclaimed asphalt pavement materials mixes and the degree of blending between reclaimed asphalt pavement and virgin materials. The level of blending between virgin and reclaimed asphalt pavement materials was investigated under the scope of this thesis. The level of blending was investigated based on the nano-mechanical properties of mastic and interfacial transition zone measured using

nanoindentation. Results were validated using scanning electron microscopy and the overall performance of warm mix asphalt incorporating reclaimed asphalt pavement materials in terms of stiffness and fatigue. Accordingly, a simple protocol is proposed to obtain a complete blending between reclaimed asphalt pavement binder and virgin binder, which is a key component of suitable practices in the pavement industry.

The implications of this work for industry are that, firstly, warm additives offer a superior performance in producing asphalt mixtures that have better fatigue performance than traditional hot mix asphalt. Moreover, the study revealed that warm additives improve the strength bond between aggregate and binder. Secondly, highway agencies are advised to specify a minimum production temperature for warm mix asphalt to reach acceptable mixture stability. A complete blending between reclaimed asphalt pavement and virgin materials can be achieved using the proposed protocol; therefore a more sustainable and cost-effective pavement structure can be constructed.

Declaration

I declare that the contents and the work described in this thesis were performed at the University of Liverpool, School of Engineering from Juan 2013 to Juan 2016. I hereby certify that this thesis is my own and has not been submitted in whole or in part to any other university or any other educational association for a higher degree.

Duraid Muayed Abd

Liverpool, 2017

Acknowledgements

Before all and after all, I am ultimately grateful to **Allah** for giving me the knowledge, intellect, patience, ability and great blessings to accomplish this work

The current thesis was performed with the help and encouragement of many people to whom I would like to express my grateful thanks and appreciation.

The first two people to whom I would like to express my great special thanks and gratitude are my supervisors **(Dr. Hussain Al-Khalid & Dr. Riaz Akhtar)**. It was my honour to work with them. Without their guidance and persistent help, this thesis would not have been possible. I will never forget their great assistance, motivation and encouragement in introducing me to the craft of scientific research.

I would also like to acknowledge the Iraqi government represented by the Iraqi Ministry of Higher Education and Scientific Research and Iraqi Cultural Attaché in London for the award of a study scholarship to pursue this research.

Appreciation must also go to Naylor Chemicals, UK, and AkzoNobel, Sweden, for their assistance in providing the WMA additives and Nynas for supplying the straight-run binders. Great thanks must also go to Aggregate Industries, UK, for their assistance in providing the relevant material. I am also indebted to all technical staff in the School of Engineering for their help in the experimental work, especially **Mr. Marc Bratley, Mr. Dave Atkinson and Mr. Jiji Mathew.** Especial thanks must also go to the geologist, **Mr. John Kavanagh**, for his great assistance in cutting the granite rocks and identifying the RAP aggregate. I would like also to thank **Dr. Tim Joyce** for his assistance with the AFM and SEM testing.

To my father, whose help and encouragement in enabling me to reach this level of education, my great appreciation and thanks are due.

To the nearest person to my heart, my wife **Sumaya**, and my little princess, **Layan**, my words are not enough to express my deepest gratitude and sincere love to you for your patience, help and encouragement. Finally, to my lovely brothers and sisters, your continuous support and precious encouragement are highly appreciated

Duraid 2017

Contents

List of Abbreviations and Mixture Codes

Abbreviations

AASHTO	American Association of State Highway and Transportation Officials
AFM	Atomic Force Microscopy
ANOVA	Analyses of Variance
BBS	Bitumen Bond Strength
CAM	Cold Mix Asphalt
DSR	Dynamic Shear Rheometer
DSC	Differential Scanning Calorimetry
GHG	Green-Houses Gases
GPC	Gel Permeation Chromatography
HMA	Hot Mix Asphalt
ITZ	Interfacial Transition Zone
ITZ Virgin	Interfacial transition zone between virgin aggregate and virgin binder
ITZ RAP	Interfacial transition zone between RAP aggregate and RAP binder
NCAT	National Centre for Asphalt Technology
NCHRP	National Cooperative Highway Research Program
NDSs	Nanoindentation Disc Samples
NIST	National Institute of Standard and Technology
PATTI	Pneumatic Adhesion Tensile Testing Instrument
PFQNM	Peak Force Quantitative Nano-mechanical Mapping
RAP	Reclaimed Asphalt Pavement
SEM	Scanning Electron Microscopy
SFE	Surface Free Energy
SHRP	Strategic Highway Research Program
SPM	Scanning Probe Microscope
USA	Untied State of America
VECD	Viscoelastic Continuum Damage
WMA	Warm Mix Asphalt
WMBB	Warm Modified Bituminous Binder

Mixture codes

H + Sa	40/60 binder grade with addition of Sasobit
H + Rw	40/60 binder grade with addition of Rediset WMX
H + Rl	40/60 binder grade with addition of Rediset LQ
S + Sa	100/150 binder grade with addition of Sasobit
S + Rw	100/150 binder grade with addition of Rediset WMX
S + Rl	100/150 binder grade with addition of Rediset LQ
HH155	Hot mix asphalt manufactured at 155°C using 40/60 binder
HS145	Hot mix asphalt manufactured at 145°C using 100/150 binder
WHSa135	Warm mix asphalt manufactured at 135°C using 40/60 binder with addition of Sasobit
WHSa145	Warm mix asphalt manufactured at 145°C using 40/60 binder with addition of Sasobit
WHRw135	Warm mix asphalt manufactured at 135°C using 40/60 binder with addition of Rediset WMX
WHRw145	Warm mix asphalt manufactured at 145°C using 40/60 binder with addition of Rediset WMX
WHRl135	Warm mix asphalt manufactured at 135°C using 40/60 binder with addition of Rediset LQ
WHRl145	Warm mix asphalt manufactured at 145°C using 40/60 binder with addition of Rediset LQ
WSSa125	Warm mix asphalt manufactured at 125°C using 100/150 binder with addition of Sasobit
WSRw125	Warm mix asphalt manufactured at 125°C using 100/150 binder with addition of Rediset WMX
WSRl125	Warm mix asphalt manufactured at 125°C using 100/150 binder with addition of Rediset LQ
HSP145	Hot mix asphalt manufactured at 145°C using 60% virgin materials (100/150 binder and granite) mixed with 40% RAP materials
WSSaP125	Warm mix asphalt manufactured at 125°C using 60% virgin materials (100/150 binder and granite) mixed with 40% RAP materials with addition of Sasobit

WSSaP155 Warm mix asphalt manufactured at 155°C using 60% virgin materials (100/150 binder and granite) mixed with 40% RAP materials with addition of Sasobit

WSRlP125 Warm mix asphalt manufactured at 125°C using 60% virgin materials (100/150 binder and granite) mixed with 40% RAP materials with addition of Rediset LQ

WSRlP155 Warm mix asphalt manufactured at 155°C using 60% virgin materials (100/150 binder and granite) mixed with 40% RAP materials with addition of Rediset LQ

List of Tables

List of Figures

Publications

(1) Abd, D. & Al-Khalid, H., 2015. Fatigue performance characterization of warm-modified bituminous binders. **Bituminous Mixtures and Pavements VI, 105.**

(2) Abd, D.M., Al-Khalid, H. & Akhtar, R., 2017. Nano-scale properties of warm-modified bituminous binders determined with atomic force microscopy. **Road Materials and Pavement Design**, 1-14 Available from: http://dx.doi.org/10.1080/14680629.2017.1304262.

(3) Abd, D. Al-Khalid, H. and Akhtar, R. 2016. An investigation into the impact of warm additives on asphalt mixture phases using a nano-mechanical approach, Paper submitted to the **Journal of Construction and Building Material.**

(4) Abd, D. Al-Khalid, H. and Akhtar, R. 2017. Adhesion properties of Warm-Modified Bituminous Binders (WMBBs) determined using Pull-off tests and Atomic Force Microscopy. Paper submitted to the **Journal of Road Materials and Pavement Design**

(5) Abd, D. Al-Khalid, H. and Akhtar, R. 2016. A novel methodology to investigate and obtain a complete blending between RAP and Virgin materials. **Journal paper submitted to journal of Materials in Civil Engineering/ASCE**

(6) Abd, D. Al-Khalid, H. and Akhtar, R. 2016. Impact of mixture phases properties on the overall fatigue performance of WMA. **Journal paper under preparation.**

Chapter One

Introduction

1.1 Introduction

Over the last two decades, great attention has been paid to improving the overall performance of asphalt mixtures, particularly to achieve environmental and economic objectives. More attention has been paid recently to reducing energy consumption throughout the process of manufacturing asphalt mixtures without having a negative impact on their in-service mechanical performance (Capitão *et al.* 2012). Furthermore, there is growing international pressure to minimise fossil fuel consumption and the emission of greenhouse gases (GHG) such as carbon dioxide (CO_2). Unfortunately, the production of hot mix asphalt (HMA) makes a considerable contribution to energy consumption and to the release of pollutant gases due to the process required to dry and heat the mineral aggregates and binder at temperatures above 150°C. In fact, the asphalt industry has been trying to mitigate these challenges by promoting three strategies. Firstly, through the use of inexhaustible and non-polluting new energy sources, secondly, through the use of renewable natural resources and synthetic adhesive binders to replace the traditional binders, and, thirdly, through the development of new technologies to produce sustainable asphalt mixtures that can be constructed and compacted at lower temperatures without sacrificing the mixtures' properties (Jamshidi *et al.* 2013).

The introduction of innovations and technologies in the form of warm mix asphalt (WMA), which can be manufactured at temperatures ranging from 100°C to 140°C (using one of warm technologies either organic, chemical or foaming) compared to mixing temperatures of 150-180°C for traditional HMA (Mo *et al.* 2012), can lead to significant improvements in energy consumption and the release of pollutant gases. It was reported that the use of WMA produced a clear reduction in various emissions throughout the production process in the plant as follows: 30-40% for CO_2 (carbon dioxide) and SO_2 (sulphur dioxide), 50% for

volatile organic compounds, 10-30% for CO (carbon monoxide), 25-55% for dust and 60-70% for NO_x (nitrous oxide). Moreover, reductions of between 30% to 50% have also been reported for asphalt aerosols/fumes and polycyclic aromatic hydrocarbons (Capitão *et al.* 2012,Zaumanis 2010,D'Angelo *et al.* 2008). In addition, a 30% reduction in energy consumption was found using WMA (Kheradmand *et al.* 2014). However, in spite of these remarkable economic and environmental improvements, there is still uncertainty with respect to using them due to lack of data concerning their long-term performance, moisture susceptibility due to lower production temperatures, and coating and bonding problems (Rubio *et al.* 2012). Added to that, the use of WMA technologies may involve increasing cost associated with the cost of materials such as Advera, Aspha-main, Sasobit, Rediset, Evotherm etc., and with equipment modifications in the case of foaming technology (Kristjánsdóttir *et al.* 2007). However, the use of reclaimed asphalt pavement (RAP) materials can reduce the cost of WMA in the production process (Hamzah *et al.* 2015). Indeed, it was reported there is a potential benefit in using recycled materials and industrial by-products instead of traditional materials in highway structures, as this can result in a 20% reduction in global warming, 16% reduction in energy consumption, 6% reduction in hazardous waste generation and 11% reduction in water consumption (Lee *et al.* 2010). Of course, one of the most important recycled materials in pavement structures is RAP materials.

The current school of thought in the asphalt industry is that WMA can be used to incorporate a higher percentage of RAP materials (Tao and Mallick 2009,Mallick *et al.* 2008,El Sharkawy *et al.* 2016). There is already a controversial point among pavement researchers regarding the level of blending between RAP and virgin materials and the hypothesis behind the inclusion of RAP materials in HMA, which needs to be resolved. Therefore, the incorporation of RAP materials in WMA is a more complicated scenario than in the case of HMA, as WMAs are produced at a lower temperature than that required to manufacture HMA. A recent study by Zaumanis and Mallick (2015) recommended the need for a methodology to evaluate the level of blending between RAP and virgin materials in the laboratory. This point and others

concerning the performance of WMA that have not been addressed or studied before are investigated in detail in this thesis.

1.2 Need for the research

The innovation of warm asphalt technologies started in Europe and the research area has more recently been gaining momentum in the USA. And since then extensive studies have been conducted to evaluate the performance of WMA. However, although significant attention has been paid to investigating the performance of different warm technologies, there are still some issues that need to be investigated before a conclusion can be made about replacing the current HMA with WMA. One of the issues that need to be investigated in detail is the fatigue performance of WMA.

In fact, it is particularly difficult to characterise the fatigue life of hot mix asphalt for a number of reasons, such as the composite nature of the material, the gradation of aggregate particle size, asphalt film thickness variation within the mastic, air void size distribution, and the dependency of asphalt binder behaviour on time and temperature (Masad *et al.* 2008). Therefore, this fatigue-cracking phenomenon should be even more difficult to characterise in WMA as the mixing temperature is lower than HMA; thus, another two factors or questions should be addressed. The first is whether the fatigue life improves because of the lower production temperature or because of the effect of warm additives. The second is to what extent the production temperature can be decreased without causing a negative impact on the degree of bonding between the binder and the aggregate in the asphalt mixtures. Both of these questions are investigated in detail in the current study.

SuperPave's fatigue parameter which has received extensive criticism characterises the fatigue life of bituminous binder (Hamzah *et al.* 2015). It is therefore clear that there is a need to evaluate the effect of warm additives on the fatigue life of binders using a time sweep test. Based on the results, the fatigue life of WMA can be further investigated taking into account the effect of production temperatures, warm additives, binder grade and the effect of ITZ and mastic on the overall fatigue life.

Furthermore, there is little understanding of the fundamental properties of asphalt mixtures' phases at the nano-scale because of the inability to characterise their mechanical properties at this scale. Undoubtedly, there is a lack of understanding of the behaviour of asphalt mixture at the nano-scale and, as recommended by Igarashi *et al.* (1996), there is a need to characterise and understand the mechanical properties at the nano-scale because the interactions among the composite phases happen at this level. Atomic force microscopy (AFM) and nanoindentation are powerful techniques to characterise asphalt mixtures at the nano-scale. Up to date, there has been very limited research conducted in this area, whilst no research has investigated the nano-mechanical properties of warm-modified bituminous binders and mix. There is a need to investigate and gain further understanding of the effect of warm additives on virgin binder and mixture phases, aggregate, interfacial transition zone (ITZ) between aggregate and binder/mastic and mastic, without separating them from the mixture. Therefore, under the scope of this study, investigation into the effect of warm additives on nano-mechanical properties of binder using AFM and of mixture phases using nanoindentation was conducted in order to firstly evaluate the effect warm additives and production temperatures on the mixture phases; secondly, the nano-mechanical properties of ITZ can be used to investigate the degree of bonding between aggregate and binder/mastic; and, thirdly, evaluate the effect of each phase on the overall fatigue performance of WMA as cracks occur either in mastic or along the interface between aggregate and binder.

Regarding the inclusion of RAP materials, a limited number of researchers have investigated the level of interaction between aged and virgin asphalt binders (Al-Qadi 2007) and a recent study has recommended the need for a methodology to evaluate the level of blending between RAP and virgin materials in the laboratory (Zaumanis and Mallick 2015). At present, the level of interaction between RAP and virgin materials is still ambiguous. To date, the interaction between RAP and virgin materials has not been investigated at the nano-scale, which can practically reflect the real level of materials' interactions.

In summary, the research objectives were defined in order to achieve the aims given in this chapter (Section 1.5) based on the following considerations:

- Even though extensive studies have focused on the performance of WMA compared to that of HMA, there are no clear conclusions about the fatigue life of WMA or, in other words, there is no answer as to whether fatigue life improves because of the lower production temperature, or because of the effect of warm additives.
- Very limited research studies have used AFM and nanoindentation to investigate the nano-mechanical properties of virgin binder and mix. There is a need to address and investigate the effect of warm additives on binder and mix at the nano-scale.
- To date no research has been conducted to investigate the effect of mixture phases, aggregate, ITZ and mastic on overall performance of asphalt mixtures.
- To date, the adhesive bond strength between aggregate and binder has only been investigated indirectly, out the mixture. In terms of asphalt mixture, no method has been developed to evaluate the bond strength between aggregate and binder in the mixture.
- To date, the level of blending between RAP and virgin materials is a controversial point. In fact, there is a need for a method to accurately evaluate and obtain the level of blending between RAP and virgin materials.

1.3 Significance of the research

It has already been mentioned that WMA can greatly reduce energy consumption and the emission of greenhouse gases (GHG). However, there remain a number of challenges to overcome. One of these challenges is the effect of production temperature on the performance of WMA. The production temperature greatly influences the durability of an asphalt mixture; therefore, any thoughts about reducing the production temperature should be made cautiously, without sacrificing the required properties of the mixtures. The effect of production temperature on the performance of WMA needs to be further investigated considering the effect of binder grade as well, so that highway agencies can specify minimum reduction in the production temperature to produce asphalt mixtures with an equal or better performance than HMA, thus achieving great

positive economic and environmental improvements. The reason for that is because, if the WMA is not as durable as the HMA, the cost of maintenance may increase and, in severe conditions, the highway or the road may need to be reconstructed before the time specified in the design for that infrastructure.

Although an effort was made to explore the nano-mechanical properties of virgin mixture phases, aggregate, and mastic using nanoindentation (Tarefder *et al.* 2010,Tarefder and Faisal 2013), so far no research has been conducted to investigate the nano-mechanical properties of the ITZ in asphalt mixtures, which reflects the real bonding and interaction between aggregate and binder. Understanding the real bonding or interaction between aggregate and binder without separating them from the mixture can contribute to accurately assessing the performance of the asphalt mixture. Furthermore, understanding the effect of warm additives on the mechanical properties of ITZ of WMA can contribute to establishing a new mixture design procedure. To date, the design procedure for HMA has served as that for WMA. In the future, if the WMA is to replace the HMA, a mixture design procedure must be established. Therefore, investigation into the effect of warm additives on mixture performance, especially at the nano-scale, is required.

In addition, establishing a methodology to investigate and obtain a complete blending between RAP and virgin materials is necessary to give pavement designers more confidence in incorporating RAP materials in pavement structure, through which economic, environmentally friendly improvements and sustainable structures can be constructed.

1.4 Scope of the research

The asphalt industry has been pressured in recent years to mitigate the significant contribution to increasing energy consumption and the release of pollutant gases due to using hot mix asphalt (HMA). One of the main solutions to overcome this problem is to manufacture asphalt mixtures at lower temperatures than that required for HMA without sacrificing the mixtures' properties.

Under the scope of this thesis, a considerable amount of work was conducted to characterise the performance of WMA and WMA incorporating

RAP materials at different levels. Three warm additives, Sasobit, Rediset WMX and Rediset LQ, were used and these warm additives were incorporating into two binder grades, namely 40/60 and 100/150. Granite aggregate and rocks of granite supplied from the same granite aggregate quarry were used. Real reclaimed asphalt pavement materials (RAP) were also adopted. The effects of different dosages of warm additives on the viscosity and rheological properties of binders were investigated in depth. More importantly, a time sweep method was used to characterise the fatigue life of warm-modified bituminous binders (WMBBs). In terms of the nano-mechanical properties of WMBBs and mix, the study also focused on the impact of Sasobit, Rediset WMX and LQ on topography, modulus, adhesion and deformation of warm-modified bituminous binders using Atomic Force Microscopy (AFM) with the PeakForce Quantitative Nanomechanical Mapping (PFQNM) modality, whereas the nano-mechanical properties of the WMA phases were investigated using nanoindentation. Regarding the use of nanoindentation, a very smooth sample surface is required; therefore, a technique was developed to prepare the asphalt mixture samples for nanoindentation. In order to validate the adhesion results measured using AFM and nanoindentation, the effects of warm additives on the adhesive bond strength of an aggregate-binder system was investigated using the pull-off test. In terms of asphalt mixtures, the time sweep method was also used to measure the fatigue life of cylindrical DSR samples (12mm diameter and 50mm height) taking into account the effect of production temperature and binder grade and study how asphalt mixture phases with particular reference to ITZ and mastic contribute to the overall fatigue performance. A methodology to investigate the level of blending between RAP and virgin materials was proposed based on the nano-mechanical properties of the mixture phases, ITZ and mastic.

1.5 Aims and objectives of the research

1.5.1 Overall aims

On the basis of the foregoing, the overall aim of the present investigation was to evaluate the effect of warm additives on the rheological properties of WMBBs. A further aim was to investigate the effect of warm additives, production temperatures, and binder grade on the nano-mechanical properties of WMBBs and

WMA to gain more insight into the behaviour and response of binder and asphalt mixtures to different conditions. Moreover, understanding of the individual mixture phases and how the interaction between aggregate and binder contributes to the overall performance of asphalt mixtures is required to aid pavement designers design more sustainable and cost-effective asphalt mixtures. In term of level of blending between RAP and virgin materials, further aim was to propose a methodology or protocol to investigate and achieve complete blending in the laboratory.

1.5.2 Objectives

The specific objectives of the research are summarised as follows:

- To review the international literature on the performance of WMA.
- To review the international literature on the level of blending between RAP and virgin materials.
- To investigate the effect of different dosages of Sasobit, Rediset WMX and Rediset LQ on the viscosity and rheological properties of binder.
- To investigate the fatigue life of WMBBs using the time sweep method.
- To evaluate the impact of warm additives Sasobit and Rediset WMX and LQ on topography, modulus, deformation and adhesion of warm-modified bituminous binders using Atomic Force Microscopy (AFM) with the PeakForce Quantitative Nanomechanical Mapping (PFQNM) modality.
- To quantify the effect of warm additives, production temperatures and binder grade on the mechanical properties of mixture phases aggregate, ITZ and mastic.
- To propose new approaches to evaluate the strength of the bond between aggregate and binder without separating them from the mixture.
- To link the effect of warm additives on the work of fracture to the adhesion force determined using AFM and the work of indentation approach.
- To evaluate the fatigue life of WMA taking into account the effect of production temperatures and binder grade
- To assess the effect of mechanical properties of mixture phases on the overall fatigue life of asphalt mixture.

- To investigate the effect of warm additives and production temperatures on the level of blending between RAP and virgin materials at micro- and nano-scales.
- To establish a protocol or methodology to obtain and approve complete blending between RAP and virgin materials in the laboratory.

1.6 Thesis layout

The thesis is organised into ten chapters. Chapters 1 and 10 are the introduction and conclusion respectively while Chapter 9 summarises the effect of warm additives on bituminous binder and mixture properties. The main body of the research is presented in chapters 2 to 8, as follows:

Chapter 2- Warm Mix Asphalt (WMA)/Reclaimed Asphalt Pavement (RAP) State-of-the-Art: the state-of-the-art chapter reviews the more common available warm technologies with particular reference to the organic technology and chemical technology. The chapter also reviews the hypotheses regarding the level of blending between RAP and virgin materials, as well as the performance to date of including RAP in WMA.

Chapter 3- Viscosity, Rheological Properties, and Fatigue of Warm-Modified Bituminous Binders (WMBBs): in this chapter, the effect of warm additives on the viscosity of bitumen is investigated in detail. Furthermore, the effect of these additives on the rheological properties of bitumen is also identified using a Dynamic Shear Rheometer (DSR). The investigation of rheological properties includes the effect of these additives on the linear viscoelastic region using amplitude strain sweep and also their effect on the stiffness and phase angles of bitumen using sweep frequency. Furthermore, the fatigue performance of WMBB is investigated using a time sweep test, and data are modelled using the Viscoelastic Continuum Damage approach (VECD).

Chapter 4- Nano-scale Properties of WMBBs Determined with Atomic Force Microscopy (AFM): this chapter presents firstly a brief background on the general utilisation of AFM in pavement engineering. This is followed by experimental details, results and discussion about an investigation into the impact of warm additives on topography, modulus, adhesion and deformation of binder

using Atomic Force Microscopy (AFM) with the PeakForce Quantitative Nanomechanical Mapping (PFQNM) modality.

Chapter 5- Nano-Mechanical Properties of WMA Determined with Nanoindentation: this chapter presents an investigation into the impact of warm additives, production temperatures and binder grades on the mechanical properties of mixture phases aggregate, ITZ and mastic. It also presents a technique to prepare asphalt mixture samples to be used in nanoindentation.

Chapter 6- Adhesion Performance of WMA: this chapter presents the results of an investigation to evaluate the effect of the warm additives on the adhesive bond strength of an aggregate-binder system using the pull-off test. It also presents a new approach called work of indentation to evaluate the strength bond between aggregate and binder/mastic in the mixture based on the ITZ properties. In addition, it presents a comparison between the required work of fracture to break the adhesive bond of the aggregate-binder system and adhesion force between the probe and the bitumen surface using atomic force microscopy (AFM) and the work of indentation.

Chapter 7- Fatigue-cracking Characterisation of Warm Mix Asphalt (WMA): this chapter presents stiffness measurements and fatigue life of WMA tested in a DSR. The chapter also presents results of sweep stress measurements to select the stress value for the fatigue test after the region damage. Moreover, it presents the effect of mixture phases ITZ and mastic on the overall fatigue performance of WMA.

Chapter 8- Level of Blending between RAP and Virgin Materials: this chapter presents the effect of warm additives and production temperature on the level of blending between RAP and virgin material using the advanced technology of nanoindentation. The chapter also presents the validation of complete blending between RAP and virgin materials based on and high-resolution images obtained using a scanning electron microscopy (SEM) and the stiffness and fatigue life of asphalt mixtures. It also introduces a new protocol to investigate and obtain a complete blending between RAP and virgin materials in the laboratory.

Chapter Two

Warm Mix Asphalt - Reclaimed Asphalt Pavement -State-of-Art

2.1 Introduction

In recent years, pavement researchers have increasingly focused on reducing production and compaction temperatures to improve the environmental and economic impacts of hot mix asphalt (HMA) without adversely affecting the workability, durability and performance of asphalt pavements. The introduction of innovations and technologies in the form of warm mix asphalt (WMA), which is one of the main focuses of future pavement technology endeavours, will lead to substantial improvements in quality of life and economic prosperity. Warm mix asphalt (WMA) is an environmentally friendly asphalt mixture that can typically be manufactured at a temperature of approximately 20°C less than the typical temperature used in HMA production using one of warm technologies organic, chemical or foaming. Moreover, in order to maximise the benefits of such technology, the inclusion of higher percentages of reclaimed asphalt pavement (RAP) in WMA allows the development of a more sustainable and cost-effective pavement structure in terms of reducing greenhouse gas emissions and fuel consumption, and conserving the natural resources of the materials used. The current state-of-the-art chapter reviews the more common available warm technologies with particular reference to the organic technology (Sasobit) and chemical technology (Rediset). The chapter also reviews the hypotheses regarding the level of interaction between RAP and conventional materials, as well as the performance of including RAP in WMA to date.

2.2 Asphalt mixtures

In general, pavement is a composite material used to surface roads, car parks and airports. It consists of mineral aggregates bound together with bitumen. The production of asphalt mixtures can be conducted using either hot mix asphalt (HMA), warm mix asphalt (WMA) or cold mix asphalt (CMA). Traditionally, hot mix asphalt is used to manufacture asphalt mixtures by heating the bitumen to decrease its viscosity, and drying the aggregate to remove moisture from it prior to mixing. Hot mix asphalt is generally manufactured at temperatures between 150°C and 180°C, whereas warm mix asphalt can be manufactured at temperatures ranging from 100-145°C using one of a number of warm technologies, either zeolites, waxes, surfactant or asphalt emulsions. Cold mix asphalt is manufactured by emulsifying the asphalt in water. While in its emulsified state, the asphalt is less viscous; therefore, the mixture is easy to work and compact. Whatever mixture type is used, the flexible pavement structure, as shown in Figure 2.1, should provide: good ride quality at high speeds by reducing noise levels both inside and outside the car, superior night-time visibility, an adequate level of skid resistance, adequate drainage, low maintenance, and, more importantly, reduce traffic stress to a level that can be sustained by sub-grade level.

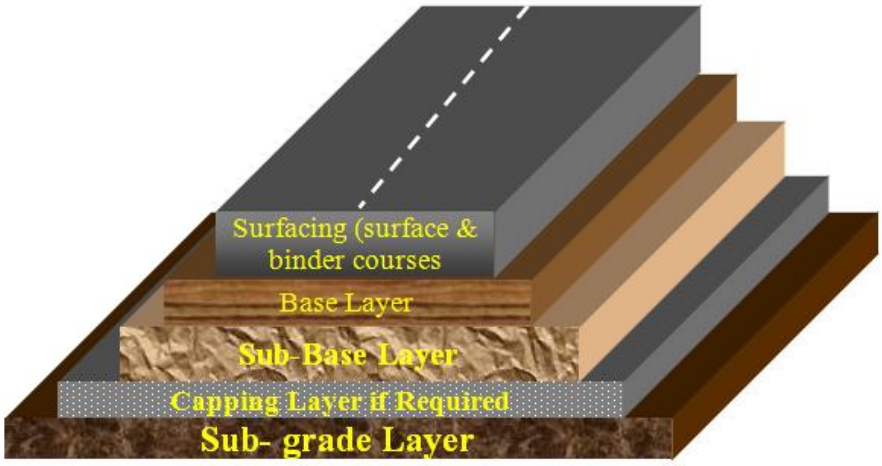

Figure 2.1 Typical flexible pavement structure (Abd 2011)

Bitumen is a binding agent like Portland cement but it has very different properties. Cement creates a rigid material which cannot deform appreciably unless it first cracks, while bitumen exhibits viscoelastic behaviour at normal-in

service temperature; the latter therefore has the ability to deform. However, despite this viscoelastic behaviour, it can still crack and it is impossible to define a tensile strength since this will vary with temperature and rate of loading; the relevant parameter is the fatigue characteristic, which is defined as the resistance to cracking under repeated load. The key properties for design are therefore stiffness, resistance to deformation under repeated load and fatigue characteristics (Thom 2008).

2.3 Background history of warm mix asphalt development

From a historical point of view, the concept of using lower production and compaction temperatures is not completely new. The earliest work was started by Professor Ladis Csanyi in 1956 at Iowa State University, when the potential of foamed bitumen was investigated for use as a soil binder. From that time, successful foamed asphalt technologies have been developed in many countries (Chowdhury and Button 2008). However, despite the fact that the concept of introducing steam into hot bitumen was successful, the work was impractical for in situ foaming operations. For this reason, in 1968, Mobile Oil Australia obtained the patent rights for Csanyi's invention and made modifications to the original process by supplying cold water instead of steam to the hot bitumen (Muthen 1998,Kristjansdottir 2006).

Further advancement in this technology was introduced to the market in the USA as the Conoco product, which was evaluated as a base stabiliser in both the field and the laboratory (Little *et al.* 1983,Chowdhury and Button 2008). In the early 1970s, new methodologies of pavement mixtures stabilised with emulsified asphalt were successfully developed by Chevron, who published the *Bitumuls Mix Manual* as a practical guideline in 1977 (Chowdhury and Button 2008,Zettler 2006).

In terms of producing mixture at an ambient temperature, in 1994, Houeran and Maccarone investigated and studied cold-mixed asphalt-based foamed bitumen, which is produced at approximately 20–49°C and highlighted that, due to the lower emissions and greater energy efficiency of this system, cold mix was broadly gaining acceptance. Indeed, it was stated that "Cold technologies

represent the future in road surfacing" (Chowdhury and Button 2008). However, despite the fact that cold asphalt mixes (CAMs) have many good properties, they have not taken the place of hot mixes. CAMs cannot replace HMAs as the primary road surfacing materials because of their requirement for curing time, which means that there is a long delay after laying before the road can be opened to traffic, and they also have an inadequate overall long-term performance in comparison with HMAs (Gandhi 2008b). However, rising fuel prices, global warming and more stringent environmental regulations have resulted in more demand to reduce production and compaction temperature. It is therefore necessary to heat the aggregate to at least above the ambient temperature so that appropriate coating occurs between the aggregate and the binder. From this idea, in 1999, Jenkins *et al.* introduced a new concept of half-warm foamed bitumen treatment, which can enhance mix cohesion, tensile strength and compaction.

A warm asphalt mixture process has been developed in Europe. Between 1996 and 1999, several road trials in Europe were conducted to study and demonstrate the warm mixture's performance in the field with three major asphalt companies in Norway, the UK and the Netherlands, and the results were first reported by Harrison and Christodulaki at the First International Conference of Asphalt Pavement in Sydney, 2000 (Jones 2004). Afterwards, a more comprehensive and complete report was introduced by Koenders *et al.* (2000) at the Eurobitume Congress in 2000, which described the innovative warm asphalt mixture and its performance based on laboratory tests and large-scale field evaluation . It can therefore be said that some of today's versions of warm asphalt technologies are the brainchild of European researchers trying to reduce mixing/compaction temperatures.

In recent years, and despite the fact that the innovation of warm asphalt technologies remarkably started in Europe, the topic has been gaining momentum in the USA. In May 2007, a team of 13 materials experts from the USA visited four European countries, Belgium, France, Germany and Norway, to assess and evaluate various WMA technologies (D'Angelo *et al.* 2008). Since then, extensive research has been carried out to establish the potential benefits of using WMA and evaluate its performance compared to the traditional HMAs and, to date; there have been no negative reports about the performance of WMA in the field.

2.4 Available warm technologies

In general, despite the fact that different WMA technologies have different methods of reducing the manufacturing and paving temperatures, they obviously tend to follow the same patterns. Different methods of classification can be used for the WMA technologies. One is to classify the technologies based on the degree of temperature reduction. Warm mix signifies an asphalt mix that can practically be achieved at temperatures around 20-30°C less than the typical temperature used in HMA production, and slightly above 100°C and, for some technologies, even below the boiling point of water. Figure 2.2 illustrates the different production temperatures of flexible pavement mixtures.

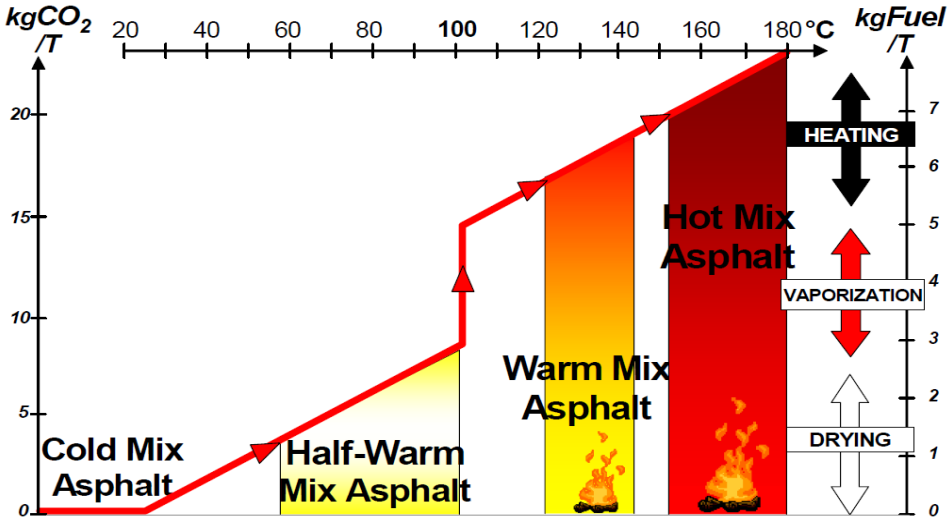

Figure 2.2 Production temperatures of asphalt mixtures (Bueche 2009)

However, for a more instructive and comprehensive definition, warm technologies can be classified based on their products into foaming processes, which could be sub-divided into water-containing and water-based processes, organic additives such as Fisher-Tropsch synthesis wax, fatty acid amides and Montan wax, and the addition of chemical additives (surfactants), which can be either emulsification agents or polymers (Rubio *et al.* 2012). Table 2.1 presents the available warm technologies.

In general, reduction in the production temperatures using warm additives can be achieved based on the three mechanisms:

(1) First mechanism: the organic additives reduce the viscosity of the asphalt binder; therefore, the aggregate can be fully coated at lower production temperatures.
(2) Second mechanism: foaming the asphalt binder by using injected water or hydrophilic (zeolite) in the vaporisation process.
(3) Third mechanism: surfactants decrease the internal frictional forces between the interfaces of the aggregate and the binder and decrease the surface tension of the asphalt binder (Banerjee *et al.* 2012,Capitão *et al.* 2012), which leads to improve wettability of aggregate by asphalt binder.

This section of the research literature mainly focuses on the best-known technologies, which have been extensively studied by researchers. However, more attention will be paid to the performance of Sasobit and Rediset to date.

Table 2.1 Available warm technologies

Product	Company
Low Energy Asphalt	Advanced Concepts Engineering Co.
Rediest WMX and Liquid	Akzo Nobel
CECABASE RT^{R}	Arkema Group
Double Barrel Green	Astec Industries
Aspha-Min	Eurovia Services
Ultrafoam Gx^{TM}	Gencor Industries
Aquablack WMA	Maxam Equipment Inc.
Low Emission Asphalt	McConnaughay Technologies
Evotherm^{R}	MeadWestvaco Asphalt Innovations
Advera	PQ Corporation
Sasobit	Sasol Wax Americas
WAM Foam	Shell Bitumen
Warm Mix Asphalt System	Terex Roadbuilding

2.4.1 Foam technology

With this technology, a small amount of water is injected into the preheated asphalt binder or it can be injected directly into the asphalt mixing chamber. This will result in the evaporation of the water and the liberated steam is encapsulated in the binder, which can then produce a large volume of foam. This action will rapidly and considerably lower the viscosity of the binder by increasing the surface area of the bitumen, leading to a better distribution of the binder with the mixture, which enhances coating and workability. However, careful attention should be paid during this process: just enough water to produce foam must be added otherwise stripping problems may well occur. To overcome this problem, anti-stripping additives can act as a bridge between the aggregate surface and the asphalt binder so that moisture susceptibility is minimised. Foaming technologies are sub-categorised into two groups: water based and water containing.

2.4.1.1 Water-bearing/Containing additives

From the perspective water-containing warm processes there are two synthetic zeolites, Aspha-Min and Advera, which work in a similar manner.

2.4.1.1.1 Aspha-Min

Aspha-Min is a fine white powdered synthetic zeolite. Zeolites are crystalline hydrated aluminium silicates that exist in the natural environment and are also produced artificially. In general, synthetic zeolite has the ability to hold different quantities of water; therefore, in order to utilise this advantage to lower the production temperature of asphalt mixtures, Eurovia Services GmbH, based in Bottrop, Germany, developed Aspha-Min, which is a manufactured synthetic sodium aluminium silicate (Hurley and Prowell 2005a). From the chemical structure point of view, zeolite generally has a framework of silicates with large empty spaces in its structure that allow the establishment of large cations such as sodium, barium and calcium. Groups of large molecules, such as water molecules may also be available. The available water can be driven from the zeolite structure by heating; the available spaces can be interconnected and form long, wide channels of varying sizes depending on the mineral. These channels allow the easy movement of the resident ions and molecules into and out of the zeolite;

therefore, zeolite acts as a delivery system for the new fluid (Button *et al.* 2007,Corrigan 2005). The released water, which is typically up to 20% by mass, will evaporate and the liberated steam will be encapsulated in the binder, leading to a volume expansion of the binder, which results in asphalt foam and enhances the workability of the mixture as well coating the aggregate at lower temperatures.

The recommended dosage of Aspha-Min is 3.0% by the total weight of the asphalt mixture mass, which can yield and promote a reduction in the production temperature of approximately 30°C and save 30% energy (Kristjánsdóttir 2007). As declared by Eurovia, it accommodates the addition of RAP and uses different polymer-modified binders. The foaming can effectively last up to 6hrs (Zaumanis 2010).

In 2005, Hurley and Prowell studied the influence of Aspha-Min extensively at the National Centre for Asphalt Technology (NCAT). It was highlighted that Aspha-Min decreased the air voids by 65% on average and in parallel the compaction was improved at temperatures as low as 88°C. Moreover, the resilience modulus was not adversely affected by the addition of Aspha-Min at any compaction temperatures, but the compactability improvement of Aspha-Min mixtures led to improved resilience modulus values in this research. The rutting potential was not increased by the addition of zeolite. On the other hand, apparently incomplete drying of the aggregate due to decreasing production and compaction temperature attributed to a reduction in tensile strength; therefore, visual stripping was noticed in WMA mixes manufactured at 121°C. In order to mitigate the moisture damage problem, 1.5% of hydrated lime was added to enhance the cohesion and moisture susceptibility of WMA in comparison with mixtures without the hydrated lime. This was remarkable in enhancing the results obtained from the Hamburg wheel-tracking test, which confirmed that the hydrated lime improved the rutting resistance of warm mixtures compacted at lower temperatures.

The authors concluded that the addition of Aspha-Min should not be taken into account during the determination of the optimum asphalt content. Furthermore, if the manufactured temperature is higher than 135°C, the same binder can be used in the design; otherwise, the high temperature grade has to be

increased by one grade, or it is possible to minimise the tendency towards decreased rutting resistance by adding hydrated lime. It is also recommended that tensile strength ratio testing should be carried out for WMA manufactured at temperature same to the expected site production temperature (Hurley and Prowell 2005a). It was, however, concluded in a study by Gandhi *et al.* (2010) that the moisture susceptibility of warm asphalt additives was improved when Sasobit and Aspha-Min were used. They showed that tensile strength ratio values of the unaged mixes increased. But, more importantly, according to Kheradmand *et al.* (2014) and Xiao and Amirkhanian (2010), warm asphalt mixtures containing Aspha-Min have the worst moisture susceptibility in comparison with other warm additives. However, Medeiros Jr *et al.* (2012) highlighted that Aspha-Min mixtures did not indicate moisture susceptibility.

Goh *et al.* (2007) also highlighted that the use of Aspha-Min has no influence on the dynamic modulus. It has also been demonstrated that the addition of Aspha-Min does not significantly affect the asphalt binder grading (Wasiuddin *et al.* 2007,Barthel *et al.* 2004). At temperatures of 135°C and 120°C, Aspha-Min has no significant effect on the viscosity of the binders in comparison with base binder and, more importantly, the viscosity is notably higher than the viscosity of conventional binders after 60 to 90 minutes (Gandhi 2008b). This is surely because of the addition of fine solid material to the binder. In 2009, it was shown that Aspha-Min has a negative effect on the viscosity of recycled binders, as the viscosity increases when Aspha-Min is used. The study also found that it had no positive effect on the resistance to fatigue cracking of recycled binders (Lee *et al.* 2009).

2.4.1.1.2 Advera

Advera is another type of synthetic zeolite, which is developed and manufactured by PQ Corporation in Malvern, PA, USA. Advera has the ability to store approximately 20% water in its chemical structure (Hanz *et al.* 2011), and the water is released at a temperature of 99°C which allows a reduction in the production temperature of approximately 10–21°C (Perkins 2009). It is worth mentioning that, although Advera's mechanism of working is very similar to that

of Aspha-Min, it has no notable effects on the rheological properties of the mix because the zeolite will reabsorb the water again (Kheradmand *et al.* 2014).

Several studies have been carried out to investigate the physical and mechanical properties of WMAs containing Advera. A study conducted by Mogawer *et al.* (2011a) showed that, in terms of moisture resistance, as the ageing time increased, the moisture susceptibility of the warm mixtures including Advera improved significantly, and the greatest improvement in Advera's performance was observed with the addition of hydrated lime over the use of liquid anti-strip.

Another study conducted by Mogawer *et al.* (2011c) showed that, based on the foaming process, Advera was more susceptible to moisture damage than other warm technologies such as Evotherm, Sasobit and Sonnewarmix. This issue may result from water enclosed in the aggregate, which weakens the interface between the asphalt binder and aggregate, leading to stripping problems. This corresponds to a study conducted by Hill *et al.* (2012a), who reported that Advera reduced the tensile strength ratio by 23% in comparison with the control HMA mixture. However, a study conducted by other researchers revealed that the addition of Advera did not make the mixture more prone to moisture damage, and also concluded that Advera did not confer favourable properties on mixtures with highly acidic aggregates such as granite (Ghabchi *et al.* 2013). In 2011, Goh and You demonstrated that warm mixtures with Sasobit and Advera had lower dynamic modulus values at most mix and compaction temperatures (100°C, 115°C and 130°C) and frequencies tested (from 0.1 Hz to 25 Hz). This issue was particularly significant at higher testing temperatures. In terms of WMA fatigue life, most WMAs performed similarly to or even better than the control HMA, apart from warm mixtures manufactured at 130°C. More importantly, WMAs tested at 115°C had the highest fatigue life as compared with other WMAs (Goh and You 2011b). However, in another study, the presence of Advera decreased the number of wheel passes required to reach 12.5 mm of rutting in the Hamburg device by 38% (Hill *et al.* 2012a).

2.4.1.2 Water based

2.4.1.2.1 Double barrel green

The concept of this technology is to use some type of nozzle to inject a small amount of water into an asphalt binder stream. The nozzle should be computerised to control the amount of water and the foaming rate (Button *et al.* 2007). The additional water, which is delivered to the system using a positive displacement piston pump capable of accurately rating water induced into the system, will microscopically foam the binder, which creates encapsulated steam in the binder, leading to a forceful increase in the volume of the binder and a decrease in its viscosity.

G1 and G2 are two generations of this technology, which has been in existence since 2007, and was developed by Astec Industries in the USA. The main difference between these two types is the nozzle system functionality. However, there is typically no need to make any changes to the mixture design process, but a foaming device should be used in the laboratory in order to simulate plant mixing.

Middleton and Forfylow (2009) reported that the properties of asphalt binder and mixtures were the same as those of HMAs. The rutting susceptibility of mixtures produced with the Double Barrel Green process was identified to be adequate; moreover, this technology has no negative influence on the moisture susceptibility of mixtures. Environmentally, a 10% reduction in nitrogen oxide, carbon monoxide and carbon dioxide was determined and reported in this process as well as a 24% reduction in energy consumption.

It is thought that this technology may eliminate the need for expensive additives because only a small amount of water is required to be injected into the binder stream, provided that the water is accurately injected to avoid potential stripping problems. However, despite the fact that this technology has gained more popularity in the USA, not much research has been conducted in this area compared with other technologies such as Advera and Aspha-Min. The following figure illustrates the process of this technology.

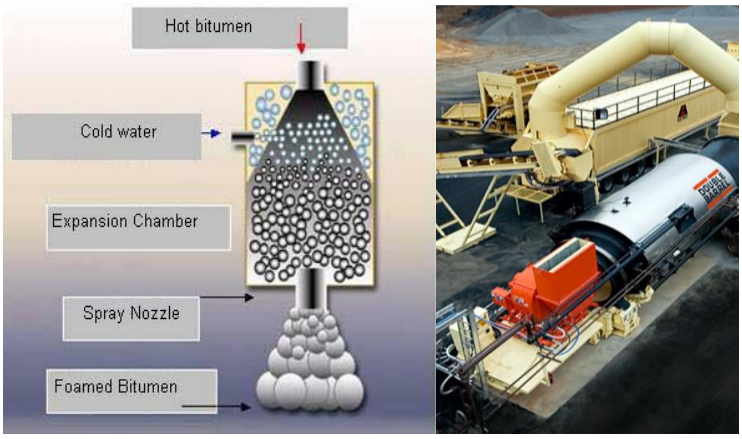

Figure 2.3 Double Barrel Green (Equipment and Lounge 2010,Jenkins *et al.* 1999)

2.3.1.2.2 Low energy asphalt

Low Energy Asphalt WMA technology is developed by Advanced Concepts Engineering and distributed in the USA by McConnaughay Technologies. This technology has a different process to Double Barrel Green. The process involves mixing the hot bitumen (140-180°C) with hot coarse aggregate at a temperature of around 290°F/145°C and then incorporating wet fine aggregates at an ambient temperature. This process releases the moisture in the fine aggregates as steam and, therefore, a foaming action results, which facilitates the fine aggregate coating (D'Angelo *et al.* 2008,Perkins 2009,Rubio *et al.* 2012). This technology is reported to reduce the production mixing temperature to approximately 90°C, which yields significant reductions in energy costs and gas emissions. However, the author thinks that coating and adhesion promoters should be introduced into this technology to enhance the performance of the asphalt mixtures by minimising stripping problems.

Despite the fact that this technology offers a great advantage in terms of the production temperature, it requires a major plant modification. In 2006, Romier *et al*. developed a kit that can be attached to a batch plant. The kit can control the amount of cold sand by the addition of a specific hopper and is also integrated with a device for adding water to the fine aggregate. The RAP can also be introduced directly into the mixer (Chowdhury and Button 2008,Romier *et al.* 2006). They also interestingly highlighted the reduced soiling of production

equipment resulting from this method due to the available moisture, which results in minimising the cleaning requirements and corresponding use of solvents.

Between 2005 and 2010, more than 400,000 tonnes of low energy asphalt were manufactured in Worldwide (LEA-CO 2014) and it is reported that specific multifunctional system were mostly used to enhance the foamability and the coating ability of the binder. This technology has been used successfully mainly in France by EIFFAGE and FAIRCO and the USA by Suit Kote, and to a lesser extent in the UK by PetroPlus, in Spain by EIFFAGE Infrastructures and in New Zealand by Fulton Hogan. However, few studies have been published in this area; therefore further work is highly recommended in order to gain more understanding of the properties of asphalt mixtures and also to check the validity of this process with other materials, climates and mix design methods in order to discriminate the process from other warm technologies, as Gaudefroy *et al.* (2007) believes it is a WMA process with a great deal of potential.

2.3.1.2.3 Warm asphalt mix foam

Warm asphalt mix foam is a water-based foaming technology that was presented for the first time at the Eurasphalt and Eurobitumen Congress in 2000 and was a result of work from a cooperation between Kolo Veidekke and Shell-initiated work on WMAs with laboratory experiments back in 1995 (Koenders *et al.* 2000, 2002). From a practical point of view, Warm asphalt mix foam is slightly different from other water-based technologies because soft and hard binders are introduced at different times in the mixing cycle. The first stage involves heating up the aggregate to around 130°C and then coating it with the soft binder, which accounts for about 20% to 30% of the total binder. At the second stage, the hard binder is foamed by introducing water at 2–5% of the mass of the hard binder at a temperature of about 180°C. The main advantage of this process is to ensure adequate bitumen absorption of the coarse aggregate by the use of the soft binder (which may not be satisfactory with the hard binder at a lower temperature), which then leads to sufficient distribution of the binder in the mixture and an adequate coating and workability for paving.

In spite of a reported 30% plant fuel reduction and 30% reduction in emission rates (Larsen *et al.* 2004), it is still necessary to heat the hard binder to

the temperature required for HMA, and stripping problems may occur because of incomplete water evaporation. However, some researchers have demonstrated that warm asphalt mix foam can successfully be used in the base course and in the wearing course and, in terms of volumetric properties, its performance is very similar to that of HMA using the same materials. Consequently, the mechanical properties of warm asphalt mix foam are equal to those of HMA. Furthermore, field studies have reported that the paved sections utilising warm asphalt mix foam were equivalent to HMA in terms of permanent deformation and surface texture (Larsen *et al.* 2004). Another study, by Losa *et al.* (2009), confirmed good results for this process in terms of fatigue life and permanent deformation.

2.4.2 Chemical technology

Another technology that is utilised to reduce manufactured and compaction temperature is chemical additives, which work in a different way to produce WMAs when added to the mix. This technology involves different packages such as surfactants, emulsification agents, aggregate coating enhancers and anti-stripping additives. This summary of the research focuses on the most important chemical additives such as Evotherm and Rediset.

2.3.2.1 Evotherm

Evotherm is a chemical package that is manufactured by MeadWestvaco Asphalt Innovations, USA, and was introduced to the market in 2005. It includes materials to improve workability, adhesion promoters and emulsification agents. It is currently delivered with relatively high asphalt residue (around 70%) (Hurley and Prowell 2006b,Bennert *et al.* 2010). MeadWestvaco has developed and distributed three kinds of Evotherm to the market, Evotherm DAT, ET and 3G (Kheradmand *et al.* 2014). It is reported by the manufacturer that no special requirements or modifications are needed to pump Evotherm to the asphalt plant. In the field paving to date, Evotherm has been pumped directly from a tanker truck. When Evotherm is mixed with the hot aggregate, the water in the emulsion will be liberated in the form of steam, enhancing mixture workability and aggregate coating. This process allows asphalt application at a temperature 50°C to 70°C lower than traditional HMA. It has been reported in field testing that production

temperature has been successfully reduced by up to 56°C. This allowed energy savings of up to 55%, with a 45% reduction in CO_2 and SO_2 emissions as well as a 50% reduction in NO_x and a 41% reduction in the total organic materials (Sampath 2010).

Evotherm has a minor effect on the rheological properties of bitumen. Xiao *et al.* (2012a) looked at the performance of different warm additives including Evotherm, and found that Evotherm did not exhibit a significantly different failure temperature to control binder. Moreover, in spite of the increasing *m*-value of Evotherm-modified binder (m-value is the measure of binder ability to resist low temperature cracking obtained from bending rheometer testing), which can enhance low temperature properties, in terms of strain response, amplitude sweep testing at 60°C did not reveal any difference in the complex modulus and phase angle of any of the evaluated warm additives in the study, apart from Sasobit. In addition, Evotherm exhibited the highest value of creep compliance. It is therefore thought that Evotherm may be more prone to permeant deformation. It is also important to mention that Evotherm generally has no influence on the viscosity properties of asphalt binder when investigated based on both the rotational viscosity and NCHRP 9-39 Method (Bennert *et al.* 2010). As a matter of fact, as recommended by supplier, Evotherm enhances the workability of asphalt mixtures where they can be compacted at lower temperatures.

In 2006, Hurley and Prowell highlighted that the addition of Evotherm reduced air voids measured in the Gyratory Compactor for given asphalt content. However, as per their recommendation, further research is required to fully investigate this issue because favourable performance, in terms of compaction, resulting from the addition of Evotherm may be negated by a reduction in the optimum asphalt content (Hurley and Prowell 2006b). In addition to the fact that Evotherm has the potential to decrease rutting compared to controlled HMA as found by certain authors (Hurley and Prowell 2006b,Xiao *et al.* 2010,Mogawer *et al.* 2011c,Sampath 2010), visual stripping problems have also been observed. However, Hill *et al.* (2012a) also addressed the effect of Evotherm and found that Evotherm performed approximately 13% better than the control mixture in terms of tensile strength ratio, although a 40% reduction in the required number of wheel passes for the Hamburg device to reach a depth of 12.5 mm was reported.

Consequently, liquid anti-strip or hydrated lime could be utilised in order to remediate the WMA mixture's susceptibility to moisture damage. Having mentioned this, there is a need to simulate the required ageing time in the laboratory because, in fact, to date, no problem with WMA moisture damage has been highlighted in the field.

2.3.2.2 Rediset WMX and LQ

Rediset is a product delivering significant advantages to road construction in one very convenient chemical package. This is the most recent innovation of AkzoNobel, Sweden, the United States and The Netherlands, and Rediset WMX was firstly introduced in 2007 in the United States (Bonaquist 2011) in order to reduce the deficiencies of some existing WMA additives (Hamzah *et al.* 2015). Two kinds of Rediset have been supplied by AkzoNobel, Rediset WMX and Rediset LQ, which do not significantly differ from each other. Rediset WMX is a solid palletised additive and is designed in such a manner that it does not have a negative effect on the binder in terms of the high-temperature or low-temperature properties of bitumen at a wider dosage level (Akzonobel 2011,Logaraj and Almeida 2009). This additive is classified as both a viscosity reducer and a surfactant because it includes a long chain aliphatic hydrocarbon structure and an $-NH_3^+$ group which could chemically react with the aggregate surface (Syroezhko *et al.* 2011).

Rediset LQ, which was recently developed by AkzoNobel, is a surfactant, compaction aid and active adhesive, as it enables the bitumen to displace residual water from the incompletely dried aggregate surface and creates a strong chemical bond between the aggregate and the bitumen that is resistant to moisture damage. It is reported by the manufacturer that Rediset LQ does not alter the binder properties and bitumen grade at the recommended dosage between 0.4 and 0.75% of the total effective binder weight. As mentioned, Rediset LQ also functions as an adhesion promoter; therefore, the potential need for additional anti-strip is eliminated. Moreover, Rediset LQ could potentially improve the stress characteristics of asphalt concrete (Hill *et al.* 2012b). However, in spite of its superior performance, Rediset LQ has not been extensively studied, and there has been limited research on the effect of this warm additive on the performance of

asphalt binder and mixtures (Hamzah *et al.* 2015). Thus, researchers are highly recommended to deeply investigate its performance.

The next sub-sections will mainly focus on the effect of Rediset WMX on binder and mixture because of the aforementioned reason.

2.3.2.2.1 Effect of Rediset on asphalt binder properties

Studies conducted by Xiao *et al.* (2011a, 2011b, 2012a) to investigate the rheological properties of non-foaming additives revealed that the viscosity values of all asphalt binder modified with Rediset WMX decreased as the test temperature increased, and it should also be mentioned that no negative effect of storage duration on viscosity was found. Therefore, the modified binder could be stored for a certain period if this is required. This is also confirmed by Arega *et al.* (2011) and Sengoz *et al.* (2013). However, Arega *et al.* (2011) highlighted during their study that some warm additives involving Rediset WMX reduced the binder viscosity measured at 135°C with minor exceptions. This fact agreed with a study conducted by Sengoz and Oylumluoglu (2013), who reported that Rediset WMX decreased the mixing and compaction temperatures of WMA by only 8°C and 6°C respectively, based on the results of rotational viscosity. It seems that the estimation of reduction in the production temperatures based on rotational viscosity test cannot predict the real reduction in the production temperatures of WMA as obtained in the current thesis, which will be discussed in detail in the next chapter. However, another study conducted by Arega *et al.* (2011) observed a negative effect of using 2% of Rediset WMX on the rotational viscosity of a PG76-22 asphalt binder, which contains a high amount of natural wax.

Attention should be drawn to the performance of Rediset WMX in terms of permanent deformation because researchers have reported different behaviour. Some studies have shown that binder modified with Rediset WMX exhibited high levels of compliance in terms of the creep and creep recovery test and was more stress sensitive relative to the virgin binder but without a significant adverse effect on high-temperature continuous grade (Hanz *et al.* 2011,Xiao *et al.* 2012a). This means that asphalt binder modified with Rediset is more prone to rutting issues. However, these findings do not agree with other studies (Xiao *et al.* 2011a,Doyle

et al. 2013). Xiao *et al.* (2011b) claimed that modified binders with Rediset WMX increased the high temperature failure of asphalt binders while a study by Doyle *et al.* (2013) showed that incorporating 1.5% of Rediset WMX increased the rutting factor ($G^*/Sin\ \delta$, G* is complex shear modulus and δ is the phase angle) of asphalt binders by 48% and 15% for un-aged and short-term ageing conditions at 70°C. In spite of the controversial point about the effect of Rediset WMX on permeant deformation among the aforementioned researchers, Kim *et al.* (2011a) studied the impact of warm additives on rheological properties of polymer-modified asphalt binders, highlighted that the performance grade of asphalt binders at low and higher temperatures was not affected by adding 2% of Rediset WMX.

Most researchers (Arega *et al.* 2011,Xiao *et al.* 2013) investigated the fatigue performance of Rediset WMX-modified binders based on Superpave fatigue cracking ($G^*\ Sin\delta$, G^* is complex shear modulus and δ is the phase angle), which has received extensive criticism (Hamzah *et al.* 2015). In most scenarios, Rediset WMX decreased the value of $G^*\ Sin\delta$ of the asphalt binders, which implies that Rediset WMX makes the asphalt binder less stiff than the control binders. It was also found that it has a high *m*-value in comparison with virgin binder, and therefore the addition of Rediset WMX may well lead to better fatigue life performance. This matter has been highlighted by Arega *et al.* (2011), who also reported that the recommended strategies to compensate for the reduced initial stiffness in WMA (such as addition of RAP) must be tailored to the specific kind of WMA mixture, because subjecting the short-term aged modified binder to long-term ageing led to low-temperature and fracture properties similar to or lower than the long-term ageing residues of conventional or control asphalt binders, which means that long-term ageing may erase the variation in reduced short-term ageing of WMA. Consequently, the incorporation of RAP materials or any other strategy to overcome the reduced initial stiffness in WMA may adversely affect the low-temperature behaviour of warm asphalt mixtures.

This finding does not correspond with another study carried out by Banerjee *et al.* (2012), who studied the effect of long-term ageing on the rheology of warm-modified binders. Results suggested that warm-modified binder not only reduced the influence of short-term ageing on rheological properties, but could also retard the rate of ageing in which stiffness increases over time. Surprisingly,

and more importantly, Rediset WMX exhibited the lowest rate of ageing of the additives used in this study.

During all the aforementioned studies, unsurprisingly, the binder source also significantly affected the viscosity values and rheological properties of the same binder grade. This fact indicates that the chemical interaction between warm additives and different asphalt binder sources should be thoroughly investigated in order to select the appropriate additive dosage to enable the warm mixture to have a similar or better performance than HMA. The author of this thesis believes – and it is also the recommendation of a recent study by Hamzah *et al.* (2015) – that the intermediate temperature properties of asphalt binders in terms of fatigue cracking should be evaluated by time sweep tests. This point is one of the objectives in the framework of this thesis.

Rediset LQ has not been investigated in detail in the literature; therefore, researchers are encouraged to thoroughly investigate it, as the author of this thesis believes it is expected to display superior performance.

2.3.2.2.2 Effect of Rediset on asphalt mixture properties

Some researchers have investigated the effect of Rediset on reducing the manufacturing and placement temperatures of WMA. It has been reported that the recommended dosage of Rediset WMX, which is 2% of binder weight, exhibited the best workability and compactability compared with 1% (Bennert *et al.* 2010). This was certainly achieved by the action of Rediset WMX in reducing binder viscosity and enhancing the wetting of the aggregate surface. Recently, this has been confirmed by a study carried out by Hamzah *et al.* (2013), who proclaimed that there is a slight decrease in the Marshall stability if 3% Rediset is used instead of 2%; therefore, one can deduce that 2% of Rediset gives the desired and adequate Marshall stability. In addition, the higher the Rediset content, the higher its softening role in the asphalt mixtures will be.

In terms of fatigue performance of asphalt mixtures, there is little information and study evaluating the effects of both Rediset WMX and LQ on the fatigue performance of asphalt mixtures (Hamzah *et al.* 2015). The fatigue properties of asphalt mixtures containing Rediset WMX in both wet and dry

conditions were investigated by Jones *et al.* (2010). They conducted fatigue tests at two different strain levels and at three different temperatures using a flexural controlled-deformation fatigue test. It was concluded that the fatigue life of asphalt mixtures at 50% stiffness reduction and also on the initial phase angles was not affected by addition of Rediset WMX in both wet and dry conditions. However, this fact does not agree with a study conducted by Bennert *et al.* (2011), who claimed the fatigue life based on the number of cycles measured by overlay tester for asphalt mixtures containing Rediset was higher than that of controlled HMA produced at normal temperatures. It is therefore believed that the effect of Rediset on the fatigue cracking of asphalt mixtures should be further studied, taking into account the effect of fabricated temperature and binder grades.

The susceptibility of chemical additives to thermal cracking was explored by Hill *et al.* (2012b). They found that the fracture energy of chemical-modified WMA mixtures including Rediset LQ and Evotherm slightly increased, by 7%, in comparison with the control HMA and displayed the greatest creep compliance, whereas the addition of an organic additive (Sasobit) and a foaming additive (Advera) decreased the fracture energy by 12.7% and 11.1%, respectively. This finding exactly coincides with another study conducted by Hill *et al.* (2012a), who indicated that the use of chemical technology (Evotherm and Rediset LQ) increased the fracture energy by 7% and increased the resistance to moisture damage by 13% and 23%, respectively; however, at the same time these additives reduced the resistance to permanent deformation by 40%. It can therefore be demonstrated that low-temperature characteristics are sensitive to the kind of warm technology used. The influence of manufactured temperature was not clear, as two WMA systems had higher fracture energy values, whereas others had lower values. Study of the performance when including RAP materials in WMA is urgently required to find the counterbalance between potential low-thermal cracking issues and an adequate level of rutting performance.

Bennert *et al.* (2011) conducted a study to evaluate the impact of production temperatures on the rutting properties of WMA with the inclusion of 1% and 2% of Rediset WMX using the Hamburg wheel-tracking test. It was reported that the resistance of mixtures to permeant deformation deceases as the production decreases, and the resistance of asphalt mixtures containing 2% of

Rediset WMX was higher than those containing 1% of the same additive. This positive performance was also observed by (Sampath 2010), who showed that mixtures containing Rediset WMX had sufficient capability to pass the requirement of 10,000 cycles in a simple performance tester. On the other hand, Mo *et al.* (2012) reported that WMAs containing Rediset WMX do not have a comparable performance to that of HMAs.

Regarding the effect of Rediset on moisture damage, it was found that the indirect tensile stress ratio of mixtures containing Rediset WMX was less than 80% (Sampath 2010). However, the addition of Rediset WMX had no effect on the moisture sensitivity of the asphalt mixtures investigated based on the Hamburg wheel-tracking test (Jones *et al.* 2010). Furthermore, a study on the mechanisms of adhesion between aggregate and binder conducted by Alavi *et al.* (2012) pointed out that the bond strength ratio of binder containing Rediset WMX was higher than 0.7, which implies that Rediset WMX could provide acceptance resistance to moisture damage. It seems that the mechanisms used to evaluate the degree of bonding between aggregate and binder exhibited different behaviour, and there is a need to find a way to directly estimate the degree of aggregate-binder bonding in the mixtures.

In fact, in order to reach acceptable and adequate mixture stability, rutting and fatigue resistance, and also to produce asphalt mixtures that have equal or even better performance than traditional HMA, highways agencies may need to specify minimum production temperatures for WMA taking into account the effect of production temperatures and binder grade and source as well.

2.4.3 Organic additives

This technology is based on using waxes, which contain high molecular weight hydrocarbon chains, in the asphalt mixture because when the temperature reaches the melting point of the waxes, they melt, leading to a viscosity reduction in the asphalt binder. However, when the mixture cools these additives will solidify into microscopically small and uniformly distributed particles in the bitumen (Rubio *et al.* 2012). This phenomenon leads to stiffening of the binder in a similar manner to fibre-reinforced materials. Some researchers have highlighted that complicated

problems exist when the melting point of the wax is below the in-service temperature, and careful selection of wax type is needed to avoid potential temperature problems (Silva *et al.* 2010,Shang *et al.* 2011). As a matter of fact, not only the kind of wax but also the type of binder plays an important role in determining the performance of included synthetic waxes, as the internal crystallising fraction depends on the bitumen type and source (Edwards and Redelius 2003). In general, the introduction of synthetic waxes to the asphalt mixture will boost the permanent deformation resistance by increasing the mixture stiffness properties. On the other hand, there may be an adverse effect on the fatigue response because stiffer materials exhibit less ductile behaviour (Barbati *et al.* 2009).

Three well-known technologies of synthetic waxes are available: per Fischer-Tropsch wax, fatty acid amide and Montan wax. This research is only going to focus on the most frequently used wax in WMAs, whether in the field or in the laboratory, which is Fischer-Tropsch wax, with particular reference to Sasobit.

Sasobit is a Fisher-Tropsch synthetic wax produced by Sasol Wax GmbH in Germany. From the industrial point of view, the Fischer-Tropsch synthesis, coal or natural gas is partially oxidized to carbon monoxide that is subsequently reacted with hydrogen under catalytic conditions producing a mixture of hydrocarbons which have molecular chain length of carbon C_{45} to C_{100} plus carbon atoms. The process starts with generation of synthesis gas then reacted with cobalt or iron catalyst to form products such as kerosene, gas oil, synthetic naphtha and waxes. Finally, recovered Sasobit is carbon in the chain length range of C_{45} to C_{100} plus, which is longer than microcrystalline bituminous paraffin wax, with chain lengths from C_{25} to C_{50} (Hurley and Prowell 2005b,Butz *et al.* 2001,Wasiuddin *et al.* 2011b).

Sasobit is supplied in the form of greyish-white to yellowish pastilles and pills (Jamshidi *et al.* 2013). It does not require high-shear mixing apparatus and can be easily blended manually and/or mechanically, and the method used has no effect on the properties of Sasobit-modified asphalt binder (Sasolwax 2014,Ji and Xu 2010). Therefore, no major modification is required to introduce Sasobit into

the asphalt plant because it can be either mixed with hot bitumen or added directly to the aggregate. The recommended dosage of Sasobit is 0.8–4% of binder mass. However, more than 4% has a negative effect in terms of the low-temperature properties of bitumen (Edwards and Isacsson 2002).

2.4.3.1 Performance of asphalt binder containing Sasobit

2.4.3.1.1 Effect of Sasobit on asphalt binder rheological properties

As mentioned above, Sasobit has a predominant range of hydrocarbons of chain length from 45 to 100 carbon atoms, while natural asphalt paraffin waxes are normally in the range of 25 to 45 carbon atoms. The long chains of carbon atoms increase the plastic limit and also increase the asphalt binders' range of melting temperatures (Wasiuddin *et al.* 2011a, 2011b). It has been determined that the melting point of Sasobit is approximately 100°C. Above this temperature Sasobit liquefies the asphalt binder, resulting in a reduction of asphalt binder viscosity; therefore, the production temperature at which the mixture should be produced decreases. However, below the melting point of wax, Sasobit forms a lattice structure which acts as a bridge between molecules and prevents their movement; consequently, it increases the viscosity of asphalt binders at lower temperatures. It should also be mentioned that Sasobit exhibits Newtonian behaviour at higher temperatures and non-Newtonian behaviour below its melting point (Jamshidi *et al.* 2013). According to the manufacturer, with the addition of Sasobit the production temperature can be reduced by approximately 20–30°C. However, this is not always true because the reduction in the production temperature is also highly affected by the binder source and grade. Silva *et al.* (2009, 2010) reported that, in order to maximise the benefits of using Sasobit, softer base bitumen should be used, and it was found that a maximum temperature reduction of 15°C was achieved by using 4% of Sasobit with a softer binder.

Many researchers have investigated the rheological properties of Sasobit-modified asphalt binder. In all scenarios, Sasobit increases the complex shear modulus (G^*) of asphalt binder while decreasing the phase angle (δ) regardless of binder type and grade. Moreover, the addition of Sasobit increases the failure temperatures of all binders and leads to lower creep compliance and high creep stiffness with lower *m*-value. It subsequently enhances the permanent deformation

of asphalt binder but may adversely affect its low-temperature properties (Xiao *et al.* 2012a,Xiao *et al.* 2011a,Xiao *et al.* 2011b,Gandhi *et al.* 2010,Doyle *et al.* 2013). However, a study conducted by Kim *et al.* (2011a) highlighted that the addition of Sasobit increased the elastic behaviour of warm-modified polymer-modified binders at lower temperatures and enhanced the rutting resistance properties at high pavement temperatures. Based on these studies, it is the author opinion, although there is a clear conclusion that Sasobit improves the rutting resistance of asphalt mixtures, the fatigue cracking of asphalt mixtures is still a controversial point.

However, a study conducted by Banerjee *et al.* (2012) showed that Sasobit causes a slower increase in stiffness over time, therefore retarding the rate at which binder stiffness increases over time in comparison with conventional asphalt binder. Moreover, 2% of Sasobit increases the cohesive strength of the asphalt binder evaluated by surface free energy measurements (Wasiuddin *et al.* 2011a). It must also be mentioned that the interaction between Sasobit and asphalt binder is only physical, because a study conducted by Menapace *et al.* (2014) outlined that nuclear magnetic resonance did not detect any chemical interaction due to the addition of Sasobit.

From a sustainable engineering point of view, the Sasobit dosage should be carefully selected because it has been reported that low-temperature cracking resistance of both un-aged and long-term-aged binder decreases as the Sasobit dosage increases. In other words, asphalt binder containing a high percentage of Sasobit will be more prone to cracking issues (Liu *et al.* 2012).

2.3.3.1.2 Effect of Sasobit on the topography of asphalt binder structure

The surface of the asphalt binder can be investigated by using the recently developed and sophisticated Atomic Force Microscopy (AFM) in order to subsequently bridge and link observed behaviour of the asphalt binders with their chemical make-up and bulk properties (Menapace *et al.* 2014,Rebelo *et al.* 2014a,Masson *et al.* 2006). Briefly, bitumen can be separated into four fractions: saturates, aromatics, resins and asphaltenes (Masson *et al.* 2007,Nahar *et al.* 2013b). The more asphaltenes there are in the asphalt binder, the harder and more

viscous that bitumen is likely to be, because molecules can form easily as they carry positive and negative charges at different points; therefore, bonds between molecules are easily made. At the other end of the scale, the more saturates there are, the softer the binder will be. Saturates are a non-polar fraction and they form a soup surrounding the other molecules. However, the other kinds of molecules, aromatics and resins, are intermediate components in the soup. Resins are similar to the asphaltenes and are highly polar, which influences the degree to which asphaltenes are readily dispersed within the bitumen, whereas aromatics behave as a solvent to both resins and asphaltenes (Thom 2008).

These components are explained by a bee-like structure which consists of the catana phase, which is assigned to the most rigid and polar bitumens, the asphaltenes; the peri phase, which is attributed to the less polar aromatics and resins; and the para phase, which refers to non-polar saturates. It was therefore possible to investigate the effect of different polymers on the components of asphalt binders and make a link between the morphology of the bitumen's structure and its rheological properties (Loeber *et al.* 1996, 1998).

It was reported that Sasobit greatly affected the morphology of asphalt binder. Menapace *et al.* (2014) found Sasobit enlarges the bee-like structures of bitumen. In other words, Sasobit caused the catana phase and the peri phase to grow. The following Figures, 2.4 and 2.5, illustrate the effects of Sasobit on 60/70 Pen and PG 76-22 observed by using Atomic Force Microscopy (AFM).

60/70 Pen ***PG 76-22***

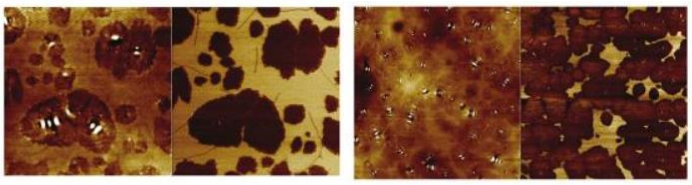

Figure 2.4 Height (left) and Phase (right) images with scan size 10 and 25 μm as presented exactly in (Menapace et al. 2014)

60/70 Pen + Sasobit ***PG 76-22 + Sasobit***

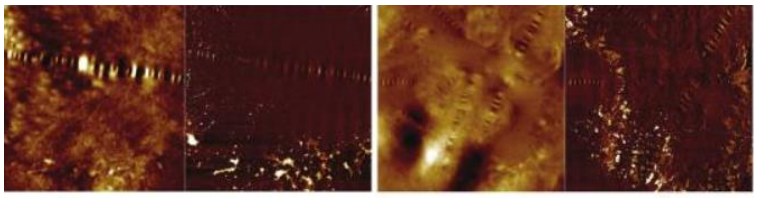

Figure 2.5 Height (left) and Phase (right) images with scan size 25 μm as presented exactly in (Menapace et al. 2014)

2.4.3.2 Performance of asphalt mixture containing Sasobit

2.4.3.2.1 Effect of Sasobit on mix design and volumetric properties

Sasobit is a flow modifier and viscosity reducer; therefore, it is expected to have an influence on the volumetric properties and mix design of asphalt. Hurley and Prowell (2005b) found that air voids in asphalt mixtures decreased when Sasobit was added, which may result in a reduction in the optimum asphalt content. It was found that using 2.5% of Sasobit improved the compactability of the mixtures in both the Superpave gyratory compacter and the vibratory compactor, with a reduction in air voids of up to 0.87%. However, another study highlighted that the addition of Sasobit has no significant influence on optimum asphalt binder content, and 3% of Sasobit resulted in an energy saving of up to 12% (Hamzah *et al.* 2010). This could be used to confirm that achieving the required density is quicker for Sasobit-WMA mixtures than for HMA even at lower compaction temperatures, as reported in a study by Zaumanis (2010). In this study, the asphalt mixtures modified with Sasobit reached the final density after 100 gyrations at 135°C, whereas HMA reached the final density after 170 gyrations at 155°C. In fact, it was noticed that Sasobit improved the workability of the asphalt mixtures (Sanchez-Alonso *et al.* 2011). A later study conducted by Zhao and Guo (2012) agrees with this finding, as they noticed the workability of Sasobit asphalt mixture manufactured at 145°C is equivalent to that of control HMA fabricated at 175°C. It can therefore be said that Sasobit generally has no negative effect in terms of mix design and volumetric properties.

2.4.3.2.2 Effect of Sasobit on rutting susceptibility

In terms of lower production temperature, warm mixtures may be softer because of reduced oxidative ageing and incompletely drying aggregate. The performance

of Sasobit with particular reference to rutting susceptibility has been investigated by a number of researchers. Testing conducted using the Hamburg wheel-tracking test showed that Sasobit-modified mixtures were within the allowable rutting limit after 10,000 loading cycles (Hurley and Prowell 2005b,Kim *et al.* 2012,Estakhri *et al.* 2010). The superior performance of Sasobit was also confirmed by using an asphalt pavement analyser. It was reported that the control HMA and Sasobit-WMA performed similarly and met the criterion for rutting resistance. In other words, warm mixtures containing 1.5% Sasobit had a similar performance to HMA after 8000 loading cycles (Hearon and Diefenderfer 2008,Goh and You 2009).

Moreover, although Mohammad *et al.* (2008) reported that Sasobit-modified mixtures presented lower modulus values, other researchers (Petit *et al.* 2012,Haggag *et al.* 2011,Yang *et al.* 2009) have shown that Sasobit-modified mixtures had a higher stiffness value, and it has also been revealed that Sasobit-WMA exhibited an added stiffness, particularly at higher reduced frequencies and/or lower temperatures, because the addition of synthetic wax resulted in a more stable asphalt binder and consequently led to a more stable asphalt mixture due to its crystallised form (Petit *et al.* 2012).

Sasobit-modified mixture containing moist aggregate has been investigated by Xiao *et al.* (2010), who declared that using Sasobit in moist aggregate mixtures did not require additional treatment to satisfy the required pavement performance in terms of rutting, and concluded that the mixture with Sasobit exhibited the best rutting resistance. This coincides with another study undertaken by Bennert *et al.* (2011) to study the effect of production temperature and aggregate moisture content, which revealed that, as the mixing temperature reduced, the flow number also decreased, but not in the case of Sasobit-modified mixture, which was able to maintain flow number values at the 132°C production temperature at the 1.0% and 1.5% dosage rates, and achieved high-temperature stiffness and permanent deformation that surpassed the baseline mixture.

In general, as highlighted by Edwards *et al.* (2006), Sasobit-modified mixture offered the smallest strain in dynamic creep testing; thus, it can be

concluded that the rutting performance of Sasobit-WMA is similar to or even better than HMA.

2.4.3.2.3 Effect of Sasobit on low-temperature performance and fatigue life

The fatigue performance of asphalt mixtures can be affected by a number of factors such as an inadequate structural design, repeated heavy loads, poor drainage and construction and asphalt binder stiffening due to ageing at low and intermediate temperatures (Jamshidi *et al.* 2013). Sasobit stiffens the asphalt binder, which consequently leads to a stiffer asphalt mixture; however, the lower production temperature may offset the negative effect of the addition of Sasobit in terms of low-temperature properties and fatigue life because it is expected that the binder will be less oxidative, which results in a more ductile mixture. However, this may not be true because Hill *et al.* (2012b) found that the effect of manufactured temperature was not conclusive and the selection of warm additive affects the low-temperature properties. In that study, the organic additive presented in the form of Sasobit reduced fracture energy by approximately 12.7% in comparison with chemical technologies, which were able to increase the fracture energy by around 7%, because chemical technologies may have had a tendency to emulsify the neat asphalt binder, whereas Sasobit resulted in stiffer asphalt mixtures. This corresponds with the results of another study, which indicated the inclusion of Sasobit increased the chances of low-temperature cracking as lower tensile strength and failure strain were reported for Sasobit-modified binder, especially at lower temperatures (Liu *et al.* 2012).

In fact, the effect of warm additives including Sasobit on fatigue performance is not clear, as some studies have shown that the fatigue life of Sasobit-modified mixtures was similar to or even better than the control HMA when evaluated based on four-point beam fatigue testing and the cyclic direct tension test (Goh and You 2011b,Haggag *et al.* 2011). The substantial effect of the synthetic wax additive was detrimental in terms of the fatigue cracking resistance, as highlighted by Silva *et al.* (2010), who also recommended that fatigue resistance may only improve without compromising the rutting resistance if softer binders are used, due to the brittle behaviour of wax additives. Therefore,

the issue may be more challenging when RAP materials are considered, as stiffer materials make the mixtures more prone to fatigue deterioration.

2.4.3.2.4 Effect of Sasobit on moisture resistance

Loss of bonding between aggregate and asphalt binder, known as stripping, is the major problem with which pavement engineers are concerned, and it causes many surface manifestations such as rutting, corrugations and cracking (Xiao *et al.* 2012b,Caro *et al.* 2008,Kim and Amirkhanian 1991,Xiao and Amirkhanian 2009). Generally, the strength of an asphalt pavement structure is affected by three major factors: the adhesive bond between the aggregate and the asphalt binder, the cohesive strength of the binder, and the frictional resistance and development of interlock between aggregate particles (Jamshidi *et al.* 2013). Anything affecting these factors can result in deterioration of the pavement structure. In fact, stripping can be caused by the following mechanisms, as identified in the literature: detachment, displacements, spontaneous emulsification, pore pressure, hydraulic scour and pH instability (Little and Jones 2003,Kiggundu and Roberts 1988,Mogawer *et al.* 2011c). However, these mechanisms are beyond the scope of this research.

The lower production temperature of WMAs may well make those mixtures more prone to moisture damage because of incomplete drying of entrapped water in the aggregate. A study conducted by Buddhala *et al.* (2012) pointed out that Sasobit had no detrimental effect on the surface adhesion, as the adhesion increased in wet and dry conditions; moreover, the rate of increase in the surface adhesion was more conspicuous between 0 and 2%, whereas little increase was noticed between 2 and 3%. However, this study is not consistent with another finding, by Arabani *et al.* (2011), who highlighted that the aggregate–asphalt surface energy of adhesion of WMA with Aspha-Min and Sasobit was lower than the adhesive surface energy measured in the reference mix; and likewise those warm additives have the ability to increase the acid component, which leads to a significant decrease in adhesion, especially when acidic aggregate is considered, such as granite. Medeiros Jr *et al.* (2012) evaluated the moisture and low-temperature cracking susceptibility of WMA included Sasobit and Aspha-min. It

was concluded that Sasobit mixtures were more susceptible to moisture damage while Aspha-min mixtures did not appear to be affected by moisture.

Despite the fact that Sasobit enhances and increases the wettability of asphalt binder over aggregates, it has also been mentioned that it shows a general trend of decreasing the adhesion between asphalt mixture components (Wasiuddin *et al.* 2008). However, its behaviour in the development of moisture damage in asphalt mixes and using different measurement methods is yet to be fully understood. The results of research on the cohesive strengths of Sasobit-modified asphalt binder did not correlate well between the surface -free energy value (SFE) and the pull-off test, as the SFE indicated that Sasobit increased cohesive strength, whereas the latter indicated the reverse (Wasiuddin *et al.* 2011b, 2011c). Furthermore, fracture energy-based parameters (energy ratio and ratio of energy ratio) were sensitive to moisture susceptibility of asphalt mixtures, while the tensile strength ratio seemed to be insensitive to moisture susceptibility of the mixes under investigation (Gong *et al.* 2012). It seems that there is no final conclusion about the effect of Sasobit on adhesion and moisture susceptibility of asphalt mixtures, because field evaluation from a WMA study carried out by Sargand *et al.* (2011) revealed that WMA including Sasobit has a better performance in terms of moisture-induced damage three months after opening to traffic.

The utilisation of anti-stripping agents to mitigate moisture sensitivity is widespread. In the USA, 56% of asphalt mixtures are treated with liquids, 15% with liquid and lime, and 29% with lime only (Jamshidi *et al.* 2013). Sasobit was also investigated with the addition of anti-stripping additives. The addition of Zycosoil as an anti-strip agent for Sasobit-modified WMA increased the surface energy of adhesion between aggregate and asphalt in dry conditions and also in the presence of water (Arabani *et al.* 2011). In addition, the addition of 2% of hydrated lime satisfied the criteria of 80% for tensile strength ratio and a remarkable increase in saturated indirect tensile strength values over dry indirect tensile strength values was achieved (Khodaii *et al.* 2012).

In general, hydrated lime has the ability to act as a mineral filler, which results in stiffening of the asphalt binder and mixture, improving resistance to

fracture growth, altering oxidation kinetics, and also altering the plastic properties of clay fines to improve moisture stability and durability (Little *et al.* 2001). The efficiency of hydrated lime depends on its content and the considered method (Little *et al.* 2001); particle size plays an important role in determining its effectiveness as well (Shen *et al.* 2010). Cheng *et al.* (2011) used different-sized hydrated lime particles: 1.3 μm (regular hydrated lime) and 660 nm (sub-nano-sized hydrated lime). In that study, most warm asphalt mixtures containing sub-nano-sized hydrated lime had greater indirect tensile strength values than mixtures containing regular hydrated lime. It is also worth mentioning that the values of indirect tensile strength in both wet and dry conditions were dependent on the aggregate type. Therefore, it is recommended that better aggregate stockpile management and the addition of anti-strips are necessary to minimise and mitigate the potential for moisture damage.

The effect of ageing time and temperature on the ageing of asphalt mixtures is evident. Aged WMA mixtures including Sasobit demonstrate a significant improvement in moisture sensitivity performance, and exposure of WMA to longer ageing times at higher ageing temperatures results in the best performance (Gandhi *et al.* 2010,Mogawer *et al.* 2011a,Mogawer *et al.* 2011c).

In general, the performance of Sasobit-modified mixtures is a function of many factors: Sasobit content, production and compaction temperatures, the type of anti-strip agents, the size and type of aggregate, and the ageing time and ageing temperatures.

2.5 Advantages and drawbacks of warm technologies

2.5.1 Advantages

WMA technologies exhibit a number of benefits. Based on the literature and field performance, the advantages of WMAs can be categorised into four groups: environmental benefits, production benefits, paving benefits and economic benefits

2.5.1.1 Environmental benefits

1- Lower production temperature leads to reduced greenhouse gas emissions.

2- Reduced emissions and odours, which improves the working conditions for production and paving workers.
3- Because of the enhanced workability of WMA, recycling materials such as crumb rubber and RAP could be used. This will therefore minimise the landfill area by recycling materials and conserve the natural resources of asphalt mixture materials (bitumen and aggregate).

2.5.1.2 Production benefits

1- Greater use of RAP could be achieved because of the increased workability of WMA (Rubio *et al.* 2012).
2- Less oxidative binder is used during production and placement of asphalt mixtures, which results in a more durable mixture.
3- Easier to obtain the legislation to implement plant sites in urban areas because of reduced emissions, dust and noise (Zaumanis 2010).

2.5.1.3 Paving benefits

1- Possibility of paving in cold weather because the difference between WMA production temperature and the ambient temperature is less than for HMA.
2- Longer haulage distances because of possibility of paving at lower temperatures.
3- Improved volumetric properties of WMA can be obtained by reducing the viscosity of the asphalt binder (organic additives or foam additives) or by decreasing the surface tension between aggregate and binder (chemical additives).
4- Reduced temperature difference makes road construction and the time before the road can be opened shorter.

2.5.1.4 Economic benefits

1- Reduced fuel consumption.
2- Less wear on the asphalt plant.

2.5.2 Drawbacks

1- Rutting. Less ageing of the asphalt binder makes the mixture prone to rutting issues.
2- Moisture susceptibility. Lower production temperature leads to incomplete drying of entrapped water in the aggregate.
3- Long-term performance. As WMAs are relatively new, less information is available about their long-term performance.
4- Economics. The costs of additives and plant modifications may outweigh the advantages of WMA technologies.
5- The low-temperature properties of organic-modified mixtures can be slightly different to those of HMA. The issue is more complicated when stiffer materials are adopted such as RAP; therefore careful selection of binder type and grade should be made to avoid low-temperature cracking.

2.6 WMA incorporating reclaimed asphalt pavement

One of the most important objectives of warm mix asphalt (WMA) technologies is to increase the possibility of using high percentages of Reclaimed Asphalt Pavement (RAP) due to the ability of these technologies to reduce binder viscosity and the internal fraction between asphalt binder and aggregate, which enhances the workability of the mixtures, resulting in an adequate aggregate coating. However, some warm technologies such as organic additives increase the stiffness of asphalt mixtures; therefore, the inclusion of RAP materials, which are also stiff materials, may have a negative impact on the performance of those mixtures in terms of low-temperature cracking and fatigue performance. Another issue is that the level of interaction between RAP materials and conventional materials is unclear and yet to be investigated (Al-Qadi 2007). This issue is more ambiguous in the case of WMAs as they are produced at temperatures 20–30°C lower than traditional hot mix asphalts (HMAs). This research also reviews the different opinions of researchers regarding the degree of blending between RAP and conventional materials and the performance of WMA-RAP mixtures to date.

2.6.1 Reclaimed asphalt pavement (RAP)

One of the most important recycling materials used in asphalt mixtures is the recycled HMA itself, which results in a reusable mixture of aggregate and asphalt binder known as reclaimed asphalt pavement (RAP). The use of RAP is a valuable approach for paving, economic and environmental reasons. The reuse of recycled asphalt mixtures decreases the amount of waste produced and significantly helps to resolve the problems associated with disposal of highway construction materials (Al-Qadi 2007). In Europe, data from 19 countries showed that 47% of the available RAP was reused in HMA and WMA, while about 22 million tonnes were used in other applications (Zaumanis *et al.* 2014). In the USA, approximately 100 million tonnes of reclaimed asphalt pavements are annually produced. Sixty million tons are reused in the construction of new asphalt pavement, while 40 million tonnes could be employed in other pavement applications. In Canada, over a period of 17 years, RAP was used to pave approximately 3,500,000 m^2 (Association 2009,Jamshidi *et al.* 2013). Moreover, it was reported that using RAP in the base and sub-base layers of the pavement structure potentially reduced global warming by 20%, energy consumption by 16%, water consumption by 11% and hazardous waste generation by 6% (Lee *et al.* 2010). Despite many states in USA have reported limits on the maximum percentage of RAP that can be reused in the asphalt pavement structure in the range between 10 and 50% (Al-Qadi 2007), high percentages of RAP are not ordinarily used in practice because it leads to durability problem.

Researchers (Al-Qadi 2007,Roberts *et al.* 1996,Karlsson and Isacsson 2006) have identified six mechanisms that age asphalt mixtures during their construction and service life:

- Oxidation as a result of a reaction between the asphalt binder and oxygen
- Volatilisation as a result of evaporation of the lighter components
- Polymerisation because of a chemical interaction between molecular components
- Syneresis and separation as a result of the absorption of oily components, asphaltenes and resins by aggregate and exudation of thin oily constituents

- Thixotropy because of the formation of the structure of the asphalt binder over a long period of time.

All the above mechanisms result in stiffer materials; therefore, some studies have indicated that the RAP materials should be mixed with soft asphalt binder and/or rejuvenating agents. The soft binder will restore the rheological properties of recycled binder, while the rejuvenating agents can lower the viscosity of the aged binder (Roberts *et al.* 1996,Sondag *et al.* 2002). It is also worth mentioning that Dunning and Mendenhall (1978) recommended the use of rejuvenating agents with low saturate content and high aromatic content in order to be compatible with the aged binder and to offset its stiffer components.

In order to establish more confident design procedures with the inclusion of RAP materials, many durability concerns regarding the level of interaction between RAP and conventional materials need to be addressed.

2.6.2 Hypotheses on including RAP materials in asphalt mixtures

The level of interaction that occurs between the RAP materials and the virgin materials directly influences the performance of asphalt mixtures and the economic competitiveness of the recycling process. If RAP materials are considered as a black rock and do not mix with the virgin materials during the mixing process, while RAP binder may mix and blend with virgin binder, then the total binder will stiffen, resulting in a stiffer mixture overall. However, if the designer assumes that the RAP will totally blend with virgin materials and actually it behaves as black rock, the mixture will not be stiff enough as insufficient asphalt binder is used. The issue is more complicated if there is a partial interaction between materials.

A limited number of researchers have investigated the level of interaction between aged and virgin asphalt binders (Al-Qadi 2007). McDaniel *et al.* (2000) in NCHRP 9-12 investigated three possible levels of interaction between RAP and virgin materials: black rock (no blending), total blending (100%) and actual practice (mixing as it usually happens in practice). Two RAP percentages were considered in this study: 10 and 40% as the minimum and maximum percentage used practically. In all scenarios, the gradation and the total asphalt binder content

were constant. It was found and concluded that, at 10% of RAP, no remarkable difference was reported between the various blends, whereas the black rock assumption was statistically not similar to the actual practice and the total blending at 40% of RAP content. In other words, out of 66 possible comparisons made, there were 11 and 16 inconclusive cases at 10% and 40% RAP, respectively. With 10% RAP, the majority of the cases (about 70%) supported the conclusion that all cases were similar; on the other hand, only 42% of the comparisons supported the assumption of total blending. However, the authors believed that it was unlikely that total mixing occurred in all scenarios, even with high RAP content. Figure 2.6 summarises the possible level of interaction in the NCHRP study. From the results, it was indicated that there is no requirement to change the binder grade at low RAP content, and total blending between RAP and virgin materials can be assumed at higher RAP percentages.

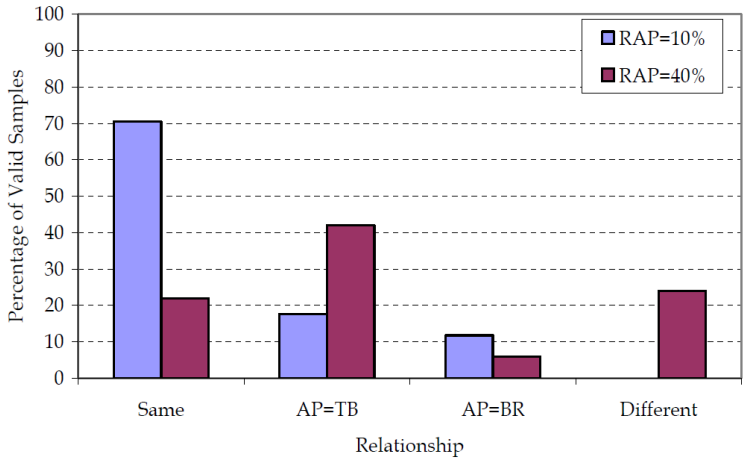

Figure 2.6 Statistical results of interaction between aged and virgin binder evaluated in NCHRP 9-12(McDaniel *et al.* 2000,Al-Qadi 2007)

Same: Actual Practice = Total Blending = Black Rock

AP = TB: Actual Practice = Total Blending ≠ Black Rock

AP = BR: Actual Practice = Black Rock ≠ Total Blending

Different: Actual Practice ≠ Black Rock ≠ Total Blending

Oliver (2001) also investigated the influence of RAP binder on recycled asphalt pavement. Artificial RAP material was manufactured in the laboratory by using bitumen class 320 similar to a 50/65 Pen. The loose mix was exposed to

high temperatures in the oven in order to oxidise and harden the binder film. It was then compacted and broken up to produce artificial RAP. After that, 50% of the manufactured RAP was mixed with 50% of new HMA (binder grade 180/200) and compacted again. Binder was recovered from the recycled asphalt mixture in order to prepare a binder with similar viscosity to the recovered-recycled binder. The viscosity of the extracted binder was 29500 Pa.s at 45°C. Class 600 bitumen was oxidised by heating and then blended with 23% of Class 170 bitumen in order to obtain the same viscosity value of extracted recycled binder. In this way, a manufactured mix identical to the recycled asphalt was produced but with virgin materials. The performance of the two mixes should have been similar; however, their performance in terms of rutting and fatigue resistance was different, and it is postulated the recycled and virgin binders may not completely mix.

Stephens *et al.* (2001) also conducted a study to evaluate the degree of blending between RAP and virgin binders in terms of the RAP preheating time before being mixed with conventional materials. The RAP preheating time was varied from zero to 540 minutes. The preheating time should not have any effect on the mix properties if RAP is considered as black rock. It was in fact found that the preheating time had a considerable effect on the mixture strength, indicating that blending does occur between aged and virgin binders. This finding corresponds with the findings of a study conducted by Nguyen (2009), who also reported that long RAP reheating time, which never occurs industrially, enhanced the reaction between RAP material and virgin materials. Based on his findings, he deduced that RAP material does not act as black rock, nor is it fully blended in recycled asphalt production.

Huang *et al.* (2005) also conducted a study to investigate the level of interaction. RAP materials (passing through No. 4 sieve only) were mixed with virgin coarse aggregate (retained by No. 4) to assess the blending due to pure mechanical mixing. The aim was to find out to what extent the aged binder can get away from the RAP particles under pure mechanical blending, as RAP materials and virgin coarse aggregate can easily be separated after mixing to assess the residual binder content in the RAP. It was found that the asphalt binder content in the RAP was decreased only by about 11% due to pure mechanical mixing. However, the use of pure mechanical mixing alone is not sufficient to

determine the level of interaction between RAP materials and virgin materials because asphalt binder can diffuse in the RAP, and the intermixing between recycled and virgin binders can also rejuvenate the aged binder, resulting in more interaction between aged and virgin binders. Huang *et al.* (2005) also conducted staged extraction and recovery for a mixture of one type (20%) of screened RAP with virgin coarse aggregate. After blending, it was found that the outside layers of the RAP particles were much softer than the inside layers in terms of binder stiffness. In other words, the experiment indicated that only a small portion of recycled asphalt binder in the RAP (40%) indeed participated in the remixing process, while other portions (approximately 60%) did not have any interaction with the virgin binder and acted as composite black rock.

More recently, experimental investigation of the homogeneity of aged binder and virgin binder has been conducted by Eddhahak-Ouni *et al.* (2012) based on conventional tests and infrared spectroscopy analysis in order to assess and quantify the evaluation of the mass proportions of RAP and virgin binders during the stripping process (percentage of extracted bitumen). Results indicated that poor remobilisation of the virgin binder in the blended binder correlated with the hypothesis of the heterogeneous asphalt.

With more recent innovations in WMA technologies, the issue of the level of interaction between RAP and virgin materials is more complicated because of the lower production temperature of the WMA. Research carried out by the NCHRP to assess the level of interaction between aged and conventional binders at WMA temperatures revealed that the aged binder and conventional binder do mix when they are subjected to elevated temperatures; however this may not be valid in the actual mixture as this study only used solvent casting of a thin film of new binder on a simulated RAP binder (Bonaquist 2008). Furthermore, a study by Nahar *et al*. (2013a) showed that the interface between the RAP binder (with a penetration value of 21 0.1mm at 25°C and a softening point of 60°C) and the virgin binder (with a penetration value of 144 0.1mm at 25°C and a softening point of 43°C) was completely blended. The investigation was conducted using Atomic Force Microscopy (AFM) and a DSR. In the DSR, 100g of RAP binder and 100g of virgin binder were blended for 5 minutes at 160°C. The rheological properties of three binders were characterised, and the complex modulus and

phase angle were used to construct a master curve for each binder. In Atomic Force Microscopy (AFM), a bead of 15mg of RAP binder was applied to one side of the 12mm metal sample substrate and the same amount of virgin binder was applied to from the other side. Although, a complete blending was observed in AFM images and confirmed by DSR, the results did not rule out the black rock hypothesis altogether.

Bowers *et al.* (2014) also investigated the effect of mixing time, mixing temperatures and the inclusion of WMA additives (surfactant beads and wax-based additives) on the efficiency of blending between RAP and virgin materials. The study involved a large virgin aggregate, a PG64-22 virgin asphalt binder and a fine RAP aggregate, therefore upon separation, it was possible to distinguish between the virgin binder recovered from coarse aggregate and aged binder recovered from fine aggregate. Rheology and molecular weight distribution of the recovered binder from coarse and fine aggregate were determined using a Dynamic Shear Rheometer (DSR) based on master curves, and Gel Permeation Chromatography (GPC) based on large molecular size was conducted. Several conclusions were reported in this study. Firstly, mixing temperature has a higher impact on the level of blending that the effect of mixing time. It was reported that the blending ratio increased from 59% at 130°C to 70% at 180°C. Secondly, including warm additives had a positive effect on blending ratio: a 76% blending ratio was achieved using surfactant-based WMA produced at 130°C for 105s, which was equivalent to that of the control mixture, mixed at 160°C for 150s. It was also found that the wax-based WMA was the most workable mixture; therefore, a suggestion was made to investigate the effect of wax-based additives on the level of blending at higher temperatures. However, one can see some issues in this study in that the type of wax and surfactant are unknown. In addition, the effect of surfactant additives on the complex modulus of recovered fine and coarse binders was higher than the effect of wax on the complex modulus, which is different to the findings of all previous studies.

Diffusion of virgin asphalt binder into the recovered binder in RAP is further being investigated. It has been reported that the current AASHTO (American Association of State Highway and Transportation Officials) *M323* specification which recommends using one grade softer performance grade

asphalt at higher than 15% of RAP may not be justified. This fact has been exhibited by Kriz *et al.* (2014), who demonstrated that it is unnecessary to change the binder grade up to 25% of RAP. The ability of RAP binder to blend with virgin binder by diffusion mechanism was measured in a DSR and the results showed that complete binder blending in both HMA and WMA applications was reached a few minutes after mixing. A similar study was conducted by Rad *et al.* (2014). The rate of diffusion of virgin asphalt binder into the RAP binder was investigated using two layers of binder (1mm of virgin binder and 1mm of artificial RAP binder) tested in a 2mm gap of DSR. The DSR measurements, diffusion coefficient and Fick's law were used to estimate the diffusion rate of virgin binder into artificial RAP binder. It was reported that the rate of diffusion increased with increasing temperature as the viscosity of asphalt binder decreases at higher temperatures. More importantly, the chemical compositions of the asphalt binder had an effect on the rate of diffusion. Therefore, it is hypothesised that other factors rather than viscosity can have an effect on the rate of diffusion of virgin binder into RAP binder.

Mobilisation rate of recycled binder derivative from Gel Permeation Chromatography testing (GPC) was investigated by Zhao *et al.* (2015a). In that study, a laboratory procedure to quantify the rate at which aged binder could be mobilised and made available to coat aggregate was developed based on a new term called large molecular size percentage derived from GPC testing for recovered binder. The researchers reported the RAP binder mobilisation rate decreased with increase in the percentage of RAP. It was noticed the RAP binder mobilisation rate was close to 100% at low RAP mixtures (10% and 20%); however, as the RAP percentages increased from 30% to 80%, the rate of mobilisation decreased from 73% to 24%.

Based on the above information, one should note that the degree of blending between aged and virgin binders still needs to be further investigated. In fact, most studies investigating the level of blending have been based on the traditional mechanical properties or only the level of blending between aged and virgin binders, which does not rule out the black rock hypothesis or complete blending assumptions. Therefore, one of the main objectives of this study is to directly investigate the level of blending between RAP and virgin materials using

the advanced technology of nano-mechanical properties, as the author believes the sophisticated technology of nano-indentation can be practically adopted in order to characterise the mechanical properties of the interfacial zone between RAP materials and virgin binder with the advantages of including warm additives in order to gain more understanding about the level of interaction at the micro- and nano-scales.

2.6.3 WMA-RAP performance

2.6.3.1 Permanent deformation

The lower production temperature of WMA may adversely affect the rutting sensitivity of the asphalt mixture as the binder is less oxidised due to lower production temperature compared to that of HMA. However, this is not always the case in WMA as some warm technologies such as Sasobit can offset the reduced stiffness of the mixture. From an engineering point of view, adding stiffer materials such as RAP to the WMA resulted in stiffer asphalt mixtures regardless of whether it was completely mixed with virgin materials or considered as a black rock. Rheology studies (Lee *et al.* 2009,Kim *et al.* 2011b) have agreed that warm-modified binder including aged binder exhibited better rutting resistance, based on the elastic properties, creep recovery and repeated creep recovery testing, regardless of the type of warm additives.

The rheology investigations are in agreement with the performance of WMA-RAP. Despite the belief that the lower mixing temperature leads to less binder oxidisation, which makes the mixture prone to rutting issues, RAP significantly increases the rutting resistance of WMA regardless of the kind of warm technology, type of asphalt binder and aggregate (Doyle *et al.* 2011,Hill 2011,Wu *et al.* 2011,Zhao *et al.* 2013,El Sharkawy *et al.* 2016,Xiao *et al.* 2015). Surprisingly, the permanent deformation performance when including RAP with WMA is better than for HMA (Zhao *et al.* 2012). However, another study reported the inverse, and high RAP-WMA showed lower rutting resistance than low RAP-HMA (Zhao *et al.* 2013). Vargas-Nordcbeck and Timm (2012) also reported that the WMA technologies have a tendency to increase permanent deformation but the inclusion of high RAP results in fewer rutting issues. It was also added that, although the lower production temperature influenced the

magnitude of rutting depth, variation in the materials was found to be more significant than the lower temperature.

Consequently, it can be said that the permanent deformation of WMA-RAP mixtures may not be a major concern when it comes to the incorporation of RAP in practice.

2.6.3.2 Low-temperature properties and fatigue life

The current school of thought in the asphalt industry is that the lower manufacture temperature associated with reduced ageing in the asphalt binder in WMA mixtures allows additional headroom for the inclusion of higher percentages of RAP. However, more attention should be paid to the low-temperature properties and fatigue life of asphalt mixtures because the greater the RAP content, the more brittle materials are included in the mixture. Studies have revealed that the addition of RAP had no significant effect on the low-temperature properties compared to the influence on high-temperature properties, as the low-temperature grade only increased by approximately 3°C when adding up to 25% RAP, while using 50% RAP increased the low-temperature grade by 8°C (Doyle *et al.* 2011). Despite the RAP's lack of effect on low-temperature grade, it was found to slightly reduce the fatigue life of WMA, based on the results of Zhao *et al.* (2012), who investigated fatigue life based on the Superpave indirect tension test and beam fatigue test. The incorporation of RAP into the WMA led to lower fatigue life based on the results of the dissipated creep strain energy threshold ($DCSE_f$), whereas it appeared that WMA with a higher RAP content was able to tolerate more load cycles than the control HMA and HMA-RAP, according to the beam fatigue test. This study is in agreement with Xiao *et al.* (2015), who noticed that, although increasing the RAP binder concentration improved the rutting resistance, a reduction in the fatigue resistance was observed.

There is more concern about the structural characterisation and longer-term field performance. As part of an objective to characterise the performance of high RAP and WAM, the National Centre for Asphalt Technology (2009) constructed four sections including WMA with high RAP content (50%) and a control section without either technology. Each section was investigated based on

strain versus temperature at three reference temperatures (10, 20 and 43°C) Moreover, beam fatigue testing was carried out to investigate the fatigue transfer functions. It was indicated that, based on the combination of the laboratory-derived beam fatigue transfer functions with temperature-corrected strain responses, the WMA-RAP section would have the better performance at 20°C (Timm *et al.* 2011).

Hill *et al.* (2012a) evaluated the performance of WMA-RAP in terms of low-temperature cracking behaviour based on disc-shaped compact tension, indirect tension creep compliance and acoustic emission tests. All these tests correlated well and indicated that incorporating RAP led to a decrease in fracture energy and an increase in thermal cracking potential.

Based on the above studies, although the inclusion of brittle materials may negatively affect the low-temperature cracking performance, it seems the preference for WMA-RAP mixtures is still a point for discussion. More investigations regarding the performance of WMA-RAP in terms of fatigue resistance are required, taking into account other considerations such as the effect of warm additives and fabricated temperature.

2.6.3.3 Moisture damage

Stripping issues are the main problem associated with WMA, as the lower production temperature leads to incomplete drying of entrapped water in the aggregate, which subsequently weakens the interface and adhesive characteristics between the aggregate and the asphalt binder. In spite of some moisture damage issues being reported, particularly associated with foaming and some chemical technologies, RAP significantly increases moisture resistance (Doyle *et al.* 2011,Hill *et al.* 2012a); however, the percentage of RAP should be no more than 30%, based on the tensile strength ratio and resilient modulus ratio results, as the results did not diverge much when more than 30% RAP was used (Zhao *et al.* 2013). In fact, RAP has the ability to reduce moisture susceptibility, because the bond between aged asphalt and aggregate particles is greater than in the virgin asphalt binder–aggregate system.

2.7 Conclusion

1. Foam technology is more prone to moisture damage because of incomplete aggregate drying and the residue of incomplete water steaming. It has been reported that the addition of hydrated lime has the ability to increase the resistance of foam technology to moisture damage.

2. Chemical technology has the ability to emulsify the asphalt mixtures, resulting in increasing fracture resistance. Moreover, it can also increase the resistance to moisture damage because it contains anti-strip, which expels the residual moisture in the aggregate and provides an adequate bonding between the asphalt binder and the aggregate.

3. Some warm additives, such as Alpha-Min, are not suitable to long-haul distances, because this technology remarkably increases the viscosity of asphalt binder in comparison with the base binder after 60 to 90 minutes. This results in inadequate compaction of asphalt.

4. Sasobit significantly decrease the viscosity of asphalt binder at higher temperatures while remarkably increasing the viscosity at pavement service temperatures. This results in increasing the rutting resistance of asphalt mixtures while perhaps decreasing the low-thermal properties as the pavement will be more brittle. However, binder source and grade play an important role in determining the effect of Sasobit in decreasing production temperatures.

5. There is a need to investigate the fatigue resistance of asphalt binder and warm-modified binders using Time Sweep test in order to firstly estimate the effect of warm additives on the fatigue resistance of asphalt binder and then address other factors such as production temperatures on the fatigue performance of WMA.

6. Highway agencies are advised to specify the minimum production temperature for WMA to reach acceptable mixture stability in terms of rutting and fatigue performance, taking into account the binder source and grade.

7. Sasobit significantly increases rutting resistance of asphalt binder and mixtures regardless of binder source and type.

8. In terms of WMA field performance, there is a high demand to simulate the required aging time in the laboratory because in fact up to date no such problem concerning WMA moisture damage has been highlighted in the field.

9. The inclusion of RAP in WMA increases the moisture and rutting resistances of WMA whereas it may decrease the fatigue life and fracture resistance, especially in the organic technology case.

10. It should be mentioned that there is a high demand to evaluate the fatigue life and fracture resistance of WMA technologies with/without RAP because different methods of identifying those properties exhibit irreconcilable performances.

11. The level of interaction between RAP and virgin materials is still ambiguous. To date, the interaction between RAP and virgin materials has not been investigated at the nano-scale, which can practically reflect the real level of materials' interactions.

Chapter Three

Viscosity, Rheological Properties and Fatigue of Warm-Modified Bituminous Binders (WMBBs)

3.1 Introduction

In this chapter, the effect of warm additives on the viscosity of bitumen is investigated in detail using Brookfield Viscometer. Furthermore, the effect of these additives on the rheological properties of bitumen is also identified using a Dynamic Shear Rheometer (DSR). The investigation of rheological properties included the effect of these additives on the linear viscoelastic region using amplitude strain sweep and also their effect on the stiffness and phase angle of bitumen using frequency sweep. Furthermore, the fatigue performance of Warm-Modified Bituminous Binders (WMBBs) is investigated using time sweep test and data are modelled using the Viscoelastic Continuum Damage approach (VECD).

3.2 Materials

3.2.1 Binder grades

Two binder grades were used, namely 40/60 and 100/150, which are commonly used in the UK and are expected to have different response capacities. Table 3.1 shows the basic properties of the binders. Penetration and softening point were conducted based on (BS EN 1426 2007,BS EN 1427 2007) respectively.

Table 3.1 Properties of straight-run binders

Binder grade	Penetration 0.1mm	Softening point °C
40/60	45	54.3
100/150	104	43.0

3.2.2 Warm additives

Three warm additives were adopted: Sasobit, Rediset WMX and Rediset LQ as presented in Figure 3.1. They were supplied by their subsidiary companies, Naylor Chemicals Ltd, UK and AkzoNobel, Sweden. The recommended dosages of Sasobit, Rediset WMX and Rediset LQ are 2%, 2% and 0.5% by the weight of the bitumen respectively. Properties of warm additives are presented in Table 3.2.

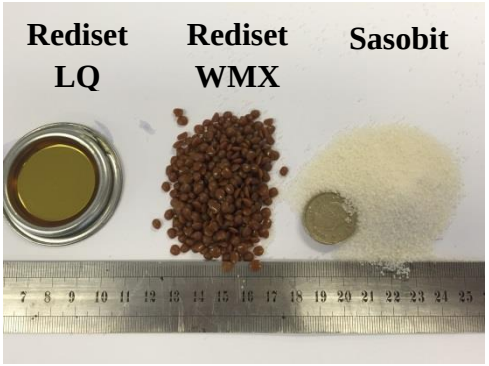

Figure 3.1 Warm additives

Table 3.2 Properties of warm additives

Properties	Rediset WMX	Rediset LQ	Sasobit
Form	Pastilles	Liquid	flakes
Colour	Light brown	Dark brown	Off-white
Odour	Ammoniacal	Slight	Practically odourless
pH	Not applicable	10 at 0.1 solution	Neutral
Melting point	80–95°C	-	Above 100°C
Boiling point	>100°C	215°C	-
Flash point	253°C	165°C (Pensky-Martens	285°C (ASTM D92)
Solubility in water	Practically insoluble	Partly soluble	Insoluble

3.3 Preparation of warm-modified bitumen

Sasobit, Rediset WMX and Rediset LQ were incorporated into the two binders in the study, namely 40/60 and 100/150 penetration grades. All warm additives were added at rates within specified manufacturers' tolerance. The recommended dosages for Sasobit, Rediset WMX and Rediset LQ which were adopted in this study are 2%, 2% and 0.5% by the weight of the bitumen respectively. However, the effect of different levels of warm additive dosages on viscosity was also investigated. The modified binders were prepared using the Silverson high shear mixer under controlled temperature, time and shear rate conditions, as shown in Figure 3.2.

It has been reported and recommended that Sasobit and Rediset do not need a high shear rate for mixing; therefore, the adopted shear rates for mixing and mixing time were 700 rpm and 5 minutes respectively, as adopted by some researchers (Xiao *et al.* 2012a). In addition, the mixing temperature for both hard binder 40/60 grade and soft binder 100/150 grade was 150°C. The asphalt binder was preheated in an oven to the selected mixing temperature while, during mixing, the mixing temperature was maintained using an iso-mantle heater in order to keep a uniform temperature to achieve consistent mixing; and the

container was also covered with an insulation mantel which was preheated to the required temperature, as can be seen in Figure 3.2. After mixing, the viscosities of the modified bituminous binders were measured directly while the mixing container was kept in the fridge at a temperature below 10°C to avoid the effect of ageing. Prior to rheological and fatigue testing, the virgin and modified binders were heated up using an oven maintained at 150°C. It should be noted that the binders were just heated up for a certain time to soften them to prevent ageing, and then they were stirred manually before being poured into a mould, as the received sample must be homogenised. For the rheological and fatigue tests, silicon moulds were then used to prepare samples for the amplitude sweep and fatigue tests. For brevity in this chapter, the binder grades of 40/60 and 100/150 are named H and S respectively, while the warm additives are named based on the first litter of the word: Sa, Rw and Rl for Sasobit, Rediset WMX and Rediset LQ respectively.

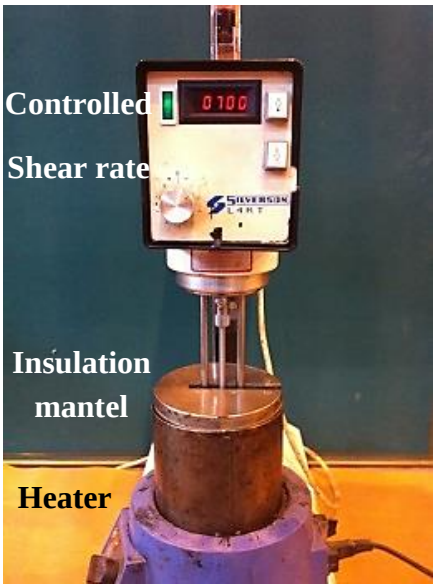

Figure 3.2 Silverson shear mixer

3.4 Viscosity

Physically, viscosity is defined as a measure of the internal friction of a fluid. In other words, it is used to identify the flow characteristics of asphalt binder in order to ensure that the binder can be adequately pumped and handled at the hot mixing facility. Therefore, viscosity measurements can be adopted to identify the possible production and compaction temperature of the asphalt binder so that the aggregate can be perfectly coated.

3.4.1 Viscosity measurements

3.4.1.1 Procedure

The maximum allowable torque was adopted (torque range between 30 and 100% (modified hard binder) and 10 and 100% (modified soft binder). Viscosity of modified asphalt binders was measured between 110 and 160°C at intervals of 10°C and the shear rates varied from 12 rpm to 100 rpm depending on temperature and warm additive contents. The recommended sample weight is 11.5 gm. The procedure followed the recommendation and standards of (BS EN 13302 2010). Two samples were measured for each control and WMBB at different dosages. Figure 3.3 shows the Brookfield Viscometer (Model LVD-I+) and its accessories.

In order to further investigate the effect of warm additives on flow behaviour of asphalt binders, three dosages were used for each warm additive, as illustrated in Table 3.3

Table 3.3 Different dosages of warm additives used in viscosity measurements

Additives	Dosage 1	Dosage 2	Dosage 3
Sasobit	2%*	3.5*	6%*
Rediset WMX	2%*	3.5%*	6%*
Rediset LQ	0.5%*	1%*	1.5%*

*** by weight of binder**

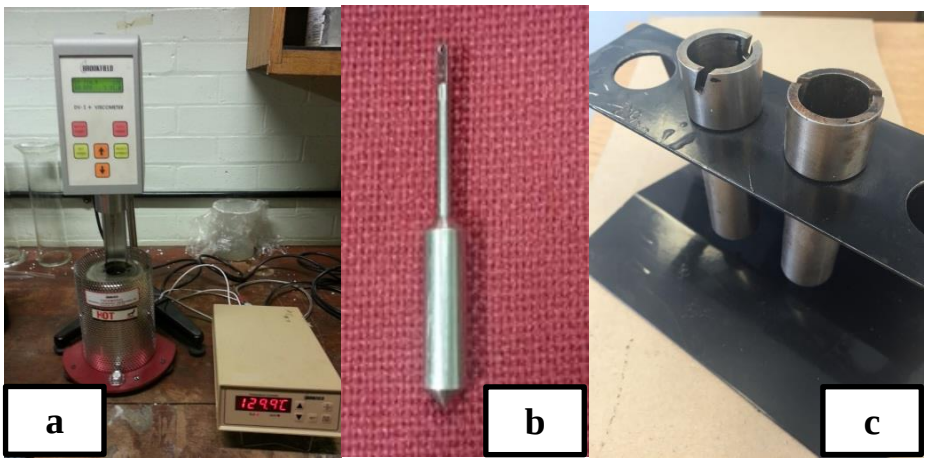

Figure 3.3 a- Brookfield Viscometer (Model LVD-I+), b- Viscometer spindle (SC-28), c- sample chamber (SC-13R)

3.4.2.2 Results and discussions

Based on the results of the viscosity measurements, Figure 3.4 shows that control binder 40/60 grade exhibited Newtonian flow behaviour at 135°C where the increase in the shear rate has no effect on the flow behaviour of the binder. As the warm additives were incorporated in this binder, Newtonian flow behaviour was not affected. It can therefore be concluded that the inclusion of Sasobit, Rediset WMX and Rediset LQ has no effect on the Newtonian flow behaviour of asphalt binder at higher temperatures. Furthermore, as expected, Sasobit and Rediset WMX slightly decreased the viscosity of the asphalt binder.

Figures 3.5 to 3.9 illustrate effect of different dosages of Sasobit, Rediset WMX and LQ on the viscosity of 40/60 binder and 100/150 binder. In fact, no significant change in binder viscosity by adding 2% Sasobit and 2% Rediset WMX was noticed. Sasobit and Rediset WMX did not decrease the mixing temperature significantly, as the maximum expected reduction was 4°C. As the amount of additives was increased, the associated viscosity of the modified binders decreased and the maximum temperature reductions of the asphalt modified by having 6% Sasobit and 6% Rediset binder added of 10°C and 12°C were possible for soft and hard binder respectively. In fact, the current results correspond with those of another study in which only a 14°C temperature reduction was obtained using Sasobit with a very soft binder (Silva *et al.* 2009) while Arega *et al.* (2011) highlighted that some warm additives involving Rediset WMX reduced the binder viscosity measured at 135°C with minor exceptions.

Rediset LQ has no effect on the viscosity of the virgin binder even when using up to 1.5% of this additive. In fact, Rediset LQ exhibits a different behaviour in decreasing the production and compaction temperature of asphalt mixtures.

It seems the real the production temperature of WMA cannot be directly predicted using a Brookfield Viscometer even with the inclusion of organic additives such as Sasobit or Rediset WMX.

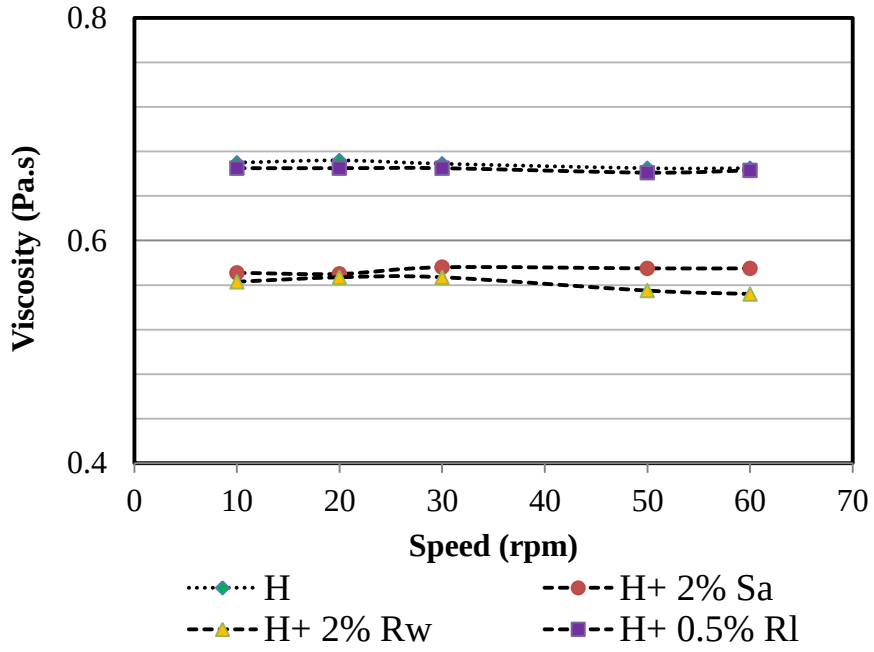

Figure 3.4 Effect of warm additives on the flow behaviour of 40/60 binder grade

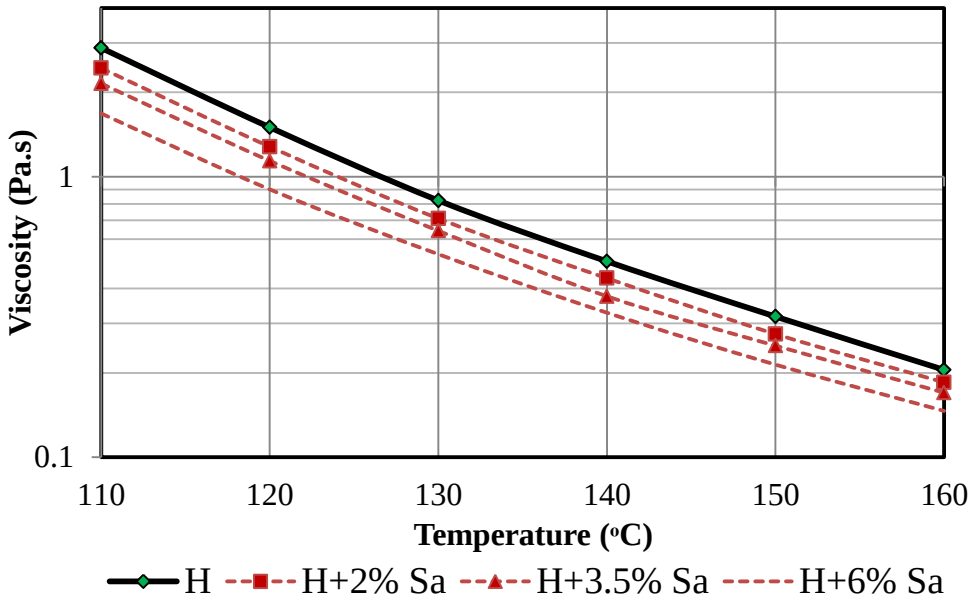

Figure 3.5 Effect of different dosages of Sasobit on the viscosity of 40/60 binder grade

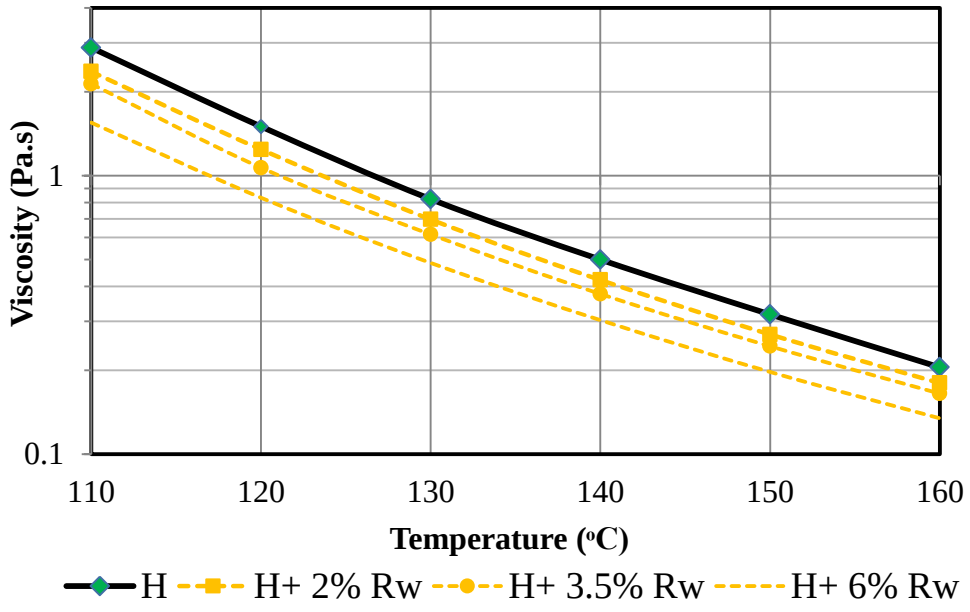

Figure 3.6 Effect of different dosages of Rediset WMX on the viscosity of 40/60 binder grade

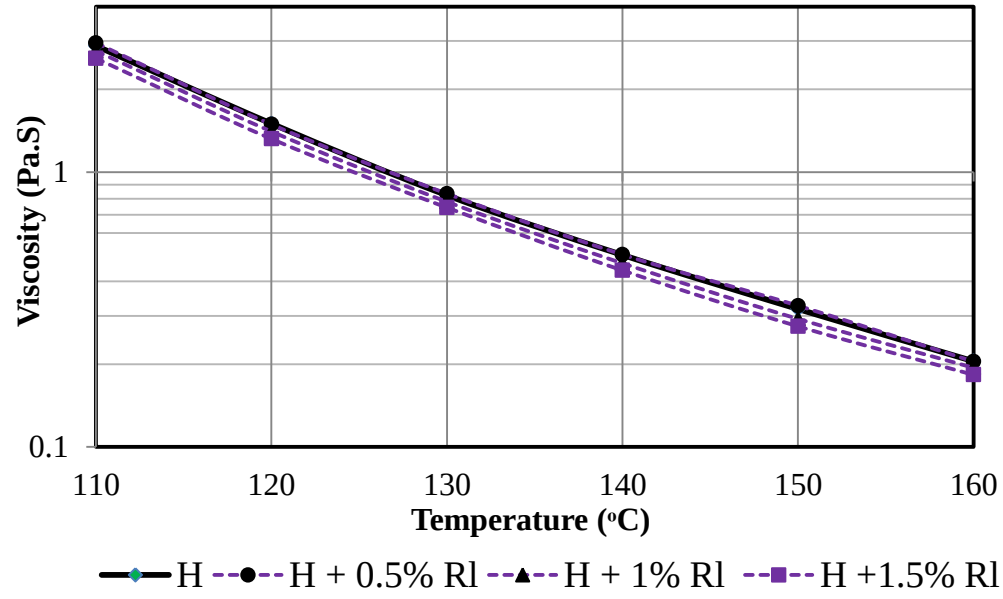

Figure 3.7 Effect of different dosages of Rediset LQ on the viscosity of 40/60 binder grade

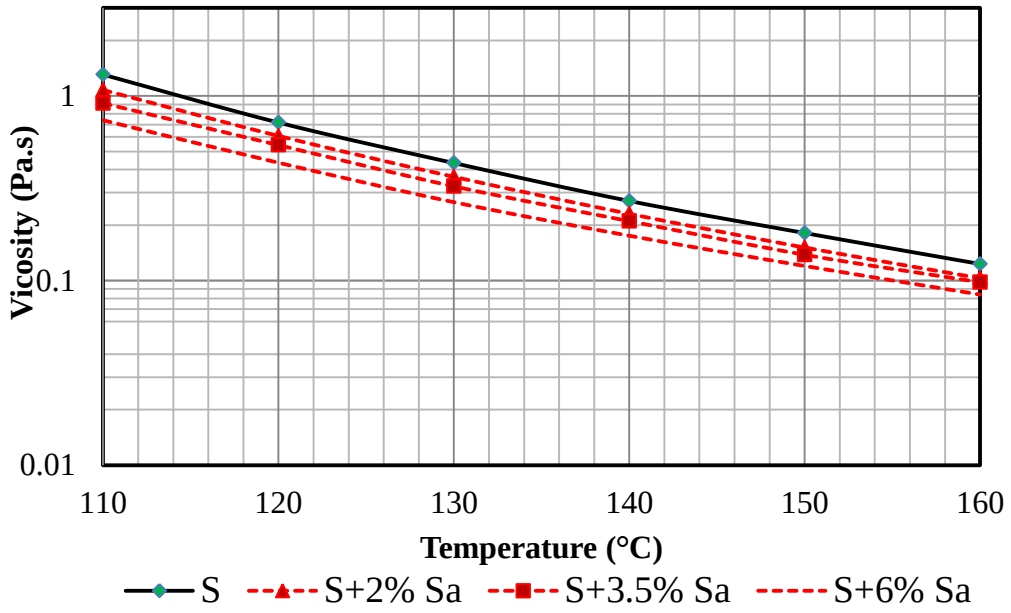

Figure 3.8 Effect of different dosages of Sasobit on the viscosity of 100/150 binder grade

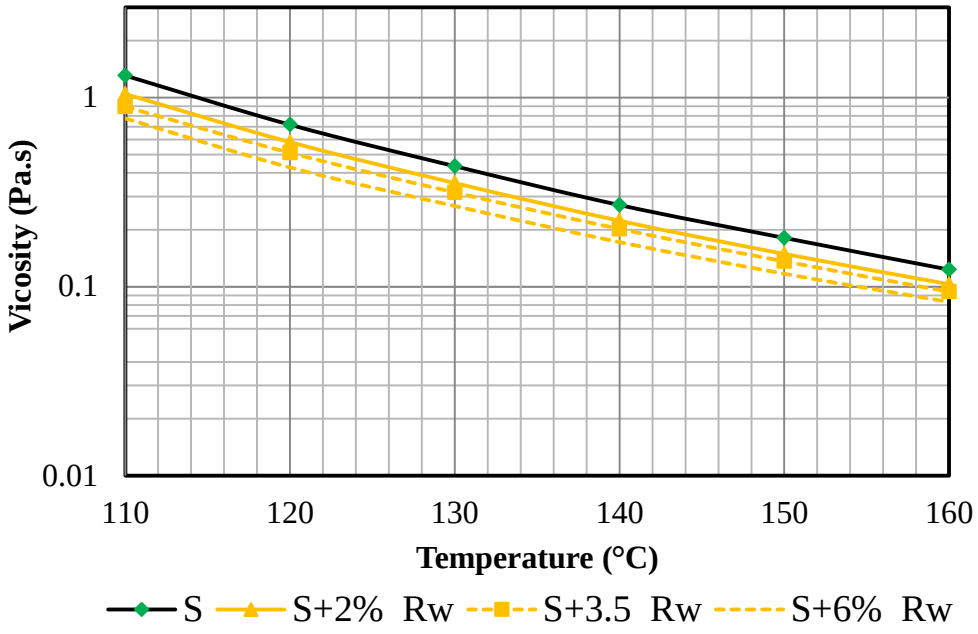

Figure 3.9 Effect of different dosages of Rediset WMX on the viscosity of 100/150 binder grade

3.5 Rheological properties

3.5.1 Dynamic viscoelastic functions

Rheological characteristics of bituminous material can be measured by means of dynamic mechanical analysis using an oscillator type, dynamic shear rheometer (DSR) tests. Historically, rheology is derived from the Greek words '$\rho\varepsilon\omega$', which is literally translated as 'to flow', and '$\lambda o\gamma o\sigma$' meaning 'word, science', which literally means 'the study of the flow' (Airey 2002). Therefore, rheology is a study of the flow properties of a material or provides indication of whether the material is deformed. The rheological properties can be identified by applying periodic strain or stress to a material sample to identify its viscoelastic behaviour. Generally, in the dynamic tests shear stress is usually applied as sinusoidal varying stress of constant amplitude and frequency. The resultant shear strain or deformation varies sinusoidally as well but its response lags behind the applied stress by the phase angle $\boldsymbol{\delta}$, as illustrated in Figure 3.10.

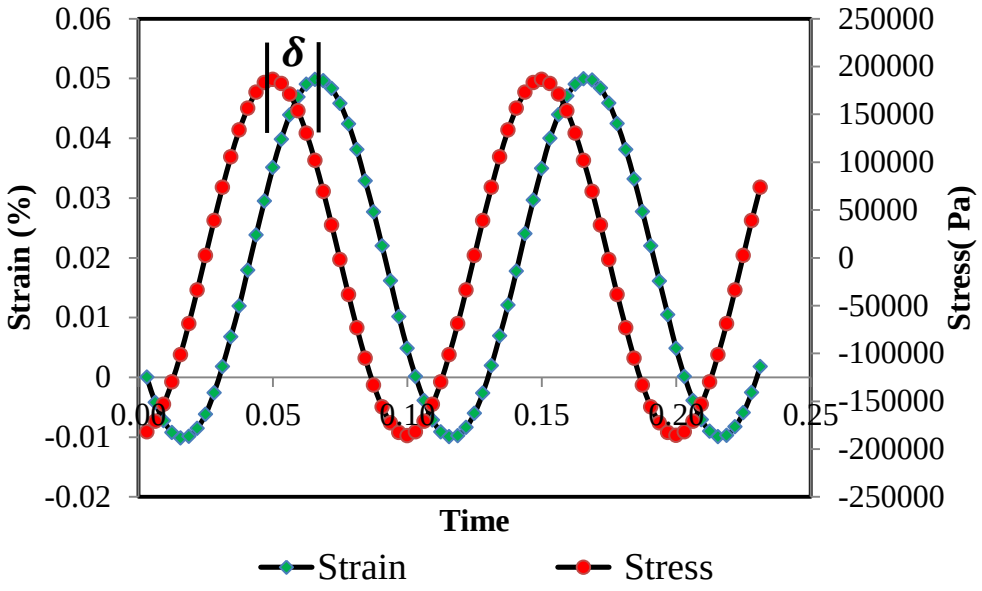

Figure 3.10 Typical shear stress and strain waveforms in a dynamic oscillatory test

As results of strain amplitude γ^{o} or stress amplitude σ^{o} amplitude, the sinusoidally varying strains and stress are given in the following equations:

$$\gamma = \gamma^{\circ}\sin(\omega t) \tag{3.1}$$

$$\sigma = \sigma^{\circ}\sin(\omega t + \delta) \tag{3.2}$$

Where ω is the angular frequency in radians/second and t is the time.

As illustrated schematically in Figure 3.11, the specimen under test with radius *r* and height *h* is held between two parallel plates. The bottom plate is fixed whilst the top plate is oscillated by applying a torque *M*. in the rheometer system; the angular rotation θ is recorded by an optical encoder system. Therefore, the shear stress and strain are calculated using equations 3.3 and 3.4:

$$\gamma^{\circ} = \theta r/h \tag{3.3}$$

$$\sigma^{\circ} = 2M/\pi r^{3} \tag{3.4}$$

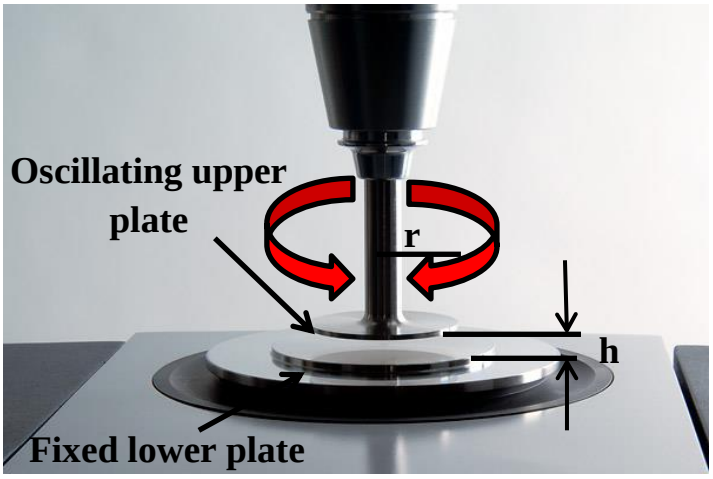

Figure 3.11 Schematic representation of oscillatory test

The most usually quoted quantities are known as the complex modulus (G^*)-complex modulus because it includes both an elastic and a viscous component-, and phase angle(δ).

The complex modus includes both the elastic modulus (G') and viscous modulus (G''). The complex modulus, which gives an idea about the stiffness of a material at a given temperature and loading time, is defined as the absolute magnitude of shear stress divided by the absolute magnitude of shear strain, disregarding any time lag between them as a result of viscous effects. The elastic modulus or storage modulus is the ratio of the amplitude of the in-phase component of stress to the strain amplitude, and also it describes the amount of energy stored and released in each oscillation. On the other hand, the viscous or loss modulus is the ratio of the amplitude of the out-phase stress component to the strain amplitude, describing the amount of dissipated energy rate as a result of viscous impact.

The viscoelastic character of a material is investigated using the phase angle(δ). In perfect elastic behaviour, the material would exhibit a phase angle equal to zero, whereas, in perfect viscous behaviour, the material would exhibit a phase angle equal to 90°. Between those phases, the material would exhibit viscoelastic behaviour; therefore, the phase angle varies between 0° to 90°, based on the conditions of the test temperature and frequency or loading time.

3.5.2 Dynamic shear rheometer (DSR)

Asphalt binder is classified as a rheological material. The stiffness of asphalt binders is time dependent and also temperature dependent; consequently, both the time of loading and temperature at loading must be considered when characterising its flow properties (Anderson *et al.* 1994). Viscoelastic properties can be identified quite easily nowadays using a dynamic shear rheometer (DSR). The Kinexus DSR as shown in Figure 3.12, which was developed by the Malvern Instrument Company, UK, has overcome the weaknesses of the previous generation of rheometers, combined with advances in shear and vertical (axial) testing, can provide a rotational rheometer platform with unprecedented dual-action capabilities (Malvern 2014)

Figure 3.12 Kinexus DSR Pro+

3.5.3 Sample preparation

WMBB preparation was explained in Section 3.3. As mentioned previously, prior to measuring the rheological properties of a WMBB, the sample's container was heated in an oven maintained at 150°C for a certain time in order to soften the bituminous binder. After that, it was stirred manually before being poured into a mould, as the received sample must be homogenised. Customised silicon moulds were then used to prepare the samples for rheological measurement and fatigue tests. Figure 3.13 illustrates the WMBB samples for different geometries, 8mm

and 25mm. It should be mentioned that sample preparation were performed based on (BS EN 14770 2012) using manufactured silicon moulds.

In all scenarios, in order to assure a good adhesion between the samples and the plate-spindle, 8mm or 25mm, the spindle was firstly lowered down to the associated plate until the gap between them is zero. It was then heated to 60°C. After that, the spindle was raised and the sample was moulded into the rheometer. In any scenario, the sample should start flowing to get adequate adhesion to both plates. Prior to testing, the gap was firstly decreased to 2.05 mm or 1.05 mm using an 8 mm base plate or 25 mm base plate respectively and then cooled down to 20°C. Then it was trimmed using a sharp unheated knife, because using a heated tool for trimming may deform the edges of the sample and result in inaccurate data. Afterwards, prior to testing, the gap was decreased to exactly the required setting.

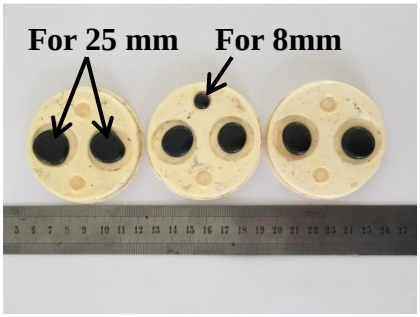

Figure 3.13 WMBBs samples for different geometries, 8mm and 25mm

3.5.4 Linear viscoelastic performance of warm modified bitumen/ Amplitude Sweep Strain

Linear viscoelastic region is defined as a linear viscoelastic representation of the flow properties of the asphalt binder where the modulus is independent of stress or strain. The investigation can be performed by applying a varying (increasing) strain to the sample and observing the resulting stress or modulus (Anderson *et al.* 1994). It has been defined that the linear viscoelastic region limit is the point at which the modulus decreased to 95% of the initial modulus (Anderson *et al.* 1994,BS EN 14770 2012). Linear viscoelastic region was performed as following:

- For modified hard binder 40/60 grade (H), amplitude sweep strain at strain ranged from 0.005-10% at three levels of frequency: 10, 1 and 0.1 at 25°C. Three samples were tested at each frequency.
- For modified soft binder 100/150 grade (S), amplitude sweep strain at strain ranged from 0.005-20% at three levels of frequency: 10, 1 and 0.1 at 25°C. Three samples were tested at each frequency. Results at frequency 10Hz were only presented for brevity.

At a temperature of 25°C, asphalt binder exhibits both elastic and viscous behaviour; it was therefore decided that this temperature be adopted to perform the test. However, other researchers may select a range of temperatures to determine the limit of linear viscoelastic region. Figures 3.14 and 3.15 show the complex modulus versus strain results for the virgin binders and warm-modified binders at 25°C and 10 Hz. Similar plots were obtained at different frequencies but are not shown here for brevity. Based on the complex modulus versus strain plots, the linearity limits and the linear viscoelastic region were determined for each of the unmodified and modified binders.

Sasobit significantly increased the binder stiffness and reduced the limit of linear viscoelastic region. It was found that Sasobit increased the binder stiffness by approximately 50% and 70% for hard and soft binders respectively, whereas minor effects can be reported for the Rediset WMX and LQ. Furthermore, as presented in Figures 3.16 and 3.17, Sasobit increased the elastic behaviour of the asphalt binder. It was noticed that the phase angle of Sasobit-WMBB decreased by approximately 5°.

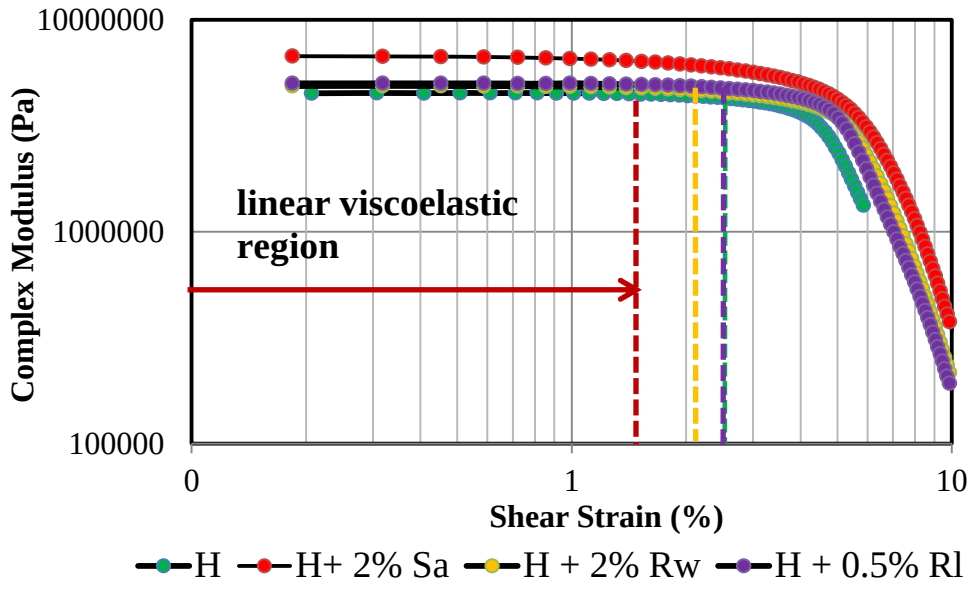

Figure 3.14 Average complex shear modulus against shear strain measured at 10Hz and 25°C for WMBB with 40/60 binder grade.

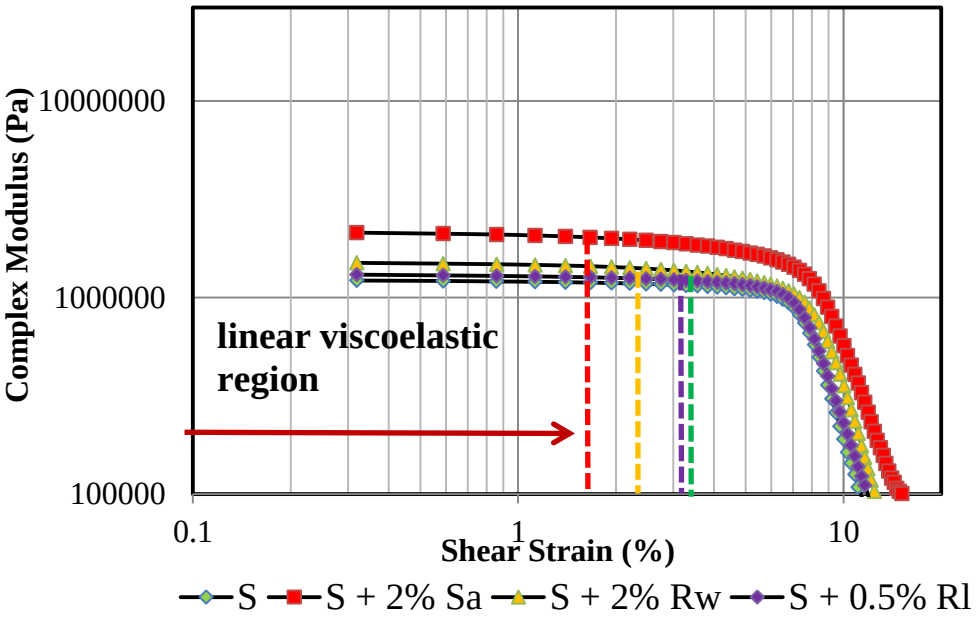

Figure 3.15 Average complex shear modulus against shear strain measured at 10Hz and 25°C for WMBB with 100/150 binder grade

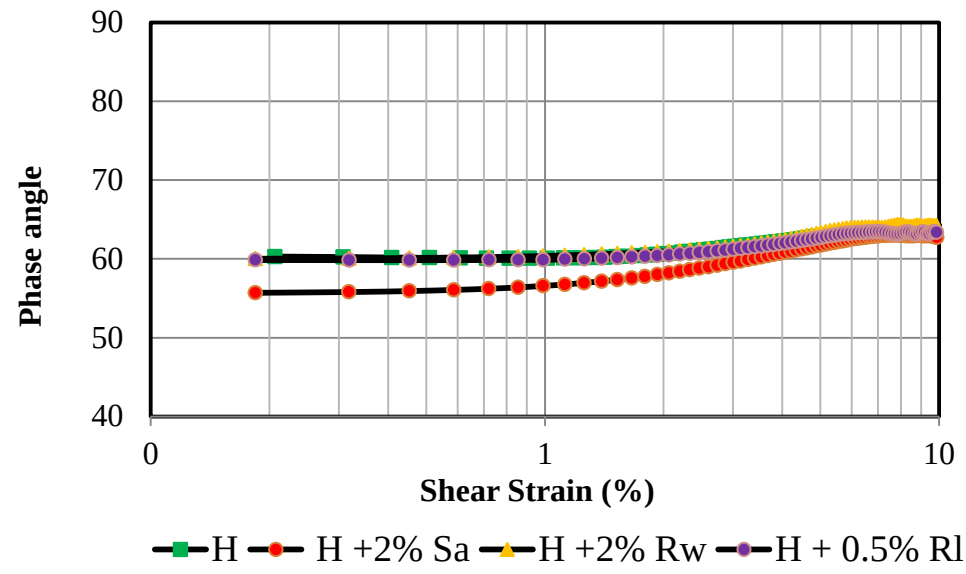

Figure 3.16 Average phase angle against complex shear strain at 10Hz and 25°C for WMBB with 40/60 binder grade.

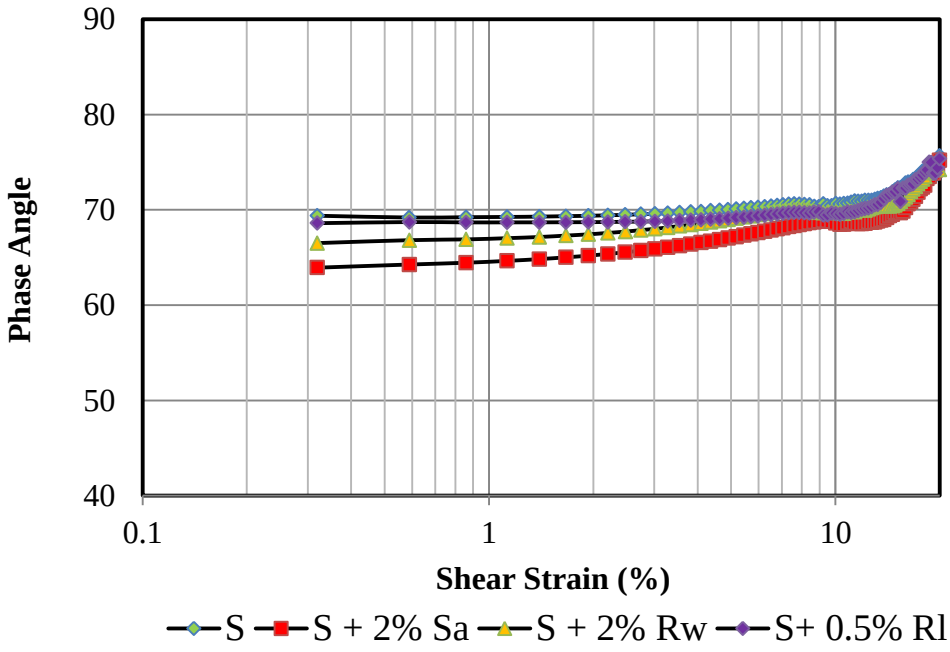

Figure 3.17 Average phase angle against complex shear strain at 10Hz and 25°C for WMBB with 100/150 binder grade.

3.5.5 Rheological properties of asphalt binder from frequency sweep tests

The frequency sweep tests were performed under controlled strain and frequencies between 0.1 to 10 Hz were adopted over a temperature range between 0°C and 60°C at intervals of 10°C and two samples were tested for each condition. All the frequency sweep testing was performed at strains well below the linear limit to ensure linear viscoelastic response behaviour during the dynamic test. In addition, the overall frequency sweep tests were run with a plate 8 mm in diameter with a 2 mm gap and a plate of 25 mm with 1 mm gap. In order to achieve consistency in rheological data, a black diagram was plotted for each virgin and modified binder. Plate geometries associated with the temperatures were as following:

- For 8 mm/2 mm (0°C 10°C, 20°C and 30°C).
- For 25 mm/1 mm (30°C, 40°C, 50°C and 60°C).

3.5.5.1 Black diagram

A black diagram of complex modulus versus phase angle can be used to identify the real rheological characteristics of bituminous binder (Airey 2002). As explained above, different temperatures and setting diameters and gaps were adopted. In linear viscoelastic, a smooth single curve should result when the phase angle is plotted against the complex shear modulus. Data presented in the black diagram show the smooth single curve of the phase angle against the complex shear modulus, which approaches a horizontal asymptote at high temperatures and low frequencies, as the asphalt binder tends to behave as a Newtonian fluid. However, at low temperatures and high frequencies, the phase angle decreases and complex stiffness increases, so the behaviour of materials becomes elastic (Artamendi 2003).

Before constructing a time-temperature superposition master curve, the sweep frequency data should be examined using a black diagram in order to report the real behaviour of virgin and WMBB binders, to ensure that type of geometry does not affect the rheological properties of tested materials in certain conditions.

It can be noticed in Figure 3.18 that at 30°C the tests run with different geometries did not yield the same results. Using an 8 mm plate with 2 mm gap

setting did not provide a smooth single curve of complex modulus versus phase angle for 40/60 virgin binder. It is therefore decided that frequency sweep data at 30°C with 8 mm/2mm is not considered to construct the master curve. This issue in fact was noticed for all modified warm additives and so sweep frequency with 8 mm/2 mm was eliminated at a temperature of 30°C. All data used to construct the master curves in Section 3.5.5.2 were firstly plotted in black diagrams, as explained previously.

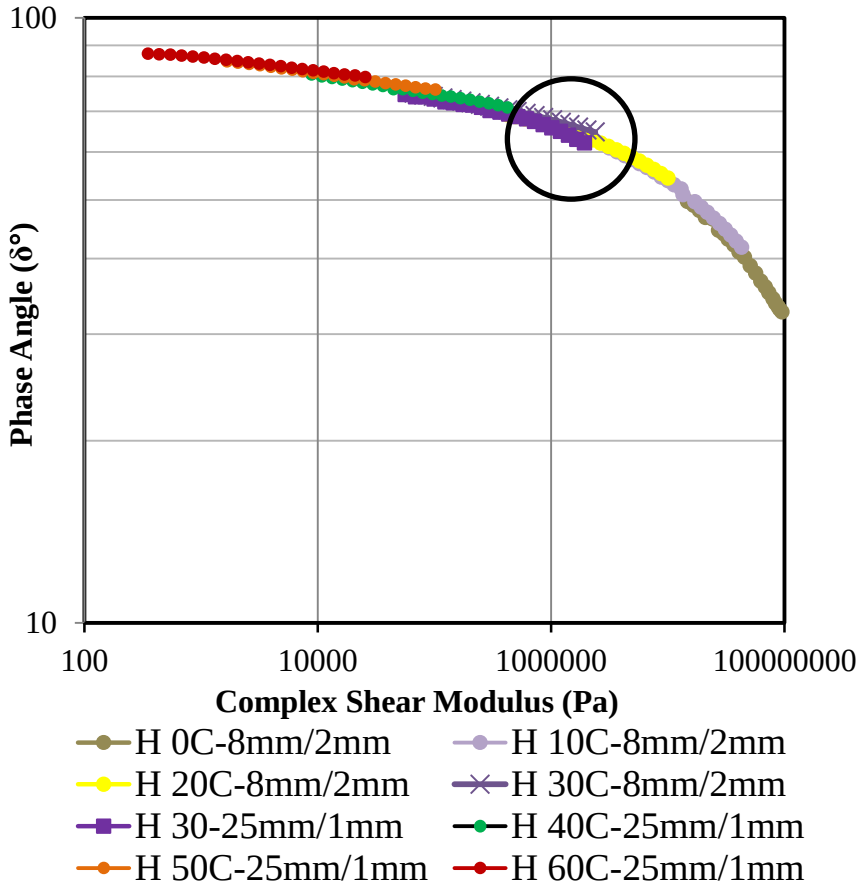

Figure 3.18 Black diagram of 40/60 binder grade

3.5.5.2 Master curves

3.5.5.2.1 Master curves of WMBB at recommended dosages

Generally, asphalt binder and bituminous mixture stiffness should be evaluated in order to identify both the load-induced and thermal stress and stain distribution in an asphalt pavement structure (Medani and Huurman 2003). The stiffness modulus of asphalt binder, which is an indicator of the stiffness or resistance of the asphalt binder to deformation under load, typically increases with increasing

loading frequency and decreasing temperature. The master curve can typically be constructed by shifting the stiffness modulus versus frequency for various temperatures horizontally to the reference temperature, which could be chosen arbitrarily. In the current study and as previously mentioned, the sweep frequency were performed at the temperature range with two samples for each test in order to construct a master curve at reference temperature 20°C. rSpace for Kinexus software version 1.6 was used to construct the master curves that can be seen in Figures 3.19 to 3.22.

It can be observed that Sasobit modified binders have higher complex modulus and exhibit a slightly lower phase angle in terms of various frequencies, and thus result in a higher rutting resistance while Rediset WMA and LQ had only minor effects. In fact, Sasobit increased the binder stiffness by approximately 30% at 0°C and 200% at 60°C while it decreased the phase angle by 12% at 0°C and 8% at 60°C. The addition of Sasobit has made the asphalt binder stiffer, despite the fact that the inclusion of recycled binder in such warm additives will increase rutting resistance; it may also make the binder more prone to cracking and fatigue failure due to decreasing the binder's ductility. This issue has been investigated in detail later.

Rediset LQ had no effect on the viscoelastic character of asphalt materials. It was expected that Rediset LQ would not alter the binder properties at recommended dosages but, as Rediset WMX is a combination of the surfactant (surface active agent) and organic additives, the organic part seemed responsible for slightly decreasing the phase angle and increasing the complex shear modulus, especially at higher temperatures and low frequencies.

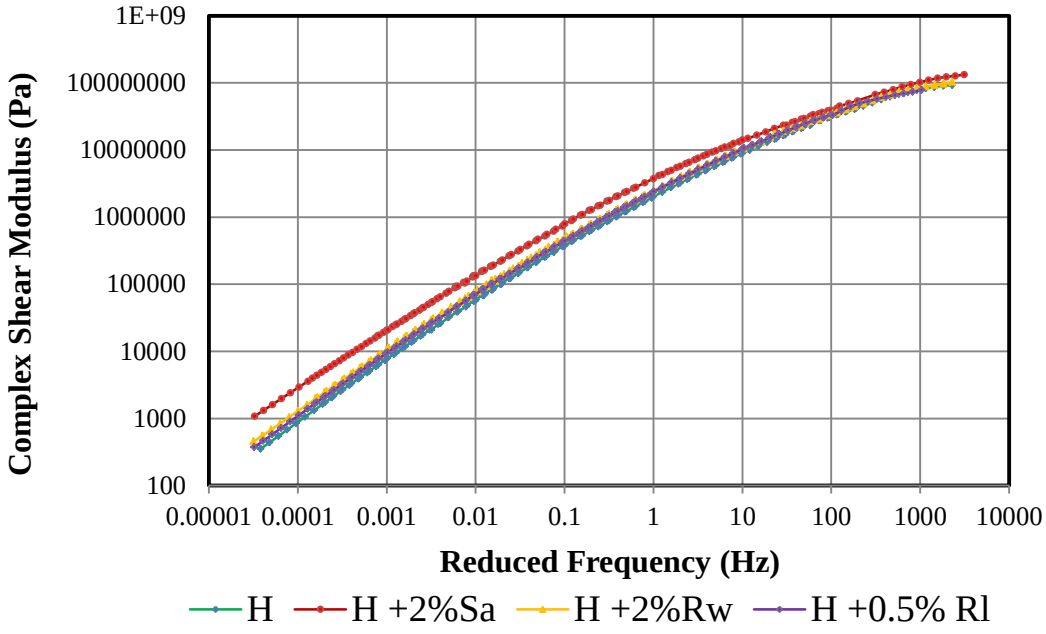

Figure 3.19 Master curves (complex shear modulus Vs. frequency) of hard-WMBB

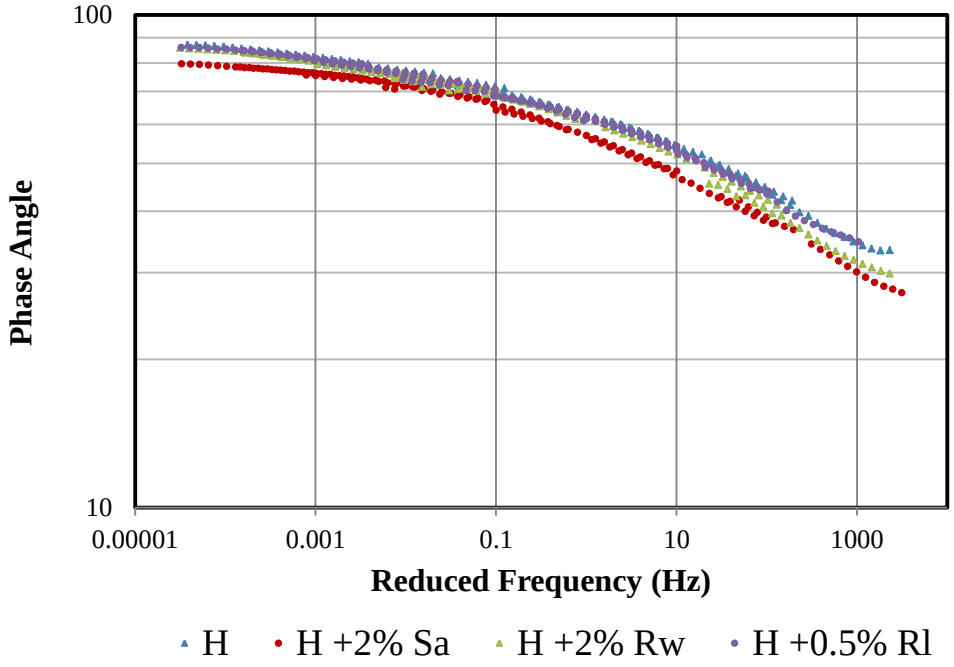

Figure 3.20 Master curves (phase angle Vs. frequency) of hard-WMBB

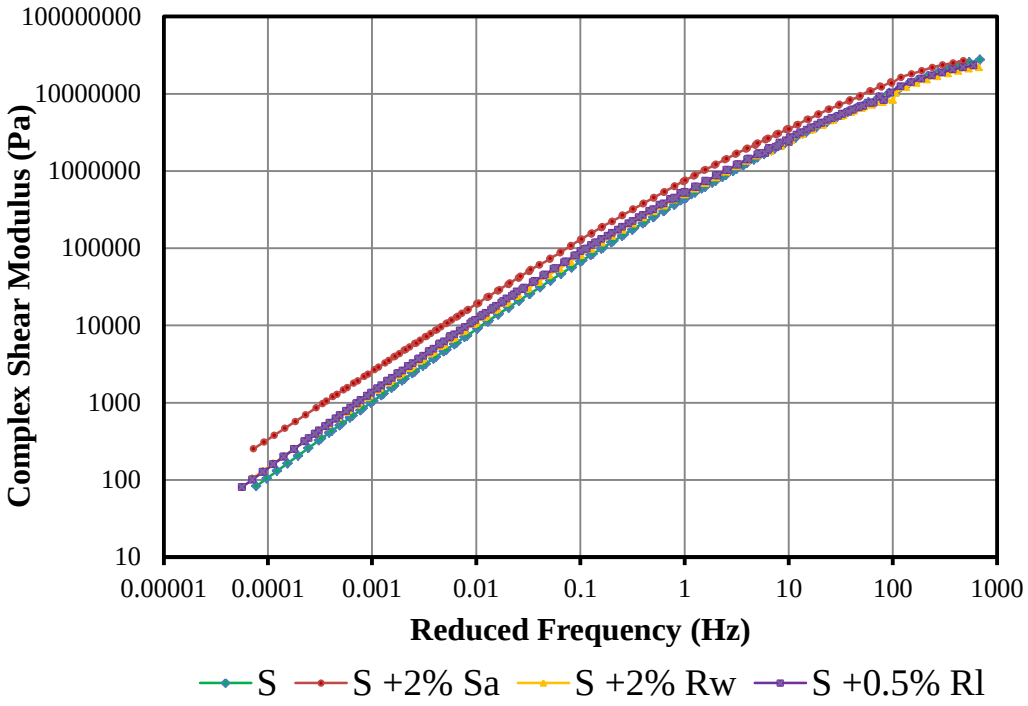

Figure 3.21 Master curves (complex shear modulus Vs. frequency) of soft-WMBB

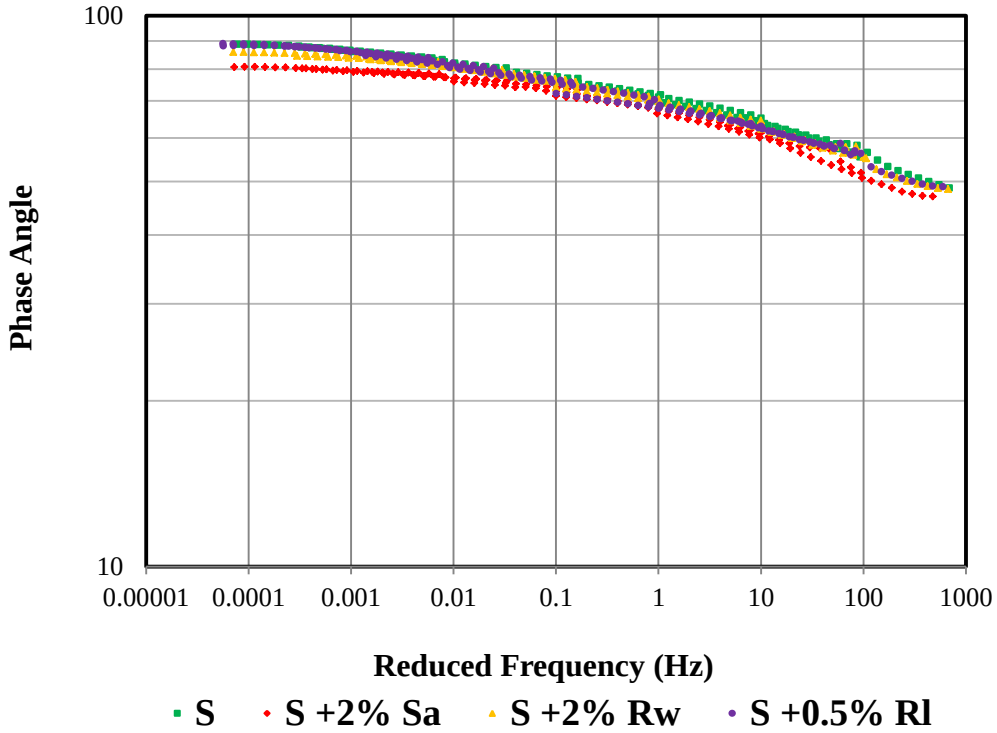

Figure 3.22 Master curves (phase angle Vs. frequency) of soft-WMBB

3.5.5.2.2 Master curves of WMBB at different levels of dosage

Figures 3.23 to 3.25 show the effect of Sasobit, Rediset WMX and Rediset LQ on the complex modulus of 40/60 binder grade tested in a temperature range from 0°C to 60°C at intervals of 10°C. The master curves were also constructed at a reference temperature of 20°C. including more than 2% of Sasobit significantly increased the binder stiffness. However, it should be noted that the effect of 3.5% of Sasobit is the same as 2% at lower temperature and high frequencies. It seems therefore that 3.5% of Sasobit increases the rutting resistance of asphalt binder but it may give the same performance as adding 2% of Sasobit in terms of fatigue cracking. Furthermore, although including 6% of Sasobit can sharply increase the rutting resistance, there will definitely be a fatigue problem, as the binder will be very stiff. This is, in fact, in agreement with (Edwards and Isacsson 2002).

Rediset WMX seems to follow the same trend as Sasobit but with less effect. As presented in Figure 3.24, Rediset WMX increases the complex modulus slightly at recommended dosages. As the dosages of Rediset WMX were increased, the complex modules also increased. However, it can be seen that, even at 6% of Rediset WMX, the complex moduli of all the modified binders were approximately the same. In conclusion, it can be recommended that higher than the recommended dosages of Rediset WMX, 3.5% or 6%, can be used in order to improve the permeant deformation of asphalt binders without perhaps adversely affecting the low temperatures properties.

Interestingly, higher dosages of Rediset LQ can be utilised to improve adhesion characteristics and wettability of asphalt mixtures without any negative impact on the mechanical properties of asphalt binder. In fact, strong bonds between aggregate and binder should result in better performance of asphalt mixtures in terms of rutting and fatigue cracking. Figure 3.25 supports the fact that it is possible to increase the dosage of Rediset LQ but the final conclusion can be made if the advantages of increasing the Rediset LQ dosage outweigh the cost of incorporating a higher dosage. This point needs to be further addressed in future work.

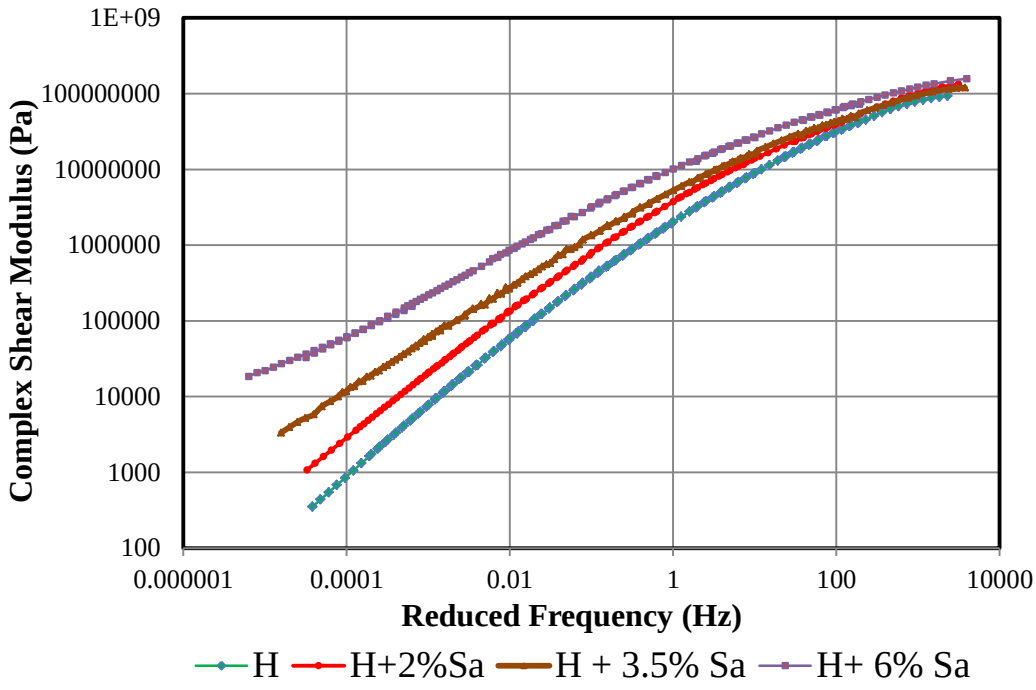

Figure 3. 23 Effect of different dosages of Sasobit on the complex modulus of 40/60 binder grade

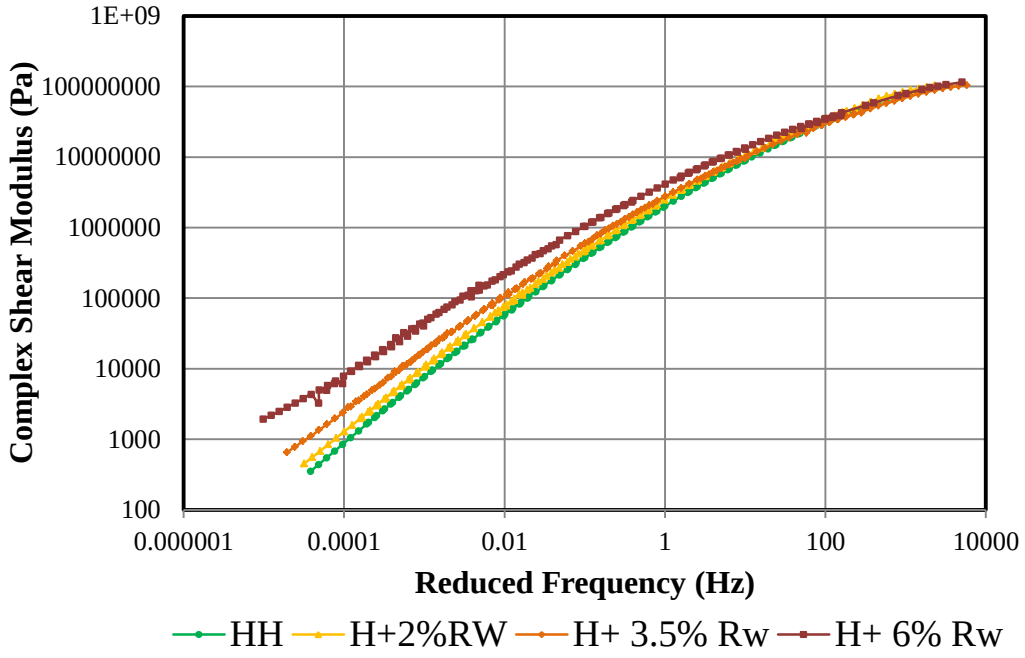

Figure 3. 24 Effect of different dosages of Rediset WMX on the complex modulus of 40/60 binder grade

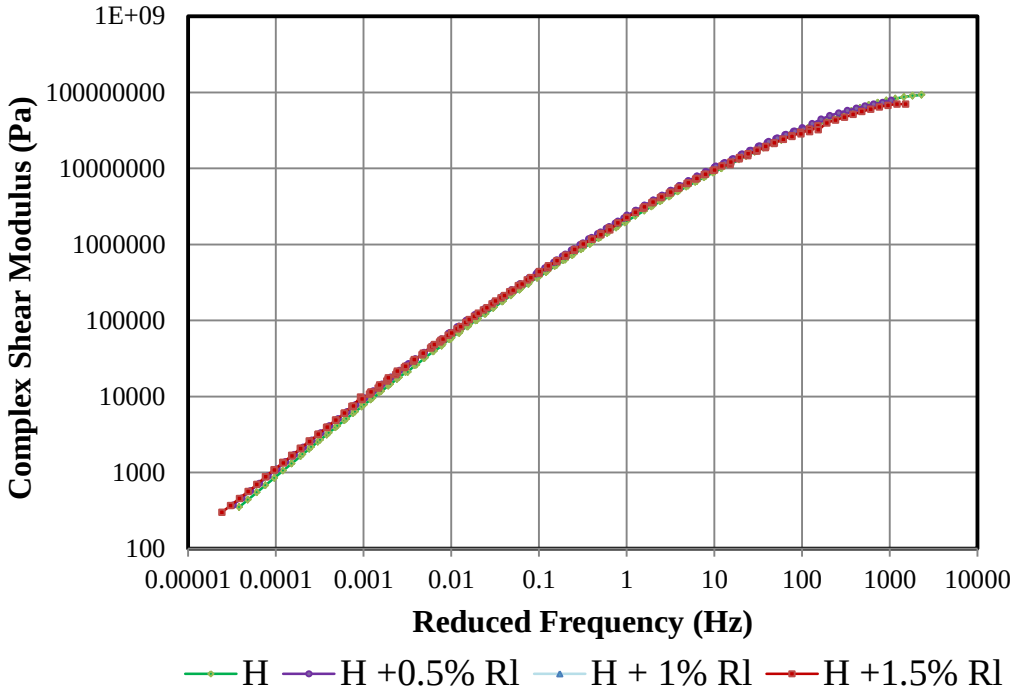

Figure 3. 25 Effect of different dosages of Rediset LQ on the complex modulus of 40/60 binder grade

3.6 Fatigue performance of WMBBs

It has been reported that binder influences asphalt distress by approximately 40, 60 and 90% in terms of rutting, fatigue and low temperature cracking respectively (Partl *et al.* 2013). In fact, fatigue is one of the main types of asphalt pavement deterioration. In reality, fatigue life is defined as the number of standard axles passing until mechanical failure while, in the laboratory, it is defined as the number of stress or strain cycles to failure of a sample predicted by fatigue criteria.

Many pavement engineers have questioned and investigated the fatigue performance of asphalt materials based on Superpave fatigue factor ($G^* Sin\delta$) (Zhou *et al.* 2012,Deacon *et al.* 1997,Tsai and Monismith 2005). In fact, this approach lacks the ability to characterise the actual damage and deterioration of bituminous binder (Hamzah *et al.* 2015) because it is measured under conditions that are relatively different from the rather complicated fatigue phenomenon, which features many more cycles of loading and fatigue damage. Therefore, to address and investigate the real fatigue resistance of bituminous binder, this study

adopts a time sweep test method to study this phenomenon under controlled stress mode using a DSR.

3.6.1 Determination of controlled stress value

The stress level for the experimental work was chosen from the results of the amplitude sweep stress test used in establishing the linear viscoelastic limits of the materials. According to the Strategic Highway Research Program (SHRP), linear viscoelastic region is defined as a linear viscoelastic representation of the flow properties of the asphalt binder where the modulus is independent of stress or strain. The investigation can be performed by applying a varying (increasing) strain to the sample and observing the resulting stress or modulus (Anderson *et al.* 1994). It was defined that the linear viscoelastic region limit is the point at which the modulus decreased to 95% of the initial modulus (Anderson *et al.* 1994).

However, in order to shorten the fatigue test testing time, a single stress level for each of the 40/60 and 100/150 binder grades was chosen after the linear viscoelastic region. Two samples were tested for each scenario. Figure 3.26 illustrates sweep stress results of the average of two samples for the 100/150 and 40/60 binder grades. It should be mentioned that sweep stress was only conducted on virgin binders and then the selected stress values were implemented on the WMBBs so that comparison could be made with the control binder. Table 3.4 shows the controlled stress values used in the fatigue tests.

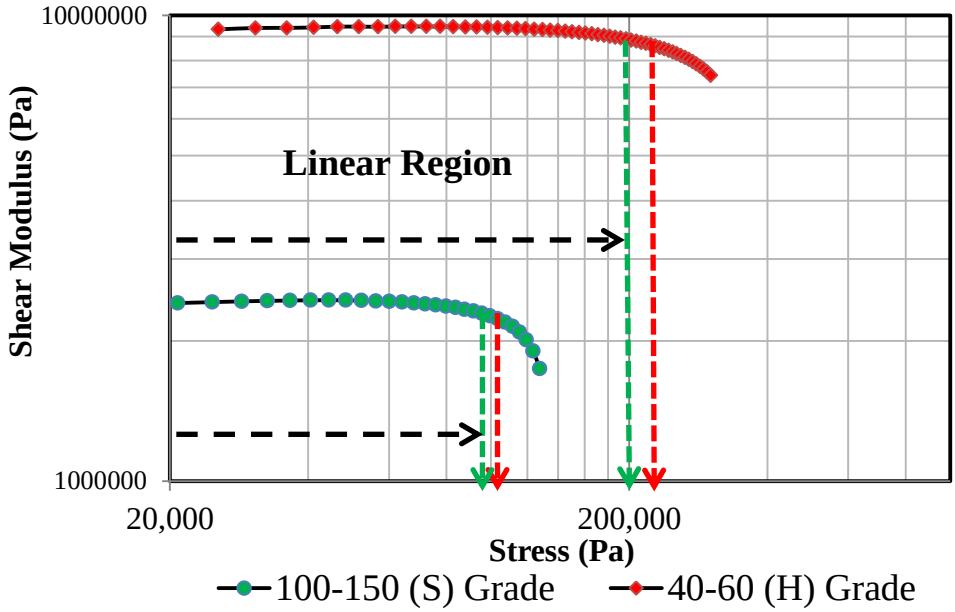

Figure 3.26 Sweep stress for the 100/150 and 40/60 binder grades

Table 3.4 Stress and strain values used in fatigue tests

Binder Grade	Stress Value (Pa)
40-60 (H)	235000
100-150 (S)	100000

3.6.2 Fatigue tests

A DSR time sweep was conducted with the 8 mm plate-plate set-up as presented in Figure 3.27. All tests were conducted at a frequency of 10 Hz, using 2 mm gap settings, and the test temperature was 20°C. It should also be noted that the fatigue test was carried out until complete failure occurs. In the fatigue test, three samples of each control binder and WMBBs were tested and the results presented in this study are the average of the samples.

Previous researchers have recommended conducting fatigue tests using a DSR at relatively low temperatures in order to minimise the edge effect of the sample, as a heterogeneous flow may accrue at high temperatures. In fact, the sophisticated Kinexus DSR has the ability to overcome this issue because of

machine capacity. This DSR incorporated a controlled hood temperature, which keeps a uniform temperature during the test.

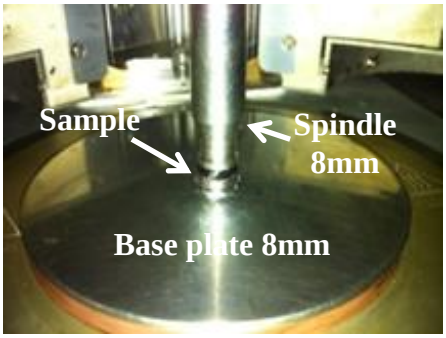

Figure 3.27 Loaded a bitumen sample between plates

3.6.3 Analyses of fatigue performance

3.6.3.1 Traditional approach

The traditional criterion, which is the commonly used and acknowledged fatigue criterion for asphalt binder and a mixture, is defined as a reduction in stiffness modulus of the material. In controlled strain mode, fatigue failure is defined as the number of cycles until the stiffness modulus decreases to 50% of its initial value (Kim *et al.* 2003,Hicks *et al.* 1993,Williams 1998); whereas, in the controlled stress mode, it is defined as a reduction of stiffness modulus of the sample to 10% of its initial value (Artamendi and Khalid 2005) or a complete fracture of the sample (Ghuzlan and Carpenter 2006). Reduction of stiffness modulus to 10% of initial value was adopted in this study.

3.6.3.2 Energy ratio

Once the load is applied to the material, the resulting stress will induce strain and the area under the strain-stress curve can be used to calculate the amount of energy being input into the material. In perfect elastic materials, all the energy being input into the material is recovered during unloading. In contrast, for viscoelastic material, not all the applied energy can be recovered; therefore, in this case, a retained part of the energy is related to mechanical fatigue of the material and can therefore be interpreted as dissipated energy.

In this regard, Van Dijk proposed an approach related to the dissipated energy to characterise the fatigue performance of asphalt mixtures (Van Dijk 1975).

Generally, in the fatigue process two stages are distinguished: initiation of micro-cracks and propagation of micro- and macro-cracks leading to specimen and material failure. In both stages some energy is dissipated during a single load cycle and can be calculated as explained in equation 3.5:

$$W_n = \pi \cdot \sigma_n \cdot \varepsilon_n \cdot \sin\theta_n \quad (3.5)$$

Where: n = cycle number; ε = strain amplitude; σ = stress amplitude; θ= phase angle.

Based on this concept and Van Dijk's work, Hopman proposed the use of an Energy Ratio to define the number of cycles (N_1) in a controlled strain mode to a point where cracks are considered to initiate (Hopman *et al.* 1989), which is calculated as equation 3.6:

$$R_i = \frac{n.w_0}{w_i} \quad (3.6)$$

Where: n number of load cycles, w_0 dissipated energy at the first cycle, and w_i dissipated energy at the *i*-cycle

However, in 1993, Rowe and Bouldin simplified the equation proposed by Hopman to identify the number of cycles (N_1) when cracks are conceded to initiate; more accurately it is a point where the micro-cracks coalesce to form a sharp crack (Rowe and Bouldin 2000).

In controlled strain mode, the energy ratio equation can be written as following:

$$R_i^{\varepsilon} = \frac{n}{E_i^*} \quad (3.7)$$

Where R_i^{ε} is Energy Ratio at controlled strain mode, and E_i^* is the complex modulus at the *i*-cycle.

N_1 can be defined in this mode as the point at which the slope of the dissipated energy ratio as a function of load cycles diverts from a straight line,

whereas, for the controlled stress mode, N_1 corresponds to the peak value when the Energy Ratio is plotted against number of load cycle and the simplified energy ratio equation is:

$$R_i^{\sigma} = n.E_i^* \quad (3.8)$$

Where R_i^{σ} is the Energy Ratio at controlled stress mode.

3.6.4 Results and discussion

The degradation in the material integrity due to fatigue is evaluated using several approaches. As mentioned previously, both the traditional approach and the energy approach were adopted. In the traditional approach, the normalised stiffness modulus and phase angles are plotted against number of cycles; and, in controlled stress, fatigue life is evaluated as the number of cycles until the stiffness modulus is reduced to 10% of the initial stiffness value.

Figures 3.28 to 3.31 present the fatigue life of WMBBs incorporating two binder grades, 40/60 and 100/150. An example of failure points (N*f* and N*1*) are given in Figures 3.28 and 3.30 respectively. It was found that Sasobit significantly increases the fatigue life of asphalt binder regardless of binder grade. This trend is not equivalent to that found by other researchers, who reported that Sasobit has lower *m*-value, which may negatively affect the fatigue life of bituminous binder. Therefore, direct fatigue tests of bituminous binder and modified binder can accurately rank their performance rather than using a bending beam rheometer test for the bituminous binder. Although rheological investigations indicated that Sasobit increases binder stiffness and slightly decreases phase angle, this does not mean it has lower fatigue life because, as mentioned previously, the interaction between Sasobit and asphalt binder is only physical but the increase in binder stiffness is because it enlarges the bee-like structures of bitumen (Menapace *et al.* 2014). In fact, Sasobit leads to stiffening of the binder in a similar manner to fibre-reinforced materials (Jamshidi *et al.* 2013) that prevent the molecules from moving. As presented in Figures 3.34 and 3.35, Sasobit decreased the initial phase angle and increased the initial shear modulus; therefore, it improves the elastic behaviour of asphalt binders, which in turn extends their fatigue life.

It can be confirmed that Rediset WMX potentially improves the fatigue life of asphalt binder. This, in fact, is because of the chemical structure of this additive. Rediset WMX is an organic-chemical: it is carbon-based with a paraffin wax and hydrocarbon wax concentration between 0 and 20%, which is thought to enhance the stress characterisations of bituminous asphalt. However, it should be noted that the improvement in the fatigue life of asphalt binders due to inclusion of Rediset WMX is not as significant as for Sasobit, because it slightly decreased the phase angle and increased the shear modulus, as illustrated in Figures 3.34 and 3.35.

Despite the superior performance of Sasobit and Rediset WMX, the trend for Rediset LQ was not clear. Rediset LQ improved the fatigue life of 40/60 binder grade by approximately 150%, as shown in Figures 3.28, 3.30 and 3.34, and slightly decreased the initial phase angles and increased the initial shear modulus of 40/60 binder grade. On the other hand, no change in the fatigue life of 100/150 binder grade was noticed with the inclusion of 0.5% of Rediset LQ. The reason for this issue may be because Rediset LQ slightly stabilised the molecules of the 40/60 binder, which was reflected by the increase in the response of shear modulus to controlled stress value, whilst, as the 100/150 binder is relatively soft, the Rediset LQ did not have any effect. In fact, the final conclusion on the performance of Rediset LQ can be made after studying its effect on the asphalt mixture.

An Energy Ratio criterion was also used to rank the performance of adopted warm additives. The fatigue performance rank for the WMBBs is the same both in the traditional approach and the energy approach. Figures 3.32 and 3.33 present the number of cycles at failure point of controlled asphalt binders and WMBBs with inclusion of error bars (standard deviation).

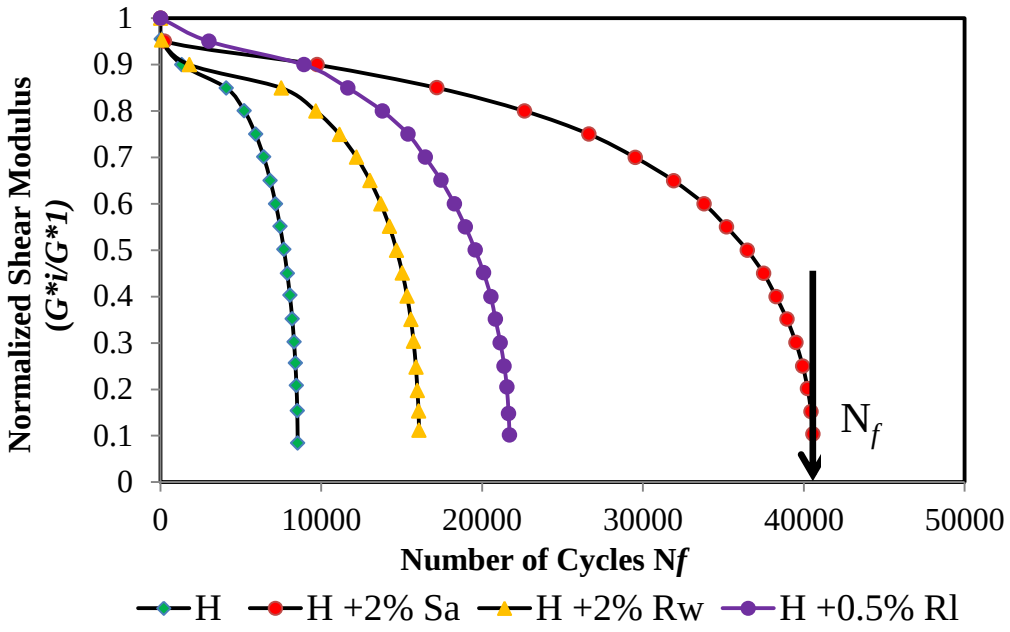

Figure 3.28 Average normalized shear modulus against number of cycles (controlled stress) mode for WMBBs with 40/60 binder grade.

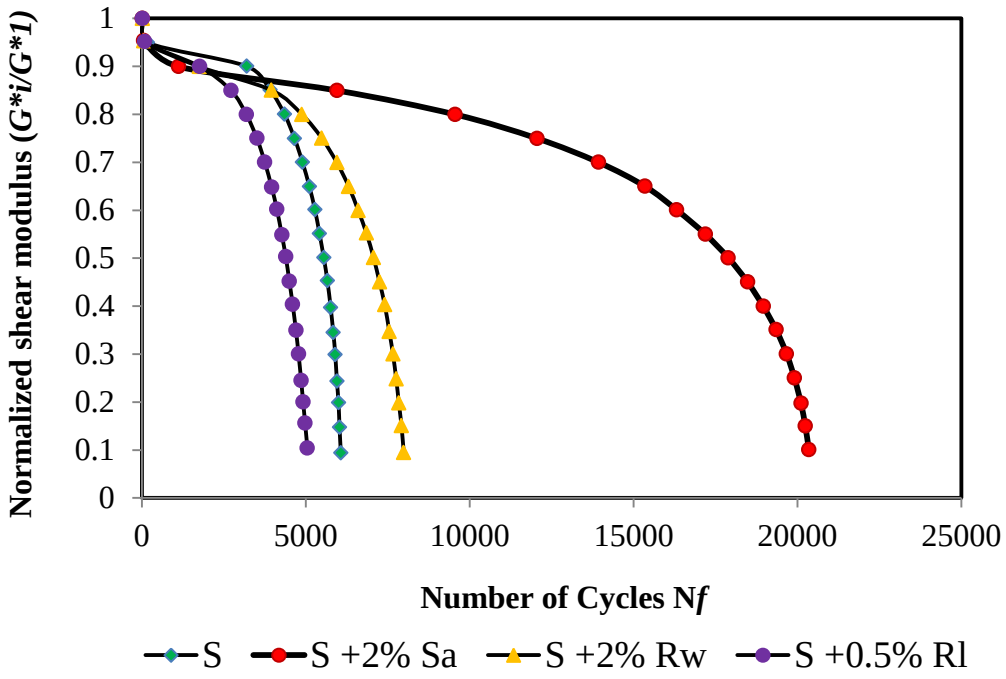

Figure 3.29 Average normalized shear modulus against number of cycles (controlled stress) mode for WMBBs with 100/150 binder grade

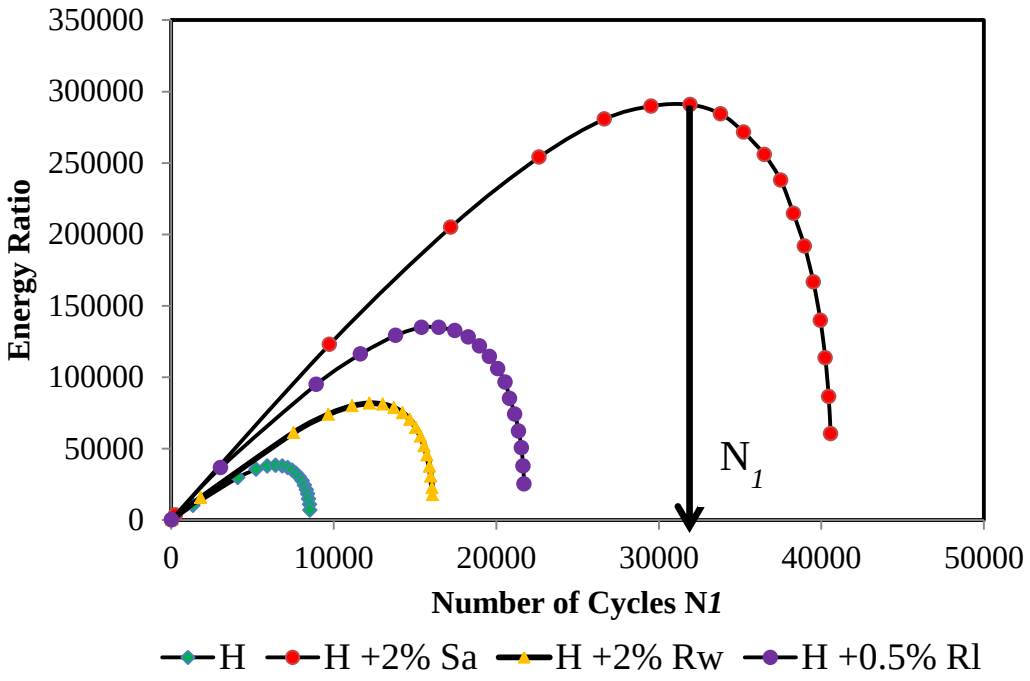

Figure 3.30 Average energy ratio against number of cycles for WMBBs with 40/60 binder grade

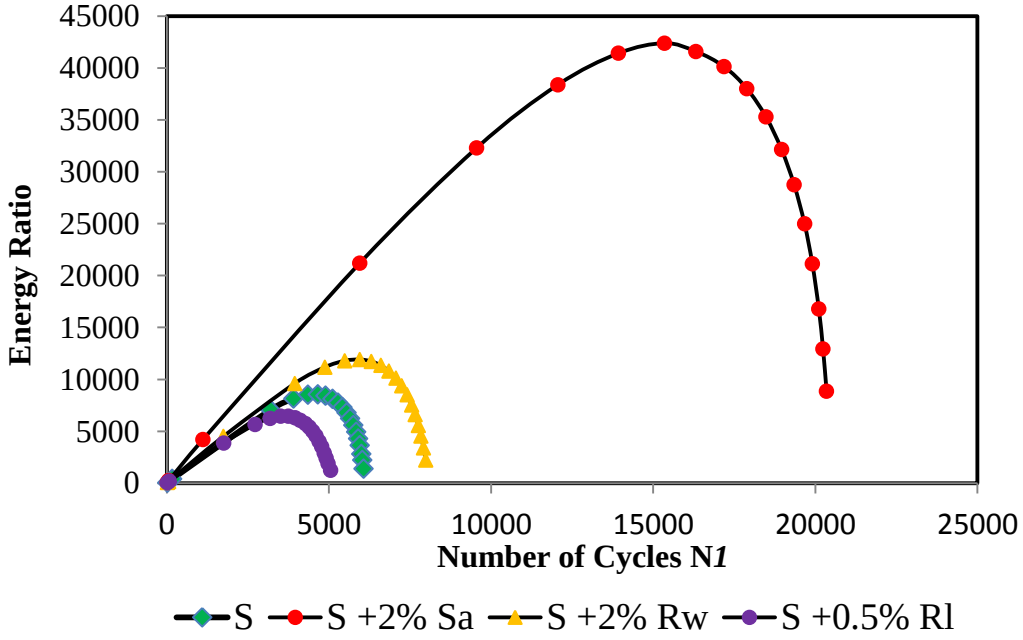

Figure 3.31 Average energy ratio against number of cycles for WMBBs with 100/150 binder grade

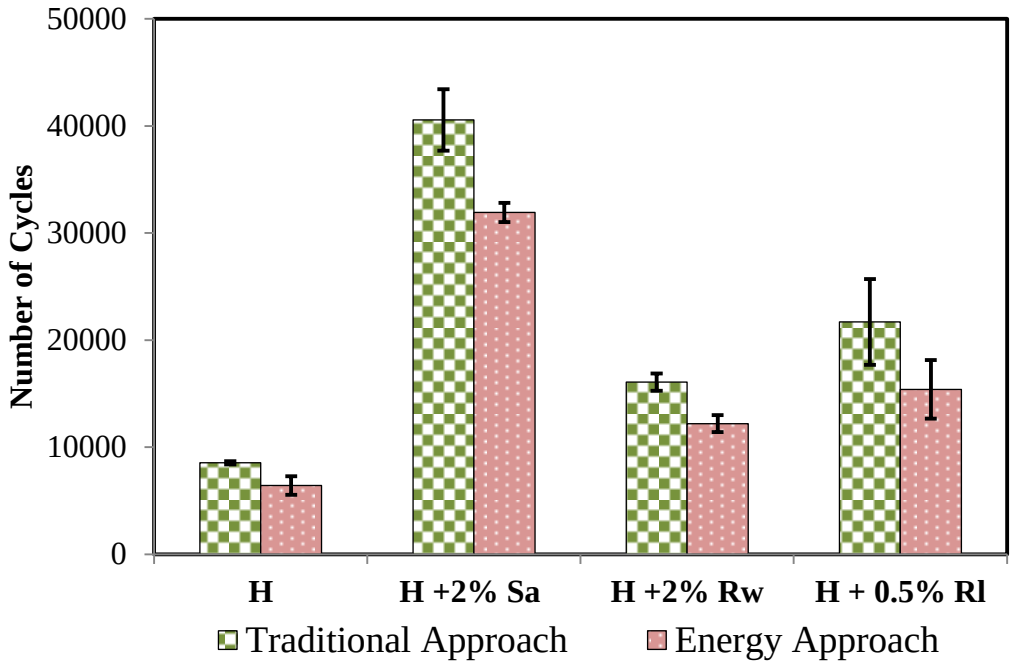

Figure 3.32 Average number of cycles (N_f and N_1) at failure point with error bars for WMBBs with 40/60 binder grade

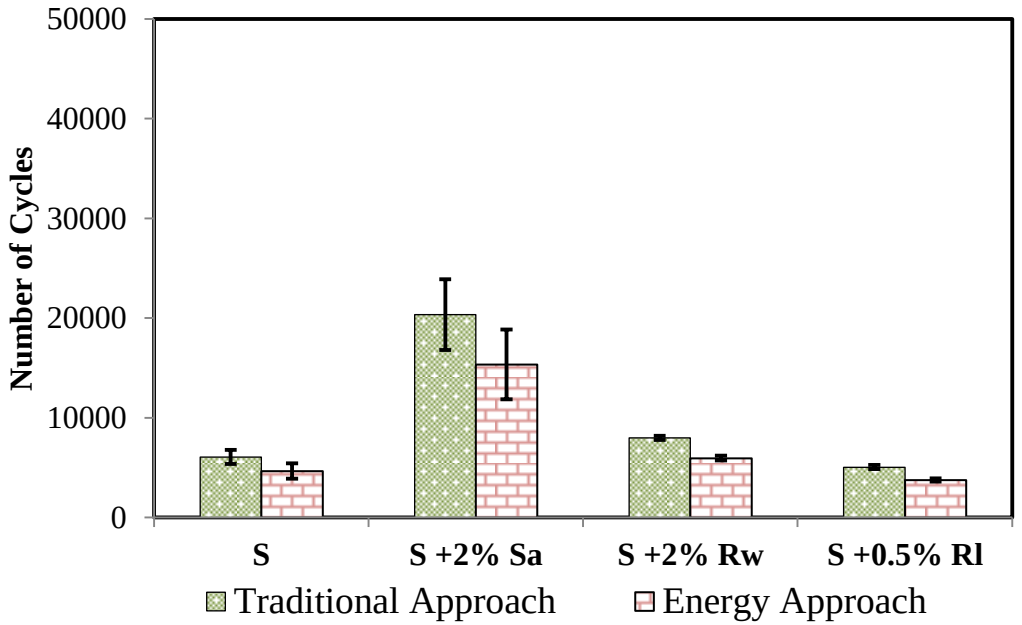

Figure 3.33 Average number of Cycles (N_f and N_1) at failure point with error bars for WMBBs with 100/150 binder grade

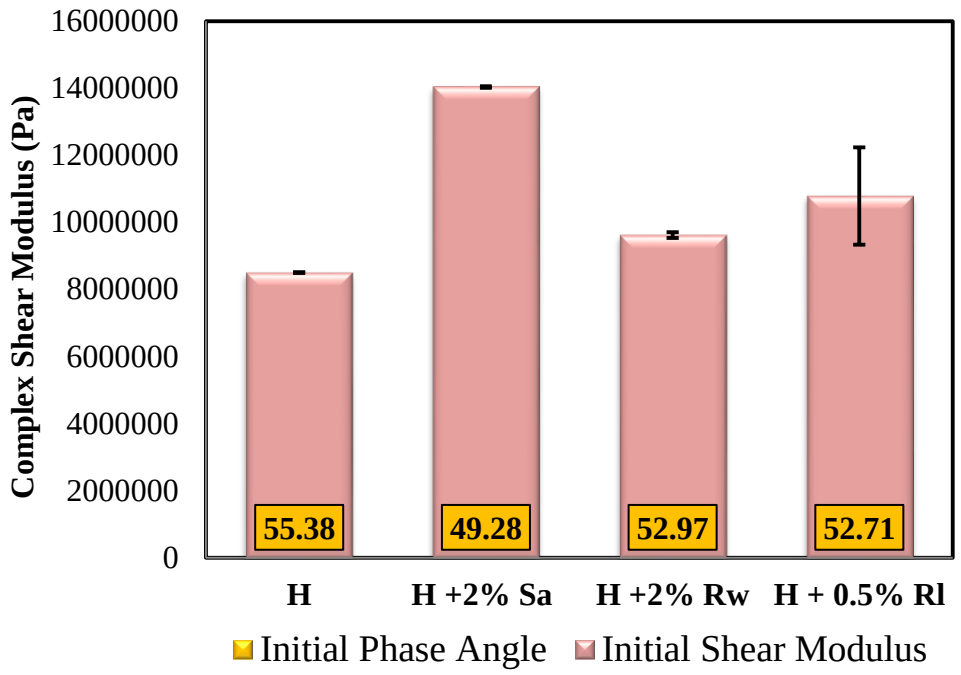

Figure 3.34 Average initial phase angle and shear modulus of WMBBs with 40/60 binder grade

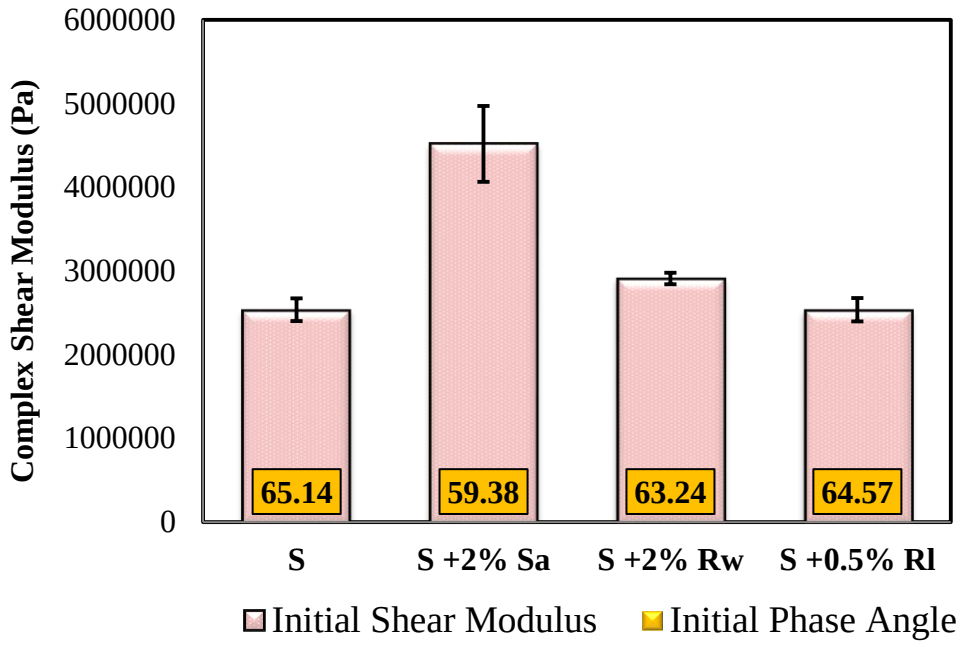

Figure 3.35 Average phase angle and shear modulus of WMBBs with 100/150 binder grade

3.7 Modelling fatigue behaviour of WMBBs using the viscoelastic continuum damage approach

In order to be able to accurately predict the fatigue performance of warm-modified bitumen, advanced mathematical models such as Viscoelastic Continuum Damage (VECD) offer a great potential for better understanding of fatigue cracking behaviour (Kutay *et al.* 2008a, 2008b) and also to model the fatigue behaviour of WMBBs. The VECD approach has been successfully used by a number of researchers. Fatigue can be identified based on the curve of *C-S*. (*C*) is pseudostiffness, which is defined as the loss of material stiffness due to loss of material integrity caused by damage, while (*S*) is a single parameter which is used to quantify the damage growth (Kutay *et al.* 2008a). Damage parameter (S) is calculated as:

$$S_{\sigma}^{N+\Delta N} = S_{\sigma}^{N} + ({}^{\Delta N}/_{f})^{\frac{1}{1+\alpha}} \left[0.5 \frac{1}{I} \sigma_{N}^{R^2} \left(\frac{1}{C_{N+\Delta N}} - \frac{1}{C_N}\right)\right]^{\frac{\alpha}{1+\alpha}} \quad (3.9)$$

Where $\sigma^R$is pseudostress, I is initial stiffness parameter, C is pseudostiffness, f is a constant frequency, S_σ is the damage parameter when σ^R is used (stress mode), N is the number of cycles, and α is a material constant related to the rate of damage.

α is calculated based on undamaged rheological properties using the slope of relaxation modulus (Hintz *et al.* 2011). Lee and Kim suggested that $\alpha = 1 + {}^{1}/_{m}$ is more suitable for strain controlled tests, whereas $\alpha = {}^{1}/_{m}$ is suitable for stress mode tests (Kutay *et al.* 2008a,Lee and Kim 1998).

m is the maximum slope of the relaxation modulus plotted against time. In this study, it was difficult to run a relaxation test; therefore, it was decided to use a method developed by Schapery and Park to convert sweep frequency test data to the relaxation data (Hintz *et al.* 2011).

3.7.1 Relaxation data

As previously stated, it was difficult to run a relaxation test on asphalt binder, therefore a method developed by Schapery and Park to convert sweep frequency test data to the relaxation data has been utilised to calculate α value. The sweep

frequency (for each control and modified bitumen) was conducted within the linear region of material behaviour at 20°C, as presented in Section 3.5.5. Then the stiffness modulus *E* was converted to the relaxation modulus *E(t)* based on the following equations:

$$\lambda = \Gamma(1-n) * cos(\frac{\pi n}{2}) \quad (3.10)$$

Where (*n*) is the slope of a log-log plot of stiffness (*E*) versus frequency (*f*), Γ is the gamma function. Once the λ parameter is calculated, complex modulus as a function of frequency can be converted to relaxation moduli as a function of time using equation 3.11:

$$E(t) = (1/\lambda)*E \quad (3.11)$$

Figure 3.36 illustrates the conversion of a log-log plot of stiffness (*E*) versus frequency (*f*) to the relaxation modulus plotted against time. Table 3.5 illustrates the values of *m* from relaxation data.

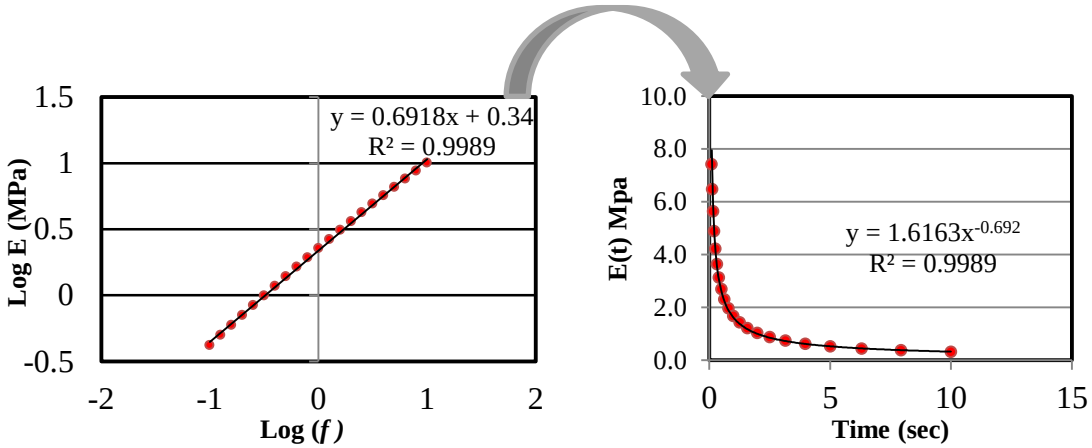

Figure 3.36 Example of conversion of the sweep frequency data to relaxation data (a) Sweep frequency data (b) Relaxation data

Table 3.5 *m* value from frequency sweep and relaxation data

Material	*m* (Relaxation)	*Material*	*m (Relaxation)*
H	0.692	S	0.782
H + 2% Sa	0.622	S +2% Sa	0.718
H +2% Rw	0.679	S +2% Rw	0.742
H + 0.5% Rl	0.689	S+0.5% Rl	0.73

3.7.2 Pseudostiffness-damage parameter curves

Data were analysed based on stress mode; however, according to the VECD theory, a single damage characteristic curve behaviour of (*C*-*S*) should exist independently of loading frequency, temperature and mode of loading, and (*C*-*S*) curves calculated at different temperatures and at different loading modes should collapse on a single curve (Kutay *et al.* 2008a).

Figures 3.37 and 3.38 describe how the micro-cracks grow and propagate for particular bitumen samples.

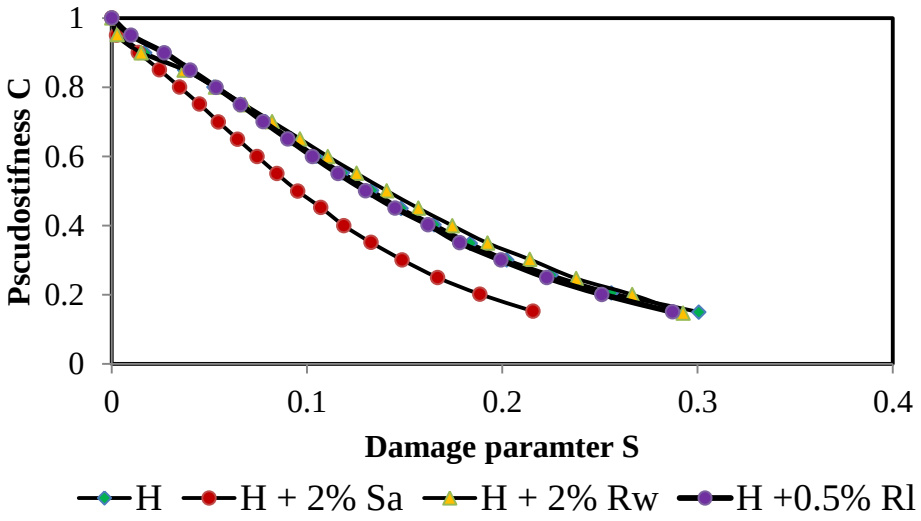

Figure 3.37 Pseudostress-based damage parameter of WMBBs with 40/60 binder grade

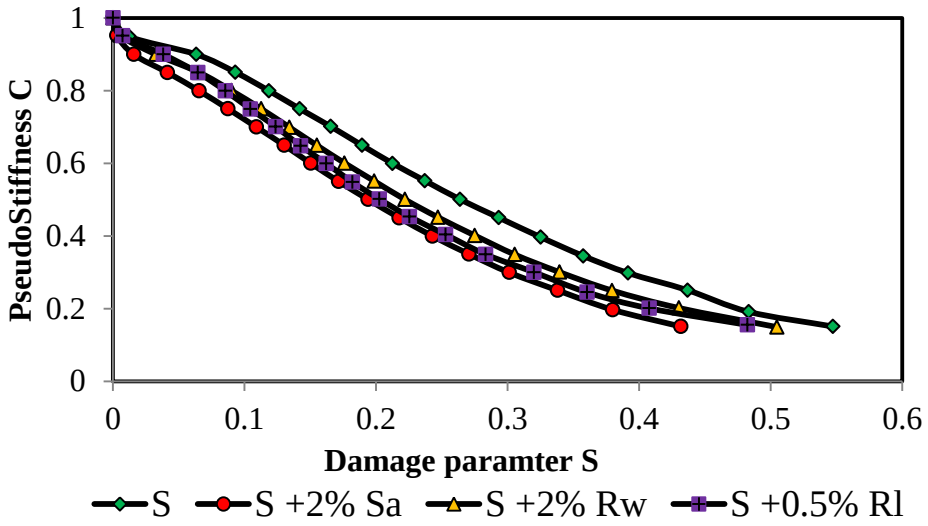

Figure 3.38 Pseudostress-based damage parameter of WMBBs with 100/150 binder grade

The main advantage of the VECD approach is that it is based on a constitutive model and the characteristic curve can be utilised to model the fatigue behaviour of the material under any load history and temperature. Once the damage characteristics of *C*-*S* curves were obtained, an exponential best-fit line was fitted to the curves using the following equation:

$$C = \exp(aS^b) \tag{3.12}$$

Where a and b are constant parameters defining the best fit. Those parameters in Table 3.6 could be further used to model the fatigue behaviour of WMBBs and predict the response of the material to a given loading history.

Table 3.6 $\boldsymbol{\alpha}$ and exponential fit coefficient of damage characteristics curves of WMBBs

Material	α	a	b
H	1.45	-8.866149	1.243603
H+ 2% Sa	1.60	-12.13045	1.208638
H+ 2% Rw	1.47	-9.398853	1.323412
H+ 0.5%Rl	1.45	-10.01931	1.278774
S	1.28	-4.436964	1.393522
S+ 2% Sa	1.39	-5.311999	1.223183
S+ 2% Rw	1.35	-4.512685	1.240143
S+0.5% Rl	1.37	-4.581165	1.186041

3.7.3 Predict fatigue of WMBBs

A procedure suggested by Kutay *et al.* (2009) to numerically predict the fatigue life of asphalt mixture was used. Once the constant parameters (a & b) defining the best fit are obtained, the following equations could be used to predict fatigue life at given loading history. The derivations of this equation are found in study of Kutay *et al.* (2008a, 2009)

$$\frac{dC^{-1}}{dS} = -\exp(-aS^{b})abS^{b-1} \quad (3.13)$$

$$S_f = \left(\frac{lnC_f}{a}\right)^{1/b} \quad (3.14)$$

$$N_f = \sum_{S=1}^{S_f}\left[\frac{\sigma^{R^2}}{2I}\frac{dc^{-1}}{ds}\right]^{-\alpha} f\Delta S_s \quad (3.15)$$

Where σ^R is pseudostress, I is initial stiffness parameter, C is pseudostiffness, f is a constant frequency, S_f is a damage parameter corresponding to failure point (in the current study, C_f =0.1), ΔS_s is the change in damage parameter within each summation increment, and α is a material constant related to the rate of damage based on the maximum slope of the relaxation modulus plotted against time.

$\frac{dC^{-1}}{dS}$ is obtained by fitting a regression model to the C-S curve and finding derivatives or by simply dividing the C-S curve into smaller intervals up to the selected failure point, S_f, and then calculating $\frac{dC^{-1}}{dS}$ within each interval.

As can be seen in Figures 3.39 and 3.40, high correlation was found between measured and predicted number of cycles.

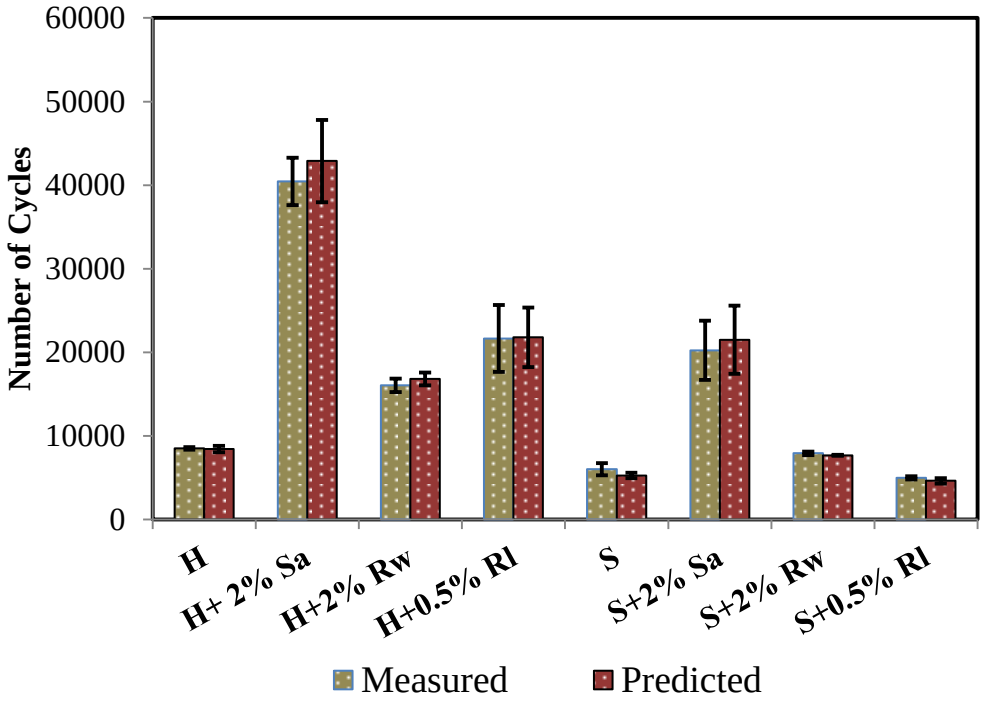

Figure 3.39 Measured and predicted number of cycles for al WMBBs

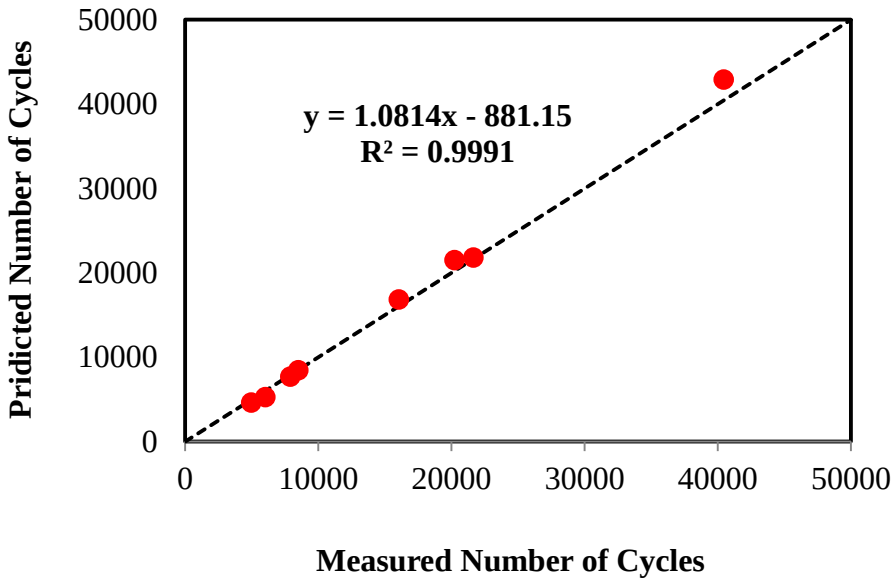

Figure 3.40 Correlation between predicted number of cycles using VECD and measured number of cycles

3.8 Conclusions

1. There is no significant change in binder viscosity by adding 2% Sasobit or 2% Rediset WMX. The Brookfield Viscometer cannot predict the adequate reduction in the mixing temperature. This finding actually corresponds with that of other researchers.

2. Addition of 6% Sasobit or Rediset WMX decreased the expected production temperature of WMA compared to control binders by only 10°C for the hard binder and 12°C for the soft binder. Finding also coincides with that from another study.

3. Rediset LQ has no effect on the viscosity of the virgin binder even when using up to 1.5% of this additive. In fact, Rediset LQ acts in a different behaviour in decreasing the production and compaction temperature of asphalt mixture.

4. Using the recommended dosages of Rediset WMX and LQ has a minor effect on the rheological properties of asphalt binder; therefore, higher than the recommended dosages can be used if required, perhaps without having negative effects on the binder's linearity viscoelastic properties.

5. Addition of 2% Sasobit increased binder stiffness by 30% at 0°C and approximately 200% at 60°C while it decreased the phase angle by 12% at 0°C and approximately 8% at 60°C. In addition, it decreased the linear viscoelastic region by approximately 45% and 55% for the hard and soft binders respectively.

6. Sasobit significantly increases the fatigue life of asphalt binder regardless of binder grade. Using the recommended dosage of Sasobit showed a superior performance in terms of resistance to fatigue cracking. This was confirmed using different criteria to rank the Sasobit-modified bitumen.

7. Despite the fact that the improvement in the fatigue performance due to of Rediset WMX was not as significant as that of Sasobit, it did improve the fatigue life of bitumen.

8. As highlighted in the literature chapter, there is no agreement or final conclusion about the performance of WMA in terms of fatigue. However, it was found that Sasobit and Rediset WMX improved the fatigue life of asphalt binders, so this improvement should also be clear on the fatigue life of warm asphalt mixtures but other factors should be addressed such as the effect of production temperatures and binder grades.

9. The VECD approach was used to predict the fatigue life of WMBBs. High correlation was found between measured and predicted number of cycles.

Chapter Four

Nano-scale Properties of WMBBs Determined with Atomic Force Microscopy (AFM)

4.1 Introduction

The effect of warm additives on the nano-mechanical properties of binder material has yet to be studied. Atomic force microscopy (AFM) has potential as a powerful technique for pavement researchers to investigate the nano-mechanical properties of film asphalt binders. It is well-established that the microstructure of bitumen is responsible for its physical properties such as elasticity, plasticity, stiffness, adhesion, and surface energy and healing. Indeed, there is a need to understand the behaviour of bituminous binders at the nanometre scale, because the interaction between the composite phases of asphalt mixtures takes place at this scale. It should then be possible to link the nano-mechanical properties of the bituminous binders and the mix to the micro and macro mechanical properties of those materials in order to accurately understand the behaviour of asphalt mixtures under applied load.

The first section of this chapter presents a brief background on the general utilisation of AFM in pavement engineering. This is followed by experimental details, results and discussion of an investigation into the impact of Sasobit and Rediset WMX and LQ on topography, modulus, deformation and adhesion of warm modified bituminous binders using Atomic Force Microscopy (AFM) with the PeakForce Quantitative Nanomechanical Mapping (PFQNM) modality.

4.2 Background

Extensive studies have focused on the performance of warm additives in relation to the traditional mechanical and rheological properties of warm modified bituminous binders and mix (Abd and Al-Khalid 2015,Hurley and Prowell 2005a,Hurley and Prowell 2005b,Hurley and Prowell 2006a,Bennert *et al.* 2011,Bennert *et al.* 2010,Silva *et al.* 2010,Silva *et al.* 2009,Gandhi 2008a,Xiao *et al.* 2012b,Kim *et al.* 2011b,Xiao *et al.* 2010,Mogawer *et al.* 2011b,Mogawer *et al.* 2011c,Hamzah *et al.* 2013,Menapace *et al.* 2014). However, there are few studies that have characterised the performance of warm additives at the nano-scale such as with the use of AFM (Nazzal and Abu-Qtaish 2013,Qin *et al.* 2014).

In fact, there is a need to understand the behaviour of bituminous binders at the nanometre scale, because the interaction between the composite phases of asphalt mixtures takes place at this scale. Such work will allow the nano-mechanical properties of the bituminous binders and the mix to be correlated with their micro- and macro- mechanical properties, and thereby better understand the behaviour of asphalt mixtures under applied load.

In terms of physical structure or topographical structure of bituminous binders, Loeber *et al.* (1996) firstly observed the well-known bee-shaped microstructure features of a heat-cast bitumen, typically several micrometres in diameter and tens of nanometres in height. Several years later, Pauli *et al.* (2001) acquired the same bee shape and correlated the bees-shape with the amount of asphaltenes in the binder by mapping the solvent-cast bitumen film. Jäger *et al.* (2004) extended the research further. They identified four phases in the topographic images of the bitumen; hard bee, soft bee, hard matrix and soft matrix, and separated the lower and higher parts of the bees and the surrounding phases. A more extensive study in this regard was conducted by Masson *et al.* (2006) who studied the morphological structure of 13 binders using AFM. The study classified the investigated binders into three groups. The first group showed a fine dispersion (0.1-0.7μm) in a homogenous matrix while the second showed domains of about 1μm. The third group manifested four different phases of vastly different sizes, named catana, peri, para and sal phases. No correlation was found between morphology and the compositions of binders based on asphaltenes, polar

aromatics, naphthene aromatics and saturates, but a good correlation was reported between the area of the bee-like structures and the contents of the vanadium and nickel in bitumen. They also reported that the method of preparing the bitumen film highly affects the final material morphology, because the morphological structure of bitumens adopted in the study was different from those observed in the study conducted by Pauli *et al.* (2001) for the same materials used in both studies.

Lyne *et al.* (2013b) conducted a study to calculate the thickness of the bee laminate phase based on the wavelengths and elastic modulus of the bee laminate and the matrix. They considered the bee catana phase and the peri phase to be a single phase named the bee laminate phase. They pointed out the bee laminate thickness was found to vary between 70 and 140 nm for the five bitumen samples that contained a significant amount of wax. In fact, it should be noted that it is not always possible to distinguish or observe all phases on the topography of the bitumen because the source of material significantly governs the morphological structural of that bitumen. For example, in the aforementioned study by Masson *et al.* (2006), it was not always possible to see all bitumen phases, catana, peri, para and sal phases, whereas, Menapace *et al.* (2014) reported three phases, catana, peri, and para, in two binders, 60/70 and PG76-22. They highlighted that the bee-like structures, measuring about 500 nm to 5 μm in length, represent the catana phase. The peri phase surrounds the catana phase. Further away from the bees, the para phase is noticed. The measurements were performed using tapping mode AFM and they characterised the effect of heat treatment and addition of Sasobit and Advera on the morphological structure of two types of bitumen, 60/70 binder grade and PG76-22, but did not measure any mechanical properties.

Dourado *et al.* (2012) investigated the mechanical properties of asphalt binders using AFM. Their study used 50/70 asphalt binder in order to relate the features observed on the surface of this binder to its local stiffness and elastic recovery. The results showed that regions belonging to the bee presented lower stiffness than the ones belonging to the matrix; therefore, it is impossible to directly link the matrix to the maltenic phase and the bees to the asphaltenes.

Das *et al.* (2013) investigated the micro-mechanics of phase separation by combining AFM with differential scanning calorimetry (DSC). Their study involved four different types of bitumen, named B1, B2, B3 and B4, the sources of which were different. B1, which was from Venezuela, was non-waxy bitumen based on DSC and B3 was prepared by adding 3% of Sasobit wax by the weight of B1. B4 was straight-run bitumen from Kuwait export crude and the source of B2 was unknown. The topographic images of each binder were captured during heating cycles from 30°C to 60°C in steps of 10°C and cooling cycles from 60°C to 30°C, also in steps of 10°C. The topographic images showed that no discernible microstructural features were visible on the surface of bitumen B1 at any temperatures in the heating cycle, which indicted that this kind of bitumen is a super flat surface. More importantly, according to the DSC results, this bitumen is classified as a non-waxy bitumen, as there was no endothermic or exothermic effect observed, which could indicate crystallising fractions. Interestingly, when Sasobit wax was added to B1, the topographic image of the bitumen produced, B3 showed long bee-shaped microstructures at all temperatures from 30°C to 60°C and the DSC revealed the presence of wax additive. Regarding bitumen B4, observed topographic images highlighted a smaller but greater number of bee-shaped microstructures, which were surrounded by similar phases. With an increase in the temperature, the microstructures started to disappear and, at 60°C, all the bee-shaped microstructures vanished. It can therefore be concluded that the presence of bee structures is closely connected to the presence of wax or paraffin in bitumen.

Fischer *et al.* (2013) used the PeakForce Tapping mode to investigate temperature- dependent nano-mechanical properties. They measured the elastic modulus, adhesion, deformation and dissipation of Q8 70/100 binder. They reported, for the first time, high-resolution, quantitative, mechanical mapping data at the nano-scale and confirmed the presence of several phases on the nano-/micro scale and presented their individual properties. They found that the peri phase is stiffer than the para phase, which is in conflict with the study of Dourado *et al.* (2012). However, it should be noted that Fischer *et al*. (2013) considered the peri/catana phase is a single phase and compared its elastic modulus to para/perpetual phases, whereas Dourado *et al*.'s (2012) study distinguished two

phases, the first is the bees and the latter is the smooth matrix which is be defined as para phase although they did not mention that. It is therefore recommend that more attention should be paid to the definition of phases in bitumen when they are reported to avoid confusion.

Using AFM to map the mechanical properties of asphalt binder film has attracted more interest recently. For example Lyne *et al.* (2013a), used PFQNM to map the mechanical properties of microphase-separated topographic morphologies of unaged 70/100 binder grade, while the effect of the ageing process (short and long term) on the topographical structure of 50/70 binder grade has been investigated by Rebelo *et al.* (2014b) measured in both contact and tapping modes. As pavement researchers are more concerned about the level of blending between reclaimed asphalt pavement (RAP) or recycled asphalt shingle (RAS) and virgin material (binder and aggregate), AFM was also utilised to investigate the microstructure of RAS and its blending with virgin material by Zhao *et al.* (2015b). In addition, the effect of short- and long-term ageing on the morphological microstructure of bitumen and polymer-modified bitumen using AFM has also been investigated by a number of researchers (Allen *et al.* 2012,Das *et al.* 2014,Poulikakos *et al.* 2014,Wu *et al.* 2009,Zhang *et al.* 2011,Zhang *et al.* 2012,Menapace *et al.* 2015)

More attention has been given recently to the performance of warm additives included in asphalt binder and mixture due to their potential to produce pavement at lower temperatures without adversely affecting workability, durability and performance of the pavement. Therefore, there is a need to study the effect of warm additives on the topographical structure of film bituminous binders and, more importantly, to map its mechanical properties.

This chapter presents new insight of the effect of warm additives, Sasobit and Rediset WMX and LQ on the topography, elastic modulus, deformation and adhesion of bituminous binders grade, namely 40/60 and 100/150, using AFM with the PFQNM modality.

4.3 Principles of AFM

Back in the 1980s, the scanning tunnelling microscope was firstly developed by Gerd Binnig and Heinrich Rohrer, who were awarded a Nobel Prize in Physics in 1986. This invention was an introduction to the AFM (Binnig *et al.* 1982, 1986). The concept of AFM work involves a cantilever carrying a probe that makes contact with the surface of the sample, the laser path and the piezo transducers, as shown in Figure 4.1. The cantilever interacts with the surface of a sample which is moved in the x, y and z directions by piezo actuators while the laser beam focused at the end of the cantilever is reflected into a detector. When the cantilever encounters a force due to a topographical, chemical or electrical feature on the sample, it is deflected, leading to a deviation of the laser beam from its original position on the detector. This deviation is reordered as a voltage which can then be converted into a force or relative height.

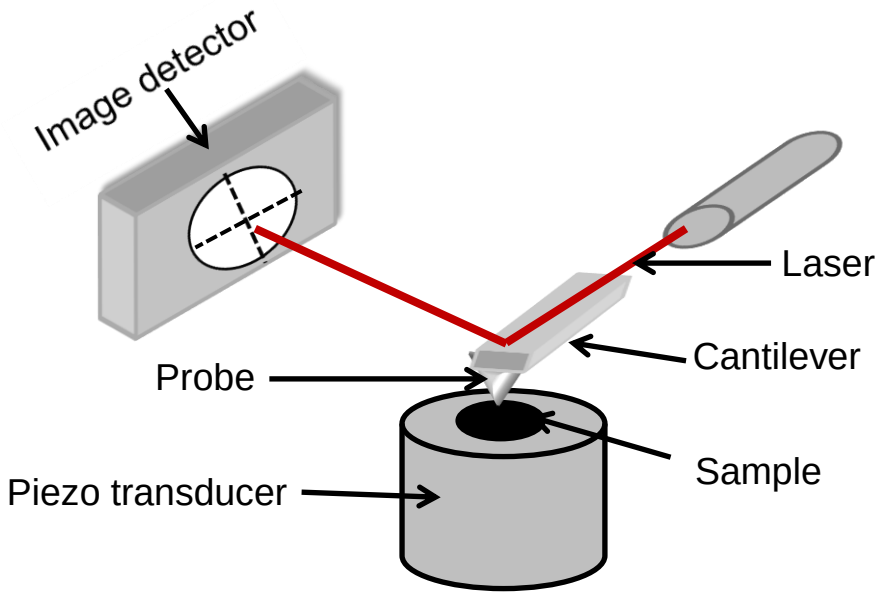

Figure 4.1 Schematic diagram of an AFM

Samples are imaged and mapped either in scanning probe microscope-contact mode (SPM-contact mode) or in tapping mode. In SPM-contact mode, the probe is in contact with surface of the sample at constant load while the surface is moving in x, y directions, whereas, in tapping mode, the probe is vibrated near the resonant frequency of the cantilever while it is scanned across the sample. Using

the SPM-contact mode, it was impossible to obtain truly quantitative material property mapping because force curves can only provide data at one point on the sample surface at a time (Pittenger *et al.* 2010). Therefore, Tapping Mode imaging was developed in 1993 by Zhong *et al.* which has the ability to generate high-quality data for a wide range of samples. In Tapping Mode, the technique involves collecting force curves at each pixel in an image and puts them together to map the properties across a larger sample. The drawback of the tapping mode technique is that the resonant behaviour of the probe also acts as a filter (Pittenger *et al.* 2010), which makes it difficult to reconstruct the force curves with adequate precision to extract the mechanical properties.

In order to overcome this problem, in 2008, HarmoniX was developed as a solution which involves adding a second sensor with a much higher bandwidth by offsetting the tip and measuring the torsional signal. However, the downsides of this approach are that it requires special probes, the operation can sometimes be complicated, and, moreover, the interpretation of the results is occasionally difficult. Bruker therefore developed PeakForce PFQNM to solve these problems and offer great advantages in providing high-resolution mapping of mechanical properties, which is non-destructive to probes and samples because it controls the maximum force on the tip and the probe oscillates far below the cantilever resonant frequency which gives unambiguous and quantitative data over a wide range of materials (Pittenger *et al.* 2010).

4.4 Materials and Methods

4.4.1 Materials

Details about adopted warm additives and binder grades were presented in Chapter 3, Section 3.2. Sasobit, Rediset WMX and Rediset LQ were incorporated into two binder grades, namely 40/60 and 100/150. In this chapter, all warm additives were also added at rates within the specified manufacturer tolerance. The recommended dosages of Sasobit, Rediset WMX and Rediset LQ adopted in this chapter are 2%, 2% and 0.5% by the weight of the bitumen respectively.

4.4.2 Sample preparation

The modified asphalt binders were prepared as presented in Chapter 3, Section 3.3. For the preparation of the AFM samples, the heat-cast method was used in preference to the solution cast method in order to avoid the solvents having an effect on the binder composition. Firstly, a metal disc of 15 mm in diameter and 0.88 mm in thickness was placed on a sheet of glass of 300×300×10 mm. The metal disc was heated using a heat gun and then a small amount of heated bitumen which was heated in an oven maintained at temperature of 140°C, was cast on it. The heat gun was then used to continue heating the bitumen samples and prepare samples with thickness varying between 100 µm and 500 µm measured using a Vernier caliper

Three samples were prepared for both the virgin bitumen and the warm-modified bitumen as shown in Figure 4.2. The samples were firstly kept in a controlled temperature unit maintained at 10°C prior to imaging; after that, the samples were left at environmental room temperature for 12 hrs and then imaged at room temperature, 22°C and the temperature was controlled using an A/C provided in the testing room.

Each sample was imaged at different locations; therefore, five images were captured for both the virgin and the modified bitumen. For brevity, the binder grades of 40/60 and 100/150 are named H and S respectively, while the warm additives are named based on the first two letters of the word: Sa, Rw and Rl for Sasobit, Rediset WMX and Rediset LQ respectively.

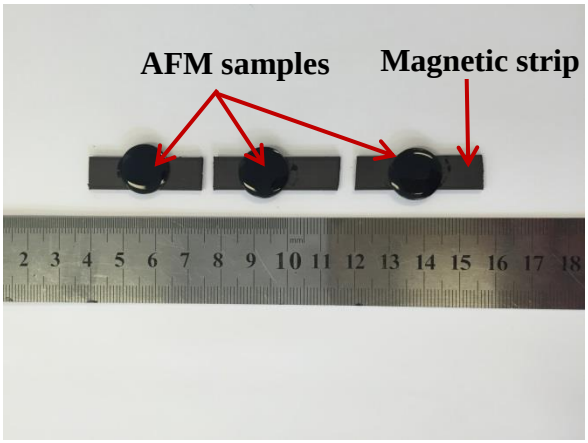

Figure 4.2 The AFM samples

4.4.3 Atomic force microscopy / PeakForce QNM

All testing was conducted with a Bruker Multimode atomic force microscope, AFM (NanoScope VIII, Bruker Nano Inc., Nano Surfaces Division, Santa Barbara, CA) equipped with a 150 x 150 x 5 μm scanner (J-scanner) operated with PeakForce Quantitative Nanomechanical Mapping (PFQNM) modality (Young *et al.* 2011). All tests were conducted in ambient conditions. The measurements were conducted with a Bruker TAP150A probe which is a silicon nitride tip with a nominal tip radius of 8 nm and a 5 N/m spring constant. The exact spring constant was determined using the Thermal Tune method and the tip radius was calibrated with a standard Vishay Photostress coating (PS1) polymer (Heilbronn, Germany) of known elastic modulus, 2.7 GPa. The exact spring constant and tip radius after calibration were 5.155 N/m and 9 nm respectively. Measurements were conducted at the peck force amplitude of 75 nm. Force mapping was conducted as follows: the sample was oscillated in the z-direction at 2 KHz at the same time as the sample was moving in the x-y directions at a rate of 0.766 Hz. Each image was composed of 384 x 384 independent force-distance curves. Topography, modulus, adhesion and deformation were measured over 10x10 μm scans. Data was analysed off-line using Nanoscope Analysis software (v.1.5, Bruker AXS).

The elastic modulus was obtained using the Derjaguin-Muller-Toporov (DMT) model (Derjaguin *et al.* 1975,Muller *et al.* 1983,Pittenger *et al.* 2010) using Equations 4.1 and 4.2.

$$F - F_{adh} = \frac{4}{3} E^* \sqrt{R(d - d_0)^3} \tag{4.1}$$

where $F - F_{adh}$ is the force on the cantiliever relative to the adhesion forc, R is the tip end radius and $d - d_0$ is the deformation of the sample. The obtained result is the reduced modulus but, if the Poisson's ratio is known, elastic modulus of the sample is obtained as follows

$$E^* = \left[\frac{1-v_s^2}{E_s} + \frac{1-v_{tip}^2}{E_{tip}}\right]^{-1} \tag{4.2}$$

where $E^*, E_s \; and \; E_{tip}$ are the reduced modulus, sample modulus and tip modulus respectively and v_s and v_{tip} are the Poisson's ratio of sample and tip respectively. The Poisson's ratio of the samples was assumed to be 0.3 for this kind of material whiles the Poisson's ratio of tip is 0.24.

The second mechanical property acquired in the mapping is the adhesion force, illustrated by the minimum force in Figure 4.3. The source of the adhesion can be any attractive force between the tip and the sample, while the deformation is the maximum penetration of the tip into the surface of the sample at the peak force. As the load on the sample under the tip increases, the deformation also increases, reaching a maximum at the peak force. Figures 4.4 and 4.5 illustrate atomic force microscopy system and setting bitumen sample in AFM respectively.

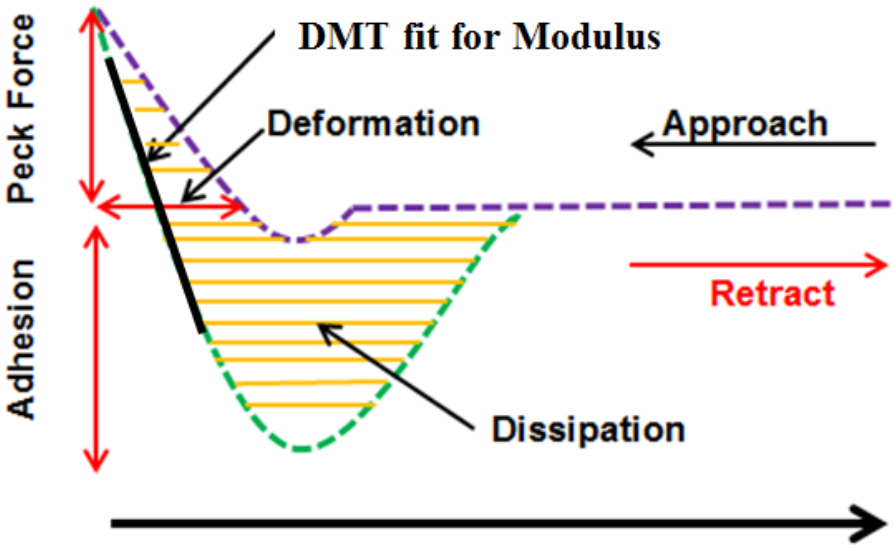

Figure 4.3 Force curve evaluation procedure

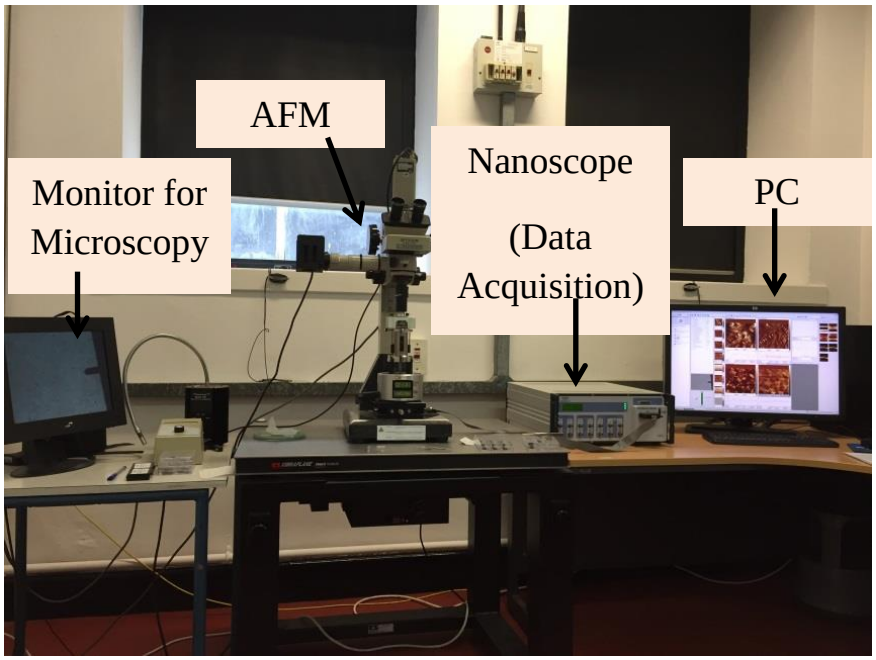

Figure 4.4 Atomic force microscopy system

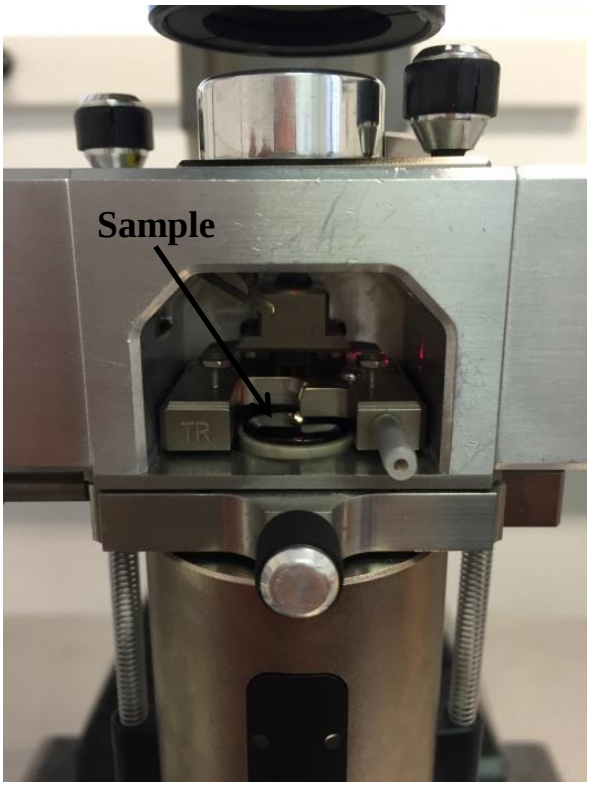

Figure 4.5 Setting bitumen sample in AFM

4.5 Results and Discussion

4.5.1 Topographical structures

Figure 4.6 shows topography images obtained for the control and warm-modified bituminous binders. As reported by other researchers, the microstructure of bitumen consisting of the peri phase and para phase can be clearly seen in the current study (Loeber *et al.* 1996,Loeber *et al.* 1998,Masson *et al.* 2006,Menapace *et al.* 2014). As can be seen in Figure 4.6-A, the peri phase is characterised by darker shade, whereas the para phase is characterised by a lighter colour in phase. However, more importantly, the catana phase does not exist, because the source of those types of binder is Venezuela, and they are classified as a non-waxy bitumen (Das *et al.* 2013). Therefore, the catana phase or the bees cannot be observed in the control binders. As Sasobit and Rediset WMX contain wax in their structures, once they were added to the control binders, the catana phase was recognized, as can be seen in Figures 4.6-B, 4.6-C, 4.6-F and 4.6-G. The effect of Sasobit and Rediset WMX is clearly noticeable. In comparison with the control binders, the peri phase is considerably larger and the para phase is significantly reduced and disappeared in the majority of the scans. Figure 4.7 shows the three-dimensional images of the same images (A, B, C and D) illustrated in Figure 4.6. Sasobit and Rediset WMX significantly changed the topographical structure of the binder. Sasobit changed the topographical structure of the control binder from approximately (-4.0/3.3 nm) and (-3.3/3.4 nm) to (-84.3/87.6 nm) and (-36/28 nm) for 40/60 and 100/150 binders respectively. The change in the topographical structure of the binder was also significant when adding Rediset WMX. The significant change in the topography caused by Sasobit and Rediset WMX may due to increasing the mobility of the different molecular species within the binder because of the presence of wax or is probably due to their lower density, which leads the wax to emerge at the surface.

Interestingly, it was noted that Rediset LQ did not have any effect on the topography of the control binders and the structure of the peri and para phases remained constant (Figures 4.6-D and 4.6-H). The result of this study clearly justifies and confirms the fact that Rediset LQ does not alter the binder properties.

Therefore, the area of the peri and para phases has not been affected and hence the Figures 4.6-D and 4.6-H are similar to Figures 4.6-A and 4.6-E.

Furthermore, the catana phase cannot be noticed in those images as there is no wax in the chemical structure of Rediset LQ. In addition, there is no difference between the range of topographical structures of Rediset LQ-modified bituminous binders and its control binders. Representative images are shown for each control and warm-modified bituminous binder topography, elastic modulus, deformation and adhesion in Figures 4.6, 4.7, 4.8, 4.10 and 4.12.

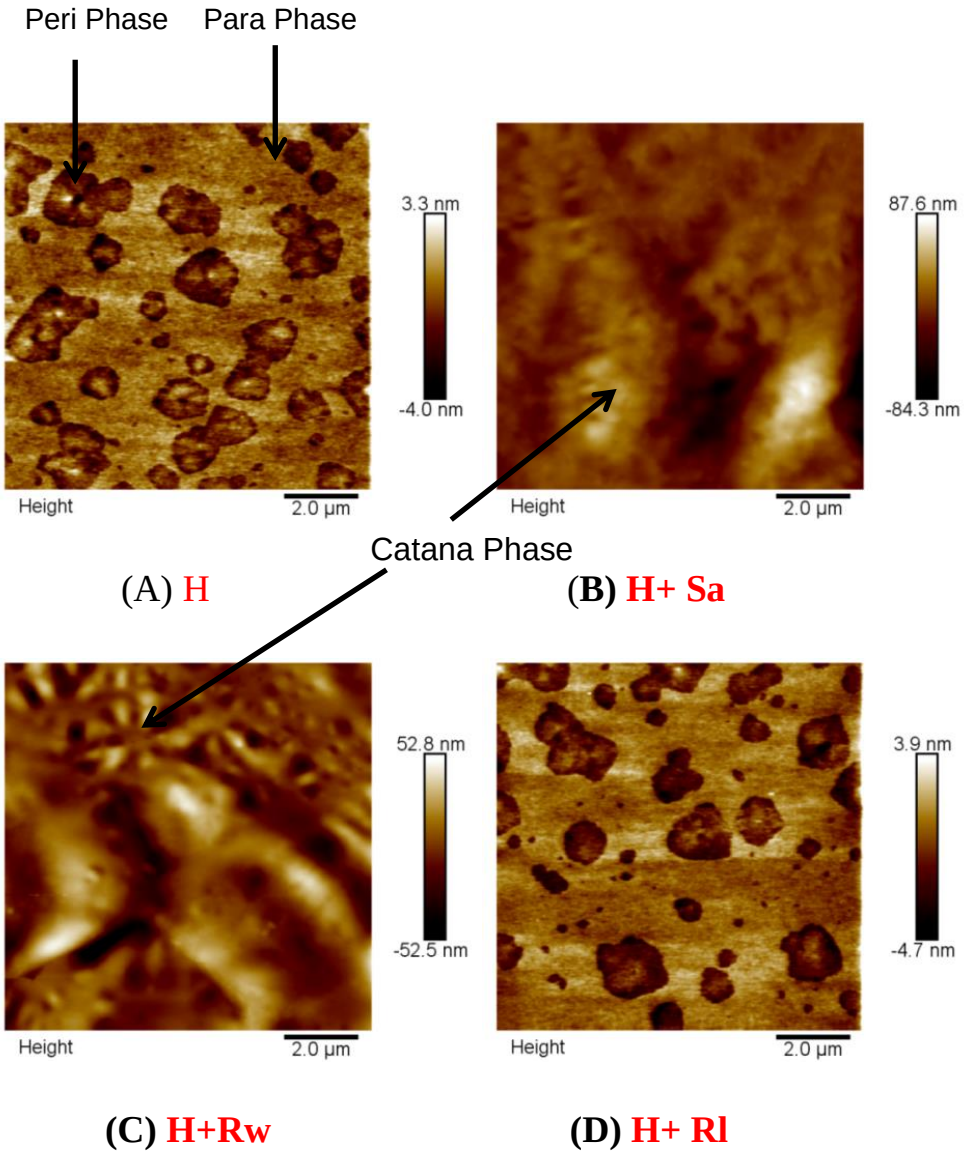

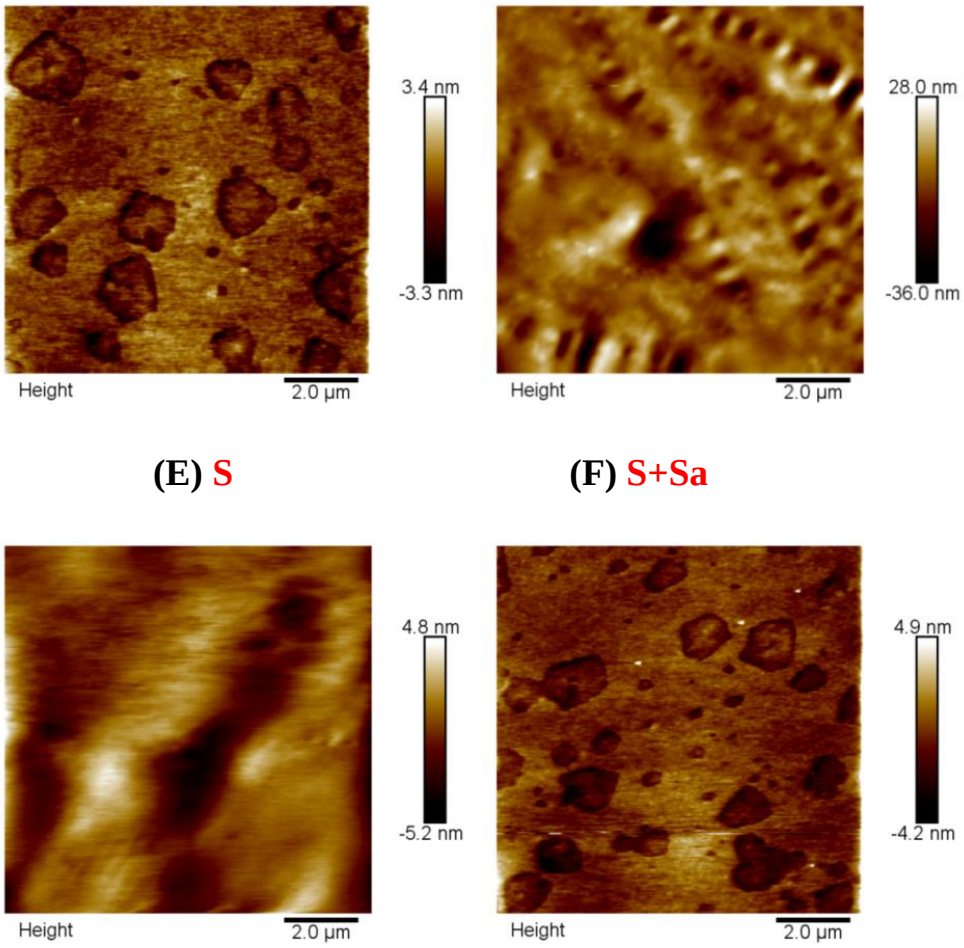

(E) S **(F) S+Sa**

(G) S+Rw **(H) S+Rl**

Figure 4.6 Representative topography (height) images control binders 40/60 and 100/150 and WMBBs

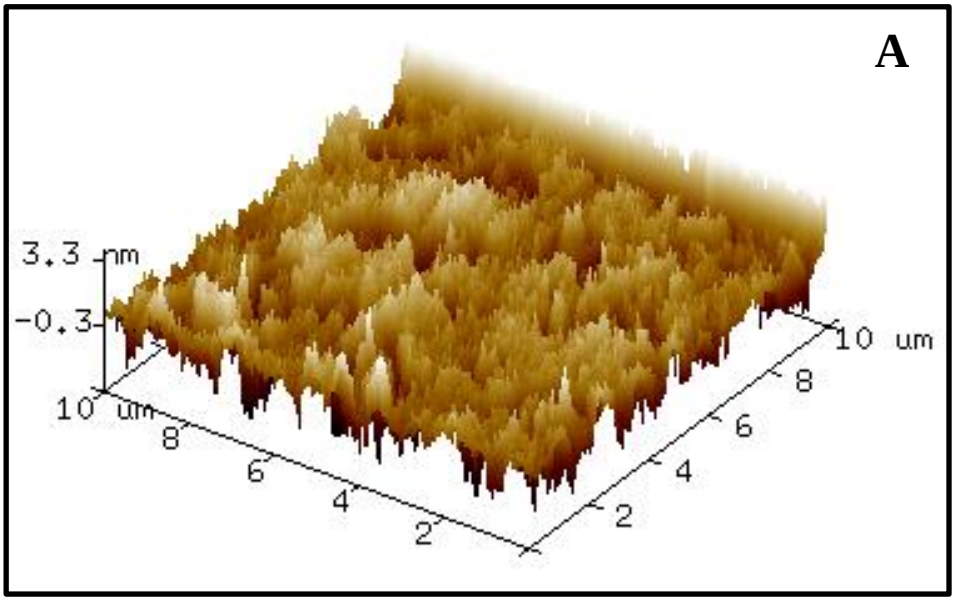

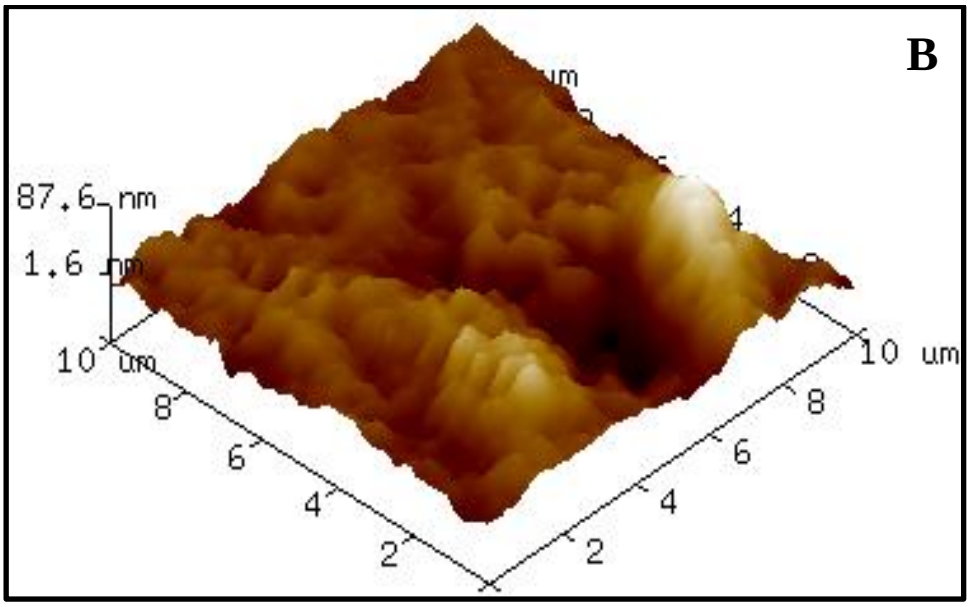
B
87.6 nm
1.6 nm
10 um
8
6
4
2
10 um
8
6
4
2

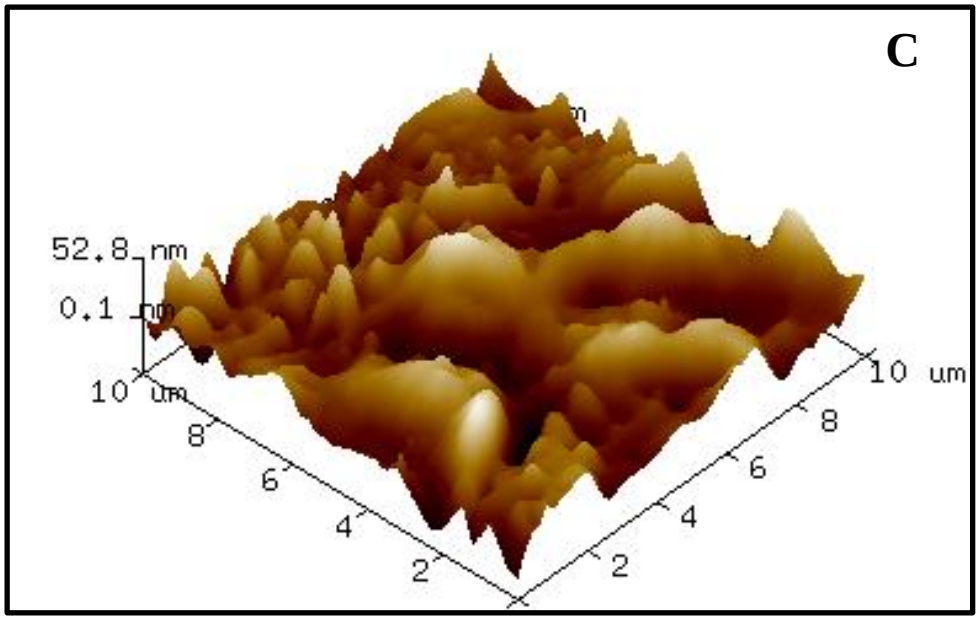
C
52.8 nm
0.1 nm
10 um
8
6
4
2
10 um
8
6
4
2

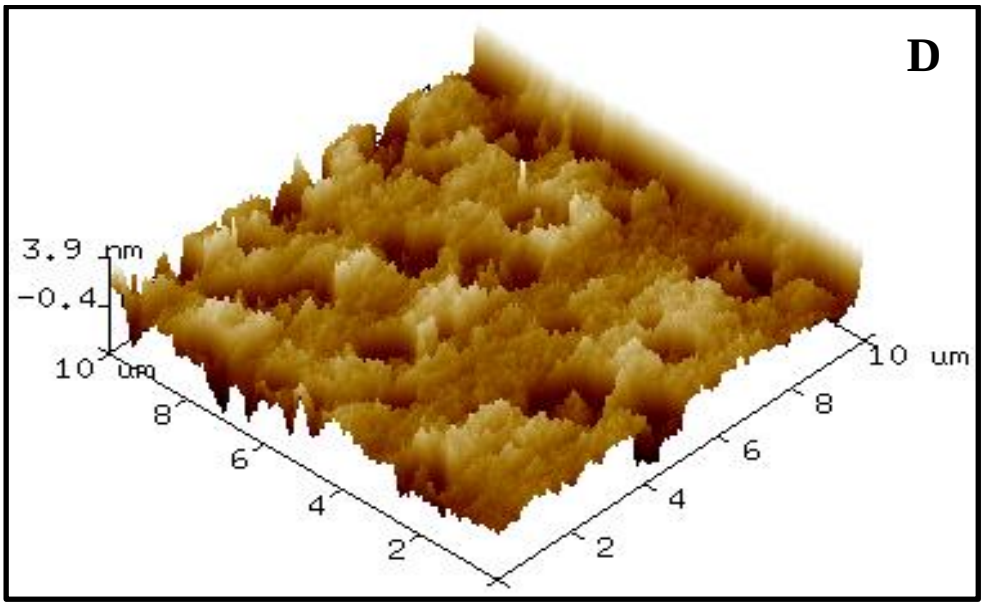

Figure 4.7 Three-dimensional images of the same images (A, B, C and D respectively) illustrated in Figure 4.6

4.5.2 Elastic modulus

Figures 4.8 shows representative elastic modulus maps for the control and warm modified bituminous binders. The modulus range is between 360.3-529.9 MPa and 148.2-262.0 MPa for controls 40/60 and 100/150 binders respectively. Localized differences in the elastic modulus are evident, with the para phase being stiffer than the peri phase, which is in agreement with Dourado *et al.* (2012). Sasobit and Rediset WMX have a significant effect on the modulus of bituminous binders. Again, the distinct modulus of the para and peri phases cannot be determined due to the effect of the wax, which increased the modulus overall significantly. Sasobit increased the modulus range of the control binder from 360.3-529.9 MPa and 148.2-262.0 MPa to 921.6 MPa-8.0 GPa and 459 MPa-2.2 GPa for 40/60 and 100/150 binders respectively. Sasobit forms a network structure that prevents the molecules from moving (Jamshidi *et al.* 2013), which in turn increases the stiffness of the binder. In fact, a significant increase in the film modulus of bituminous binder should be taken into account to accurately characterize and model the performance and behaviour of asphalt mixtures.

.

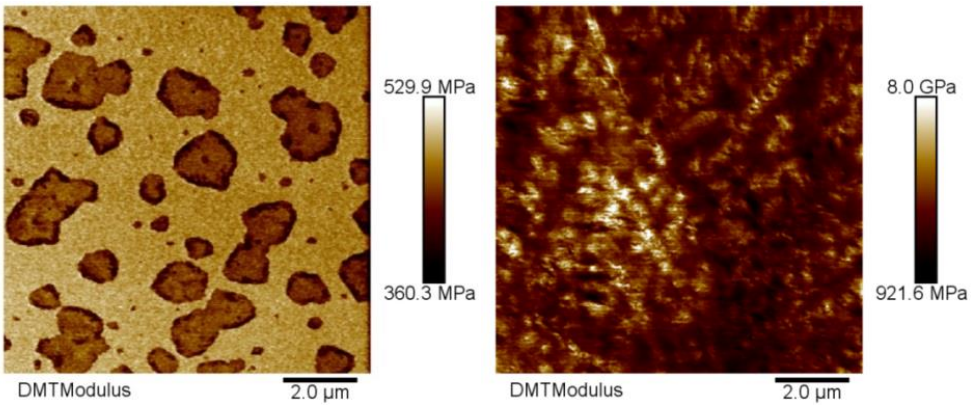

(A) H **(B) H+Sa**

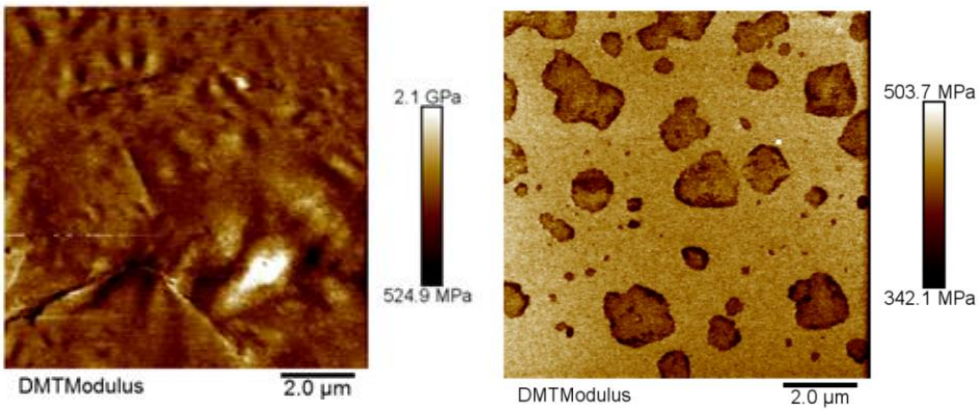

(C) H+Rw **(D) H+ Rl**

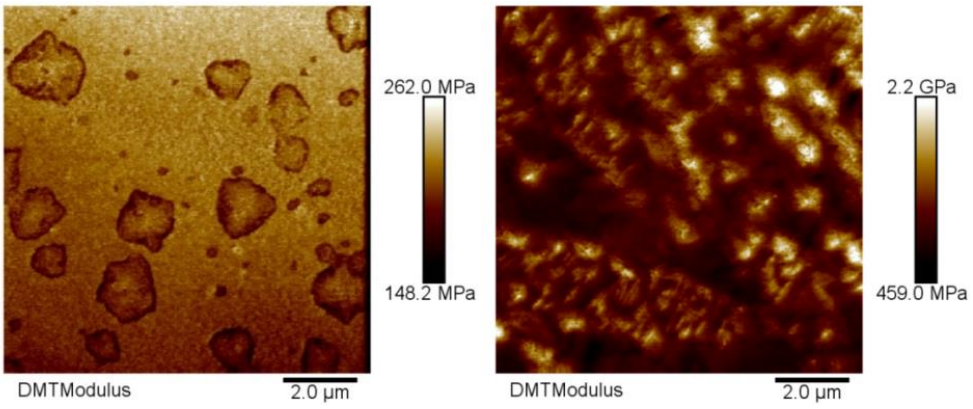

(E) S **(F) S+ Sa**

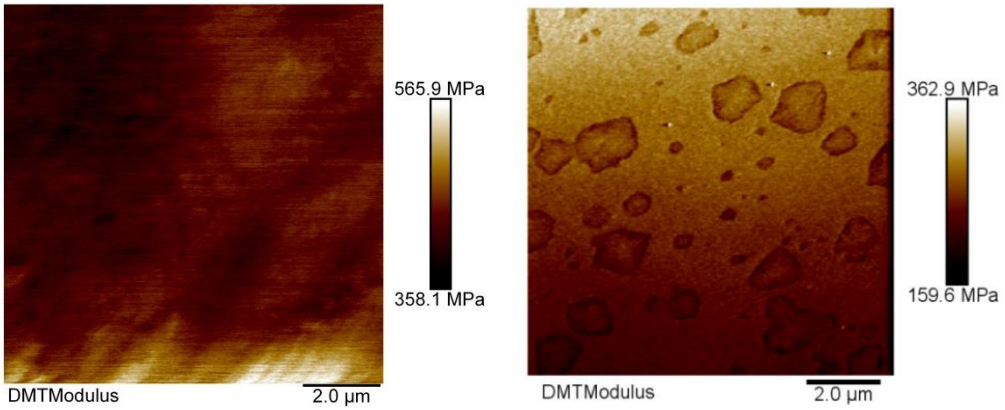

(G) S+ Rw (H) S+ Rl

Figure 4.8 Elastic modulus maps of A-H, B-H+Sa, C-H+Rw and D-H+Rl, E-S, F-S+Sa, G-S+Rw and H-S+Rl

The same behaviour was noticed when adding Rediset WMX, although it had less effect than the Sasobit. Rediset WMX also increased the modulus of the bituminous binder regardless of binder grade. Due to the presence of wax, the modulus of the peri and para phases cannot be identified because peri phase is considerably larger and the para phase is significantly reduced and disappeared in the majority of the scans. The modulus generally increased by approximately 4.5 and 2.5 times for the modified binder grades respectively. The mean and standard deviation of elastic modulus for control and modified-warm binders is presented in Figure 4.9. It should be noted that Nanoscope Analysis software integrated with AFM calculates the average elastic modulus of captured image and the mean of elastic modulus presented in Figure 4.9 is the average of five images for each control and WMBBs. Interestingly, as Rediset LQ did not alter the binder properties and acts only as workability and adhesion promoter; Rediset-modified bituminous binders had the same modulus mapping as the control binders. Furthermore, the peri and para phases can be clearly seen.

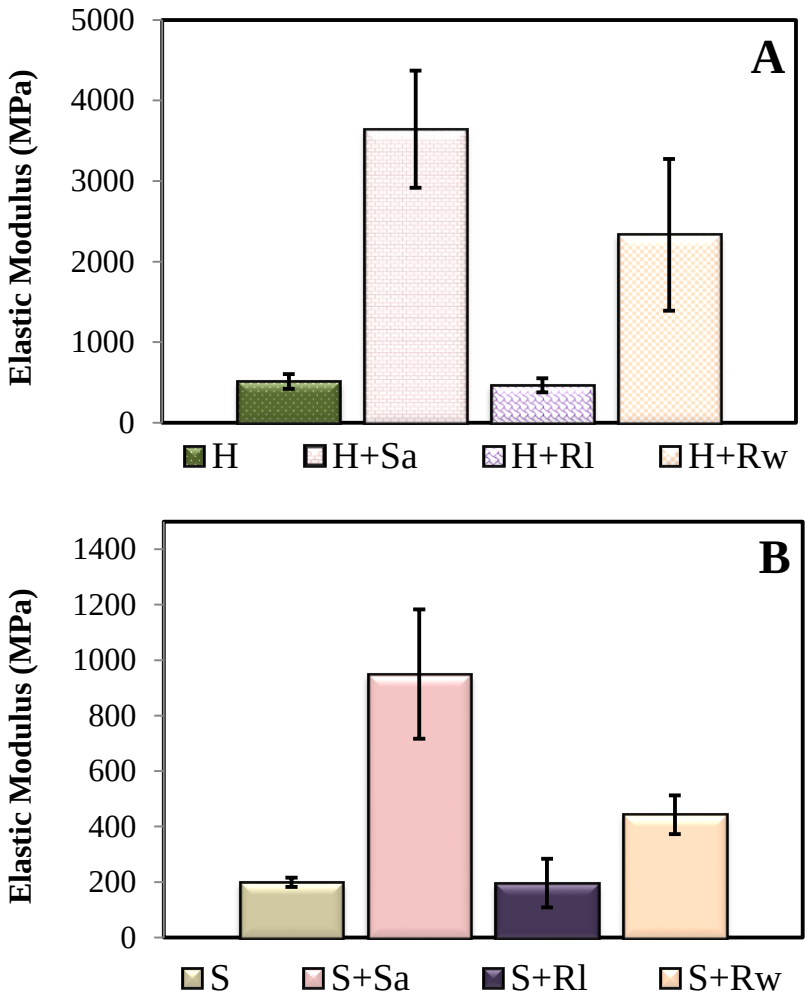

Figure 4.9 Elastic modulus of controls (A-40/60 and B-100/150) and WMBBs

4.5.3 Deformation

The second parameter is the maximum deformation, which can be defined as the penetration of the probe into the surface at the peak force after subtracting cantilever compliance. As the load on the bitumen sample under the probe increases, the penetration also increases, reaching its maximum value at the peak force. The maximum sample deformation is calculated from the difference in separation from the point where the force is zero to the peak force point. As expected, material with high modulus value exhibited less deformation value as presented in Figure 4.10. Figure 4.11 shows the mean deformation properties of warm modified bituminous binders. It is clear that Sasobit significantly increased the modulus of the bitumen and it also significantly improved the deformation of the control binders regardless of binder type.

In fact the rank of increasing the modulus of the control binders was the same as the rank of decreasing the deformation of the control binders. Moreover, as Rediset LQ did not alter the binder properties and only acted as an active adhesion, binders modified with such an additive exhibit similar values of deformation rate compared to control binders. Characterising the deformation of film binders using PeakForce QNM provides pavement engineers with new insight into the behaviour and response of virgin and modified bitumen to resist deformation or repeated load. Less deformed binder film should lead to a more durable mixtures and retard crack propagation. Because, as Sasobit forms a lattice structure which acts as a bridge between molecules and prevents them moving, it consequently increases the viscosity of asphalt binders at lower temperatures, and so the fatigue cracking should improve. This finding can explain why Sasobit significantly improved the fatigue life of bitumen as presented previously in Chapter 3. Rediset WMX exhibited the same trend but less significantly than Sasobit.

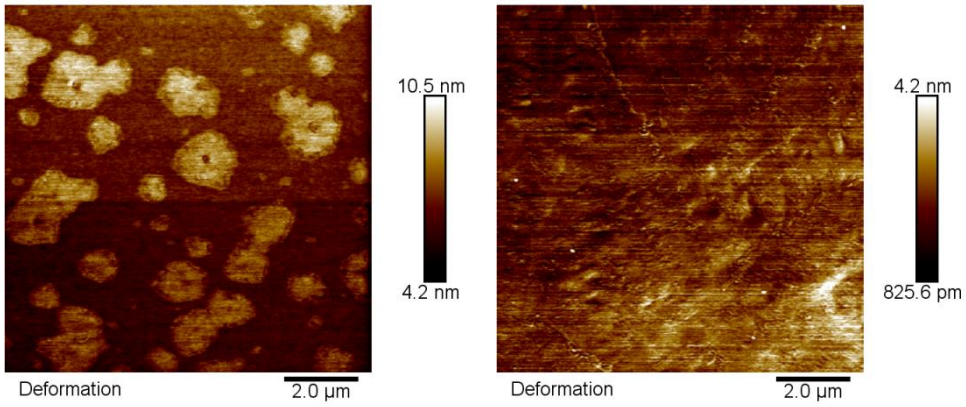

(A) H **(B) H+ Sa**

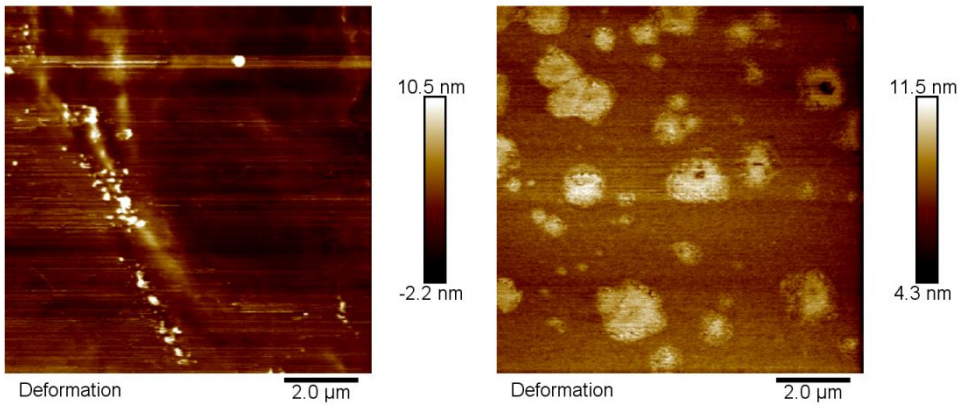

(C) H+Rw **(D) H+ Rl**

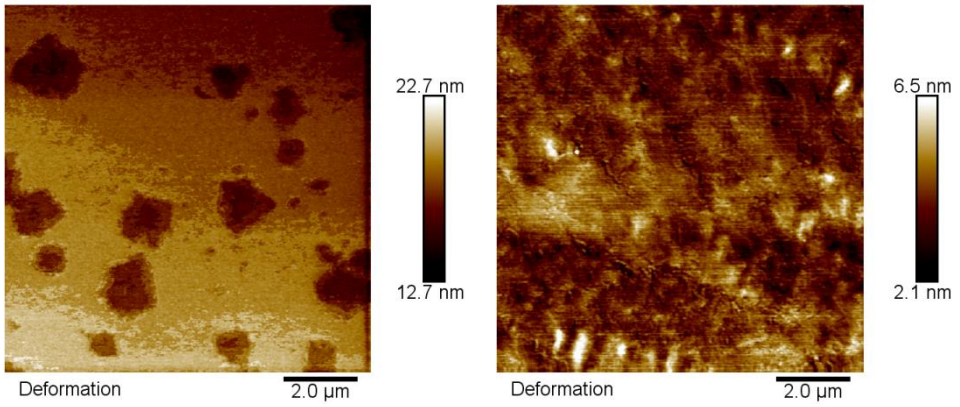

(E) S **(F) S+ Sa**

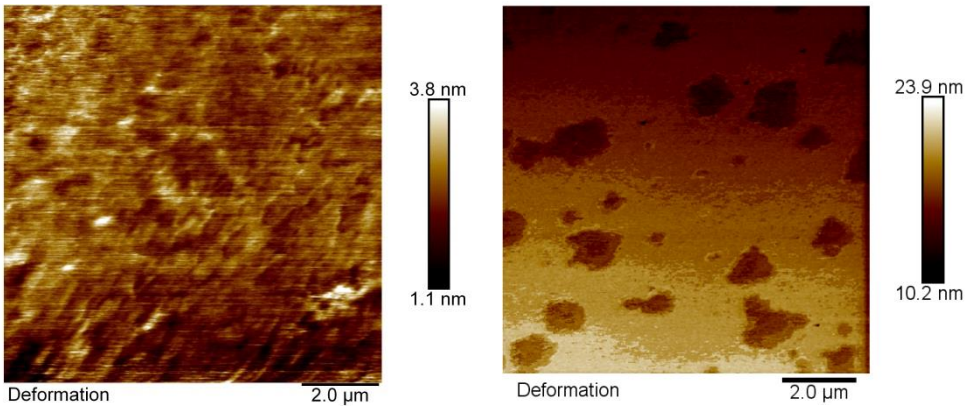

(G) S+ Rw **(H) S+ Rl**

Figure 4.10 Deformation maps of control binders and WMBBs

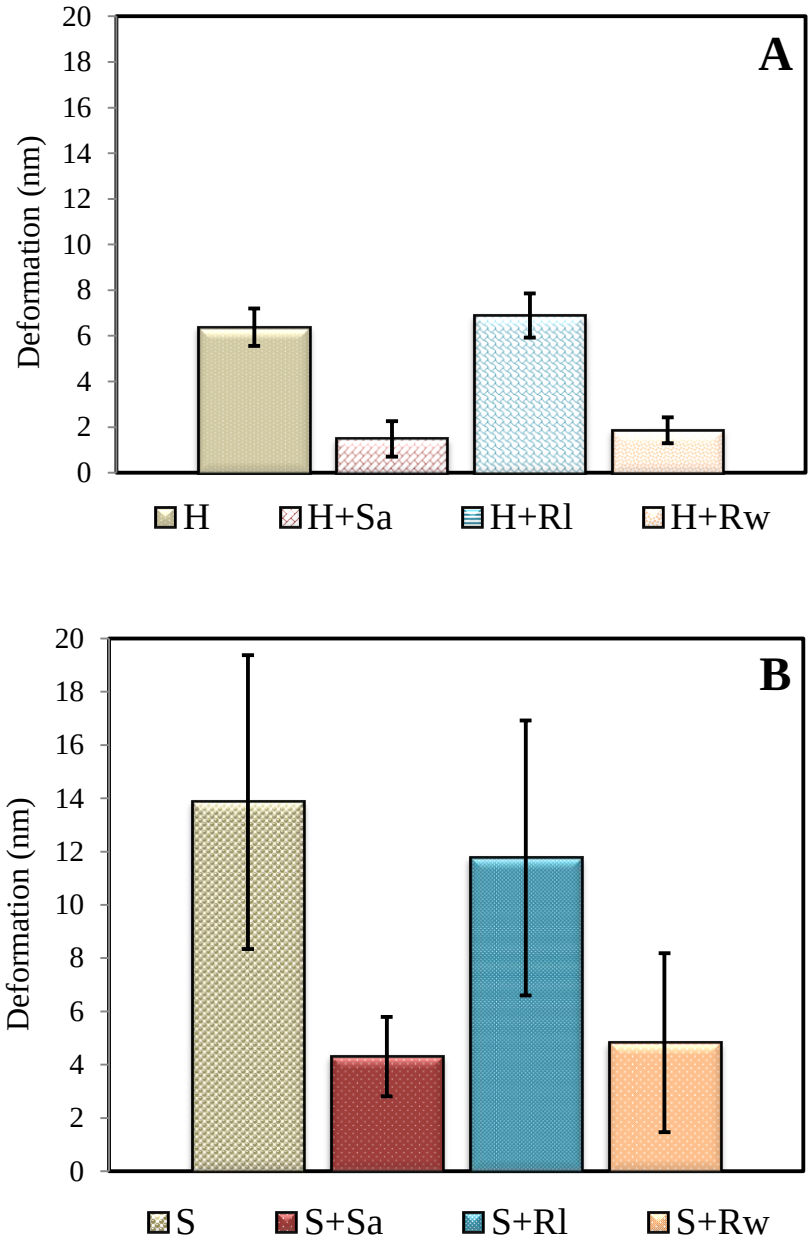

Figure 4.11 Deformation of controls (A-40/60 and B-100/150) and WMBBs

4.5.4 Adhesion characterisation

In terms of asphalt mixtures, adhesion is defined as the energy required for breaking or fracturing the force of adhesion between binder and aggregate, causing them to be isolated from each other. Many researchers have investigated the energy required to break the adhesive bond of the aggregate-binder system based on the concept of Pull-off test using different techniques such as Pneumatic Adhesion Tensile Testing Instrument (PATTI) and Bitumen Bond Strength (BBS)

(Kanitpong and Bahia 2003,Kanitpong and Bahia 2005,Copeland 2007,Miller *et al.* 2010,Greyling 2012). The failure mode between aggregate and binder can be either adhesive or cohesive or a mixture of both, depending on many factors such as the thickness of the binder film, type of aggregate and testing temperature (Al-Haddad and Al-Khalid 2015). However, with AFM, adhesion represents the attractive force between the probe and binder which is characterized by the minimum force as presented previously in the in Figure 4.3 (Young *et al.* 2011)

Figure 4.12 shows the adhesion maps of virgin and warm-modified binders. It can be noticed that the phases of virgin binders exhibited different adhesion values. The adhesive force of the para phase is higher than that of the peri phase for both 40/60 and 100/150 binders. However, with the inclusion of Sasobit and Rediset WMX, it was difficult to recognize the force of adhesion of these phases, but there was a significant increase in the adhesion force of the overall bitumen surface, which can be seen in Figures 4.12-B, 4.12-C, 4.12-F and 4.12-G, regardless of binder type. As mentioned previously, Sasobit is classified as a viscosity reducer, and it was not expected to affect the adhesion characterisation of bitumen; however, in fact it has positive improvements in terms of adhesion. Impact of Sasobit on adhesion in the current chapter agrees with what was reported previously by (Nazzal and Abu-Qtaish 2013). It is therefore that the current chapter recommends that Sasobit is used as active adhesion to increase the quality and serviceability of flexible pavements. More importantly, the tolerance dosage of Sasobit should be further investigated with binders that have different dosages of wax in their structures.

Rediset WMX exhibits the same trend as Sasobit. Rediset WMX increased the adhesive force by approximately double, while there was less improvement in the adhesive force of Rediset LQ-modified bitumen, as shown in Figures 4.13-a and 4.13-b. It can also be seen that Rediset LQ improves the adhesion force of the para phase only, without affecting the adhesion of the peri phase. This point needs to be further investigated.

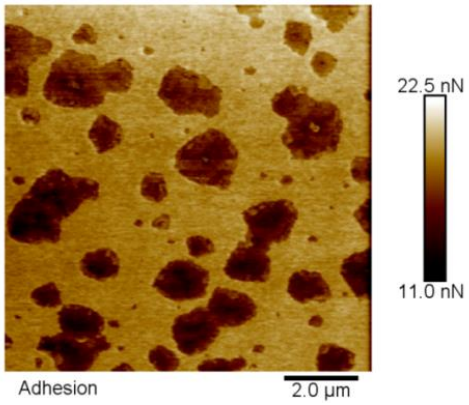

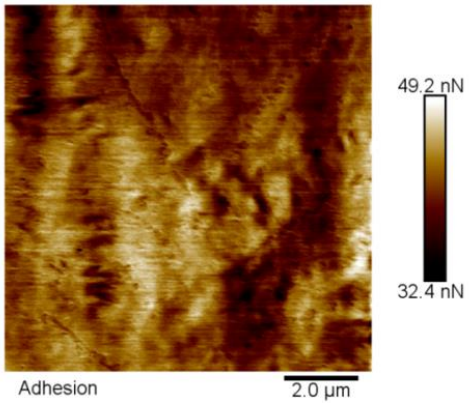

(A) H **(B) H+ Sa**

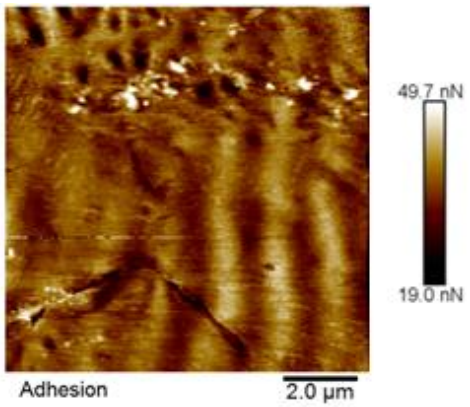

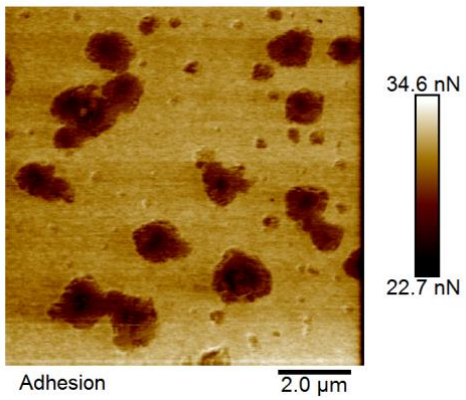

(C) H+Rw **(D) H+ Rl**

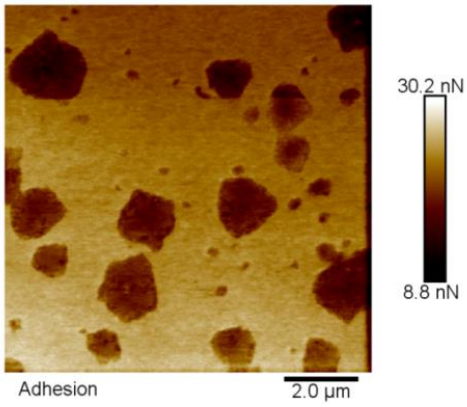

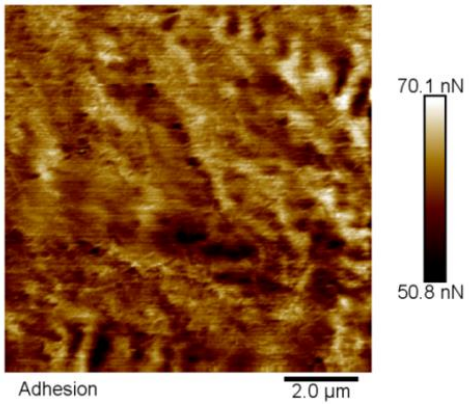

(E) S **(F) S+ Sa**

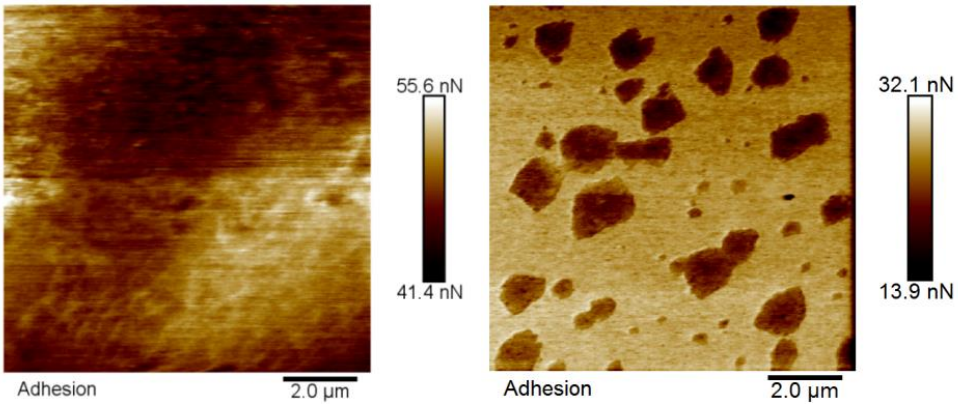

(G) S+ Rw **(H) S+ Rl**

Figure 4.12 Adhesion maps of control binders and WMBBs

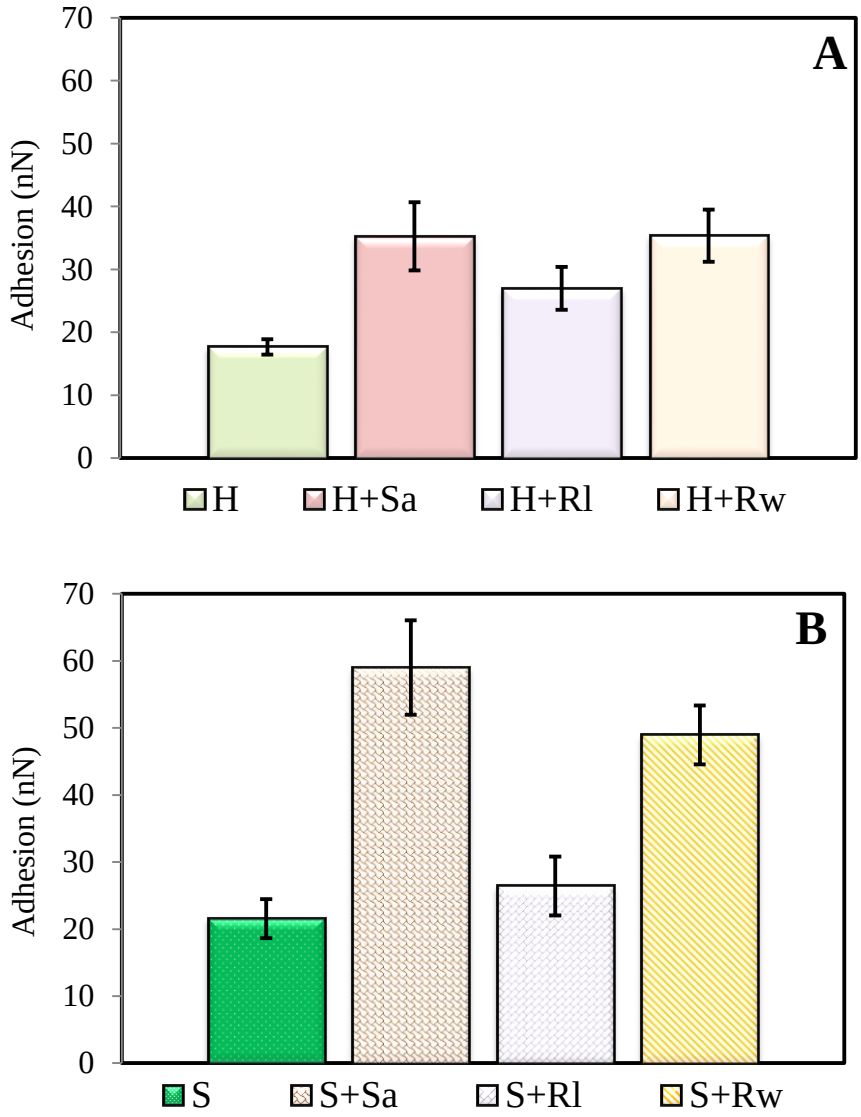

Figure 4.13 Total adhesion of control binders (a-40/60 and b-100/150) and WMBBs

4.6 Conclusions

The chapter focuses on the investigation of the effect of warm additives on the mechanical properties, topography, modulus, adhesion and deformation of micro-structure phases of bituminous binders as determined by AFM. PFQNM is a sophisticated technique for mapping mechanical properties at the nano-level, which provides new insight into the behaviour and response of virgin and modified bitumen, and mapping the micromechanical properties of phase separation in bitumen. Based on the results presented, several conclusions can be drawn:

1. The earlier observed microstructures of bitumen consisting of peri phase and para phase can also be found in this study. The interesting point is that, as the control binders are classified as non-waxy, the catana phase does not exist. However, when Sasobit and Rediset WMX were added to the control bitumen, the catana phase was noticed, which confirmed the fact that the presence of the catana phase is associated with the presence of wax in the structure of the bitumen. Rediset-modified bituminous binders had the same structure as the control binders, as Rediset has no effect on the topography and micro-structure of bitumen phases, while Sasobit and Rediset WMX changed the topographical structure of virgin bitumen due to the presence of wax.

2. Sasobit significantly increased the modulus of binders at the nano-scale by approximately seven times and five times for 40/60 and 100/150 binder grades respectively, and decreased the deformation of the modified bitumen because it forms a lattice structure and generates a bridge between molecules, which in turn prevents them from moving. The interesting point is that Sasobit also improved the adhesion characterisation of the bitumen; it can therefore be suggested that Sasobit could be used as an active adhesion to improve aggregate-binder bonding.

3. Both Rediset WMX and LQ improved the adhesion characterisations of warm modified bituminous binders by around 110% and 50% respectively. However, the deformation and modulus were only improved using Rediset WMX because Rediset LQ did not alter the binder properties of net bitumen.

Chapter Five

Nano-Mechanical Properties of WMA Determined with Nanoindentation

5.1 Introduction

In the current chapter, the effect of production temperatures and warm additives on the performance of WMAs was investigated using nanoindentation. Nanoindentation, which is an advanced mechanical testing technique, was used in the study to determine the effect of Sasobit, Rediset WMX and Rediset LQ on the nano-mechanical properties of asphalt mixture phases, aggregate, interfacial transition zone (ITZ) and mastic. The nanoindentation results were used to: firstly, evaluate the effect warm additives and production temperatures on the mixture phases, aggregate, interfacial transition zone (ITZ) and mastic, as presented in the current chapter; secondly, the nano-mechanical properties of the ITZ were used to propose a new method to evaluate the degree of bonding between aggregate and binder; and, thirdly, evaluate the effect of each phase on the overall fatigue performance of WMAs, as will be presented in Chapters 6 and 7 respectively.

5.2 Nanoindentation in pavement engineering

There has been extensive research conducted on the macro- and micro-mechanical properties of asphalt mixture composites and their constituents; however, there have been only a few studies on their nano-mechanical properties (Tarefder *et al.* 2010,Tarefder and Zaman 2009,Li *et al.* 1999,Khorasani *et al.* 2013). In fact, there is a need to characterise and understand the mechanical properties at the nano-scale because the interactions among the composite phases happen at this scale (Igarashi *et al.* 1996). The combination of asphaltic mixture, asphalt binder film, mastic (binder filled by aggregate smaller than 0.063 mm) and aggregate plays a significant role in the stress-strain behaviour of asphalt mixtures (Tarefder *et al.* 2010). The hardness and elastic modulus of the asphalt binder film have a

significant direct effect on the low temperature fracture of the asphalt mixtures (Desai 2007,Park *et al.* 1999,Chang and Meegoda 1997), whilst the mastic has a substantial effect on the healing behaviour of the asphalt mixture and the aggregate impacts the durability of asphalt mixture (Allen and Searcy 2001,Roberts *et al.* 1996).

Not surprisingly, there is little understanding of the fundamental properties of asphalt mixtures' phases at the nano-scale because of the inability to characterise the mechanical properties of asphalt mixtures at this scale. However, with the advent of nanoindentation, it has become possible to measure the mechanical properties of film and the interactions among the main components of asphalt mixture, binder and aggregate. Despite the fact that there are now efforts and endeavours made to study the influence of warm additives on the overall performance of asphalt mixtures, the effect of warm additives on the nano-mechanical properties of asphalt mixtures has yet to be studied. Therefore, there is a need to understand to what extent warm additives have an impact on the interactions among asphalt mixture components.

Generally, the evaluation of asphalt mixtures in terms of rutting, fatigue, etc., is based on the properties of the mixture as a whole, while nanoindentation is capable of differentiating the properties within mixture phases, mastic, interfacial transition zone (ITZ) and aggregate. Nanoindentation is a powerful technique to measure the hardness and elastic modulus. In terms of nanoindentation, elastic modulus is the measure of the force that is needed to compress a material sample (a stiff material needs more force to deform it compared to a soft material); while indentation hardness measures the resistance of a sample to deformation due to a constant compression load from a sharp object.

Nanoindentation is a new technique by which to measure the nano-mechanical properties of mixture phases. Stangl *et al.* (2007) conducted a study to investigate the effect of styrene-butadiene-styrene on the characteristics of bitumen using nano- and micro-indentation tests. One control bitumen (B 50/70) and one polymer-modified bitumen (60/90) were considered in the experimental work. They showed that the initial creep compliance obtained from

nanoindentation correlates with rheological properties (complex shear modulus and phase angle) obtained from a DSR.

Tarefder *et al.* (2010) investigated the nano-mechanical properties such as hardness and elastic modulus of asphalt binders and asphalt concrete using nanoindentation. Indentation tests were carried out on a base binder and two polymer-modified performance binder grades, PG70-22 and PG76-28, and also two Superpave asphalt mixes. Aggregate, matrix (Material Passing No. 4 sieve) and mastic (Material Passing No. 200 sieve) phases of each asphalt concrete sample were indented using both Berkovich (sharp and three-sided pyramidal) tip and spherical tip. It was shown that the spherical tip is suitable for asphalt binder materials, but the attempts made in their study were not successful in measuring hardness and elastic modulus of the base binder because it is soft. This is because the unloading data are linear and vertical, which could not be analysed using existing analytical tools as shown in Figure 5.1.

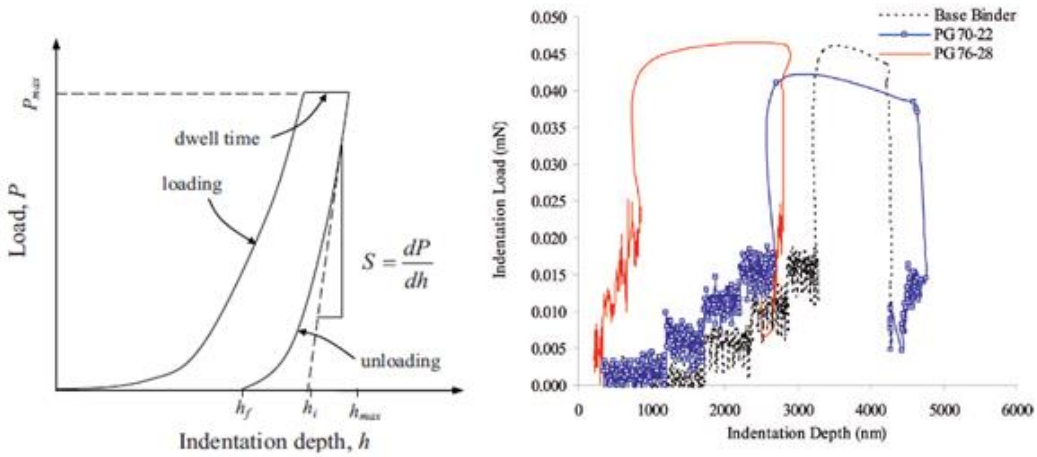

Figure 5.1 Left- typical load-displacement curve, Right- load-displacement curve on binder (Tarefder et al. 2010)

It was also reported that both Berkovich and spherical indenters can be used on asphalt concrete, but it should be noted that the Berkovich indenter penetrates the asphalt samples more than the spherical indenter under the same load. Moreover, the average values of the modulus of limestone and dolomite aggregate are within the range of commonly accepted values from the literature. The authors concluded that nanoindentation provides micromechanical properties

of mastic, aggregate and matrix without separating them from the asphalt concrete. Those properties may provide more realistic inputs for the micromechanical models such as a discrete element model of the characterisation of fracture, healing and ageing behaviour.

Tarefder and Faisal (2013) characterised the effect of ageing on aggregate and mastic of asphalt mixtures. They reported that the hardness and elastic modulus of mastic increases with ageing process and this increase resembles the age-hardening behaviour of the asphalt binder. However, the elastic modulus and hardness of aggregate remained constant after ageing process. The effect of moisture on mastic was studied by Hossain *et al.* (2016). It was reported that wet mastic was viscous than dry mastic and the surface of wet mastic was stiffer than that of dry mastic because of erosion, viscosity loss of wet surface due to conditioning effects. The authors believes that beneath the surface, the wet mastic is softer than the dry mastic and therefore they suggested the effect of moisture on properties of mastic as a function of depth from the surface should be further investigated.

Khorasani *et al.* (2013) also explored the local nano-scale mechanical properties of fine aggregate mixture phases and interfaces. The interface between aggregate and binder was found to have hardness and modulus values between those of aggregate and mastic.

5.3 Principles of Nanoindentation

5.3.1 Overview

In the nanoindentation test, an indenter is used to indent a sample surface and the load applied by the indenter is plotted continuously with the displacement of the indenter into the sample. The shape of the loading and loading curves depends on the elastic and plastic properties of the sample material (Tarefder *et al.* 2010,Mondal 2008). This technique is capable of producing contact areas and penetration depths in the order of nanometres. The forces involved are in the mili-newton range. In the conventional indentation tests, the area of the contact is calculated directly from the measurements of the residual impression left in the specimen surface upon removal of the load.

However, in nanoindentation tests, as the size of the residual impression is too small to be measured directly, the contact area is measured indirectly from the depth to which the indenter has penetrated the specimen and the known geometry of the indenter (Tarefder *et al.* 2010). Figure 5.2 shows the defined shape of some probes.

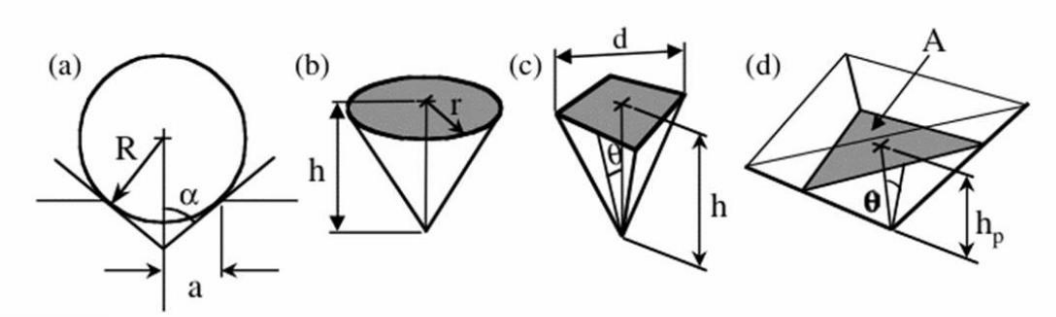

Figure 5.2 Indentation Parameters for (a) Spherical, (b) Conical, (c) Vickers and (d) Berkovich indenter tips (R, r, a and h are tip dimensions and **θ** and **α are angles**) (Mondal 2008)

5.3.2 Analytical method

In the test of indentation, a probe with a defined shape is pushed into a sample surface and the indentation load (P) and penetration depth (h) are measured as a function of time. A schematic of a typical load-indentation depth curve recorded during a nanoindentation test is presented in Figure 5.3. The quantities shown are the peak indentation load (P_{max}), the depth of peak load (h_{max}), the final depth of the contact impression after unloading (h_f), and the initial unloading stiffness (S), which is the slope of the unloading curve. Figure 5.4 demonstrates what happens during a test.

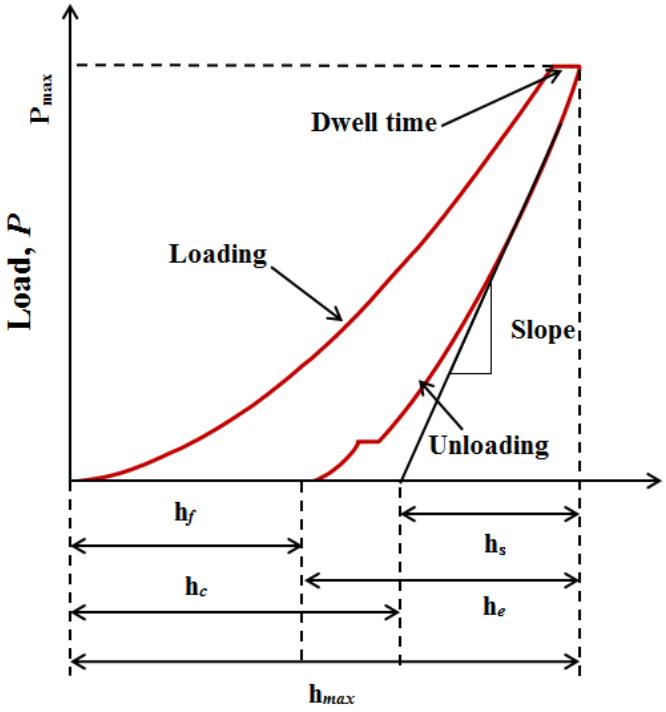

Figure 5.3 Schematic of load versus indentation depth curve, H_f: final depth after unloading, h_s: displacement of the surface at the perimeter of the contact, h_c: Vertical depth along which contact is made, h_e: elastic depth recovery during un loading, h_{max}: depth at maximum load

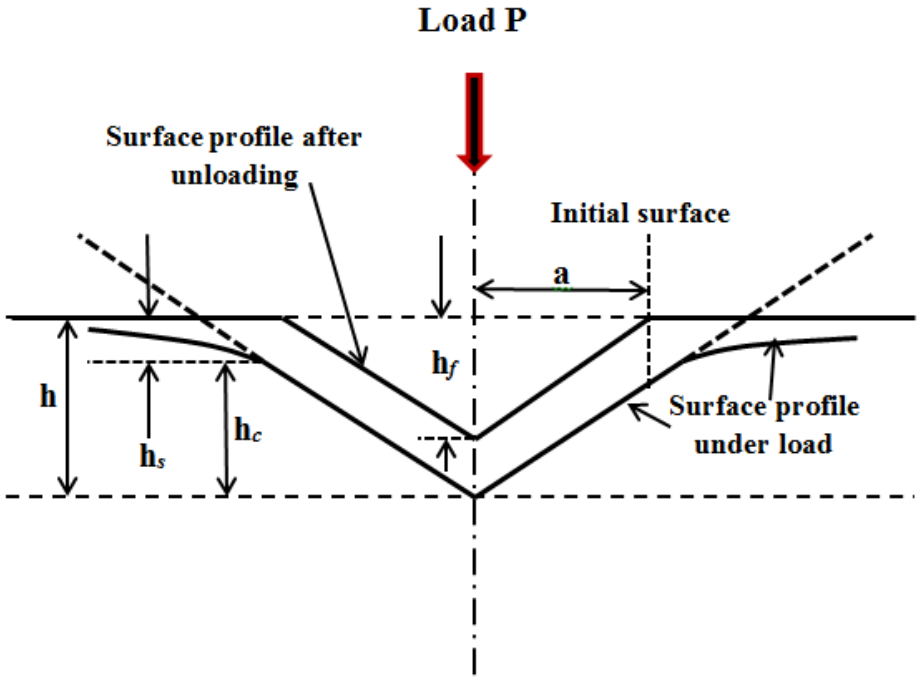

Figure 5.4 Schematic representation of a material section through indentation process

Oliver and Pharr (1992) developed an analytical method which is widely used for determining elastic modulus and hardness from nanoindentation data. This analysis procedure is essentially based on the solution to the elastic contact problem developed by Boussinesq and Hertz in the late 19th century (Johnson and Johnson 1987) and Stilwell and Tabor (1961). The Oliver and Pharr method is summarised in this subsection.

An elastic modulus of the sample, E_s, on the load-indentation behaviour can be calculated through the following equation:

$$\frac{1}{E_r} = \frac{1-v_s^2}{E_s} + \frac{1-v_i^2}{E_i} \quad (5.1)$$

Where E_s is the elastic modulus of the sample; v_s is Poisson's ratio of the sample (e.g. for asphalt material v_s is 0.3 to 0.4); E_i is the elastic modulus of the indenter tip; and v_i is the Poisson's ratio of the indenter (e.g., for Berkovich tip v_i=0.07).Once the data for the whole indentation are recorded, the elastic modulus of the sample is calculated based on equation. 5.1.

The reduced modulus is related to the unloading portion of the load-indentation curve according to equation 5.2 (Pharr *et al.* 1992).

$$E_r = \frac{\sqrt{\pi}}{2}\frac{S}{\sqrt{A}} \quad (5.2)$$

Where S=dP/dh= initial unloading stiffness and A is the contact area as presented in equation 5.3. It is therefore clear that the measured modulus relies on how initial stiffness and contact area are determined from the indentation data.

$$A=\pi a^2 \quad (5.3)$$

Where A is the contact area; and a is the contact radius as presented in Figure 5.4

In order to identify the contact area or the projected area during the indentation, Based on Oliver and Pharr's method (Oliver and Pharr 1992), S is firstly determined by fitting the depth versus loading data using the following power-law function:

$$P=\alpha(h-h_f)^m \quad (5.4)$$

Where P is the indenter load; h is the elastic displacement of the indenter; h_f is unrecoverable or plastic depth; α and m are constants; and m is a power-law exponent which is related to the geometry of the indenter. m is equal to 1 for a flat-ended cylindrical indenter, 1.5 for a paraboloid of revolution and 2 for a cone.

As shown in Figure 5.3, the total displacement, h, can be written as shown in equation 5.5, whereas the elastic depth recovery during unloading is presented in equation 5.6.

$$h=h_c+h_s \quad (5.5)$$

$$h_e=h_{max}-h_f \quad (5.6)$$

Where h_c is the vertical depth along which contact is made and h_s is the displacement of the surface at the perimeter of the contact. In order to determine the contact depth h_c from the experimental data, the authors extrapolated the tangent line to the unloading curve at the maximum loading point down to zero load. This yields an intercept value for depth h_c that estimates the h_s and re-writes the contact depth h_c associated with maximum loading point as follows:

$$h_c=h_{max}-\varepsilon\frac{P_{max}}{S} \quad (5.7)$$

Where ε is a geometric constant. The value of ε for each type of indenter probe shown in Figure 5.2, is presented in Table 5.1.

Once h_c has been determined, the area in equation 5.3 can be re-written as follows:

$$A=\pi a^2=\pi(Rh_c) \quad (5.8)$$

where R is radius of probe and hc is calculated using equation 5.7.

Hardness (H) value is calculated based on maximum load (P_{max}) divided by the projected area A of contact at the peak load, as presented in equation 5.9.

$$H=\frac{P_{max}}{A} \quad (5.9)$$

Table 5.1 Contact area for different indenter probe geometries (Mondal 2008)

Probe Type	Projected Area (A)	Semi-angle θ(deg)	Effective cone angle α (deg)	Intercept factor	Geometry correction factor β
Sphere	$2\pi R h_p$	N/A	N/A	0.75	1
Berkovich	$3\sqrt{3}\, h_p^2 tan^2\theta$	65.3	70.2996	0.75	1.034
Vickers	$4h_p^2 tan^2\theta$	68	70.32	0.75	1.012
Cone	$\pi h_p^2 tan^2\alpha$	-	-	0.72	1

5.4 Experimental work

5.4.1 Materials

The same binder grades and warm additives used in Chapters 3 and 4 are also adopted here. The only aggregate type adopted in this study is granite, which was supplied from Croft Quarry, Aggregate Industries, UK. The properties of the granite received from the supplier are shown in Table 5.2. It should be noted that the recommended dosages of Sasobit, Rediset WMX and Rediset LQ which were adopted in this chapter in all mixtures are 2%, 2% and 0.5% by the weight of the bitumen respectively

Table 5.2 Aggregate specifications

Properties	Granite
Apparent particle density	2.67*-2.71** Mg/m^3
Polished Stone Value	58*
Water absorption	1.7%*, 0.6%**
Los Angeles coefficient	27
Aggregate abrasion value	2.9
Oxidisable sulphides	0.02%*, 0.41%**
Acid-soluble sulphate	0.02%*, 0.05%**
Water-soluble sulphate	<0.01*, <0.001**

*** Coarse aggregate ** Fine aggregate**

5.4.2 Mix design

Under the scope of this study, gap-graded hot rolled asphalt is adopted to manufacture HMA and WMA. The nominal maximum aggregate size is 10mm, which is suitable for surface courses. The recipe specification method was adopted in the design of the mixes; this method provides details for the aggregate type and gradations and binder grades for particular mixes. The HMA and WMA were manufactured according to the British Standards recipe (BS 597-1 2005). Figure 5.5 illustrates the particle size distribution of the aggregates for HMA and WMA.

To manufacture slab of asphalt mixture, the laboratory asphalt mixer shown in Figure 5.6 was used. Before mixing, the aggregates and bitumen were heated at the same required mixing temperature. The aggregates were heated overnight while the bitumen was heated prior to mixing for four hours. After mixing, the mixtures were poured into steel moulds 305mm × 305mm × 100mm, which had been sprayed with silicon grease to prevent adhesion and then covered with oiled paper in order to prevent the materials adhering to the compactor. After that, the laboratory roller compactor shown in Figure 5.7 was used to compact the slab at four pressure levels, 25, 40, 50, and 72 psi; each pressure was applied for 10 cycles over the slab. The roller compactor was heated to a high temperature in order to prevent any sudden cooling the mixtures.

The procedure for manufacturing the asphalt mixtures was based on the British Standards specification (BS EN 12697-33 2003). The compacted slabs were then left for 24 hours, to cool at ambient temperature before de-moulding.

The production temperatures for hot mix asphalt (controlled mixtures) manufactured using (40/60) grade and (100/150) grade were 155°C and 145°C respectively; whereas the production temperatures of WMA manufactured using (40/60) grade and (100/150) penetration grade were 135°C and 145°C for (40/60) grade and 125°C (100/150) grade. Therefore, the reduction in the production temperature was 10°C and 20°C for WMA incorporating (40/60) grade and 20°C for WMA incorporating (100/150) grade.

For each mixture, an identification code was defined as follows: H: Hot Mix Asphalt; W: Warm Mix Asphalt; Second H: hard binder (40/60) grade; S: Soft binder (100/150) grade; Sa: Sasobit; Rw: Rediset WMX; Rl: Rediset Liquid. For example, HH155 and HS145 are the controlled hot mix manufactured using (40/60) and (100/150) grades respectively, whilst WHSa135 and WSSa125 are the WMA Sasobit-modified manufactured using (40/60) and (100/150) grades manufactured at 135°C and 125°C respectively.

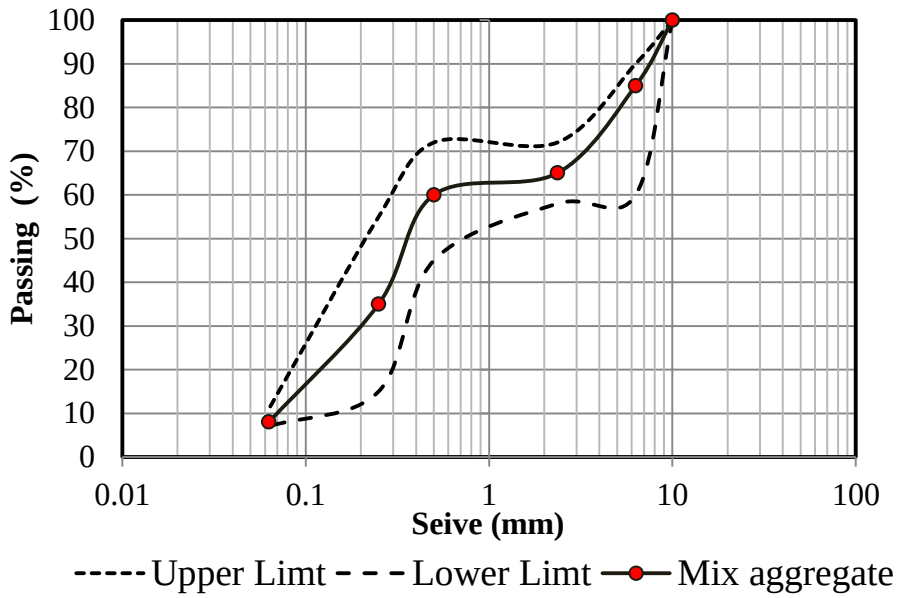

Figure 5.5 Particle size distribution of the aggregates for HMA and WMA

Figure 5.6 The controlled-temperature laboratory asphalt mixer

Figure 5.7 The laboratory roller compactor

5.4.3 Volumetric Properties of HMA and WMA

The bulk densities of controlled HMA and WMA are measured according to the British Standards (BS EN 12697-6 2012). The apparent density of gap-graded hot rolled asphalt is 2.385 (Mg/m^3).

Table 5.3 Bulk densities and air voids for all asphalt mixtures

Mix	Bulk Density(Mg/m3)	Air Voids %
HH155	2.248	5.7
WHSa135	2.258	5.3
WHSa145	2.265	5.0
WHRw135	2.264	5.1
WHRw145	2.272	4.7
WHRl135	2.255	5.5
WHRl145	2.279	4.4
HS145	2.254	5.5
WSSa125	2.260	5.3
WSRw125	2.275	4.6
WSRl125	2.279	4.4

As can be seen in Table 5.3, warm additives have a superior performance in increasing the bulk densities and decreasing the air voids of WMA. Furthermore, the effect of mixing temperature on the volumetric properties of WMA is significant. In fact, Sasobit is a flow modifier and viscosity reducer;

therefore, it is expected to have an influence on the volumetric properties and mix design of asphalt. Hurley and Prowell (2005b) found that air voids in asphalt mixtures decreased when Sasobit was added. This can be confirmed, as achieving the required density is quicker for Sasobit-WMA mixtures than for HMA even at lower compaction temperatures, as the study by Zaumanis (2010) has reported that asphalt mixtures modified with Sasobit reached their final density after 100 gyrations at 135°C, whereas HMA reached the final density after 170 gyrations at 155°C. In fact, one can say that Sasobit generally has no negative effect in terms of mix design and volumetric properties.

In this study, as presented in Table 5.3, Sasobit increased the bulk density of asphalt mixtures, which in turn leads to a decrease in the air voids in these mixtures. When WHSa145 was manufactured at 145°C (the production temperature was only 10°C lower than that of control mix HH155), Sasobit improved the volumetric properties further.

Rediset WMX and LQ also improve the volumetric properties of asphalt mixtures. As already mentioned, Rediset WMX is both a viscosity reducer and a surfactant; therefore, it decreases the internal frictional forces between the interfaces of the aggregate and binder and decrease the surface tension of binder (Banerjee *et al.* 2012,Capitão *et al.* 2012), which leads to improve wettability of aggregate by binder. This phenomenon leads to improving the bulk density and, in contrast, decreasing the air voids.

As Rediset LQ was developed to improve compaction, it also increased the bulk density and decreased air voids in asphalt mixtures. It should be noted that Rediset LQ significantly improved the volumetric properties of asphalt mixture when it was manufactured at 145°C (only 10°C lower than the control mix (HH155) using 40/60 binder grade). In fact, the level of improvement in the volumetric properties is approximately the same in case of when using 40/60 and 100/150 binder grades if reduction in the production temperatures is limited to 10°C using 40/60 binder and 20°C using 100/150 binder compared to their control mixtures HH155 and HS145 respectively. It should be noted that WMAs were successfully produced at temperatures of 20°C lower than the control mixtures and the aggregate was fully coated, whereas, Brookfield did not predict the real

reduction in the production temperature as previously presented in Chapter 3. It can therefore be confirmed that it is inadequate to estimate the expected production temperature of WMA based on Brookfield measurements.

5.4.4 Sample preparation

After manufacturing the asphalt mixture slab, firstly a beam of (305 × 65 × 25 mm) was discarded from one side of the slab and then two beams of (305 × 65 × 50 mm) were cut using a diamond cutter. The beams were tightly fixed on the wooden prisms using tape in order to prevent them moving whilst the cylindrical samples were being cored. This ensures that damage to the cylindrical -samples is avoided when the coring pet punches from the top face to the bottom face of the beam, and moreover reduces the vibration.

Cylindrical samples 25 mm in diameter and 50 mm in height were cored using an electric coring machine with continuous water in line with preparation of DSR samples as will be presented in Chapter 7. Marcrist Ø25 mm (inside diameter) crown core drill were used to prepare cylindrical nanoindentation samples. Four cylindrical samples were obtained from each Mix. The Cylindrical nanoindentation samples were left to dry for 24h at ambient temperature. They were then put in oven maintained at 20°C for half an hour to ensure they are completely dried. A small cutter as shown in Figure 5.8-A was used to prepare nanoindentation disc samples (NDSs) 25 mm in diameter and 10 mm in height as presented in Figure 5.8-B.

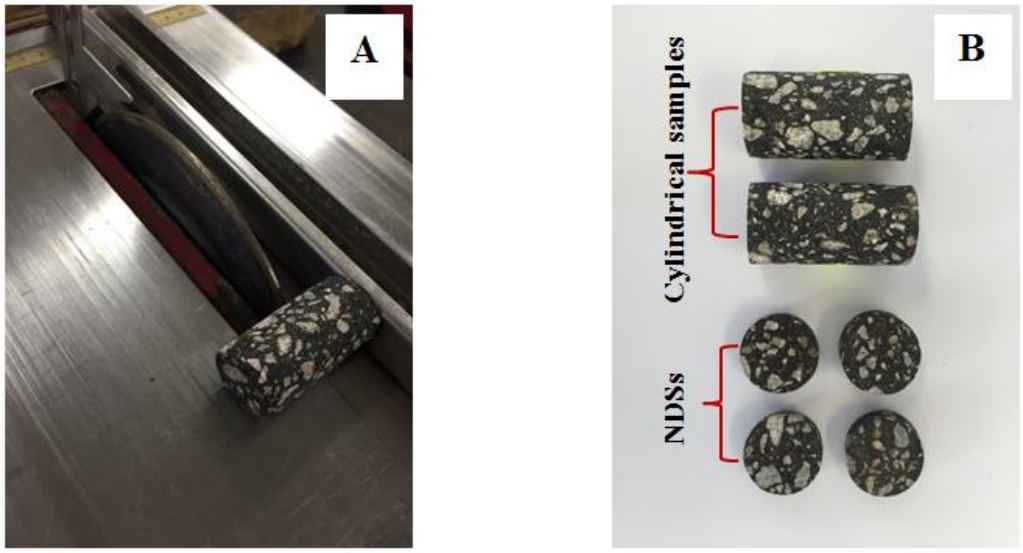

Figure 5.8 A- Preparation of nanoindentation disc samples, B- nanoindentation disc samples

It is essential that asphalt mixture samples tested using nanoindentation have a very smooth surface as the contact area is measured indirectly from the depth of penetration, as explained previously. Therefore, if the surface is rough or not adequately polished, errors in determining the area of contact may lead to obtaining inaccurate results for nano-mechanical properties, hardness and elastic modulus. In this study, a customised specimen preparation holder was used for polishing the nanoindentation disc samples (NDSs). Each NDS was fixed on the brass bar using double-sided tape. The brass bar was used in order to load the sample onto the grinding paper in the polishing machine. In order to adequately level the sample during polishing, slices of Alumina sheet were used.

A grinding machine rotating at an angular speed of 300 rpm was used to polish the sample to surface roughness finish of approximately 5µm under continuous cold water and then a grinding machine rotating at an angular speed of 150 rpm using fine aluminium powder and wet polishing cloth paper was used to obtain a finishing surface roughness of 0.05 µm (approximately 49 nm). At the first stage, the sample was firstly polished using silicon carbide abrasive paper of 80 for 10 to 15 minutes in order to adequately level it and remove any cutter effects from its surface. Polishing then continued using a sequence of silicon carbide abrasive papers of decreasing abrasiveness (120, 180, 320, 600, 1200,

2500 and 4000) under continuous cold water. Each specimen was polished for 10 minutes with each grade of paper.

After this stage, the specimens were washed in a water bath to remove any remaining dust. In order to finish the surface down to 49 nm, a second special polishing machine was used with fine aluminium powder and wet cloth paper. The NDSs were again fixed on a brass bar (32 mm in diameter and 13 mm in height) using double-sided tape. During this stage, the specimen was firstly polished down to surface roughness finish of 1μm using fine aluminium powder (its particle size is 1μm) and then was polished down to surface roughness finish 0.05μm using polishing cloth paper of 0.05μm and fine aluminium powder (its particle size is 0.05μm). Once the process had been completed, the specimens were washed in a water bath to remove any remaining dust. It should be mentioned that that the optical microscope (Nikon Epiphot Time Inverted Microscope) was used to check the microstructure between polishing steps to ensure an adequate smooth surface was obtained using this approach.

5.5 Laboratory testing

5.5.1 Test equipment

Nanoindentation tests were conducted using a Nano Indenter G200 (Keysight Technologies, Chandler, AZ, USA). The displacement resolution of this instrument is < 0.01 nm while the maximum indentation depth is > 500 μm. More importantly, the positioning accuracy allows accurate determination of and distinguishing between asphalt mixtures phases, aggregate, interfacial transition zone (ITZ) and mastic. The Nano Indenter G200, as shown in Figure 5.9, has an integrated with optical microscope, which allows users target indentation test sites with micrometre-scale precision.

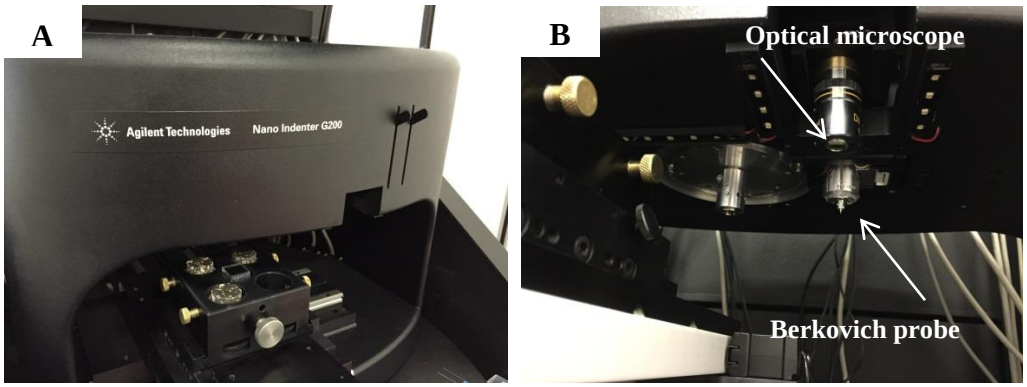

A-Nanoindenter B- Berkovich probe and optical microscope

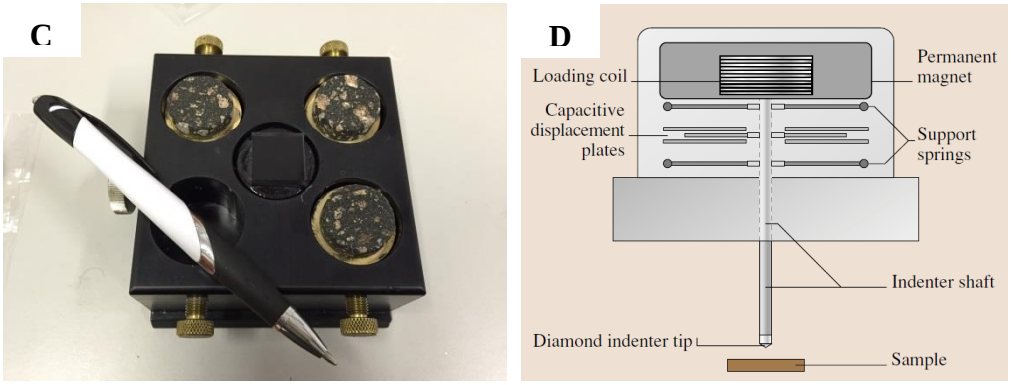

C-Sample tray D-Schematics of indenter (Mann 2004)

Figure 5.9 Nano Indenter G200

5.5.2 Loading configuration

Nanoindentation testing was conducted with a Berkovich indenter probe. The indenter was used as per the Hardness-Modulus at depth method based on Oliver and Pharr's theory (Oliver and Pharr 1992) to find the initial slope *S* of the unloading curve at maximum depth. In this study, the Hardness-Modulus at depth method was used and the controlled depth was set to 2000 nm for all asphalt mixtures, and the probe penetration stopped when the maximum depth was reached. By using this method, it is easy to distinguish between mixture phases, as each phase-loading response must be different from the others. The strain rate target was 0.05 1/s, while peak hold time was 10s (for mixtures produced using 40/60 grade) and 30s (for mixtures using 100/150 grade) and surface approach velocity was 10 nm/s.

Chudoba and Richter (2001) recommended that the maximum load should be retained for a period of 10s to 60s before the onset of unloading in order to

remove the viscous effect of asphalt materials. Tarefder *et al.* (2010) used a dwell time of 30s in their study while Khorasani *et al.* (2013) conducted their study on asphalt composites without taking the dwell time into account because of their belief that the dwell time approach did not yield consistent or repeatable results during Tarefder *et .al* study. However, Khorasani *et al.* (2013) reported that there were cases in which irregular curves were obtained, creating a negative slope, because of adherence of the binder or mastic to the probe or due to the presence of pores. In fact, the negative slope occurs because of the viscous effect of asphaltic material not because of the reasons that they mentioned because, if the binder or mastic adheres to the probe, this will affect the nano-mechanical properties (hardness and elastic modulus) of the next point as the geometry of the probe will increase. Furthermore, in the case of the presence of pores, the pop-in phenomenon will be highlighted (Tarefder and Faisal 2013). This phenomenon has also been noticed in the current study, as shown later in this chapter.

It is therefore crucial that the dwell time must be considered in order to obtain accurate results. Not only that, a very smooth surface is very important in obtaining a smooth loading and unloading curve without any noise. As mentioned previously, in this study, dwell times of 10s and 30s were used for mixtures manufactured using 40/60 binder grade and 100/150 binder grade respectively because it was difficult to remove the viscous effect of mixtures produced using 100/150 binder grade at a dwell time of 10s.

Calibration was performed using fused silica before and after testing each batch of samples to ensure that all obtained results were reliable. The elastic modulus and hardness of fused silica are 72.7 GPa and 9.38 GPa respectively. Poisson's ratio was assumed to be 0.3 for all asphalt mixture phases. All testing was conducted at 22°C and the temperature was controlled using an A/C provided in the testing room.

5.5.3 Determination of mixture phases

Three phases could be distinguished in the asphalt mixture sample, aggregate, ITZ and mastic. Mastic is the phase generated by mixing the bitumen with fine aggregate particles passing through a 0.063 mm sieve. As aforementioned, the

controlled-depth method was used to measure hardness and elastic modulus of control HMA and WMAs. Three samples were tested for each mixture. In each sample, 20 points of indentation were carried out on each mixture phase, aggregate, ITZ and mastic. The optical microscope integrated into the nano indenter was used to distinguish between mixture phases, as shown in Figure 5.10.

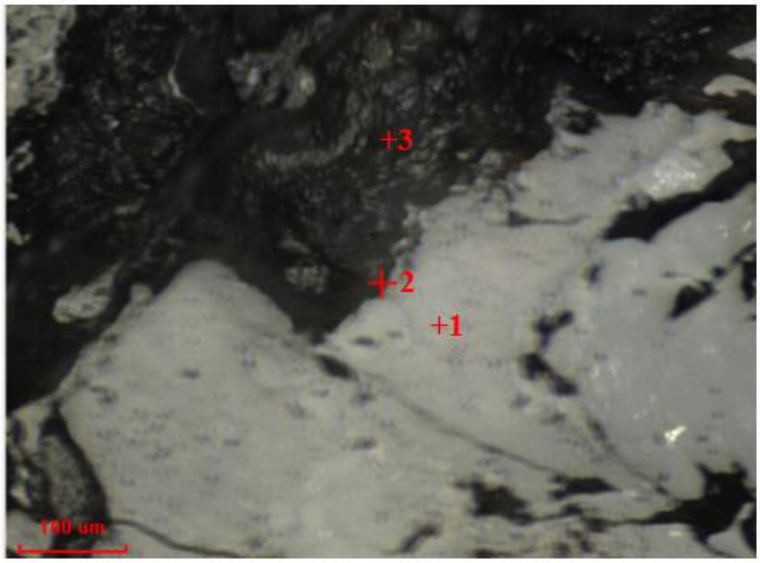

Figure 5.10 Indentation points (+1 aggregate, +2 ITZ and +3 Mastic)

As can be seen in Figures 5.11 and 5.12, a high maximum load was required to indent the aggregate 2000 nm relative to high stiffness, whereas the response load on ITZ is between the load value of the aggregate and the load value of the mastic. This was consistent for all asphalt mixtures tested in this study. It was always found that the response load on the fused silica remained constant and its hardness and elastic modulus were not affected; therefore, one can be sure that there was no dust on the probe.

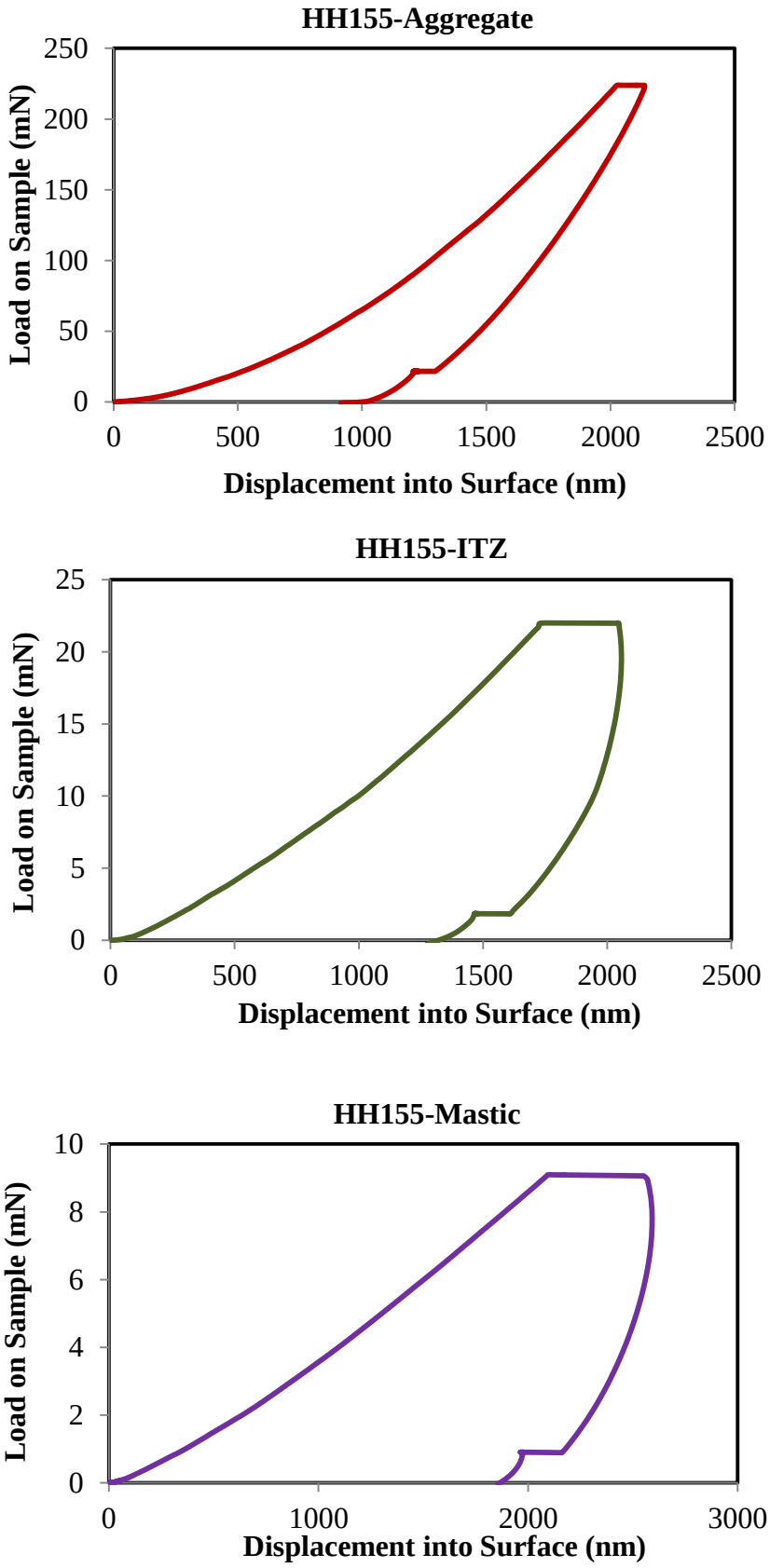

Figure 5.11 Example of response load against displacement on aggregate, ITZ and mastic for control (HH155) asphalt mixture

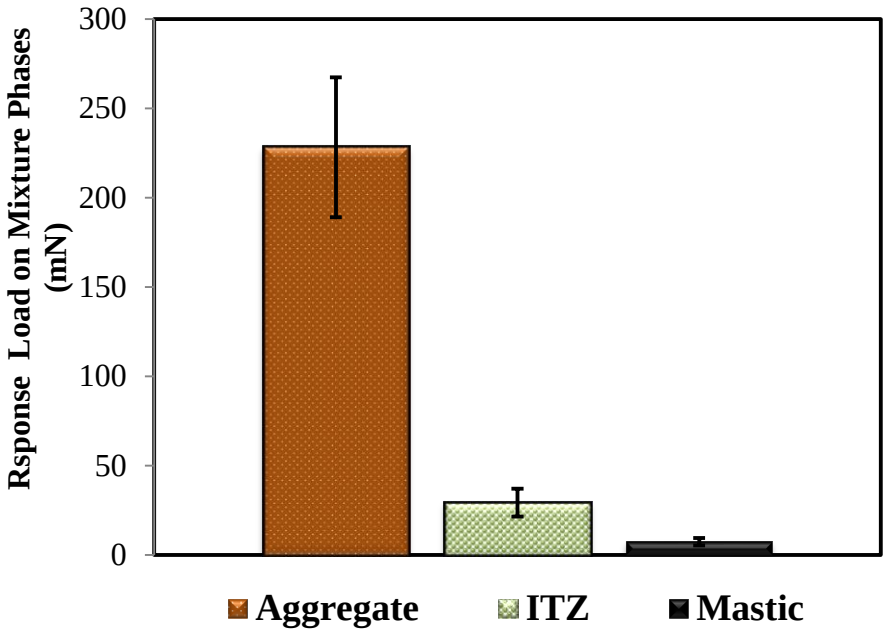

Figure 5.12 Response load on aggregate, ITZ and mastic for control (HH155) asphalt mixture

5.5.4 Statistic analysis

One-way analysis of variance (ANOVA) was used to check the statistical difference between the nano-mechanical properties of mixture phases. ANOVA analysis was performed using a statistical significance level of 5% ($\alpha = 0.05$) with aid of F-distribution. The analyses were performed using Microsoft Excel analysis ToolPak, data analyses, ANOVA-single factor. In this analysis, it was assuming that the null hypothesis is true. The null hypothesis is accepted when p-value is higher than the predetermined significance level α and F-value is less than $F_{critical}$. However, one often rejects the null hypothesis when the p-value is less than the predetermined significance level α and F-value is higher than $F_{critical}$. The hypotheses for one-way ANOVA are:

$H_0 : \mu 1 = \mu 2$ (Accept the null hypothesis)

$H_a : \mu 1 \neq \mu 2$ (Reject the null hypothesis)

Having mentioned that the analyses were directly performed using Microsoft Excel ToolPak, data analyses, ANOVA-single factor but the calculations of $F_{critical}$ and F-value can be summarised as follows:

$Df_{between} = K-1$ (5.10)

$Df_{within} = N-k$ (5.11)

$Df_{total} = Df_{between} + Df_{within}$ (5.12)

where $Df_{between}$ is degree of freedom between groups, Df_{within} degree of freedom within group, Df_{total} is total degree of freedom, K is the numbers of groups and N is the total number of values or observations . Once $Df_{between}$ and Df_{within} are calculated, $F_{critical}$ can be determined from the table of F-distribution. F-value can be calculated as follows:

$$\text{F-value} = \frac{\text{MS between}}{\text{MS within}} \quad (5.13)$$

where $MS_{between}$ is the mean square between groups and Ms_{within} is the mean square within group. In order to find F-value, the mean value of each group should be firstly calculated as presented in equations 5.14 and 5.15 respectively. And then after, the grand mean for all values is calculated using equation 5.16.

$$\mu 1 = \frac{\sum X_{i1}}{N} \quad (5.14)$$

$$\mu 2 = \frac{\sum X_{i2}}{N} \quad (5.15)$$

$$\mu^{=} = \frac{\sum xi}{N} \quad (5.16)$$

where $\mu 1$ and $\mu 2$ are the mean value of each group, $\mu^{=}$ is the mean value for all observations, X_{i1} is the observation in group one, X_{i2} is the observation in group two. The total sum of square, the sum of square within group and the sum of square between groups are calculated using equations 5.17, 5.17 and 5.19 respectively, while the mean square between groups and within group are determined using equations 5.20 and 5.21 respectively.

$$SS_{total} = \sum (X_i - \mu^{=})^2 \quad (5.17)$$

$$SS_{within} = \sum (x_{i1} - \mu 1)^2 + (x_{i2} - \mu 2)^2 \quad (5.18)$$

$$SS_{between} = SS_{total} - SS_{within} \quad (5.19)$$

$$MS_{between} = \frac{\text{SS between}}{\text{Df between}} \quad (5.20)$$

$$MS_{within} = \frac{SS_{within}}{Df_{within}} \quad (5.21)$$

Once the mean square between groups and within group are determined, the F-value is calculated using equation 5.13. As aforementioned stated, the null hypothesis is accepted when F-value is less than $F_{critical}$ and rejected when F-value is higher than $F_{critical.}$

5.6 Results and Discussion

5.6.1 Nano-mechanical properties of aggregate

It can be seen in Figures 5.13 and 5.14 that granite elastic modulus and hardness remained constant regardless of the mixture type, warm additive type, binder grade and the produced temperature of the mixture. There was no significant difference in the mean values of elastic modulus and hardness, as presented in Table 5.4, since the p-value is higher than 0.05 ($P>0.05$) for mechanical properties of aggregate, the null hypotheses was accepted and there was no difference in the data for the aggregate at 95% confidence level. However, there was a small range in the elastic modulus and hardness of the granite in the same sample because of microstructural differences and orientation of particles. For brevity, mechanical properties of granite, elastic modulus and hardness are only presented for mixtures manufactured using 40/60 binder grade, because the elastic modulus and hardness were identical for mixtures manufactured using 100/150 binder grade.

The nano-mechanical properties of the granite are equivalent to what has been reported in the literature, such as by Tarefder *et al.* (2010). Even though the type of aggregate plays generally a significant role in the overall stiffness of the mixture, it was found that asphalt binder also plays a major role in determining the mechanical characteristics an asphalt mixture portrays in resisting distress. Furthermore, the aggregate-binder bond is also a crucial parameter in evaluating the performance of asphalt mixtures.

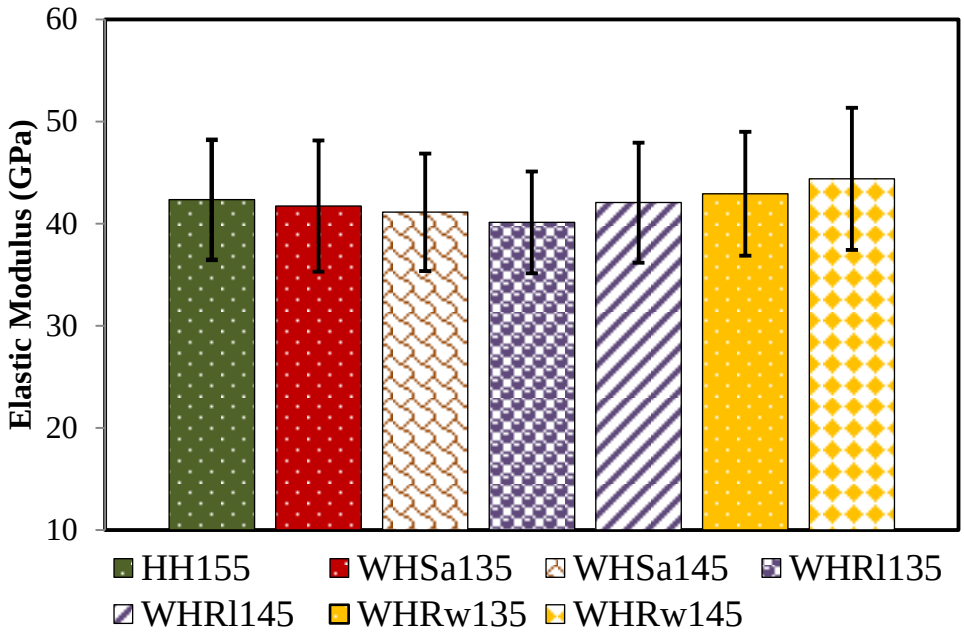

Figure 5.13 Elastic modulus of aggregate phase for all mixtures using 40/60 binder grade

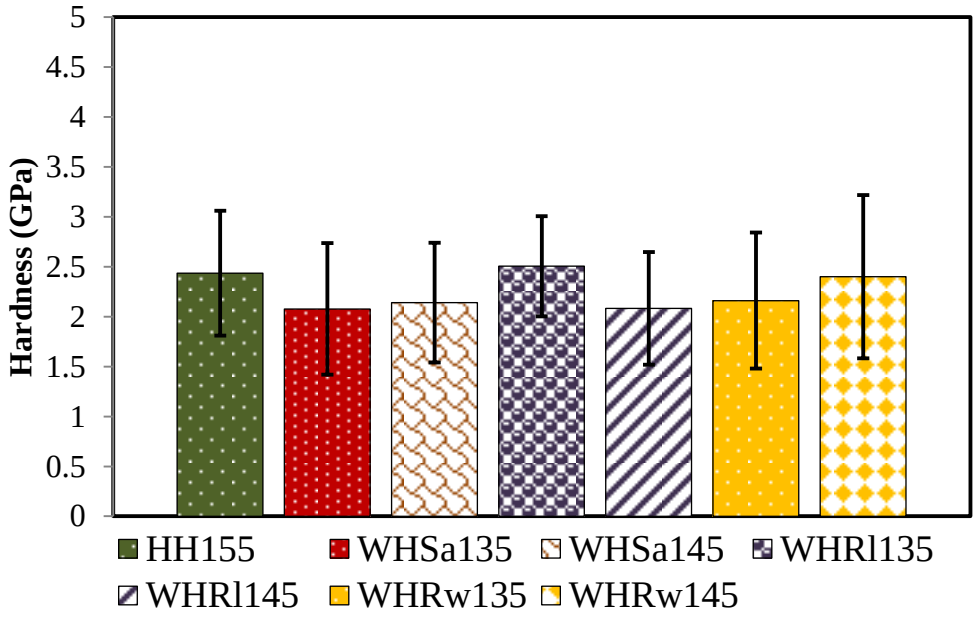

Figure 5.14 Hardness of aggregate phase for all mixtures using 40/60 binder grade

5.6.2 Nano-mechanical properties of ITZ

5.6.2.1 Response load at controlled depth on ITZ

The approach used in this chapter allowed successful determination of the nano-mechanical properties of the interfacial transition zone between the aggregate and the binder. As aforementioned elastic modulus is an intrinsic material property and is fundamentally related to atomic bonding, while indentation hardness is the resistance of a sample to material deformation due to a constant compression load from an object, it could be possible to assess the degree of aggregate-binder bond based on nano-mechanical properties of ITZ because stiffer ITZ reflects the strength bond and interaction between aggregate and binder/mastic, and this is a novel technique by which to characterise bonding using nanoindentation.

As shown in Figures 5.15 and 5.16, all warm additives have a superior performance in increasing the resistance of ITZ to deformation, which highlights that they provide better aggregate-binder bonding. It can also be seen that the production temperature has a clear effect on WHSa135, WHSa145, WHRl135 and WHRl145, which all exhibited a high load response at controlled depth regardless of any reduction in temperature, while WHRw135 had a lower load response at controlled depth. However, when the reduction in the production temperature decreased from 20°C to 10°C using 40/60 binder grade compared to that of control mix HH155, Sasobit and Rediset LQ significantly increased the resistance of the material to deformation, which was reflected by increasing the required load to reach a depth of 2000 nm. Moreover, Rediset WMX showed a positive trend when the production temperature was 145°C, lower than that of HMA by 10°C. However, in the case of incorporating 100/150 binder grade, the ITZ of WMAs produced at 125°C had higher resistance to deformation compared to the control mix HS145, which indicated that the performance of warm additives is significantly affected by the production temperature based on the binder grade.

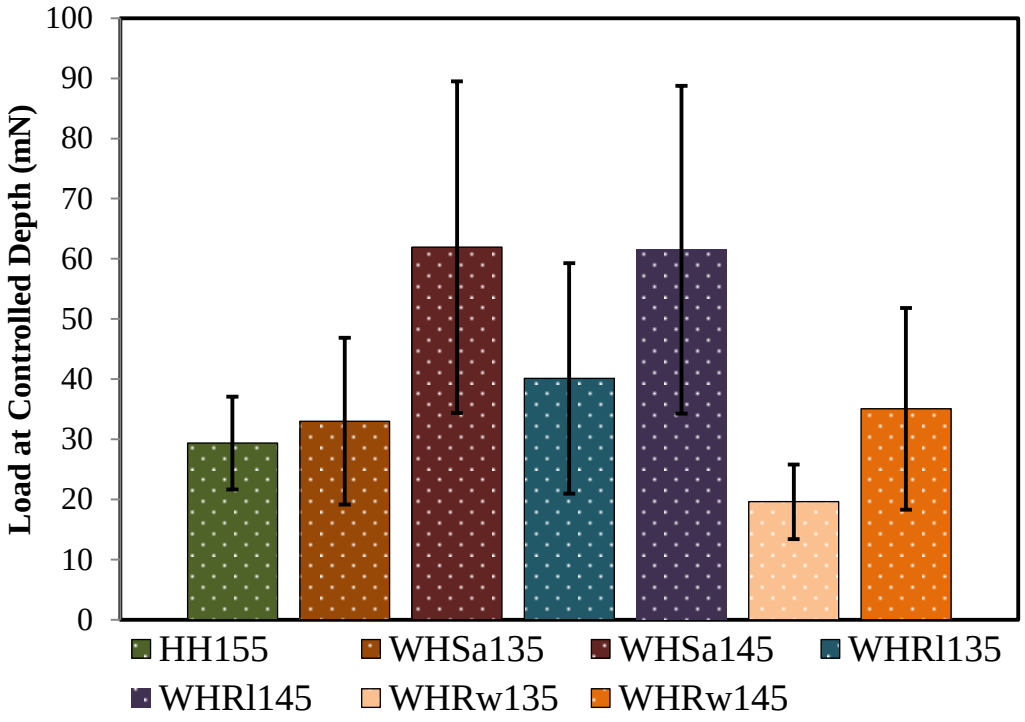

Figure 5.15 Response load on ITZ for asphalt mixtures produced using 40/60 binder grade

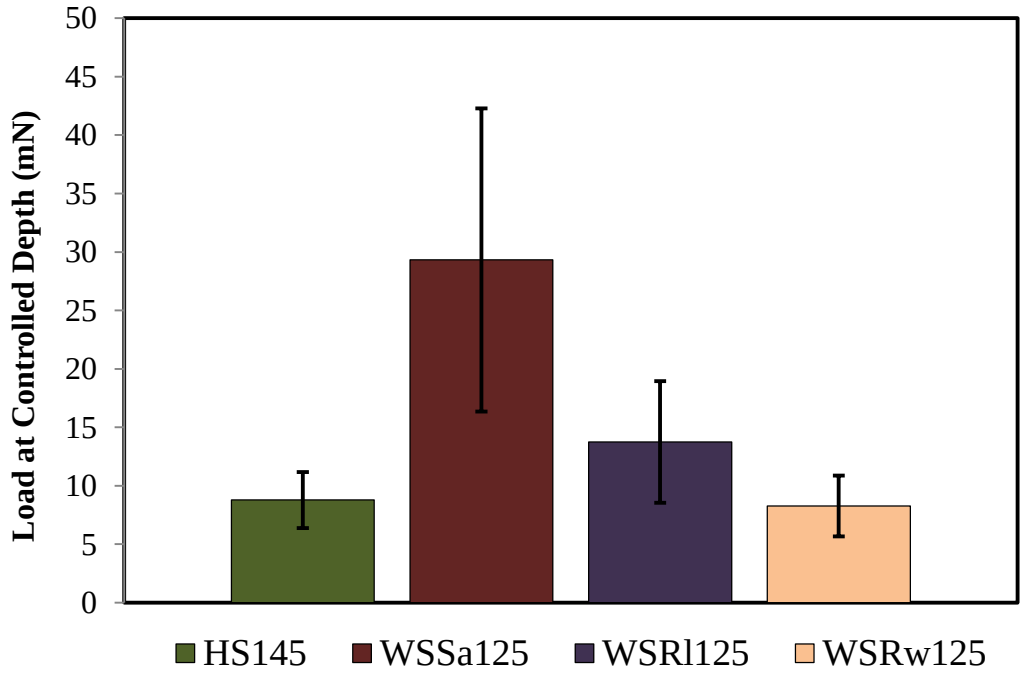

Figure 5.16 Response load on ITZ for asphalt mixtures produced using 100/150 binder grade

5.6.2.2 Elastic modulus and hardness of ITZ

Figures 5.17 and 5.18 show the elastic modulus and hardness of ITZ of asphalt mixture produced using 40/60 binder grade. It was found that the elastic modulus and hardness of Sasobit-modified asphalt mixture produced at 135°C were equivalent to control mix HH155 as there was no significant difference in the mean values of nano-mechanical properties as shown in Table 5.4. However, when Sasobit-modified asphalt mixture was manufactured at 10°C lower than the production temperature of control mix HH155, the elastic modulus of the ITZ was increased significantly by approximately 5.5 GPa in comparison with the control mixture there was statistically significant different in the mean elastic modulus ($P<0.05$) as shown in Table 5.4. In fact, Sasobit has a predominant range of hydrocarbons of chain length from 45 to 100 carbon atoms, while natural asphalt paraffin waxes are normally in the range of 25 to 45 carbon atoms. The long chains of carbon atoms increase both the plastic limit and also the melting temperature domain of asphalt binders (Wasiuddin *et al.* 2011a, 2011b). Therefore, when Sasobit is mixed with bitumen, it melts, leading to a viscosity reduction in the asphalt binder, and when the mixture cools this additive will solidify into microscopically small and uniformly distributed particles in the bitumen (Rubio *et al.* 2012). This phenomenon leads to stiffening of the binder in a similar manner to fibre-reinforced materials. Not only that, lower viscosity of bitumen due to incorporating Sasobit will allow the bitumen to diffuse more into the aggregate, thus improving the nano-mechanical properties of the ITZ.

Both Rediset WMX and LQ have active adhesion, which could displace water from the aggregate surface, enabling not only the coating of the aggregate but also creation of a strong chemical bond between the aggregate and the bitumen, but it was not possible to achieve this until the bitumen temperature was adequate for it to adhere to the aggregate. Despite the fact that the experiments in term of volumetric properties showed that WMA can be manufactured at lower temperatures, the bitumen grade must be taken into account to achieve the required mechanical properties and produce a sustainable asphalt mixture. As shown in Figures 5.17 and 5.18, Rediset LQ significantly increased the nano-mechanical properties of the ITZ, especially when the warm asphalt mixture was produced at 145°C using 40/60 binder grade. The values of elastic modulus and

hardness of WHRl145 were double those of the control mix and the mean value was statistically significant as shown in Table 5.4, while they had approximately higher values than the control mix when WHRl135 was produced at 135°C because of the functionally of Rediset LQ in improving the strength bond even at lower production temperature and the mean values were also significant.

However, Rediset WMX only improved the elastic modulus and hardness of the ITZ when the production temperature of the WMA was 145°C using 40/60 binder grade. Therefore, one can say that, in order to improve the degree of aggregate-binder bond and achieve the benefit from incorporating warm additives into the asphalt mixture, the production temperature of WMAs should be limited to only 10°C lower than that of HMA using a hard binder such as 40/60. While, as shown in Figures 5.19 and 5.20, both Sasobit and Rediset LQ improved the nano-mechanical properties of WMAs manufactured using 100/150 binder grade and mixed at 125°C (20°C lower than that of control mix HS145). A superior performance was shown when adopting Sasobit, as the further reduction in the viscosity of the 100/150 grade may have led to more diffusion of this binder into aggregate. The mean elastic modulus and hardness of ITZ for WSSa125 and WSRl125 was statistically significant compared to that values of ITZ of HS145, while it can also be noted that the WSRw125 mix performed similar to the control HS145 as there was no significant difference between the elastic modules of ITZ of WSRw125 and modulus for HS145 ($P>0.05$) as presented in Table 5.4, but Rediset WMX raised the modulus and hardness of ITZ of WSRw125 to the same level of nano-mechanical properties of ITZ of HS145 with 20°C reduction in the production temperature compared to its control mix.

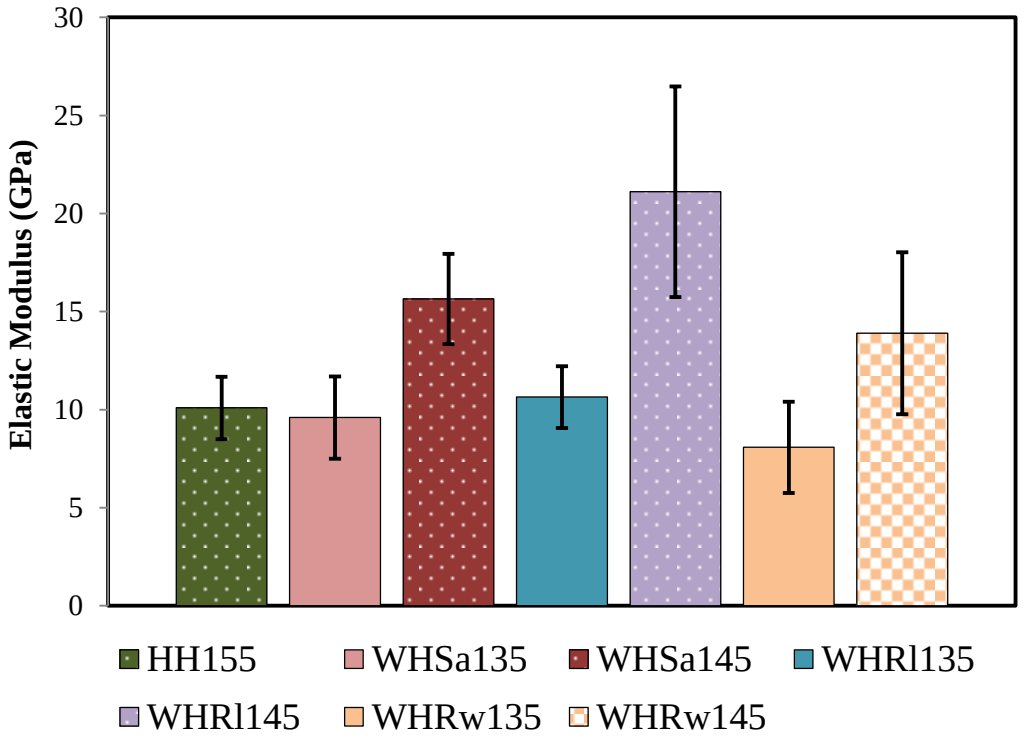

Figure 5.17 Elastic modulus of ITZ for all asphalt mixtures using 40/60 binder grade

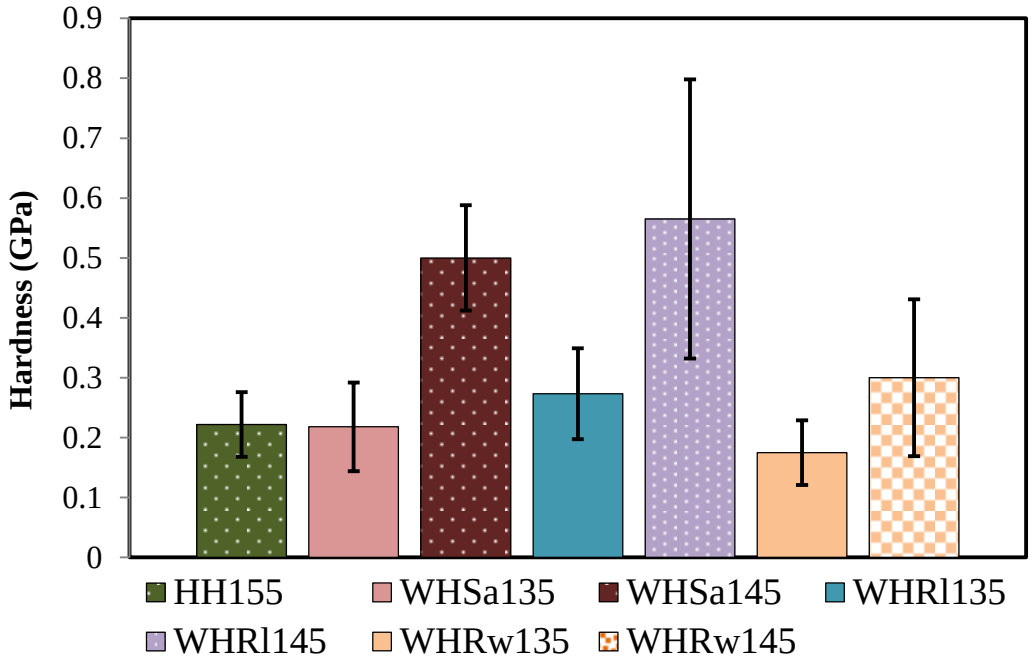

Figure 5.18 Hardness of ITZ for all asphalt mixtures using 40/60 binder grade

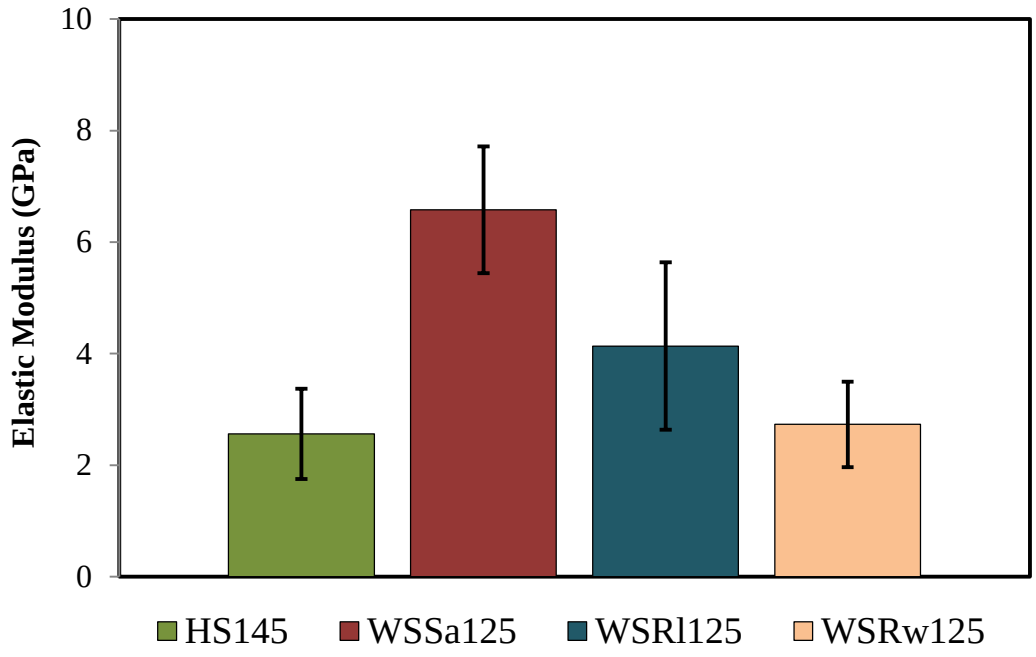

Figure 5.19 Elastic modulus of ITZ for all asphalt mixtures using 100/150 binder grade

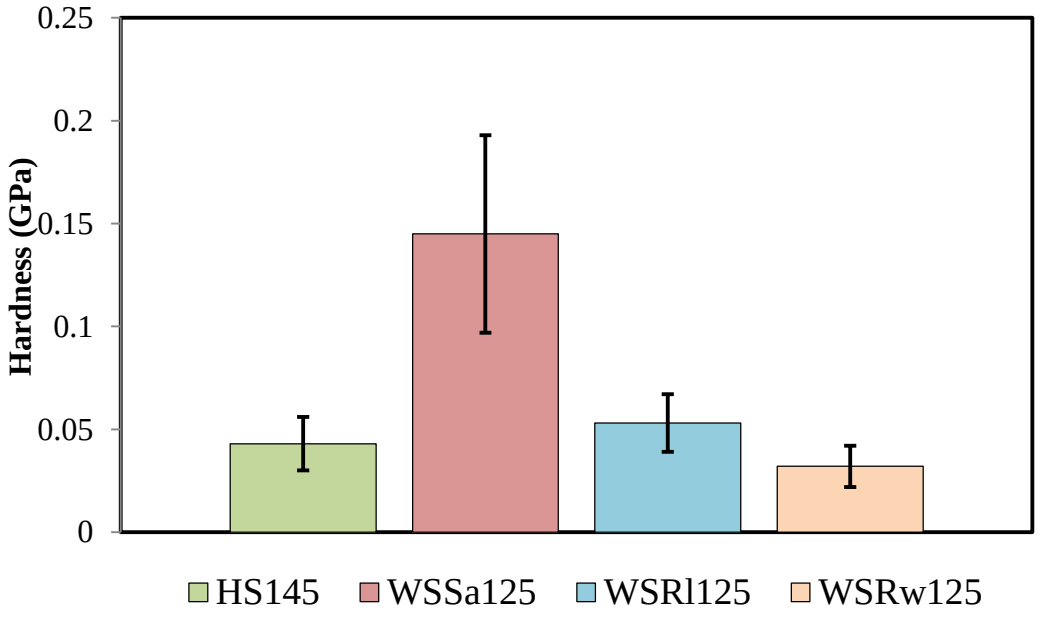

Figure 5.20 Hardness of ITZ for all asphalt mixtures using 100/150 binder grade

5.6.3 Nano-mechanical properties of mastic

5.6.3.1 Response load at controlled depth on mastic

As aforementioned, It has been highlighted that binder influences asphalt distress by approximately 40, 60 and 90% in terms of rutting, fatigue and low temperature cracking respectively (Partl *et al.* 2013). Therefore, mastic (binder mixed with fine aggregate particles passing through a 0.063 mm sieve) plays a major role in improving the durability of asphalt mixtures. As can be seen in Figure 5.21, all WMAs manufactured at a temperature of 135°C had lower resistance to loading than the control mix, although there is evidence that Sasobit increased binder stiffness (Xiao *et al.* 2012a,Xiao *et al.* 2011a,Xiao *et al.* 2011b,Gandhi *et al.* 2010) and Rediset WMX and LQ created a strong chemical bond between the aggregate and the bitumen, as stated by the supplier. However, when the production temperatures of WMAs were 145°C, only 10°C lower than the control mix HH155, the ability of WMAs to resist loads significantly improved. However, again when using the 100/150 binder grade, it was successful in producing WMAs with higher resistances to deformation using Sasobit and Rediset produced at 125°C lower than the control mix HS145 by 20°C, as illustrated in Figure 5.22.

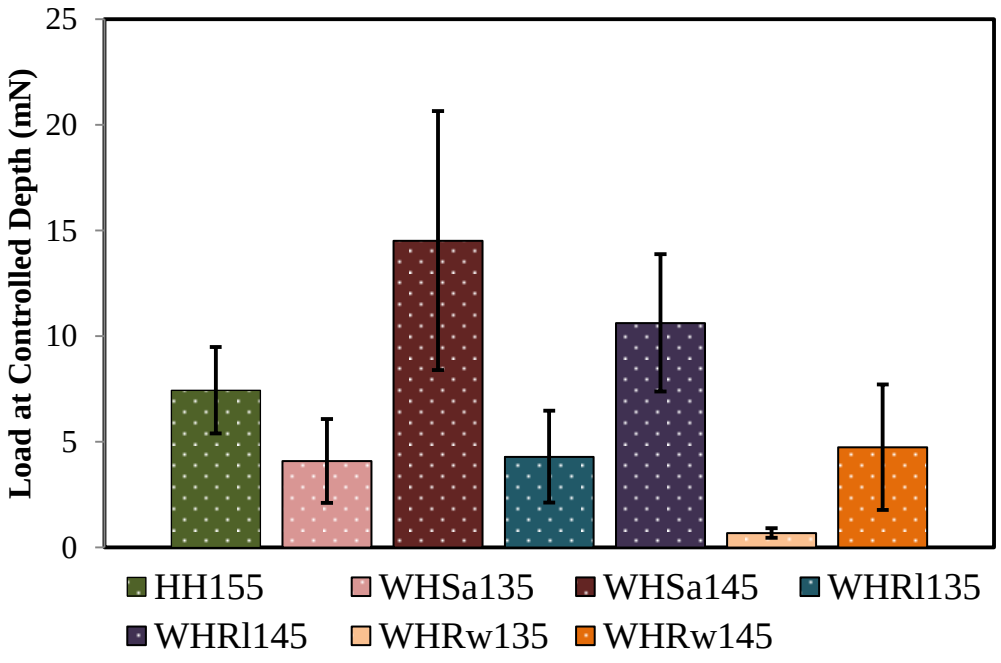

Figure 5.21 Response load on mastic for asphalt mixtures produced using 40/60 binder grade

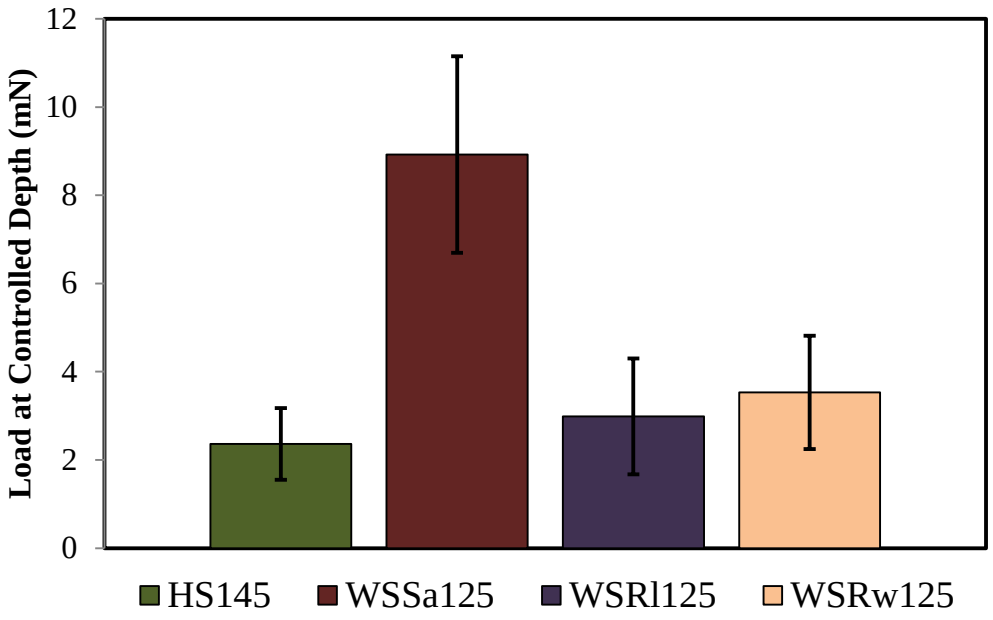

Figure 5.22 Response load on mastic for asphalt mixtures produced using 100/150 binder grade

5.6.3.2 Elastic modulus and hardness of mastic

Figures 5.23 and 5.24 illustrate the elastic modulus and hardness of control and WMAs using 40/60 binder. As is presented in those figures, Sasobit significantly increased the elastic modulus and hardness of mastic in the asphalt mixture only if the effect of production temperature is taken in account. Based on the nano-mechanical properties of mastic for WHSa135 and WHSa145, the reduction in the production temperature should be limited to only 10°C lower than that of the control mix HH155. As this limit was taken into account, the elastic modulus and hardness of Sasobit-modified asphalt mixtures increased from 2.489GPa to 5.934GPa and from 0.031GPa to 0.136GPa respectively and the mean values of elastic modulus and hardness of WHSa135 and WHSa15 were statistically significant compared to control mix HH155 ($P<0.05$). As a matter of fact, the nano-mechanical properties of WMA produced with 100/150 modified using Sasobit and manufactured at 125°C (WSSa125) had statistically higher elastic modulus and hardness than nano-mechanical properties of the control mix HS145 by approximately 2.769GPa and 0.032GPa respectively, as presented in Figures 5.25 and 5.26. The rank performance in improving the elastic modulus and hardness of mastic of WMAs using 40/60 binder grade manufactured at 145°C

and 100/150 binder grade manufactured at 125°C compared to control mixes HH155 and HS145 respectively is identical if only distinguish in the reduction of production temperatures based on binder grade is taken in account.

As Rediset LQ only improves the volumetric properties and act as active adhesion, which improves the adhesion of the aggregate-binder system, and do not alter the binder properties or bitumen grade at the recommended dosage, the WHRl145 had statistically the same modulus in comparison with the control mix but its mean hardness was statistically higher than that of the control mix by 0.035GPa due to the great advantage that Rediset LQ offers in improving the aggregate-binder bonds, even if the aggregate particles are fine, as presented in Figures 5.23 and 5.24. Moreover, WHRw145 performed as the control mix because there was no significant difference between the mean of nano-mechanical properties of WHRw145 and the control mix HH155.

However, as also presented in Figures 5.23 and 5.24, Rediset LQ- and WMX-modified asphalt mixture manufactured at 135°C had lower values of elastic modulus and hardness than the control mix, and the worst scenario was seen when Rediset WMX was adopted. The hardness of WHRw135 was significantly less than the control by approximately 0.054GPa. Again, the effect of production temperature is remarkably clear; therefore, in order to produce an asphalt mixture using a warm additive that performs the same as or even better than the traditional HMA, it seems the effect of production temperature should be into account. Figures 5.25 and 5.26 show the performance of warm additives on asphalt mixtures manufactured at 125°C using 100/150 binder grade. As can be seen in those figures, all WMAs statistically performed the same as the control mix in case of using Rediset LQ, or better than the control mix HS145 in case of using Rediset WMX and Sasobit. Sasobit Significantly increases the modulus and hardness of HS145 compared to its control mix HS145 ($P<0.05$) as shown previously the stiffness of binder increases with addition of Sasobit. As Rediset WMX has also wax in its structure, the presence of wax can also increase the binder stiffness which highlights to exhibits the same nano-mechanical of mastic for WSRw125 but 20° reduction in the production temperature can be achieved compared to control mix HS145. As presented in Table 5.4, since ($P<0.05$) for

elastic modulus and hardness of WSRw125, the means of those properties of mastic were statistically significant compared to control mix.

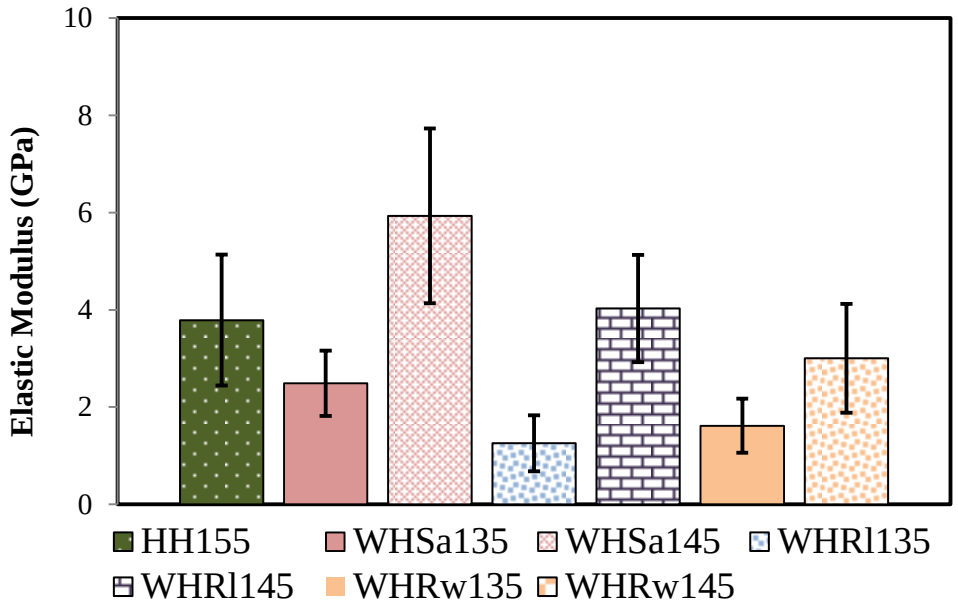

Figure 5.23 Elastic modulus of mastic for all asphalt mixtures using 40/60 binder grade

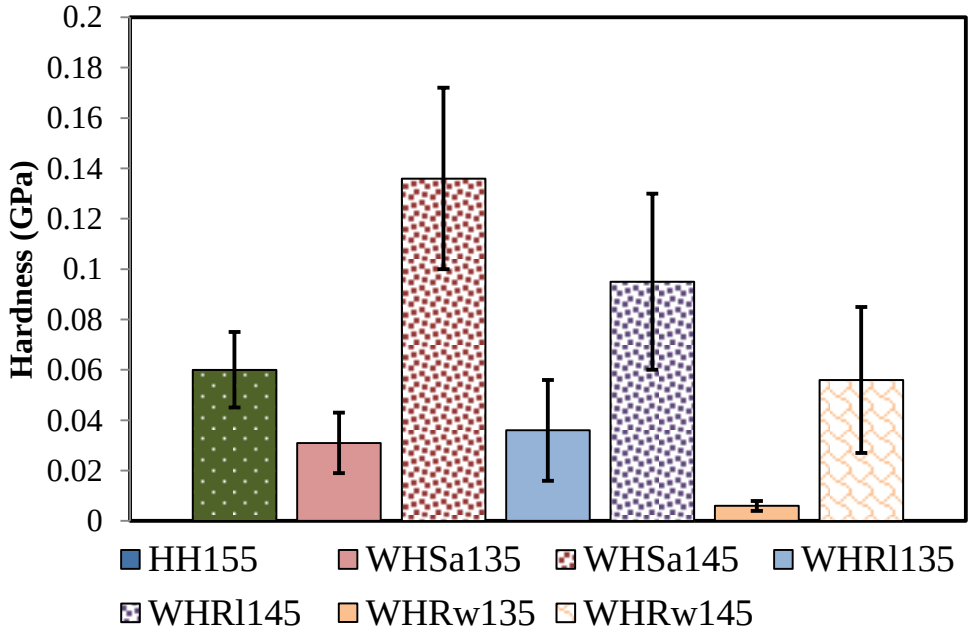

Figure 5.24 Hardness of mastic for all asphalt mixtures using 40/60 binder grade

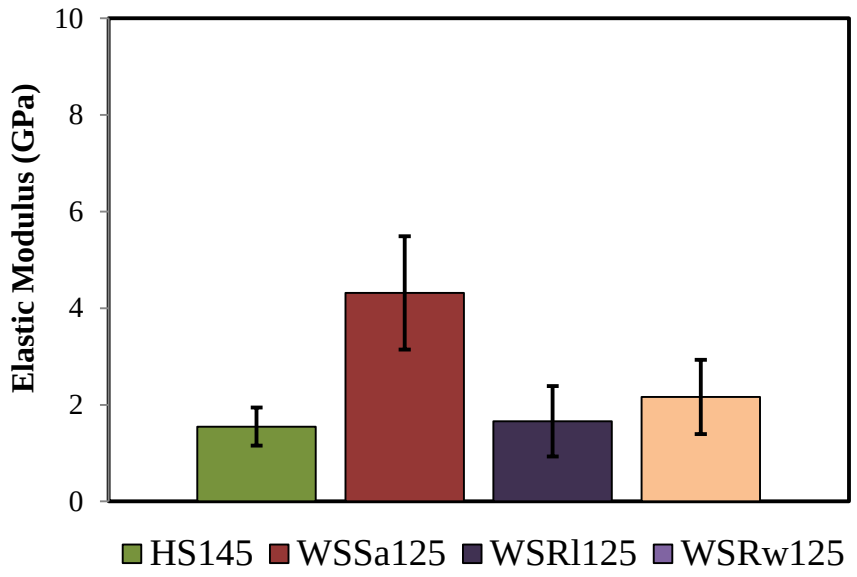

Figure 5.25 Elastic modulus of mastic for all asphalt mixtures using 100/150 binder grade

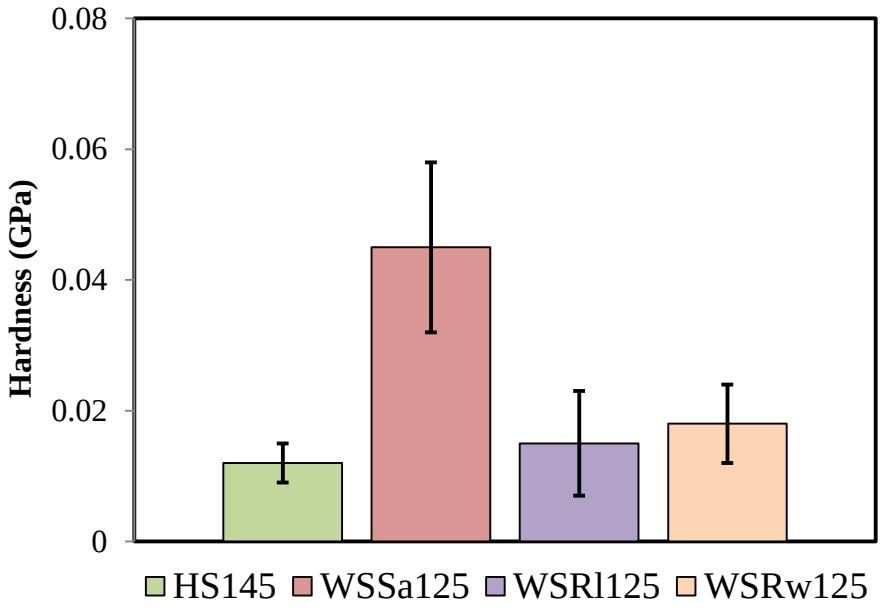

Figure 5.26 Hardness of mastic for all asphalt mixtures using 100/150 binder grade

Table 5.4 Results of ANOVA test of every mixture phase ($\boldsymbol{\alpha = 0.05}$)

Mixtures		Elastic modulus			Hardness			Difference
Between		*F*	*P-value*	*F crit*	*F*	*P-value*	*F crit*	
Aggregate								
HH155	*WHSa135,WHRw135,WHRl135,WHSa145, WHRw145, WHRl145*	0.569	0.723	2.280	1.530	0.184	2.280	**No**
ITZ								
HH155	WHSa135	0.002	0.962	4.105	0.016	0.899	4.105	**No**
	WHRw135	8.793	0.005	4.149	6.307	0.017	4.149	**Yes**
	WHRl135	8.740	0.006	4.182	26.795	0.001	4.195	**Yes**
	WHSa145	34.745	0.0002	4.210	48.107	1.87E-07	4.210	**Yes**
	WHRw145	13.121	0.0009	4.149	5.369	0.027	4.149	**Yes**
	WHRl145	68.204	4.18E-09	4.182	36.799	1.33E-06	4.182	**Yes**
HS145	WSSa125	146.024	3.14E-14	4.113	109.278	1.87E-12	4.113	**Yes**
	WSRw125	0.552	0.461	4.047	10.252	0.002	4.047	**≈ same**
	WSRl125	16.946	0.0002	4.113	4.767	0.035	4.105	**Yes**
Mastic								
HH155	WHSa135	4.566	0.055	4.844	14.348	0.003	4.844	**Yes**
	WHRw135	24.845	0.0001	4.451	160.825	4.3E-10	4.451	**Yes**
	WHRl135	15.361	0.0028	4.964	5.957	0.034	4.964	**Yes**
	WHSa145	6.835	0.028	5.117	24.922	0.0007	5.117	**Yes**
	WHRw145	1.711	0.210	4.543	0.089	0.771	5.117	**No**
	WHRl145	0.089	0.771	5.117	5.545	0.042	5.117	**No**
HS145	WSSa125	78.160	2.58E-09	4.225	100.864	1.94E-10	4.225	**Yes**
	WSRw125	7.421	0.011	4.241	10.369	0.003	4.241	**Yes**
	WSRl125	0.230	0.635	4.300	1.453	0.240	4.300	**No**

5.6.4 Pop-in phenomenon

The pop-in phenomenon was noticed in some points on the ITZ and mastic. The pop-in is defined as distinct displacement discontinuity during the loading phase of a nanoindentation test (Lorenz *et al.* 2003). However, this phenomenon was not noticed in the aggregate for all asphalt mixtures. The presence of the pop-in in some points on the ITZ and mastic may be because of the presence of voids or dust remaining from saw-cutting or polishing. It should be mentioned that the load-displacement curves with the pop-in were excluded from the results in order to obtain accurate and constant data because if they hadn't been excluded then the exiting method of analysis would be inaccurate because as mentioned previously the initial unloading stiffness is determined by fitting the depth versus loading data. Figure 5.27 illustrates examples of the pop-in phenomenon on the load-displacement curves of ITZ and mastic respectively.

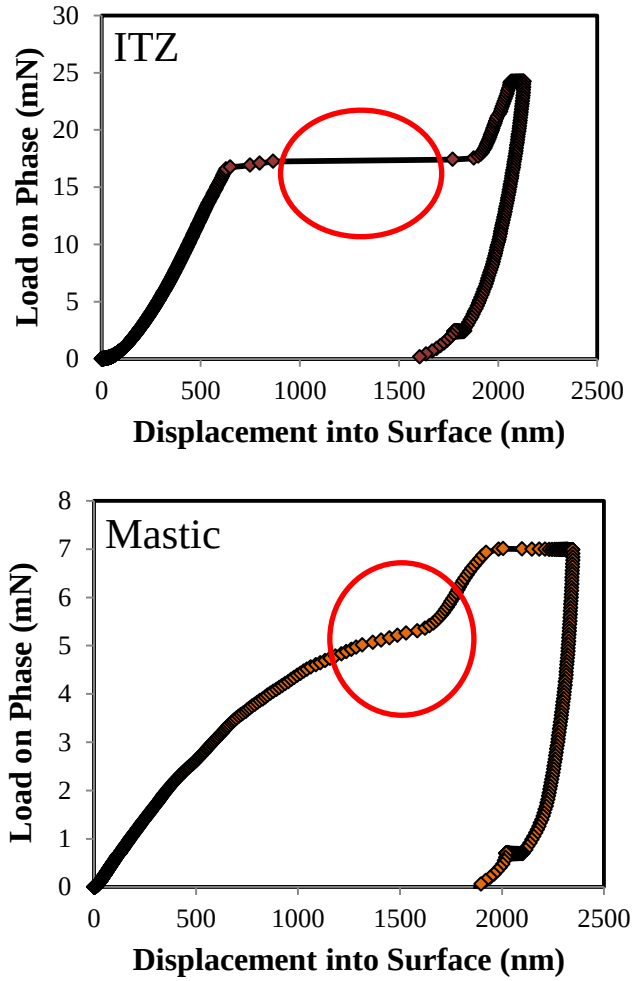

Figure 5. 27 Pop-in phenomenon on ITZ and mastic

5.7 Conclusions

Nanoindentation provides new insight about the effect of warm additives on the nano-scale properties of asphalt mixtures and explores the mechanical properties of aggregate, ITZ and mastic without separating them from the mixture. Although there have been great efforts made to study and evaluate the performance of warm additives on asphalt mixture properties, the effect of warm additives on the nano-mechanical properties of asphalt mixtures had not previously been studied. Based on the results presented in this chapter, several conclusions can be drawn:

1. No noise was noticed in any of the load-displacement curves of the aggregate, ITZ and mastic because of the well-prepared samples for nanoindentation.

2. All warm additives improved the nano-mechanical properties of the ITZ only if the production temperature was taken into account. The reduction in the reduction in the production temperature should not be more than 10°C for asphalt mixtures using such a hard binder as 40/60 compared to control mix. In this scenario, the elastic modulus value of the ITZ of WHSa145 and WHRw145 are 55% and 38% higher than that of control mix HH155 respectively, while Rediset LQ doubled the elastic modulus of the ITZ in comparison with the control mix. However, the ITZ of warm asphalt mixtures produced at 135°C was approximately the same modulus as the control mix, apart from WHRw135.

3. WHRl145 had a stiffer ITZ than all the asphalt mixtures. Its hardness value is approximately 250% higher than the hardness of the ITZ of the control mix, while the hardness of WHSa145 and WHRw145 was also higher than that of the control mix. However, the hardness of warm asphalt mixtures produced at 135°C was equal to the control mix, excluding WHRw135.

4. The production temperature had a very clear effect on the mastic. The nano-mechanical properties of mastic for all WMAs made with 40/60

binder grade and manufactured at 20°C lower than the control mix were less than the control mix. However, as the production temperature was only 10°C lower than that of control mix, the elastic modulus of the mastic for all WMAs significantly increased and so the effect of warm additives on the mastic phase was highlighted. Sasobit doubled the elastic modulus and hardness of the mastic, and Rediset LQ and WMX also improved the mastic's nano-mechanical properties.

5. In the case of WMAs produced at 125°C, the trend of improvement in the nano-mechanical properties of ITZ was the same to what was reported for WMA produced at 145°C using 40/60 binder grade. Sasobit increased the elastic modulus of the ITZ and mastic by more than double while Redist LQ only improved the elastic modulus and hardness of the ITZ but it raised the nano-mechanical properties of the mastic to the same levels as the control mix.

6. The nano-mechanical results of the ITZ demonstrate that nanoindentation is capable of differentiating among the effects of warm additives and reflecting the level of aggregate-binder bonding. Therefore, nanoindentation shows a promise to use as a novel technique to evaluate the adhesion between aggregate and binder.

Chapter Six

Adhesion Performance of WMA

6.1 Introduction

The aggregate-binder bond is one of the main factors that affect the durability of asphalt mixtures. This can be investigated based on the energy required to fracture the adhesive bond between binder and aggregate. This chapter presents the results of an investigation to evaluate the effects of Sasobit, Rediset WMX and Rediset LQ on the adhesive bond strength of an aggregate-binder system using the pull-off test. Furthermore, the current chapter introduces a comparison between the work of fracture required to break the adhesive bond of the aggregate-binder system using the pull-off test and adhesion force between the probe and the bitumen surface using atomic force microscopy (AFM). The impact of warm additives, effect of testing temperature and binder grade on the work of fracture was investigated in detail. However, all the aforementioned methods to evaluate the adhesive strength bond between aggregate and binder were conducted out the mixture. For the first time, the adhesive bond strength between aggregate and binder is evaluated using nanoindentation taking into account the production temperature, compaction, and ageing that may occur during production of asphalt mixtures.

6.2 Background

6.2.1 Techniques to evaluate adhesion in asphalt mixture

Different techniques to evaluate aggregate-binder adhesion properties have been developed based on the pull-off test concept. The Pneumatic Adhesion Tensile Testing Instrument (PATTI) was developed by the National Institute of Standards and Technology (NIST) in USA to assess the adhesive bond strength between aggregate and binder taking into account the presence of moisture. This technique was used by Kanitpong and Bahia (2005, 2003) to measure the mechanisms of

moisture damage based on the ASTM D4541 (Standard Test Methods of Coating Using Portable Adhesion Testers). Copeland (2007) modified the procedure for preparing PATTI samples by introducing a device to compress the specimens, which enables better control of the bitumen film thickness. The PATTI has been identified as an adequate tool to evaluate bond strength (Greyling 2012,Miller *et al.* 2010).

Failure in an aggregate-binder system can possibly occur in two different locations: through the bulk of the asphalt binder, i.e. cohesive failure, or along the interface between the asphalt binder and aggregate, which is known as adhesive failure (Howson 2011). The latter has been conceptually equated to the energy required to fracture the adhesive bond between aggregate and binder. Surface free energy (SFE) is another technique used to evaluate adhesion characteristics between aggregate and binder. SFE methods have been used by Howson *et al.* (2012) and Kringos *et al.* (2008) who found that work of fracture is predominantly higher than that predicated from surface energy measurements.

A relationship between ideal work of fracture and the surface free energy and work of fracture was studied by Howson (2011) and Masad *et al.* (2010). These studies produce an understanding of the mechanisms and factors that govern the fracture behaviour of asphalt binders and mixtures. The use of a servo-mechanical frame in direct tension is a simple method to fracture the adhesive bond between binder and aggregate. However, due to practical difficulties in preparing aggregate samples, binder thickness and performing the tests, it has only recently gained much attention. Several researchers have investigated the adhesive strength bond using direct tension test. Jakami (2012) produced aggregate stubs 25mm in diameter and 8mm high which were bonded with the binder inside a mounting press. The binder thickness was varied from 50 to 1000µm while the applied loading rate was 20mm/min at 25°C. It was found that a transition from adhesive to cohesive failure occurred as the binder thickness increased. However, the surface roughness of the aggregate was not clearly specified. Another study was conducted by Howson *et al.* (2012), who cored 19.1mm diameter specimens from limestone quarry rocks. The specimens were cut to 10mm stubs and polished with 6µm aluminium oxide powder. The thickness of the binder (unmodified PG64-22) between two stubs was controlled

using a DSR and was varied from 5 to 100 µm. The aggregate-binder system was tested in direct tension at 23°C with a loading rate of 0.01mm/sec. It was found that the work of fracture increased with loading rate and decreasing temperatures.

Al-Haddad and Al-Khalid (2015) conducted a similar procedure and cored 12mm diameter stubs of aggregate from quarry rocks. The aggregate stubs were polished using four stages of silicon carbide abrasive paper discs – 180, 240, 600 and 1200 – in order to obtain smooth and flat surfaces. The binder thickness was controlled using a DSR and it was varied from 10 to 100µm. Deformation rates of 30, 60 and 120mm/min were used at test temperature of 20°C and 10°C. The study demonstrated that, as the thickness of the binder increased, the failure mode transitioned from adhesive to cohesive and it was found that the transition occurs at or less than 16 µm. In other words, in order to obtain complete adhesive failure, the binder thickness between two aggregate stubs should be equal to or less than 16 µm. Apeagyei *et al.* (2014) used granite substrates of 23mm diameter and 15mm thick. The top and bottom surfaces were polished using No. 5 sandpaper. Three-mm thick mastic was sandwiched between two aggregate substrates and the measurements were conducted at 20°C with a constant displacement rate of 20mm/min. It is apparent that the authors applied a large amount of mastic; therefore, the failure mode can be questioned because it is impractical to obtain complete adhesive failure at 3.0 mm thick mastic.

As presented previously in Chapter 4, AFM has also been used by a number of researchers to investigate topographical structure of bitumen and the effect of short- and long-term ageing on the morphological microstructure of bitumen and polymer-modified bitumen (Allen *et al.* 2012,Das *et al.* 2014,Poulikakos *et al.* 2014,Wu *et al.* 2009,Zhang *et al.* 2011,Zhang *et al.* 2012,Menapace *et al.* 2015). However, very limited studies map the mechanical properties of asphalt binder. Lyne *et al.* (2013a) used PeakForce Quantitative Nanomechanical Mapping (PFQNM) modality to investigate the elastic modulus and adhesion of neat bitumen. With this method, the adhesion of bitumen is evaluated according to the attractive force between the probe and the sample. Van der Waals' forces and electrostatics were considered as contributing factors to the adhesion force between probe and bitumen surface (Pittenger *et al.* 2010).

6.2.2 Factors affecting adhesion failure in asphalt mixtures

Adhesive failure between aggregate and binder/mastic can occur under four theories, as highlighted by Hicks (1991); namely, as mechanical adhesion theory, chemical reaction theory, surface energy theory and molecular orientation theory. Terrel and Al-Swailmi (1994) reported that the mechanical adhesion failure is influenced by the physical properties of the aggregates, such as particle size, surface texture, angularity, porosity and surface area.

In the chemical reaction theory, aggregate is classified based on its affinity to attract water. Aggregates can be classified as either hydrophilic or hydrophobic. Surface chemistry and porosity are the main factors governing the characterisation. Generally, a more acidic aggregate is hydrophilic, which means it is less likely to form a strong bond with a binder, so the asphalt mixture might be susceptible to stripping. In other words, the pH values of the aggregate surface and binder affect the bond strength.

Adequate bonding between aggregate and binder/mastic can be explained by the wetting ability of the binder, which can be characterised using surface energy theory. As defined previously, surface energy is the energy required to create a unit area of new surface of a material in a vacuum, and it is highly affected by the type of aggregate, roughness of the aggregate surface and type of binder.

Molecular orientation theory is based on the concept that, when a binder is in contact with an aggregate surface, the binder molecules orient in a way to satisfy the energy demand of the aggregate surface (Jakami 2012). The energy demand of the aggregate surface can be preferentially satisfied by the water or moisture molecules, which results in degradation in the adhesive bond between aggregate and binder.

6.3 Pull-off test

6.3.1 Experimental works

6.3.1.1 Materials

6.3.1.1.1 Binder and warm additives

Details about the properties of the binders, warm additives and aggregate were presented in Chapters 3 and 5.

6.3.1.1.2 Aggregate rocks

Granite was also delivered in rocks (as presented in Figure 6.1) of approximately 8-10 kg each from Croft Quarry. The properties of granite as received from the supplier are shown in Table 5.2, Chapter 5.

Figure 6.1 Granite Rocks

6.3.1.2 Sample preparation

6.3.1.2.1 Aggregate stubs

At the first stage, the rock was cut into sheet of uniform thickness (20–40 mm) using electrical sawing in the Geology Department, University of Liverpool. Then, aggregate fingers of approximately 20-40mm height and 12mm diameter, as presented in Figure 6.2, were cored from the sheet plates using an electric coring machine with continuous water feed. Aggregate fingers were then cut to aggregate stubs of 12mm diameter and 18mm height using a small cutter in the Geology Department again. In fact, having a large contact area between aggregate and binder can increase the probability of cavitation (Al-Haddad and Al-Khalid 2015);

therefore, a decision was made to choose a small contact area, in order to reduce the possibility of cavitation occurring.

Both surfaces of the aggregate stubs were polished using silicon carbide abrasive paper discs. Firstly, both surfaces were polished using 80 silicon carbide abrasive paper in order to adequately level both faces and remove any edges caused when cutting the aggregate fingers. The polishing process was then continued for one face; this process comprised two stages using silicon carbide abrasive paper discs of 120 and 180 respectively, in order to obtain a relatively constant surface roughness so that there were no gaps when using the DSR. Dust which might have been caused by the sawing and drilling process and polishing powder was removed by cleaning the aggregate stubs by immersing them in distilled water, which was boiled for 15 min, and then drying them with hot air. The finished aggregate stubs were placed in an oven for 12 hours at 150°C to remove all moisture from them.

Figure 6.2 Preparing the aggregate stubs

6.3.1.2.2 Aggregate-binder system

Warm modified bituminous binders (WMBBs) were prepared as explained in Chapter 3. Modifications were made to the upper and lower plates of the DSR in order to run sequences on the DSR. In addition to that, aggregate stub stainless steel holders were also manufactured to be integrated into those modifications in order to fix the aggregate stubs in the proper position, as presented in Figure 6.3. The aggregate stub holders were firstly aligned in the upper holder and lower plate of the DSR. The aggregate stubs were conditioned overnight in an oven

maintained at a temperature of 150°C while the control and WMBBs were heated up to 150°C prior to setting. The preparation of the aggregate-binder system involved the following: firstly, two aggregate stubs were aligned in the aggregate stub holders, and then a zero gap setting was made between the two stubs. After that, a small drop of binder was applied to the surface of the bottom aggregate stub. Thirdly, the gap was then reduced to the desired film thickness (16μm) as recommended by Al-Haddad and Al-Khalid (2015) and the sample was allowed to cool for 15 minutes before the excess binder was removed by means of a sharp knife, as illustrated in Figure 6.4. The prepared aggregate-binder samples were kept in a controlled temperature fridge maintained at a temperature of 10°C for 24 hrs to achieve full adhesive bond.

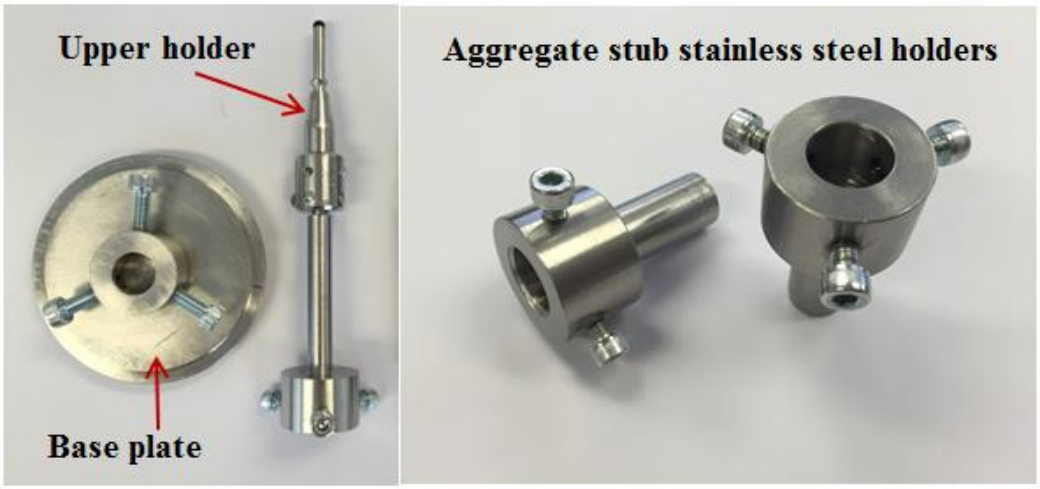

Figure 6.3 Upper holder and lower plate of DSR and aggregate stub holders

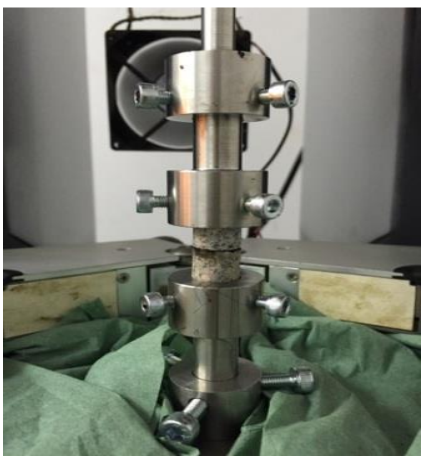

Figure 6.4 Prepare aggregate-binder system in the DSR

The aggregate-binder system were then aligned in the test aggregate-binder system holders which were manufactured in order to install the aggregate-binder system within the test machine, as shown in Figure 6.6. The surfaces of the holes for the fixing holders were cleaned of dust and had been previously cleaned with a chemical solution (white spirit solvent) in order to ensure cleanliness. The aggregate-binder system was glued to the upper and lower test holders using Araldite 2012 glue. The gluing period lasted for about half an hour, according to the company's specification in order to obtain a full connection. It is worth mentioning that the gluing process was made using a custom-made fixing device, as shown in Figure 6.5, in order to obtain perfect alignment.

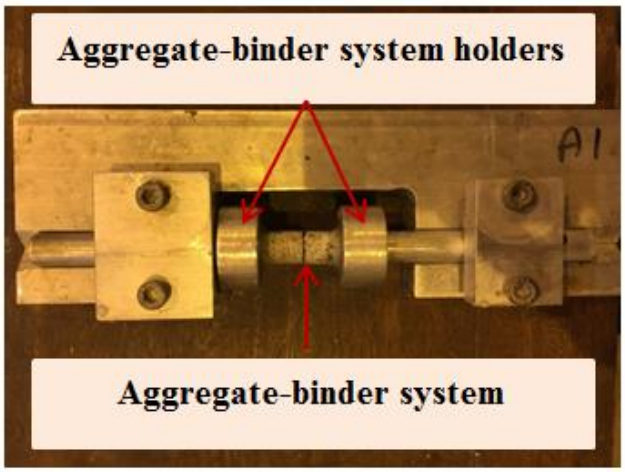

Figure 6.5 Custom device used to obtain perfect alignment

6.3.2 Testing

6.3.2.1 Data acquisition system

Testing of the aggregate-binder system samples was conducted using a servo hydraulic frame, Instron machine, model 4204 as shown in Figures 6.6 and 6.7. The Instron machine's software controlled the operation of the testing machine and recorded loading rate, force, and displacement. The entire testing process was conducted inside an environmental chamber that controlled the test temperature. The stainless steel grips were custom designed in order to hold the sample holders. The upper grip was attached directly into the load cell, while the lower grip was attached to the base of the testing chamber by means of a locking silicone-stainless steel joint that served the purpose of aligning the top and lower

grips. A prepared aggregate-bitumen system was fixed into the bottom grip, and locked in using a compression joint. In order to prevent the sample from moving during testing, the inside of the bottom grip was textured to provide a better hold.

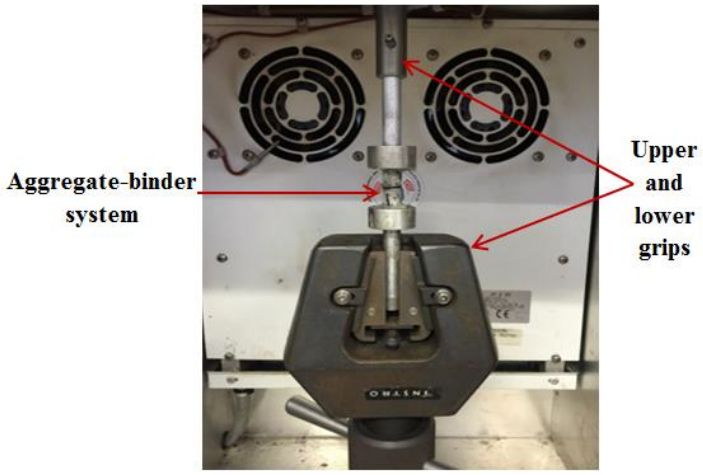

Figure 6.6 Setting the aggregate-binder system in the Instron machine

Figure 6.7 Testing apparatus

6.3.2.2 Experimental setup

A servo hydraulic frame was used to apply force while displacement of the thin binder film was measured directly using the Series IX Automated Materials Testing System version 5.3 software Instron corporation. Testing temperatures were 10°C and 20°C in order to investigate their effects on the failure mode. The deformation rate for testing all samples was 25mm/min. Three samples of the aggregate-binder system were tested.

6.3.3 Analysis of failure mode

As defined previously, adhesion in the context of asphalt mixture is defined as the attraction force between aggregate and binder/mastic. In other words, it is the required energy to break the bond between aggregate and binder. By contrast, cohesion is defined as the intermolecular force developed within the binder/mastic. Figure 6.8 illustrates the definition of adhesion and cohesion.

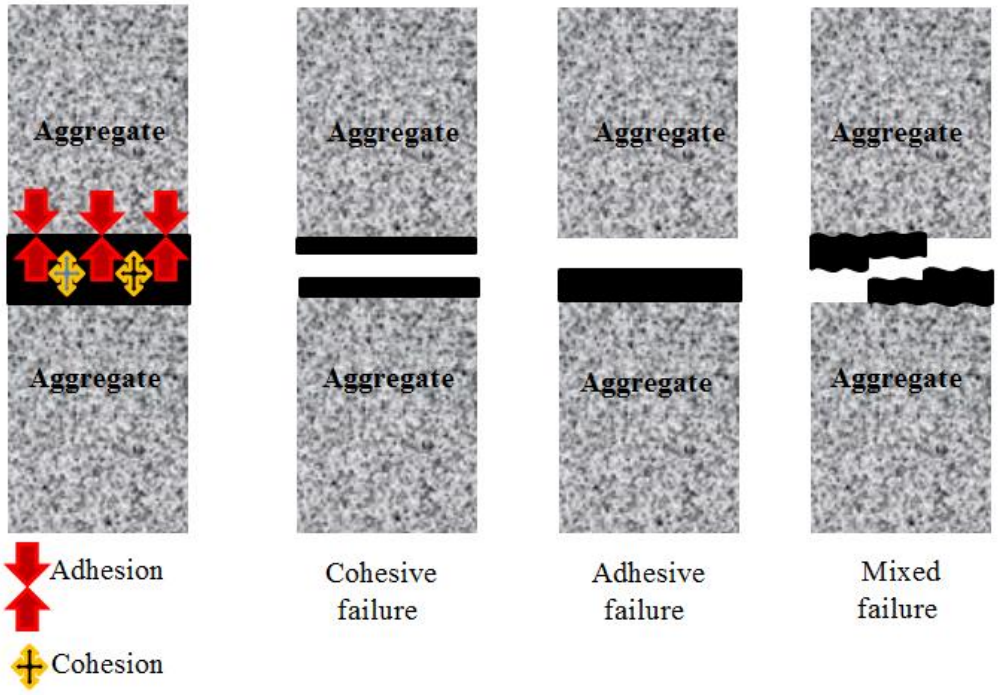

Figure 6.8 Definition of adhesive and cohesive failures between aggregate and binder

Lytton (2004) studied the relationships between film thickness and failure mode using micromechanics and reported that the transition from adhesive to cohesive occurs at film thickness of less than 100µm. However, a study conducted by Jakami (2012) observed that the transition from adhesive to mix and cohesive or complete cohesive failure occurs at film thickness of 200µm; however, he applied a factor of safety to cover the worst-case scenario that might possibly occur, so he suggested that the transition from adhesive to cohesive occurs at film thickness of 100µm. However he also mentioned that the thickness of the binder/mastic across the actual pavement structure varies considerably, and is generally within the range of 15µm to 40µm and both adhesive and cohesive failure may occur, with one of them perhaps being dominant. Howson (2011) and Masad *et al.* (2010) used image analyses software in order to calculate the grey

intensity of the surface to assess the total percentage area of adhesive failure, which was found to be in the range of 5% to 45%. The range was too low to be considered as sufficient for the occurrence of the adhesive failure mode (Al-Haddad and Al-Khalid 2015). Al-Haddad and Al-Khalid (2015) used image processing coded in MATLAB to estimate the predominant type of failure for aggregate-binder systems prepared using four types of bitumen and two types of aggregate tested at different temperature levels, loading time and binder thickness. They recommended that, at binder thickness equal to or less than 16μm, the percentage area of adhesive failure was more than 75% for the four types of binder grade and two types of aggregate. In the current study, as mentioned previously, it has therefore been decided that the binder thickness for all control binders and WMBBs should be 16μm.

In fact, there is a simple method to judge whether the type of failure is cohesive or adhesive, based on the shape of loading verses displacement as shown in Figures 6.9 and 6.10. A judgement on the failure mode using a load-displacement curve can be made based on the crest of the curve. In complete adhesive failure, the load approaches the maximum value in one point and then after failure the load drops significantly to zero value as shown in Figure 6.9. Whereas, in the case of cohesive failure, as the work is between the binder molecules, the load reaches the maximum value, it is continuing approximately at that value (the load takes in a steady state) while the viscous effect increases the displacement until failure as shown in Figure 6.10.

All WMBBs using 40/60 binder grade and the control tested at 20°C exhibited complete adhesive failure, as presented in Figure 6.9, while, when WMBBs using 100/150 binder grade were tested at 20°C, as shown in Figure 6.10, the failure mode was mixed adhesive and cohesive, although the binder thickness was 16μm in both scenarios. Figure 6.11 illustrates a typical adhesive failure as obtained when WMBBs using 100/150 binder grade were tested at a temperature of 10°C, as the failure mode transitioned from cohesive to adhesive. The reason for this phenomenon is because, the viscosity and stiffness of 40/60 binder are high, so the stored energy in the bitumen is higher than the stored energy along the interface between aggregate and binder; therefore, the failure occurs at the interface between aggregate and binder. In other words, testing the

control binder 40/60 and warm-modified binders at 20°C did not allow enough time for the cohesion force between the binder molecules to work and aid in tensile-strength resistance consequently, the resistance process will depend on the adhesion strength between aggregate and binder. Whereas, when control binder 100/150 and warm-modified binders were tested at 20°C, the viscosity and stiffness were relatively low, so the deformation rate worked further between the bitumen molecules due to the viscos effect, which resulted in decreasing the tensile load and increasing displacement at failure. However, when the testing temperature for the aggregate-binder system using 100/150 binder grade and WMBBs was 10°C, the failure mode transitioned from cohesive to adhesive.

Figures 6.9 and 6.11 show typical adhesive failure for the aggregate-binder system using 40/60 and 100/150 binder grades tested at 20°C and 10°C respectively while Figure 6.10 illustrates typical cohesive failure for the aggregate-binder system using 100/150 binder grade tested at 20°C.

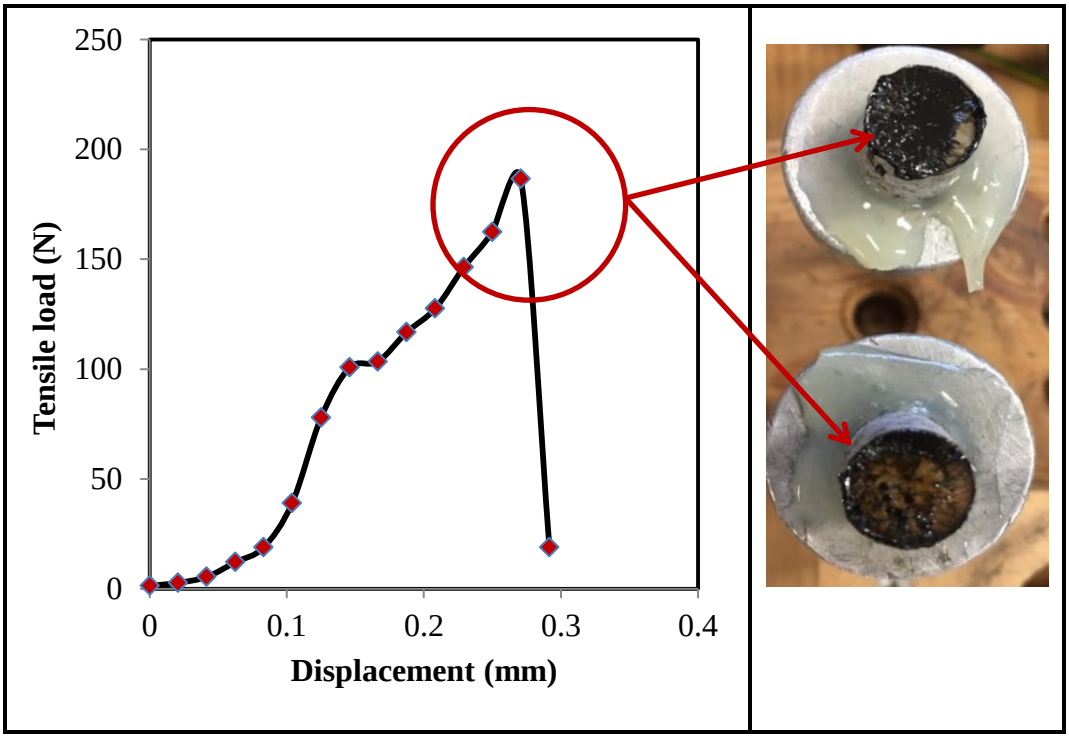

Figure 6.9 Typical adhesive failure obtained using 40/60 binder for aggregate-binder system tested at 20°C

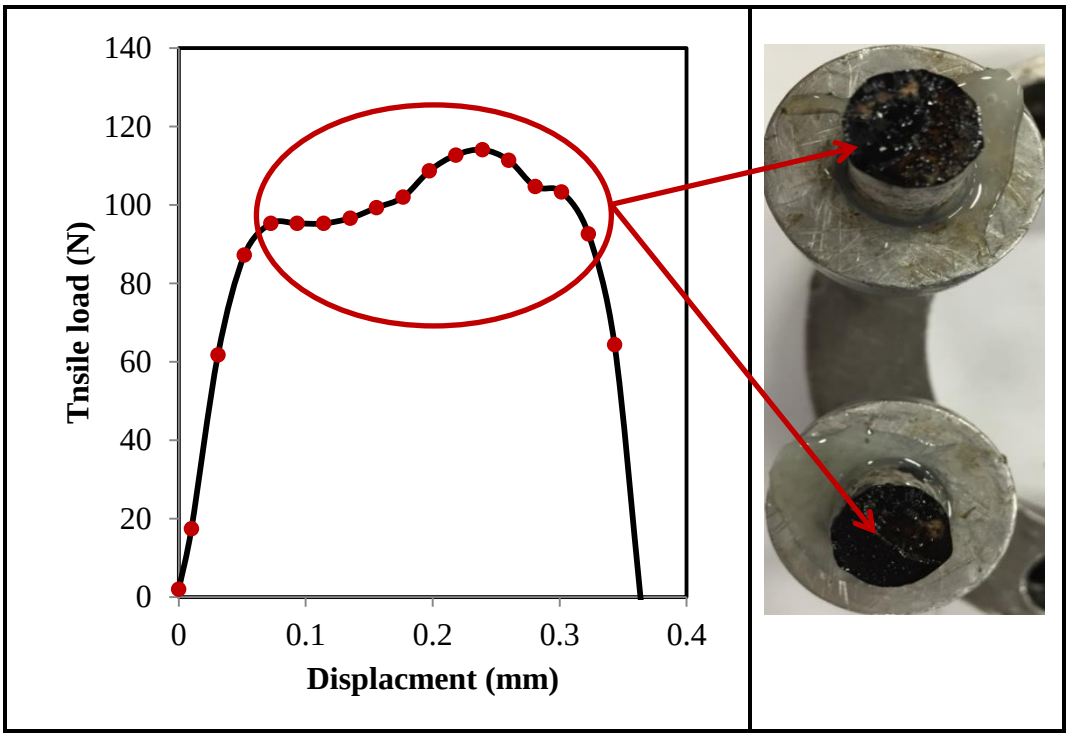

Figure 6.10 Typical cohesive failure obtained using 100/150 binder for aggregate-binder system tested at 20°C

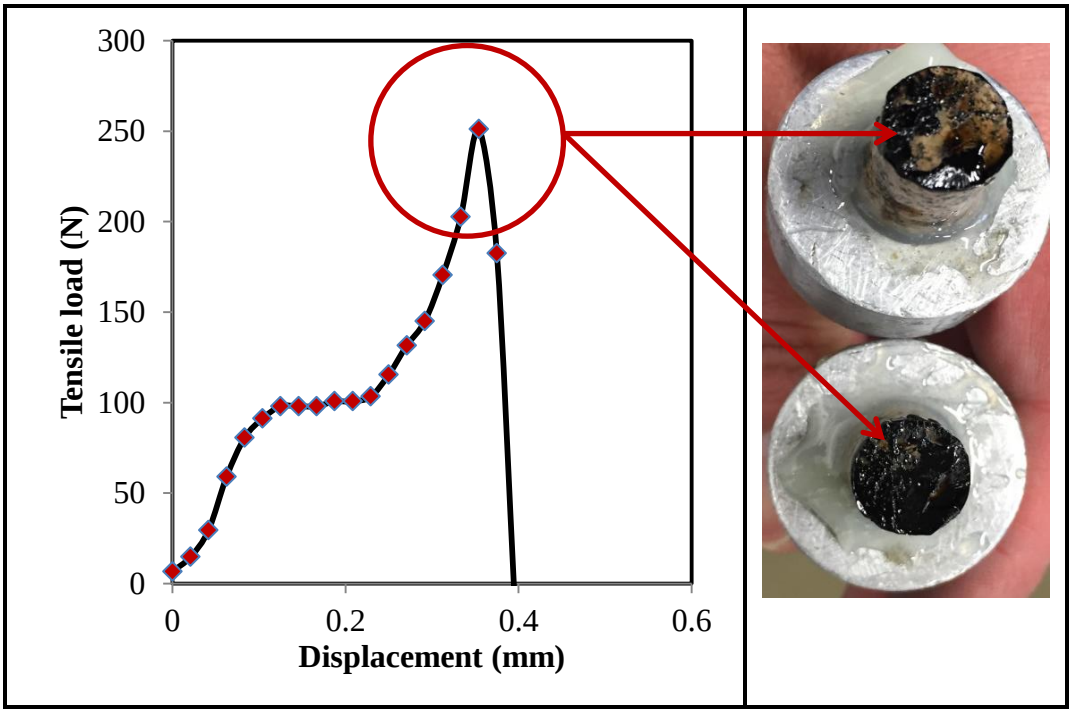

Figure 6.11 Typical adhesive failure obtained using 100/150 binder for aggregate-binder system tested at 10°C

6.3.4 Work of fracture

The work of fracture was calculated based on Harvey and Cebon (2005). The value of the required tensile energy to produce failure could be determined by calculating the area under the curve of tensile load versus displacement. Results of work of fracture for all types of control binder and WMBBs are presented in the next section.

6.3.5 Results and Discussion

Figure 6.12 presents the work fractures for control binder 40/60 and WMBBs. It was found that the failure mode for all these aggregate-binder systems tested at 20°C was adhesive. All warm additives increased the required energy to break the adhesive bond strength between aggregate and binder. Sasobit significantly increased the work of fracture. In other words, it improved the adhesive bond strength between aggregate and binder. Rediset WMX and LQ also improved the bond strength energy. It is therefore clear that the inclusion of Sasobit and Rediset can give a superior performance in providing an asphalt mixture that has better performance than traditional HMA. But again, it is necessary to specify the minimum reduction in the production temperatures in order to achieve that superior performance without having a negative impact.

Figure 6.13 shows the required work of fracture to break the aggregate-binder bond for aggregate-warm-modified binders produced using 100/150 binder grade. In this scenario, although the work of fracture of aggregate-WMBBs was equal to or better than that of the control, it was found that the failure mode between aggregate and binder was either mixed cohesive and adhesive or complete cohesive failure due to the viscous effect of those binders, so more energy was dissipated in the bulk of the viscoelastic control and warm modified binders. The failure mode was noticed in the load-displacement curve and by observation, as mentioned previously. It can be concluded that the binder grade highly affects the testing temperature of the bond strength of an aggregate-binder system. The effect of testing temperatures is in agreement to with what was reported by Al-Haddad and Al-Khalid (2015) and Howson *et al.* (2012). However, as the testing temperature decreased to 10°C for the aggregate-WMBBs system produced using 100/150 binder grade, all the failure modes were adhesive. Figure

6.14 illustrates the required energy to fracture the adhesive bond between binder and aggregate, causing isolation from each other, for the aggregate-WMBBS system produced using 100/150 binder grade tested at 10°C. It can be observed that the qualitative rank performance of improving the work of fracture using Sasobit and both types of Rediset is exactly the same after taking the effect of testing temperature and binder grade into account.

In general, in both scenarios of testing the aggregate-WMBBs system produced using 40/60 binder grade at 20°C and testing the aggregate-WMBBs system produced using 100/150 binder grade at 10°C, Sasobit, Rediset WMX and Rediset LQ increased the required work of fracture by 170%, 100% and 143% respectively for the aggregate-binder system produced using 40/60 binder, and 70%, 25% and 50% respectively for the aggregate-binder system produced using 100/150 binder grade. In fact, increasing the required energy to break the aggregate-binder bond delays the propagation of cracks along the aggregate-binder face, in which the material can resist the applied repeated load. More details about all the pull-off test results are presented in appendix C, Table C.1.

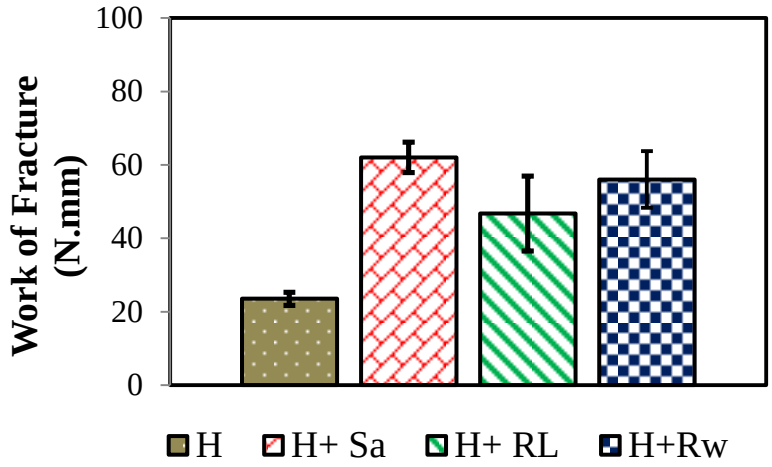

Figure 6.12 Work of fracture for WMBBs using 40/60 binder tested at 20°C

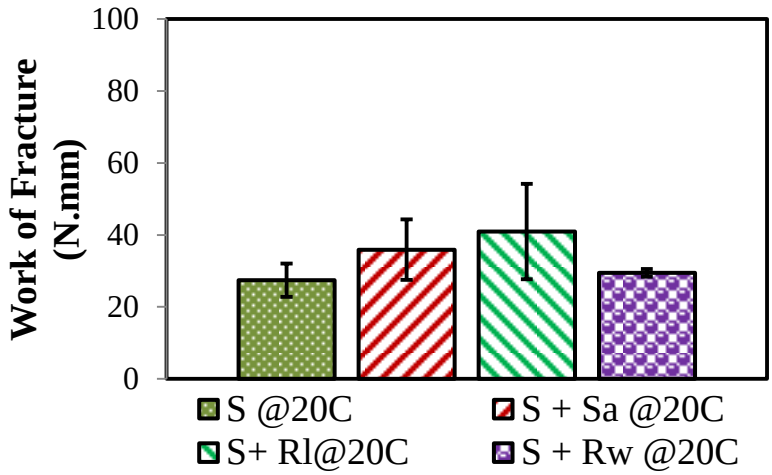

Figure 6.13 Work of fracture for WMBBs using 100/150 binder tested at 20°C

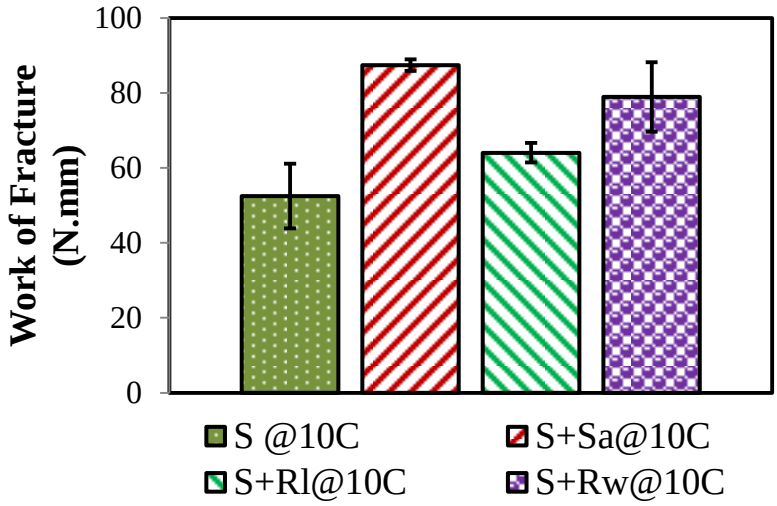

Figure 6.14 Work of fracture for WMBBs using 100/150 binder tested at 10°C

6.4 Comparison between adhesion obtained from Pull-Off test and AFM

As presented in Chapter 5, Atomic Force Microscopy (AFM) with the PeakForce Quantitative Nanomechanical Mapping (PFQNM) modality was used to characterise the adhesive force between tip and bitumen surface. The adhesion force could be any attractive force, Van der Waals or electrostatics, which could contribute to the adhesion force between the tip and bitumen surface. Based on the obtained results, the performance of warm additives in improving the work of fracture was highly associated with the measured adhesion force determined using AFM-PFQNM. Table 6.1 illustrates the performance of warm additives using both techniques.

Table 6.1 The rank performance of warm additives using Pull-off and AFM

Binder grade	Material	Pull-off		AMF		Equivalent
		Rank	Testing	Rank	Testing	
40/60 (H)	H	1	20°C	1	22°C	√
	H+2% Sa	4	20°C	4	22°C	√
	H+0.5%Rl	2	20°C	2	22°C	√
	H+2%Rw	3	20°C	3	22°C	√
100/150 (S)	S	1	10°C	1	22°C	√
	S+2% Sa	4	10°C	4	22°C	√
	S+0.5% Rl	2	10°C	2	22°C	√
	S+2%Rw	3	10°C	3	22°C	√

1: less adhesion 4: high adhesion

As presented in Chapter 4, the measurement of nano-scale properties of WMBBs determined with AFM-PFQNM was conducted at 22°C and the effects of Sasobit and both types of Rediset were exactly the same on control binders 40/60 and 100/150. However, when using the pull-off test, it was not possible to obtain the same rank performance of the warm additives on both control binders for the aggregate-binder system tested at 20°C because the failure mode of the aggregate-WMBBs system using 100/150 binder grade was a mixture of cohesive and adhesive. However, as all the measurements of the aggregate-binder system produced using 100/150 binder grade were conducted at 10°C, the effect of the warm additives was equivalent to what was noticed when using 40/60 binder

grade. In other words, the effect of testing temperature and binder grade on the failure mode is clear. This finding may be one of the advantages of using AFM to directly characterise the adhesion of binders. The main advantages also of using AFM to characterize nano-scale properties were shown to include co-localisation of nano-topography with adhesion, ease of sample preparation and reduction in experimental time relative to the direct tension pull-off test.

6.5 Comparison between adhesion obtained from Pull-off test and nanoindentation

6.5.1 Work of indentation

As aforementioned, adhesion in the context of asphalt mixture is defined as the attraction force between aggregate and binder/mastic. In other words, it is the energy required to break the bond between aggregate and binder. In terms of asphalt mixture, it is impossible to directly break this bond. However, by using nanoindentation, it has become possible to measure the properties of the interfacial transition zone (ITZ), as shown in Figure 6.15 (images captured using an optical microscope for nanoindentation), between aggregate and binder/mastic, as presented in Chapter 5 which, in fact, reflects the real interaction between aggregate and binder.

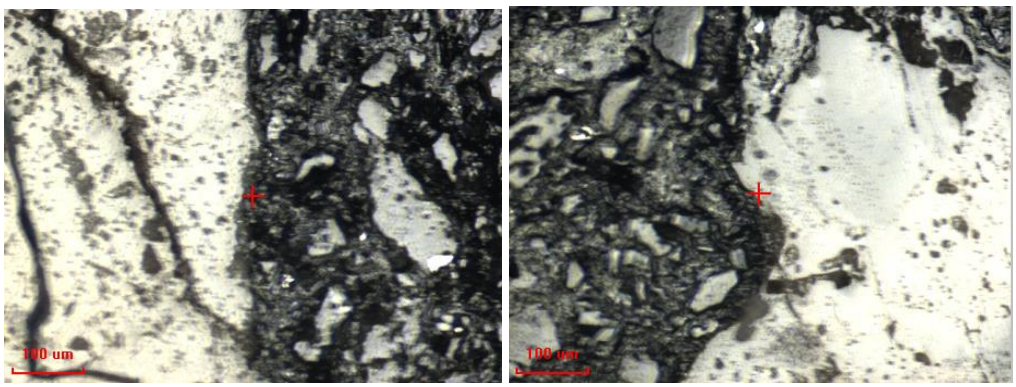

Figure 6.15 Interfacial transition zone (ITZ) between aggregate and binder

In this regard, work of indentation required to indent the ITZ was calculated based on the response load and surface displacement. The work of indentation represents the area under the curve of load-displacement excluding the dwell/hold time, as presented in Figure 6.16. Khorasani *et al.* (2013) calculated the energy dissipated as the ratio of the area inside the hysteresis loop to total area

under the loading part of the curve. Therefore, the total area under the curve (excluding dwell/hold time) represents the total energy required to indent the object. The work of indentation can accurately give pavement engineers a clear picture about the level or degree of bonding between aggregate and binder/mastic without separating them from the mixture, taking into account the production temperature, effect of mixing and compaction process and ageing that may occur during preparation.

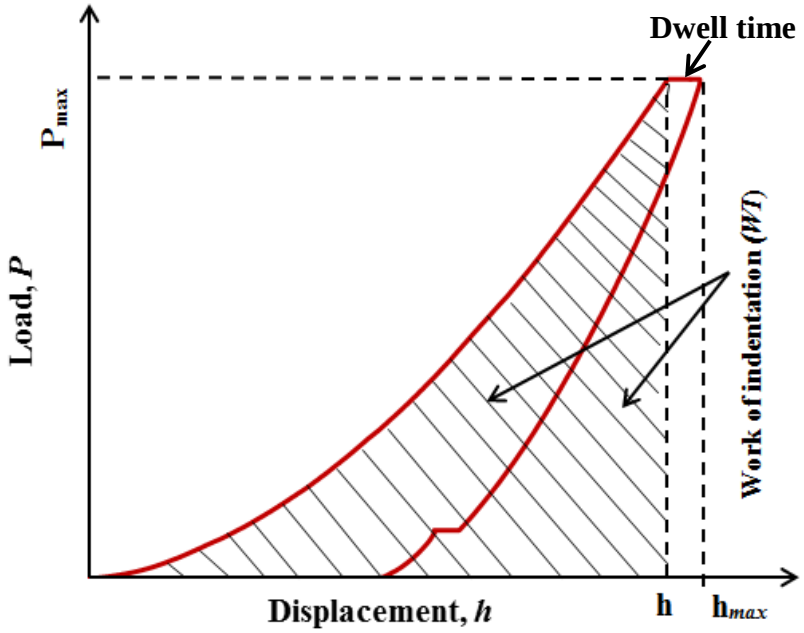

Figure 6.16 Area used to calculate the work of indentation

Figures 6.17 and 6.18 present the work of indentation of control and WMA. It can be seen that all warm additives improved the work of indentation in comparison with control mixtures. Significant improvement was noticed when adding Sasobit because, as mentioned previously, firstly, reduction in the viscosity of the control binder due to the inclusion of Sasobit may lead to making the binder further diffuse into the aggregate and, secondly, Sasobit increased binder stiffness, which also contributes to further improving the strength bond between aggregate and binder/mastic. Rediset LQ is a compaction aid, surfactant and active adhesion. Rediset LQ significantly increased the bulk density and decreased the air voids of asphalt mixtures manufactured at 145°C using 40/60 binder grade, and asphalt mixtures manufactured at 125°C using 100/150 binder grade in comparison with the associated control binders as presented in Chapter 5.

It is therefore clear that the improvement in the volumetric properties with the inclusion of active adhesion improves the bond strength of asphalt mixtures, as it is obvious in Figures 6.17 and 6.18. Although the effect of Rediset WMX on the bond strength was not as significant as that of Sasobit and Rediset LQ, WHRw145 and WSRw125 performed the same as the control mixtures HH155 and HS145 respectively in terms of strength bond, and successful reduction in the production temperature was 10°C and 20°C for Rediset WMX-modified asphalt mixture manufactured at 145°C and 125°C using 40/60 and 100/150 control binders grade respectively. However, as shown in Figure 6.19, the work of indentation of WHRw135 is less than that for the control mix (HH155); therefore, in order to produce WMA using Rediset WMX and a hard binder that has equal or better performance than that of control, WMA-Rediset WMX should be manufactured at a temperature of only 10°C using 40/60 binder grade lower than that of control mix HH155.

A summary of the response load on ITZ, surface displacement into surface and the work of indentation calculated based on those parameters for all asphalt mixtures is presented in appendix C, Table C.2.

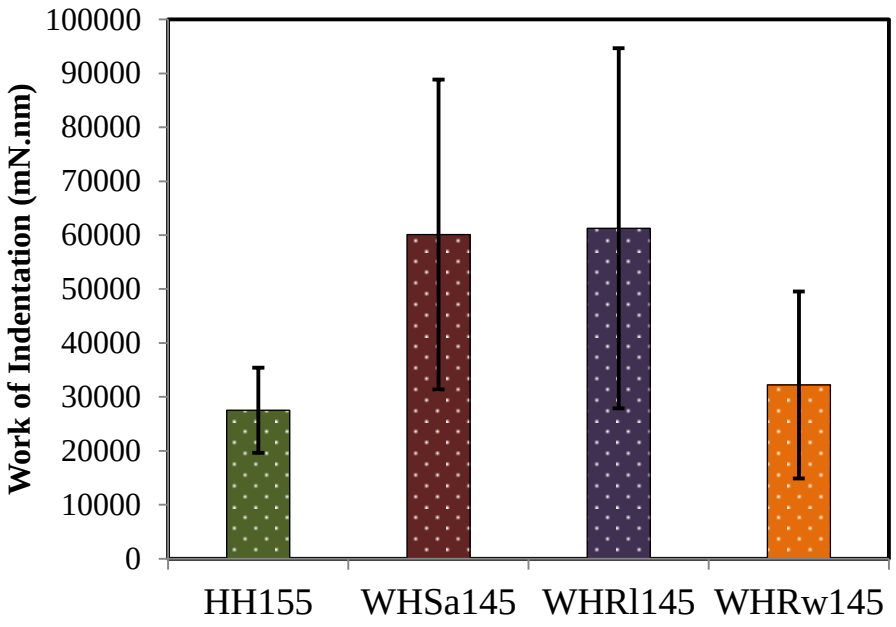

Figure 6.17 Work of indentation for HMA and WMA manufactured at 145°C using 40/60 binder grade

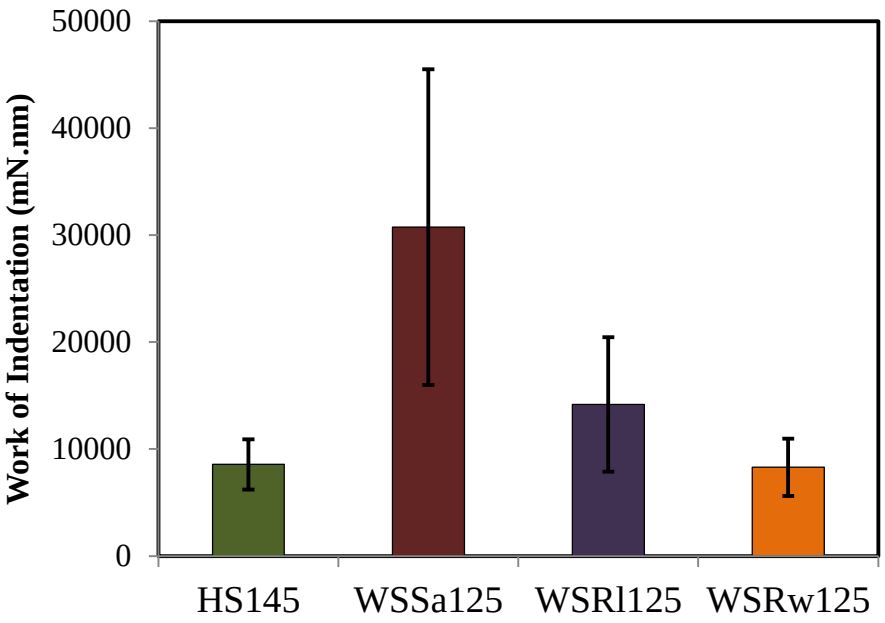

Figure 6.18 Work of indentation for HMA and WMA manufactured at 125°C using 100/150 binder grade

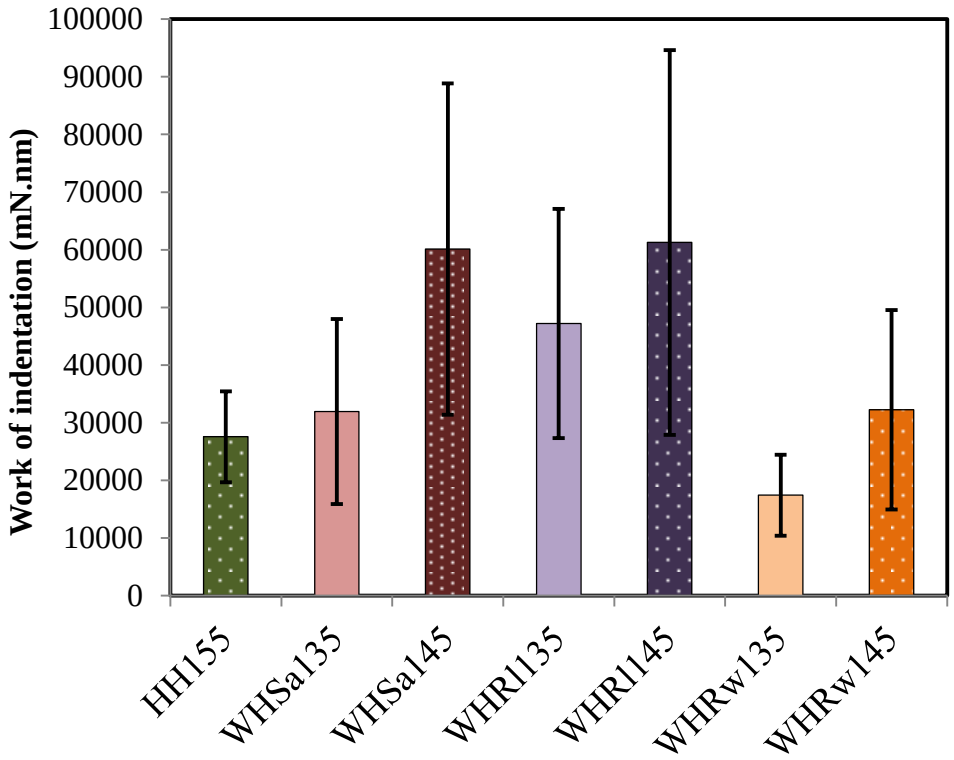

Figure 6.19 Work of indentation for HMA and WMA manufactured at 135°C and 145°C using 40/60 binder grade

6.5.2 Comparison between work of indentation and work of fracture

As presented above, the rank performance of work of fracture of aggregate-WMBBs was qualitatively associated with the adhesion force obtained from AFM-PFQNM. However, although the rank of work of indentation is as same as the work of fracture and adhesion obtained from AFM-PFQNM, in terms of asphalt mixture, Rediset LQ improved the strength bond better than Rediset WMX because Rediset LQ is also classified as a compaction aid. The significant improvement in volumetric properties (air voids and bulk density) of WHRl145 in comparison with HH155 resulted in a remarkable improvement in the bond strength of the WHRl145. This fact justifies why there is a need to characterise the adhesive bond strength between aggregate and binder in the mixture because there are different factors affecting this bond, as presented in Section 6.2.2.The required work of indentation or obtained elastic modulus and hardness can be used to directly represent the bond strength between aggregate and binder/mastic. Table 6.2 illustrates a comparison between techniques.

Table 6.2 Overall effect of warm additives on the strength bond between aggregate and binder

Binder grade	Material			Pull-off		AMF		Nanoindentation	
	Binder	Aggregate-binder system	Asphalt mixtures	Rank	Testing	Rank	Testing	Rank	Testing
40/60 (H)	H	Aggregate-H	HH155	1	20°C	1	22°C	1	22°C
	H+2% Sa	Aggregate-H+ Sa	WHSa145	4	20°C	4	22°C	4	22°C
	H+0.5%Rl	Aggregate-H+ Rl	WHRl145	2	20°C	2	22°C	3	22°C
	H+2%Rw	Aggregate-H+ Rw	WHRw145	3	20°C	3	22°C	2	22°C
100/150 (S)	S	Aggregate-S	HS145	1	10°C	1	22°C	1	22°C
	S+2% Sa	Aggregate-S+ Sa	WSSa125	4	10°C	4	22°C	4	22°C
	S+0.5% Rl	Aggregate-S+ Rl	WSRl125	2	10°C	2	22°C	3	22°C
	S+2%Rw	Aggregate-H+ Rw	WSRw125	3	10°C	3	22°C	2	22°C

1: less adhesion 4: high adhesion

6.6 Conclusion

The bond strength between aggregate and binder/mastic plays a major role in the overall performance of an asphalt mixture. In this chapter, the effect of warm additives on the bond strength of aggregate-binder systems was investigated in detail. Furthermore, a comparison was made between the work of fracture and the adhesion force between the probe and binder surface using AFM-PFQNM. In addition, a new protocol was introduced to evaluate the aggregate-binder/mastic bond strength using nanoindentation.

The main findings of this chapter are:

1. It was found that Sasobit, Rediset WMX and Rediset LQ increased the work of fracture by 170, 100 and 143% respectively for the aggregate-binder system produced using a 40/60 binder grade, and 70, 25 and 50% respectively for the aggregate-binder system produced using a 100/150 binder grade.

2. It was possible to obtain complete adhesive failure for the aggregate-binder system using 40/60 binder grade tested at 20°C but not with the 100/150 binder grade at the same temperature and binder film thickness. The reason was attributed to the mode of failure being mixed cohesive and adhesive, or at times complete cohesive failure. Therefore, control and warm-modified binders using 100/150 binder grade were tested at 10°C. The failure modes were noticed visually and confirmed by the shape of the load-displacement curve.

3. After taking into account the effect of test temperature on the adhesive bond in aggregate-binder systems produced with 40/60 and 100/150 binders grades, it was evident that the effect of Sasobit and both types of Rediset is exactly the same: they all improved adhesion.

4. The performance of warm additives in improving the work of fracture was qualitatively associated with the effect of warm additives on the adhesion force determined using AFM-PFQNM.

5. For the first time it has become possible to investigate the bond strength between aggregate and binder/mastic (or ITZ) in the asphalt mixture using nanoindentation. A new method called work of indentation to investigate the bond strength using nanoindentation depend on the total area of load-displacement has been introduced in this chapter.

6. The work of indentation was qualitatively associated with work of fracture obtained from the pull-off test and adhesion force obtained from AFM-PFQNM. The only difference noticed in the asphalt mixture is the effect of Rediset LQ. In addition to the objectives of using this additive as an active adhesion and surfactant, it is also developed as a compaction aid, which was confirmed by the significant improvement in the volumetric properties of the asphalt mixture. Consequently, its effect on the mechanical properties and bond strength of ITZ was better than that of Rediset WMX.

Chapter Seven

Fatigue Cracking Characterisation of Warm Mix Asphalt (WMA)

7.1 Introduction

Bituminous pavement layers should exhibit an adequate level of resistance to fatigue cracking when they are subjected to repeated loading by traffic. The current school of thought in the asphalt industry is that warm mix asphalt (WMA) can typically be manufactured at a temperature of approximately 20-30°C lower than that of hot mix asphalt (HMA). However, the asphalt mixture's production temperature can highly affect the durability of the pavement. This chapter presents an investigation into the fatigue performance of WMA and the effect of mixing temperature on fatigue cracking of WMA tested in a dynamic shear rheometer (DSR). As proved in Chapter 3, warm additives such Sasobit and Rediset WMX have a superior performance in the fatigue life of asphalt binders, while there is no clear conclusion about the fatigue performance of WMA. It is therefore expected that the effect of production temperatures and binder grades should be considered in evaluating the fatigue life of WMA. In other words, the question is: to what extent can the production temperature be decreased without causing a negative impact on the fatigue life of asphalt mixtures? This question is addressed in detail in the current chapter by taking in account the effect of mixture phases on the overall fatigue performance of WMA.

7.2 Fatigue test of asphalt mixtures

Degradation in pavement serviceability due to fatigue cracking is an important consideration in the design of asphalt mixtures and structural design of flexible pavements. The fatigue performance of asphalt mixtures can be affected by a number of factors such as an inadequate structural design, repeated heavy loads, poor drainage and construction quality, fluctuations in the environmental temperature, and asphalt binder stiffening due to ageing at low and intermediate temperatures (Jamshidi *et al.* 2013). It is thought that WMA has a better performance in terms of fatigue cracking resistance as the bitumen is less oxidised because of the lower production temperature, although this observation does not take into account the effect of warm additives on fatigue resistance.

Fatigue cracking is one of the most common distresses in asphalt pavements; in practice, it occurs when pavement structures undergo repeated loading specifically at intermediate temperatures in the range of 10°C to 30°C (Al-Khateeb and Shenoy 2004). Fatigue cracking may not occur if the tensile and compressive strain created by repeated load is less than the ultimate or the design strength of the material. However, if the tensile and compressive strain caused by repeated load is practically higher than the maximum allowable material strength capacity, the material rigidity decreases and, in the long term, this reduction in rigidity results in a structural failure (Di Benedetto et al. 2004). These stages are called the initiation and propagation of a micro-crack. In other words, during the first phase or stage, degradation resulting from damage is uniformly spread in the material, which causes the initiation of a micro-crack. As the damage is continually accumulated, the initial cracks will coalesce, resulting in the appearance of a macro-crack (Di Benedetto *et al.* 2004), and finally, in some extreme cases, the potholes caused by the further disintegration of the micro-cracks will be exacerbated by the action of traffic (Suh *et al.* 2010).

In fact, it is particularly difficult to characterise the fatigue life of hot mix asphalt (HMA) due to a number of reasons such as the composite nature of the material, the gradation of aggregate particle size, asphalt film thickness variation within the mastic, air void size distribution, and the dependency of asphalt binder behaviour on time and temperature (Masad *et al.* 2008a). Therefore, this fatigue-

cracking phenomenon should be more complicated in WMA, as the mixing temperature is lower than HMA, and thus another two factors or questions should be addressed. The first is whether the fatigue life improves because of the lower production temperature or the effect of warm additives. And, secondly, to what extent the production temperature can be decreased without causing a negative impact on the degree of bonding between the binder and the aggregate, and the overall mastic stiffness in the asphalt mixtures. Both of these questions are deeply investigated in the current study.

As presented and proved in Chapter 3, it has been found that some warm additives such as Sasobit and Rediset WMX have a superior performance in terms of fatigue life of warm-modified bituminous binder. It is therefore clear that the effect of the production temperature of WMA should be taken into account to characterise its effect on fatigue life.

7.3 Fatigue test configuration

In the fatigue test, there are two loading configurations, sinusoidal waveform and haversine waveform. These configurations can be illustrated in the form of a beam fatigue test. In the sinusoidal waveform, the load bends the beams in both upward and downward directions, whilst, in the haversine waveform, the load arches the beam only in the downward direction. The upward and downward directions of the sinusoidal waveform are half the magnitude of the haversine waveform, as illustrated in Figure 7.1.

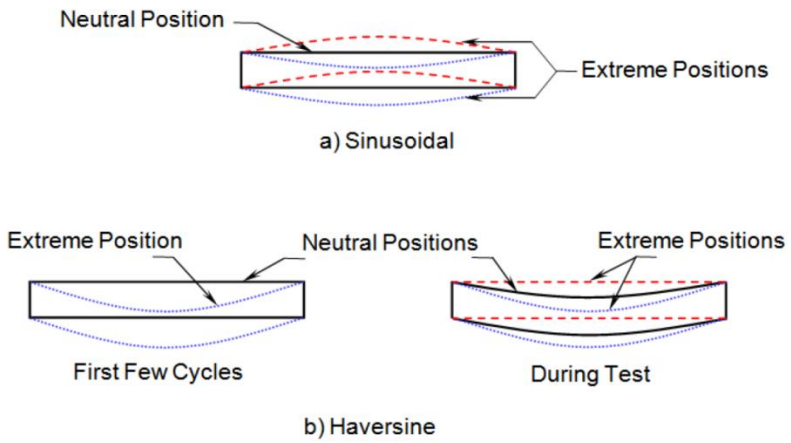

Figure 7.1 Neutral and extreme positions using sinusoidal and haversine waveform for a deflection-controlled test on HMA (Mamlouk *et al.* 2012)

In a study conducted by Mamlouk *et al.* (2012) that attempted to optimise the test conditions such as waveform type (haversine vs. sinusoidal), incorporating rest periods between loading cycles and the effect of rest period on the healing of the HMA, it was found that, in the deflection-controlled haversine test, despite the fact that the deflection input remained haversine, resulting stresses and strains followed a sinusoidal waveform in which the beam was bent in both upward and downward directions, similar to the resulting strain and stress of the deflection-controlled sinusoidal test. And, as there was no match between the assumptions and actual conditions of the test, the fatigue results were erroneous. Whereas, in the case of the deflection-controlled sinusoidal test, the results were accurate as the intended stress and strain waveforms were expected. It was therefore recommended that it is of paramount importance to use a sinusoidal waveform in order to obtain accurate and consistent data.

7.3.1 Modes of fatigue testing.

Generally, the fatigue life of asphalt mixtures can be evaluated with repeated load testing, using either a constant applied strain (controlled strain) or a constant applied stress (controlled stress). In controlled strain mode, the applied strain remains constant and the resulting stress decreases during the test. Conversely, in controlled stress mode, the applied stress is maintained and the resulting strain response increases during the test. It is recommended that the controlled stress mode is suitable for thick layers and the strain controlled is appropriate for thin

layers, as the strain level remains almost constant at the bottom of a thin pavement, while stress levels remains almost constant at the bottom of a thick pavement over a wide range of mixture stiffnesses. However, due to certain reasons such as modifications in the pavement structural design and the realisation that multiple fatigue mechanisms may happen, it has become difficult to identify criterion that specifically applies to either stress mode or strain mode conditions (Masad *et al.* 2008a).

7.3.2 Interpretation of fatigue phases

Fatigue life has traditionally been analysed by plotting the reduction in the stiffness against the number of load cycles or by plotting the normalised modulus verses number of load cycles. Three phases have been identified during the fatigue test, as illustrated in Figures 7.2 and 7.3.

Phase I (Internal heating): this phase presents a rapid reduction in the stiffness modulus and is mainly as a result of internal heating of the sample (Di Benedetto *et al.* 1996). Bituminous materials dissipate energy after each load cycle. This energy is firstly transformed into heat which initially increases the temperature of the sample and then, it diffuses through the surface (Artamendi 2003,Di Benedetto *et al.* 1996).

Phase II (Crack initiation): in controlled strain, this phase includes two parts, micro-crack formation and crack-formation, which are separated by a flection point (Rowe and Bouldin 2000), while the controlled stress mode is characterised by an approximate linear reduction in the stiffness modulus against number of cycles.

Phase III (Crack propagation and damage): is generated by a sharp and fast reduction in the stiffness modulus. This is mainly due to micro-cracks coalescing to form a sharp crack.

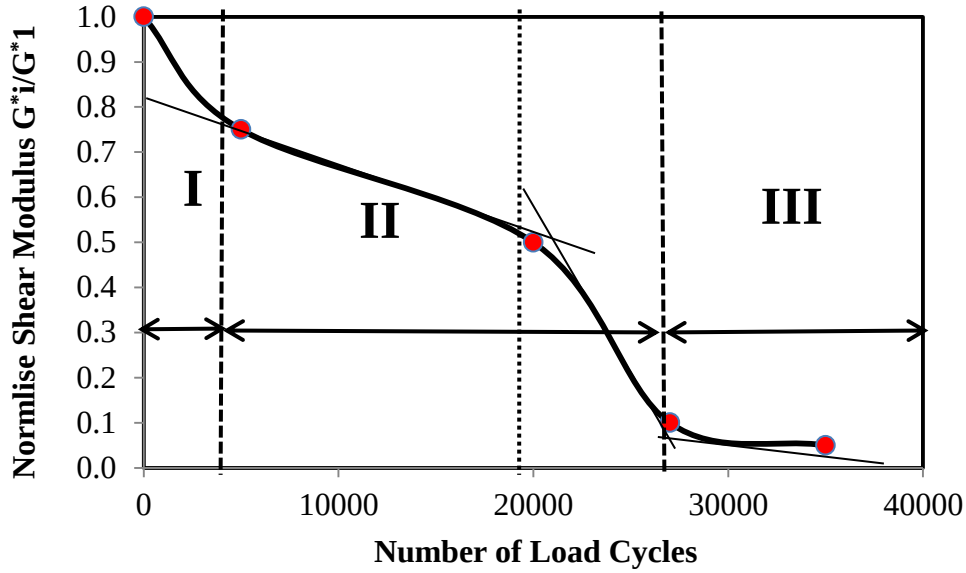

Figure 7.2 Typical fatigue phases in controlled strain mode

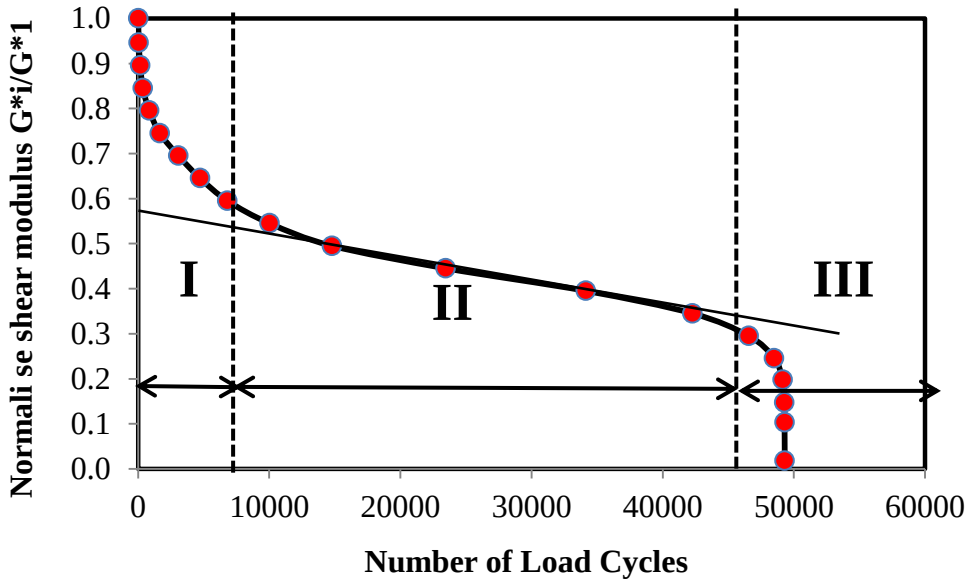

Figure 7.3 Typical fatigue phases in controlled stress mode

7.4 Available techniques for fatigue testing

There are several techniques used to characterise the fatigue cracking of asphalt mixtures, as illustrated in Figure 7.4. These techniques are divided into homogeneous and non-homogenous loading effects. In the homogeneous loading effect, the load is uniformly disseminated to all cross-sectional areas of the sample, whereas, in the non-homogenous loading effect, the load effect is different at different locations across the cross-sectional areas of the sample (Di

Benedetto *et al.* 2004). All the techniques presented in Figure 7.4 are non-homogeneous loading effects apart from the Uniaxial test (Tension-Compression test).

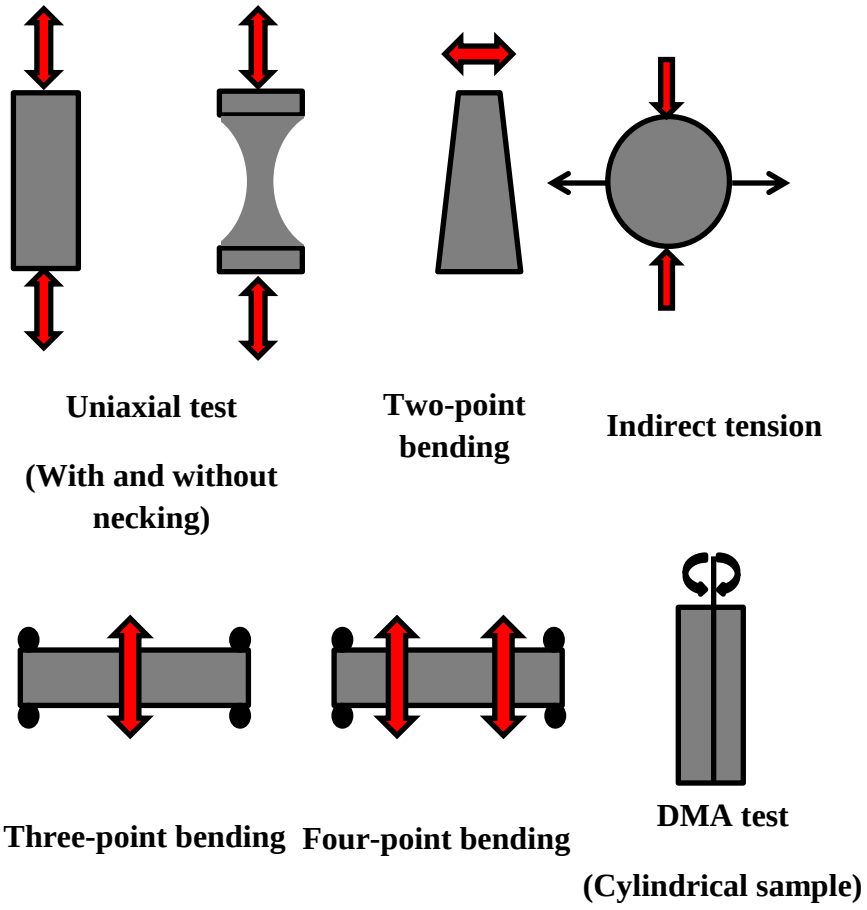

Figure 7.4 Available techniques for fatigue testing of asphalt mixtures

7.4.1 Conventional techniques

Fatigue cracking of asphalt mixtures has been extensively characterised using the traditional techniques, uniaxial (tension-compression), indirect tension, two-point bending, three-point bending and four-point bending tests.

The four-point bending beam is widely used to characterise fatigue life and evaluate the stiffness modulus of asphalt mixtures. However, despite the fact that this test is widely used and presents reliable results, it is time consuming as it may take several days to complete. Furthermore, it is also material consuming.

The four-point bending beam test is greatly utilised in the USA, compared to Europe (Maggiore *et al.* 2012).

The two-point bending test is also used to characterise fatigue life and evaluate the stiffness modulus of asphalt mixtures. This test is wide spread and more commonly used in Europe than in the USA (Maggiore *et al.* 2012). It is categorised as having a non-homogenous loading effect because the fracture commonly occurs at the first third from the bottom of the sample (Rowe 1993,Cocurullo *et al.* 2008,Maggiore *et al.* 2012). This test is only a controlled strain test as it is designed to apply only a sinusoidal loading under controlled displacement (BS EN 12697-24 2012). However, it could also be used for controlled stress if integrated with an electronic magnetic actuator (Cocurullo *et al.* 2008). In comparison with other techniques, two-point bending test has the ability to test two samples at the same time; therefore, firstly it is time saving and, secondly, it ensures the same conditions are applied to both samples. However, it is difficult to manufacture samples of high enough quality to be used in the test.

The three-point bending test has a similar concept to the 4PB. It is also a non-homogenous test (Di Benedetto *et al.* 2004). It is conducted on prismatic beams, as illustrated in Figure 7.4. However, this test is not as widely used as four-point bending beam and two-point bending tests.

The indirect tensile test is another test used to measure the fatigue life and stiffness modulus of asphalt mixtures. This test is performed on cylindrical samples. In the fatigue test, displacement transducers are used to measure the vertical displacement whereas, in measuring stiffness, the displacement transducers measure the deformation in the horizontal diameter of the cylindrical sample. The indirect tensile test is a non-homogeneous test because the tensile stress is not regularly distributed under the repeated compressive loading (Di Benedetto *et al.* 2004).

The uniaxial test (Tension-Compression) is a homogenous test (Di Benedetto *et al.* 2004) because the load is uniformly distributed on the cross section of the sample. Tension-Compression can be conducted on either cylindrical samples (Luo *et al.* 2012) or beam samples (Qian *et al.* 2013). The

main advantage of using this type of sample is that loading effect can be distributed to the whole sample.

7.4.2 Modern techniques

The dynamic mechanical analyser technique is used to apply load to a sample and its response is recorded to obtain the phase angle and the deformation data under any conditions such as temperature, frequency, magnitude of loading, etc. (Menard 2008). This configuration applies an oscillatory sinusoidal deformation to the sample. In this technique, the fatigue test can be conducted by applying controlled strain or stress.

The Dynamic Shear Rheometer (DSR) works to a similar concept as the dynamic mechanical analyser. The DSR has been extensively used to study the rheological properties of semisolid and liquid materials. More attention has been paid recently to adopting the use of the DSR to characterise the mechanical properties of asphalt binder, mastic and Fine aggregate matrix (Airey 2002,Airey *et al.* 2003,Masad *et al.* 2008a,Masad *et al.* 2008b,Branco and Franco 2008,Ahmed and Khalid 2015,Abd and Al-Khalid 2015,Ahmed 2016). In comparison to other techniques, the DSR has a great deal to offer in saving test time and also reducing the quantity of required material. In this chapter, a DSR has been used to characterise the fatigue cracking of WMA.

7.5 Preparation of fatigue test samples

HMAs and WMAs were manufactured as reported in Chapter 5, Sections 5.4. The cylindrical DSR samples (12 mm in diameter and 50 mm in height) were cored using an electric coring machine with continuous water in line with preparation of cylindrical nanoindentation samples as presented previously in Chapter 5. A Marcrist Ø12 mm (inside diameter) crown core drill was used to prepare the cylindrical DSR samples. 34 cylindrical DSR samples were obtained from each beam. The DSR samples were left to dry for 24h at ambient temperature. They were then put in an oven maintained at 20°C for half an hour to ensure they were completely dry. After that, bulk densities for all DSR samples were measured based on (BS EN 12697-6 2012), and, during the measurements, the samples were

coded and kept in PVC tubes, and then stored in a fridge at 10°C. Figure 7.5 shows the preparation of the DSR samples.

Figure 7.5 The preparation of DSR-samples

7.6 Mechanical testing

7.6.1 Modifications to the DSR

Modifications were made to the DSR Kinexus in order to use it to run sequences on cylindrical DSR samples. These modifications included design and manufacturing end alterations and adjusting the holder connections that are used to hold and set up samples in the proper position for testing, as shown in Figure 7.6-a. Moreover, in order to control the sample temperature during testing, a temperature controller unit illustrated in Figure 7.6-b was designed and added to the DSR as an essential component. End connections, the holder and the temperature controller unit were manufactured in the University of Liverpool workshop. Figure 7.7 shows the DSR sample after it has been placed in the temperature controller unit.

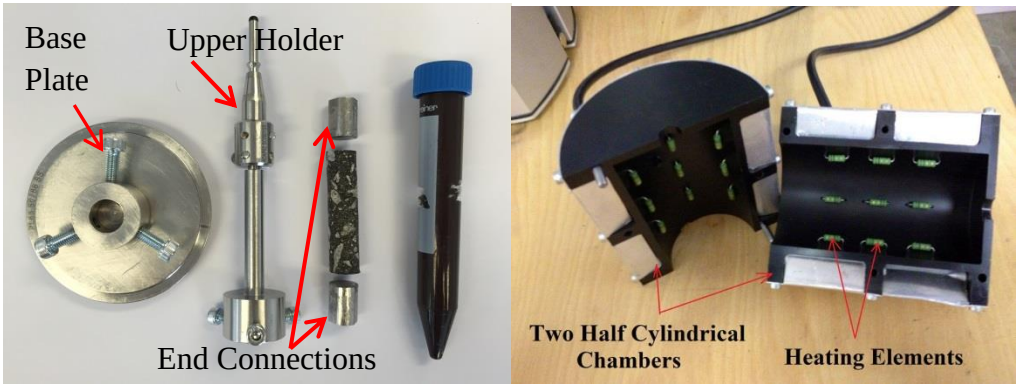

Figure 7.6a Figure 7.6b

Figure 7.6 a- End connections and holders, b- Temperature control unit

Figure 7.7 DSR sample after it has been placed in the Temperature control unit

7.6.2 Constructing the sequence using rSpace for Kinexus

The DSR Kinexus developed by the Malvern Instrument Company is an advanced rotational rheometer platform integrating advanced software to provide accurate and precise measurements with ultimate flexibility and ease of use. Using the integrated rSpace software allows the operator to construct a test sequence as required. A sequence was built in order to run a sweep frequency test within the linear limit of the DSR samples, and fatigue test within non-linear damage. Five samples were tested for each mix and the presented data are the average value of

the samples. More details about the constructed sequence are presented in Appendix D.

7.6.3 Stiffness

7.6.3.1 Loading configuration

Stiffness measurement is performed by applying a sinusoidal loading or other controlled loading on compacted bituminous material using different types of specimens and support. The European Standard specifies the methods for characterising the stiffness of bituminous mixtures by alternative tests, including bending tests and direct and indirect tensile tests. These techniques are used to rank bituminous mixtures on the basis of stiffness, as a guide to relative performance in the pavement, to obtain data for estimating the structural behaviour in the road. However, as the European Standard does not impose type of testing device, the precise choice of test conditions depends on the possibilities and working range of the used device (BS EN 12697-26 2012).

In this study, stiffness measurements of HMA and WMA are conducted within linear viscoelastic region of bituminous mixture. The controlled stress value of measurement was 25,000 Pa and the frequency was in the range from 0.1Hz to 10Hz, while the testing temperature was 25°C. More details for the DSR sequence of sweep frequency test are presented in Appendix D, Figure D-2, and a summary of all the sweep frequency results is presented in Appendix F.

7.6.3.2 Effect of warm additives on the stiffness of asphalt mixtures

It was found that Sasobit significantly increased the binder stiffness while Rediset WMX and LQ did not alter the binder properties at the recommended dosages, as presented previously. In fact, Sasobit also increased the stiffness of bituminous mixtures, as can be seen in Figures 7.8, 7.10 and 7.11. Despite the fact that it has been reported that Sasobit decreases the compaction temperature by approximately 18°C (Hurley and Prowell 2005b), this is not always true. In the current study, the maximum reduction in the production temperature was found to be 10°C and 20°C for 40/60 and 100/150 binder grades compared to control mixes HH155 and HS145 respectively, based on the stiffness measurements of the

bituminous mixtures. When Sasobit-WMA modified binder was produced at 135°C, the stiffness of this mixture (WHSa135) was lower than that of the control mix (HH155) at different ranges of loading frequencies. However, the maximum reduction in the production temperature of 20°C for the mixture incorporating the 100/150 binder grade compared to control mix HS145 was achieved. This point definitely highlights that the reduction in the production temperature should distinguish between hard and soft binders because, although the 40/60 binder grade was found to completely coat the aggregate at 135°C, the degree of bonding between binder and aggregate and the overall mastic stiffness were insufficient to reflect the required stiffness of the mixture as shown previously in Chapter 5.

As proved previously, Sasobit increased the stiffness of binder; therefore, as can be seen in Figures 7.8 and 7.9, even though the WHSa135 was produced at a temperature lower than the control mix by 20°C, its stiffness was not significantly lower than the control mix.

The effect of mixing temperature was further clear in the case of incorporating Rediset WMX and LQ, as shown in Figure 7.9. The stiffness of WHRl135 and WHRw135 was significantly lower than the stiffness of HH155. As the reduction in the production temperature was reduced from 20°C to 10°C so WMAs were manufactured at 145°C, the stiffness of those mixtures improved, as shown in Figure 7.10. The stiffness of WHRl145 manufactured at 145°C was exactly the same as the stiffness of HH155, while the stiffness of WHRw145 was slightly lower than that of the control HH155. The effect of Rediset WMX on mixture stiffness was also obvious in the case where the soft binder (100/150 binder grade) was incorporated, when the stiffness of WSRw125 was lower than that of the control mix HS145 as shown in Figure 7.11.

Despite the fact that the Rediset LQ and WMX do not increase the stiffness of asphalt mixtures, both have the ability to displace water from the aggregate surface, enabling not only the coating of the aggregate but also the creation of a strong chemical bond between the aggregate and bitumen that is resistant to the action of water, as the aggregate may not be dried completely if the mixing temperature is lower than the control mix.

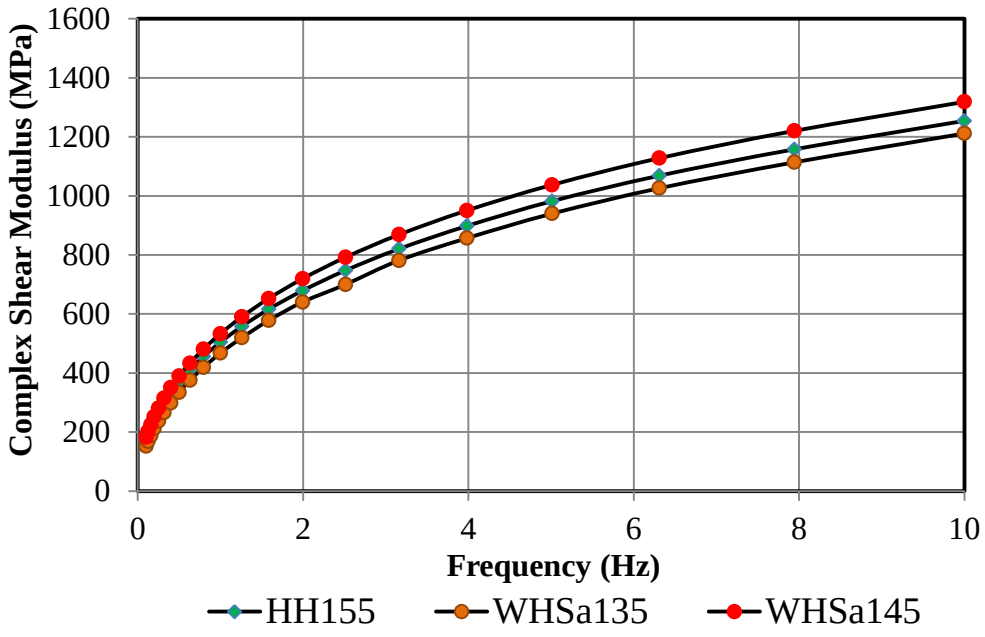

Figure 7.8 Effect of mixing temperatures on the stiffness of Sasobit modified-mixture using 40/60 binder grade

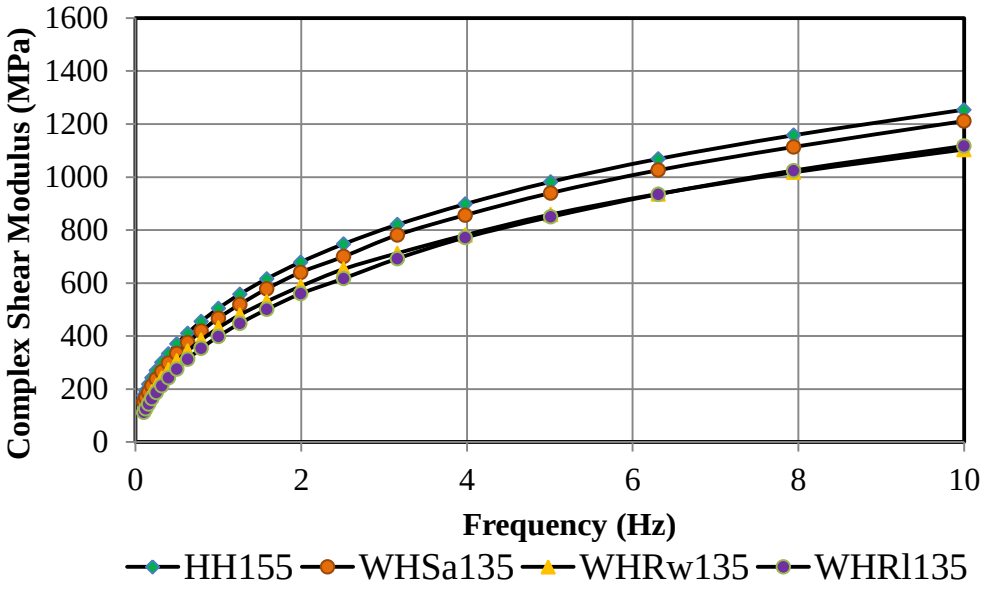

Figure 7.9 Average stiffness of WMA manufactured at 135°C using 40/60 binder grade

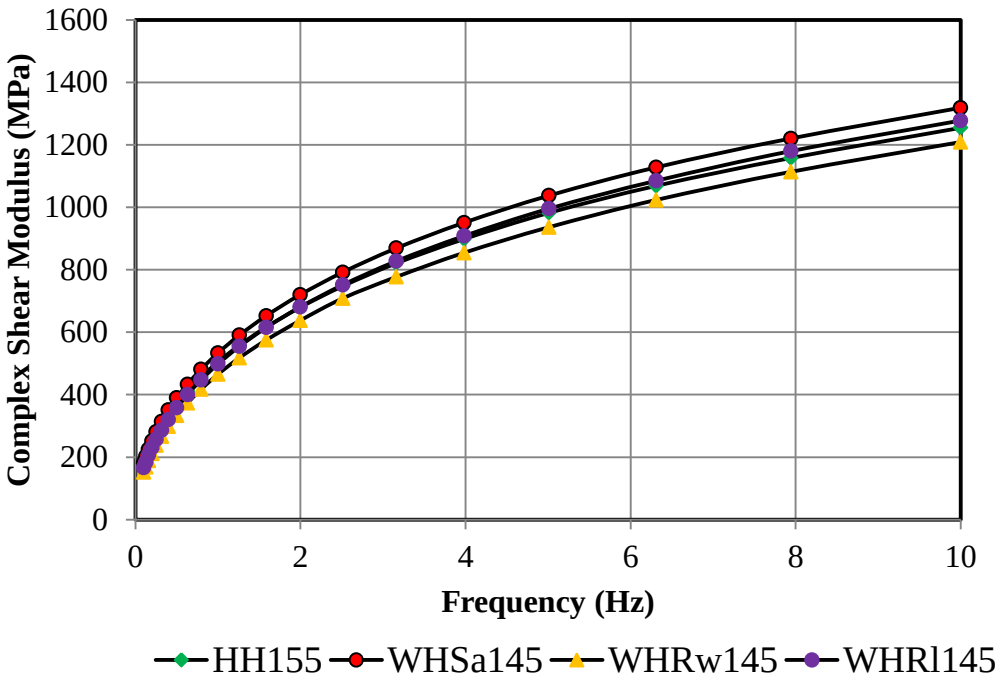

Figure 7.10 Average stiffness of WMA manufactured at 145°C using 40/60 binder grade

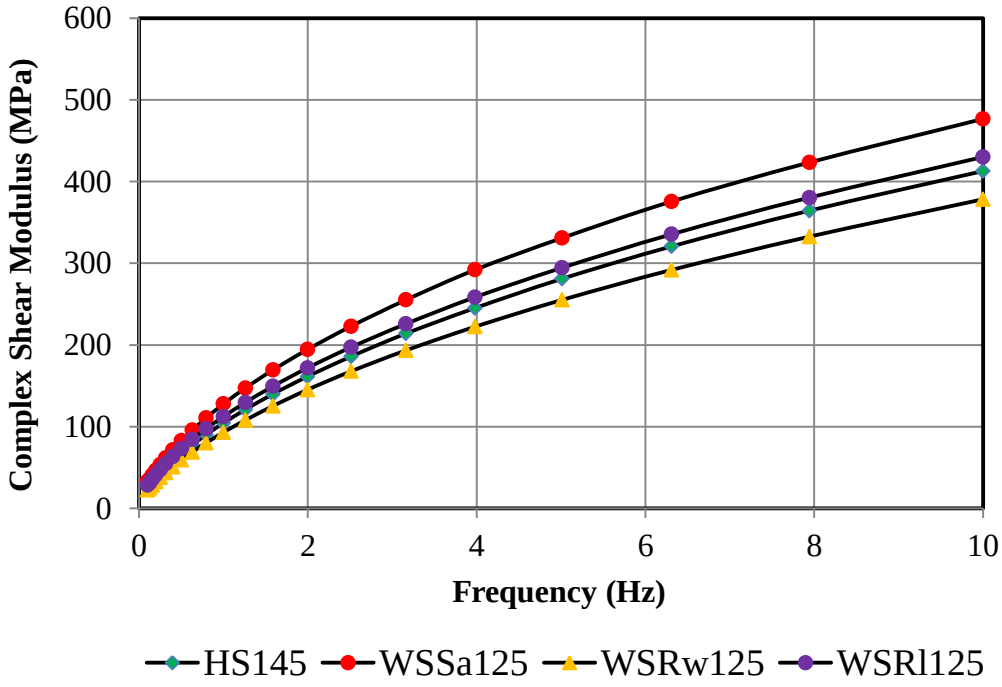

Figure 7.11 Average stiffness of WMAs manufactured at 125°C using 100/150 binder grade

7.6.3.3 Effect of warm additives on the viscoelastic behaviour of asphalt mixture

It was also found that, as Sasobit increased the stiffness of the WHSa145 and WSSa125 asphalt mixtures, it slightly decreased the phase angle in comparison with the control mixtures HH155 and HS145 respectively if only the effect of production temperature is considered, as illustrated in Figures 7.12a and 7.12b. This phenomenon is exactly same to what was noticed in the binder. However, despite the fact that there was an agreement that the phase angle of WHSa135 was slightly higher than the phase angle of the control mixture HH155 at different loading frequencies ranging from 0.1Hz to 10Hz, as displayed in Figure 7.12a, a noteworthy point can be seen in Figure 7.12b. WHSa145 had slightly higher phase angles at frequencies lower than 1Hz and lower phase angles at frequencies higher than 1Hz. This phenomenon, in fact, occurs because Sasobit forms a lattice structure which acts as a bridge between molecules and prevents their movement. Consequently, at lower frequencies, when load tends to accelerate damage in the material, the lattice structure is extended due to the availability of Sasobit, which results in slightly increasing the phase angle without adversely decreasing the modulus of the material. However, at higher frequencies, that phenomenon may not exist as the load on the material is less than its effect at low frequencies. In fact, 100/150 binder grade is relatively soft; WSSa125 had lower phase angles at different frequencies although it seems to follow the same trend at lower frequencies as the difference in the phase angles between WSSa125 and HS145 is slightly higher at 10Hz than at 0.1Hz as shown in Figure 7.12c.

Interestingly, Rediset LQ seems to act the same as Sasobit. One of the advantages of using Rediset LQ is improving the aggregate-binder bonding. It is also expected that Rediset LQ may increase the domain of ductility without negatively impacting on the modulus of material at lower frequencies in which resistance to cracking improves. On the other hand, there is an agreement that Rediset WMX slightly decreases stiffness and increase the phase angles as shown in Figures 7.12b and 7.12c due to probably the effect of production temperature, which is the inverse to what was found in its effect on the asphalt binder. However, initially the effect of production temperatures plays a significant role in determining the elastic and viscous behaviour of asphalt mixtures. As can be seen

in Figures 7.12a and 7.12b, all warm asphalt mixtures produced at temperature of 135°C, lower than the control mix by 20°C had higher phase angles than that of control mix HH155 while, as the production temperature of WMA was 145°C, only 10°C lower that of control mix HH155, the difference in the phase angle between WMA and HMA decreased.

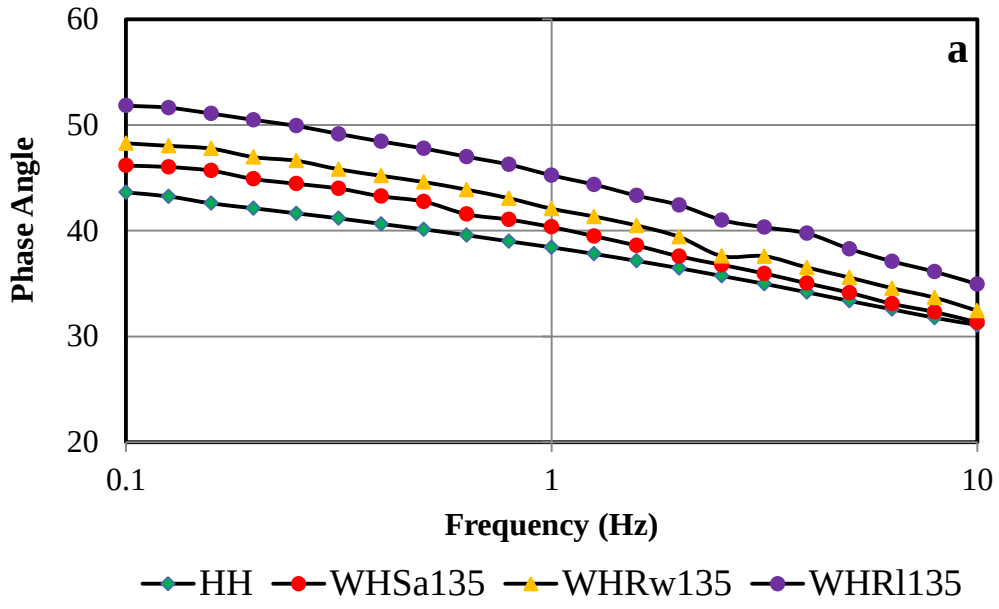

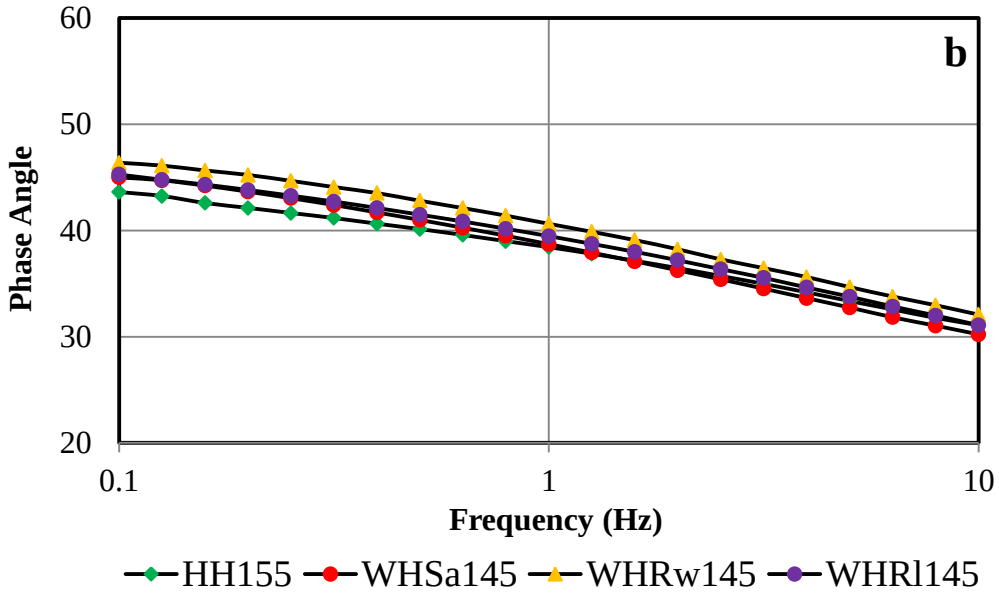

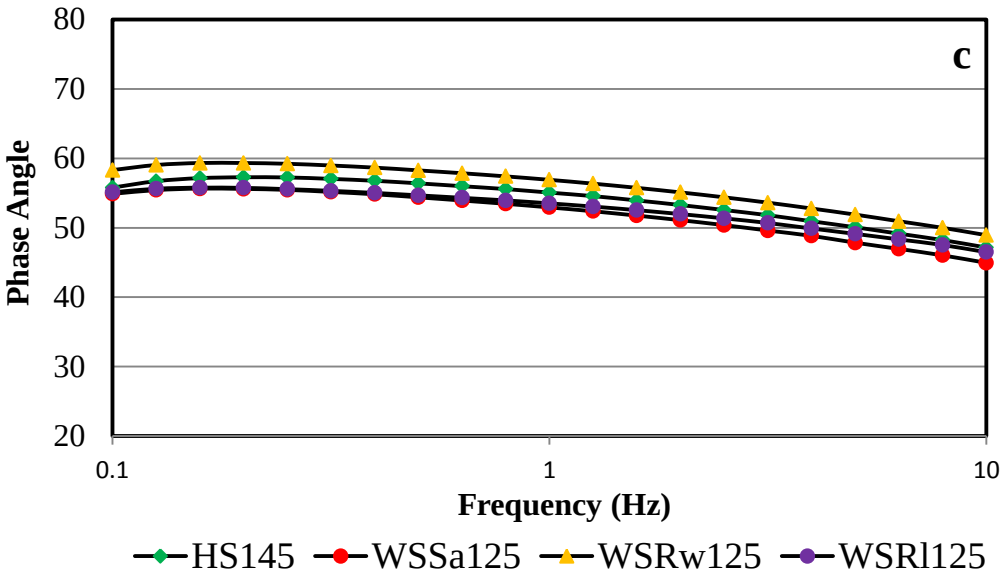

Figure 7.12 Average phase angle of WMA (a) manufactured at 135°C using 40/60 binder grade (b) manufactured at 145°C using 40/60 binder grade (c) manufactured at 125°C using 100/150 binder grade

7.6.4 Fatigue performance

7.6.4.1 Determination of the controlled stress value/stress amplitude test

In order to select an adequate value for the fatigue test, stress amplitude was performed at 25°C and 2.5 Hz frequency on three cylindrical DSR samples for HH155 and HS145 mixtures and the strain response was collected. Sweep stress increased linearly from 5KPa to 589KPa distributed at 24 values. The maximum stress value that can be applied in a DSR is 600KPa as the maximum torque that can be applied using a DSR is 0.2 N.m, which is equal to 600 KPa. The strain response against time for each amplitude stress, which was distributed along 80 points, was then plotted and fitted linearly in order to find slopes of strain-time ($d\gamma/dt$) from the fitted equations using a linear regression model. Finally, ($d\gamma/dt$) was plotted against amplitude stress to determine the point where ($d\gamma/dt$) increased dramatically as the stress amplitude increased. Figures 7.13 and 7.14 show the typical shear-strain response plotted against time for HH155 and HS145 respectively. The amplitude sweep stress results are presented an Appendix E.

As can be seen in Figures 7.15 and 7.16, the linear regain is the point where the shear-strain response slope against stress amplitude diverts from the straight line. The stress values used in the controlled-stress fatigue test are shown

in Table 7.1. It should be mentioned that this approach was applied only to the control mixtures, whilst the selection values were also used with the warm mixtures; therefore, comparisons can be made with particular reference to the control mixtures. It can be noticed that the linear limits for HH155 and HS145 are approximately 325KPa and 200Kpa respectively. Therefore, in order to shorten the fatigue test, the controlled stress values were chosen after the linear limit.

Table 7.1 Linear limits and selected values for fatigue tests

Mix	Linear Limit (Pa)	Selected value (Pa)
HH155	325000	425000
HH145	200000	250000

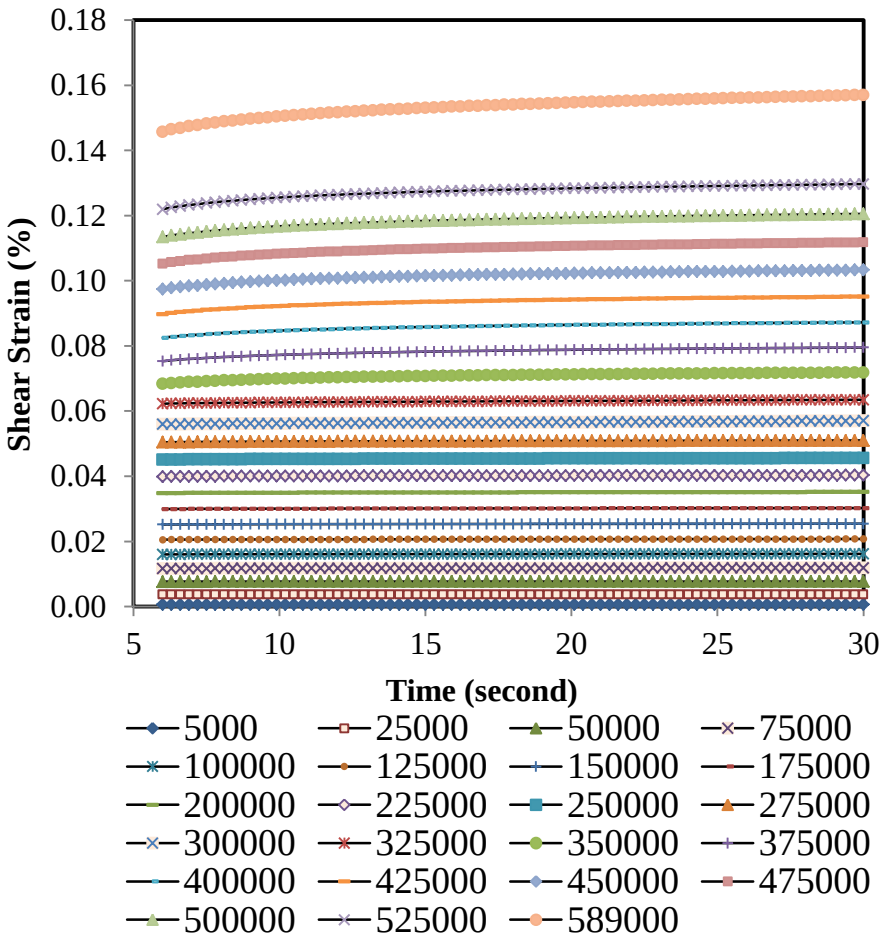

Figure 7.13 Shear strain against time at each amplitude stress for HH155

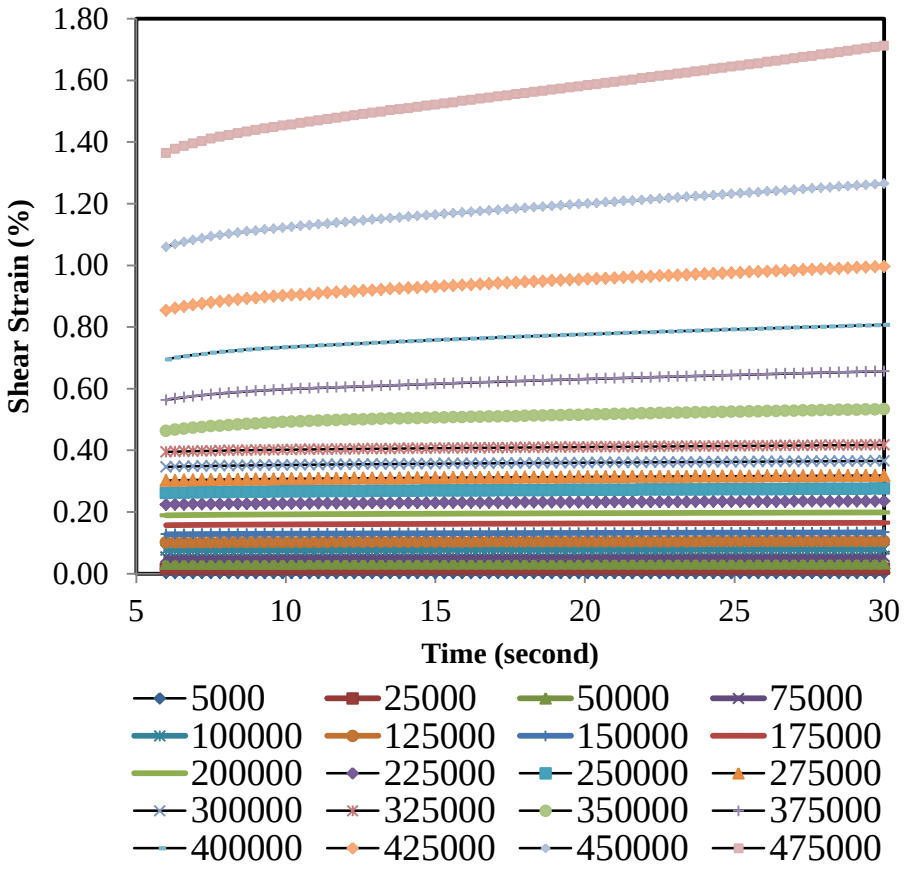

Figure 7.14 Shear strain against time at each amplitude stress for HS145

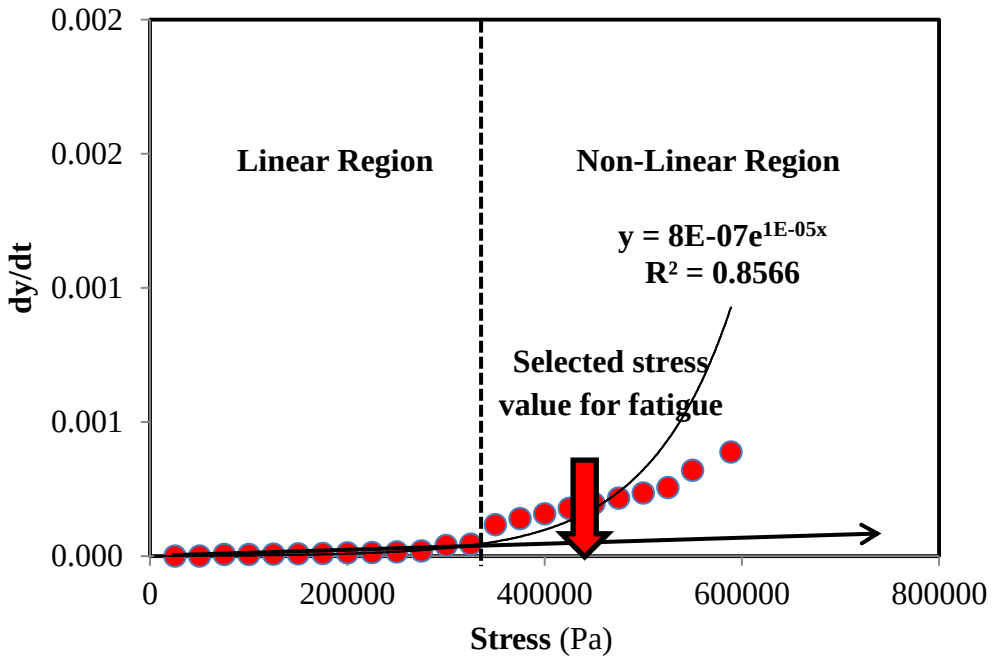

Figure 7.15 Slopes of strain-time (dγ/dt) against stress for HH155

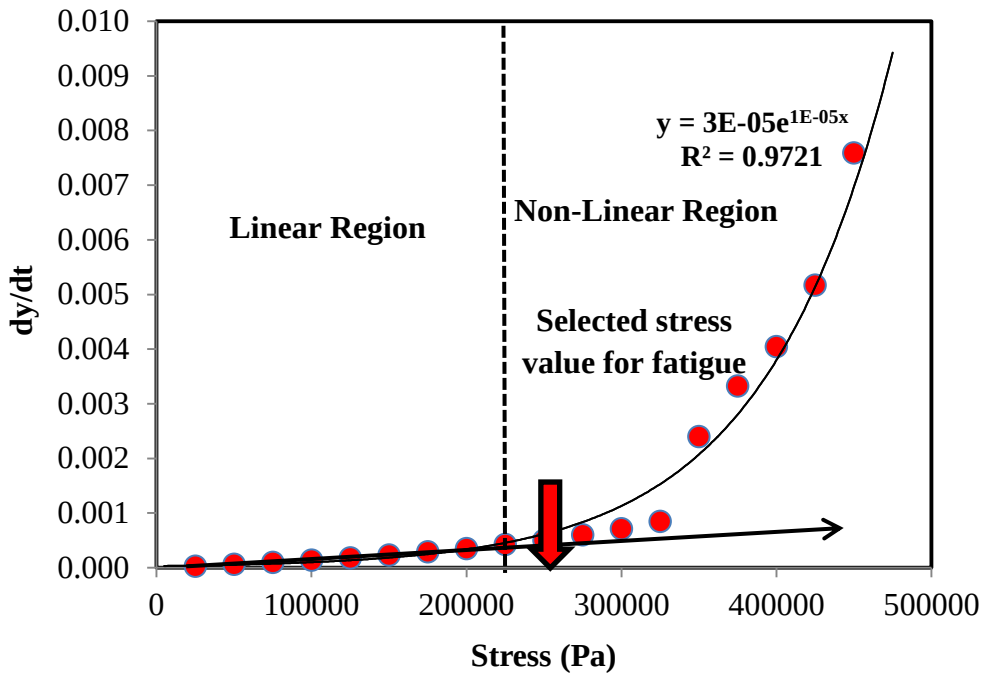

Figure 7.16 Slopes of strain-time (dγ/dt) against stress for HS145

7.6.4.2 Fatigue test configuration

The concept of measuring the fatigue performance of WMA is similar to the fatigue test applied to the bitumen. The time sweep fatigue test (controlled stress only) was also used to characterise the fatigue cracking of HMAs and WMAs. As mentioned previously, modifications were made to the DSR so that it could be used to run sequences on cylindrical DSR samples. And, as mentioned earlier, the maximum torque applied by the DSR is 0.2 N.m, according to the product specification; therefore, in order to avoid overheating and potential damage and also to shorten the fatigue test, a test temperature of 25°C and a loading frequency of 2.5 Hz were chosen while the controlled stress values were in the non-linear region. Failure due to fatigue is shown in Figure 7.17. The results in Figures 7.18 to 7.25 are the average values while standard deviations from the average values are reported in Figures 7.27 and 7.28. More details on the fatigue results are illustrated in Appendices G.

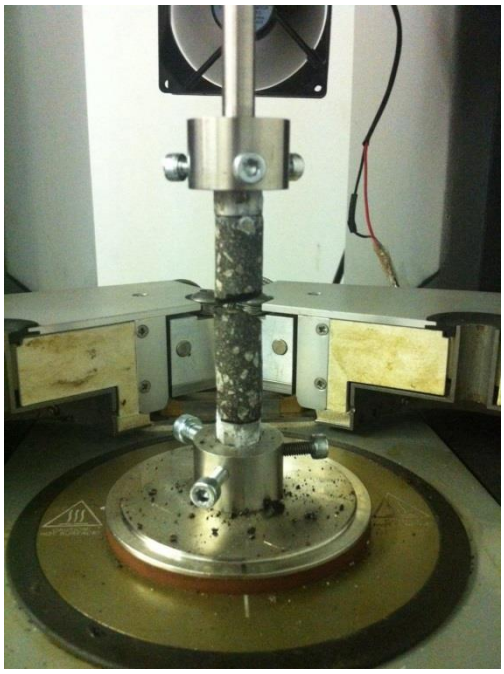

Figure 7.17 Failure in DSR sample due to fatigue

7.6.4.3 Analysis of fatigue test results

7.6.4.3.1 Traditional approach

As stated in Chapter 3, Section 3.6.3.1, the traditional approach is defined as a reduction in stiffness modulus of the material. In the controlled stress fatigue test, fatigue failure is defined as a reduction of stiffness modulus of the sample to 10% of its initial value or a complete fracture of the sample. A failure criterion of complete fracture of the sample was adopted. Figures 7.18 to 7.23 present the fatigue performance of WMA using traditional approach.

7.6.4.3.2 Energy ratio approach

Energy ratio approach was also used to rank the performance of WMAs. The equations for calculating the energy ratio were presented in Chapter 3, Section 3.6.3.2. Figures 7.24 and 7.25 illustrate the energy ratio plotted against number of cycles for WMAs manufactured using 40/60 and 100/150 binder grades.

7.6.4.4 Discussion

As presented in Chapter 3, Sasobit and Rediset have a superior performance in improving the fatigue life of asphalt binder, while there is no clear conclusion about the overall fatigue performance of WMA (Arega *et al.* 2011,Xiao *et al.* 2013,Jones *et al.* 2010,Bennert *et al.* 2011,Liu *et al.* 2012,Goh and You 2011a,Haggag *et al.* 2011,Silva *et al.* 2010,Ghabchi *et al.* 2015). It has been found, however, that warm additives have a superior performance in terms of fatigue cracking provided that the production temperatures are taken into account. The fatigue life of WMAs manufactured at 135°C was lower than the control mix HH155, as presented in Figures 7.18 and 7.19; this is because the degree of bonding between the binder and aggregate and the stiffness of the mastic are not good at resisting the deformation under repeated applied load. However, once the production temperatures were 145°C, lower than the control mix HH155 by 10°C, the warm additives performed significantly. Sasobit was proved to increase the stiffness of the binder and exhibited more elastic behaviour than the net bitumen. Therefore, once adequate bonding between the aggregate and binder and the overall stiffness of the mastic were achieved, an increase in the mixture stiffness was noticed which extended the fatigue life of WHSa145, as shown in Figures 7.20 and 7.21. Figure 7.20 illustrates the average complex shear modulus against number of cycles while Figure 4.21 presents the average response of the phase angle against number of cycles during repeating load.

Both Rediset WMX and LQ have active adhesion, which could displace water from the aggregate surface, enabling not only the coating of the aggregate but also the creation of a strong chemical bond between the aggregate and the bitumen, but it was not possible to achieve this until the temperature of the bitumen was adequate to adhere it to the aggregate. In fact, despite the fact that WMA could be manufactured at lower temperatures than that of HMA, the binder grade must be taken into account to achieve the required mechanical properties. It can therefore be said that the maximum reduction in the production temperature using hard binder such as 40/60 should be no more than 10°C compared to that of HMA. In contrast, in the case incorporating the 100/150 binder grade, WMAs were successfully manufactured at 125°C lower than that of control mix HS145,

without adversely affecting the superior fatigue performance of the warm additives, as shown in Figures 7.22 and 7.23.

The effects of Sasobit and Rediset WMA were clear. Both improved the fatigue life of the asphalt mixtures by approximately 90% and 30% respectively, which agreed with the case of WMA incorporating 100/150 binder grade produced at 125°C. Sasobit increased the stiffness and enhanced the elastic behaviour of the asphalt mixtures, which resulted in extending their fatigue life, while the improvement in the fatigue life due to the inclusion of Rediset WMX is because of the effect of the surfactant. As mentioned previously, Rediset WMX is classified as a viscosity reducer and surfactant. Surfactants are generally classified into four groups: cationic, anionic, amphoteric and non-ionic (Rosen and Kunjappu 2012). As previously mentioned, according to Syroezhko *et al.* (2011), the tail of the surfactant part of Rediset WMX is a long-chain aliphatic hydrocarbon while its head is a $-NH_3^+$ which exhibits a cationic property. Through mixing binder with aggregate, the silica atoms can bond with the cationic surfactant while calcium ions bond with both anionic and cationic. As granite is 72% silica, the surfactant part of Rediset WMX acts as a bridge between the binder and the granite surface in which adhesion between aggregate and binder should improve. This improvement makes the material more resistant to repeated applied load, which can explain the improvement in the fatigue life of asphalt mixtures.

A significant improvement in the fatigue life was achieved by incorporating Rediset LQ. Rediset LQ functions as an anti-strip and creates a strong bond between binder and aggregate, thus providing a very strong and stable mixture. Even though all WMAs manufactured using 40/60 binder grade at 135°C performed worse than the control mix HH155, WHRl135 had a slightly lower fatigue life than the control mix. However, when the effect of production temperatures was taken into account, WHRl145 had a fatigue life approximately twice that of the control mix HH155 when the production temperature of WMA was 145°C. This agreed with the fatigue performance of WSRl125.

Furthermore, a question may be raised: if the bond strength of WHSa135 and WHRl135 was better than that of the control mix, as shown in Chapters 5 and

6, why was their fatigue life lower than that of the control? The answer to this question can also be found in Chapter 5. Although the bond strength of WHS135 and WHRl135 was better than that of HH155, the mechanical properties of the mastic were lower than that of HH155. It is therefore apparent that cracks separated with mastic of asphalt mixture due to repeated load and, over time, the cracks interlocked and fatigue failure was accelerated.

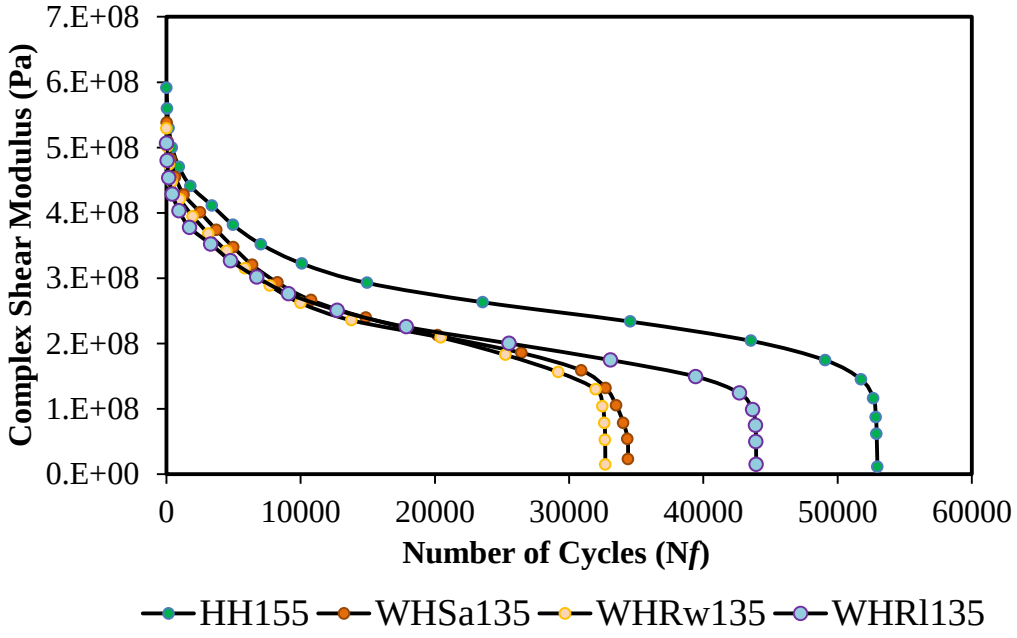

Figure 7.18 Average shear modulus against number of cycles for WMAs manufactured at 135°C

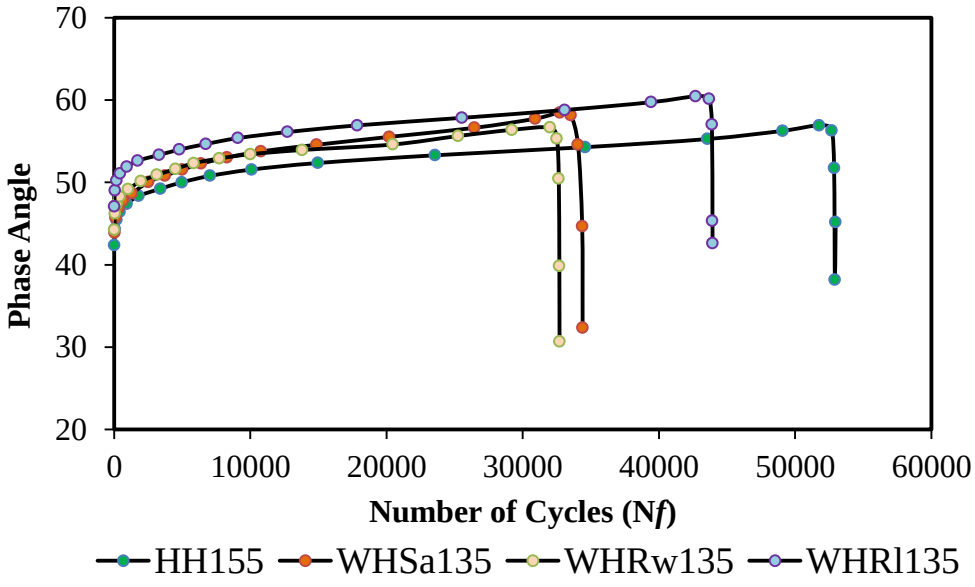

Figure 7.19 Average phase angle against number of cycles for WMAs manufactured at 135°C

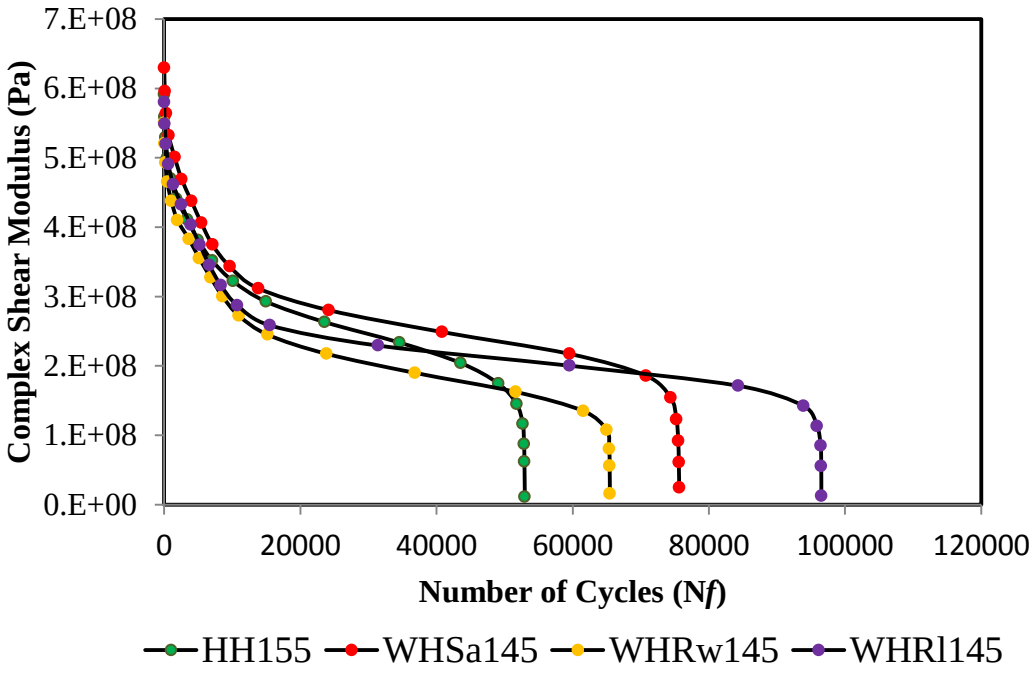

Figure 7.20 Average shear modulus against number of cycles for WMAs manufactured at 145°C

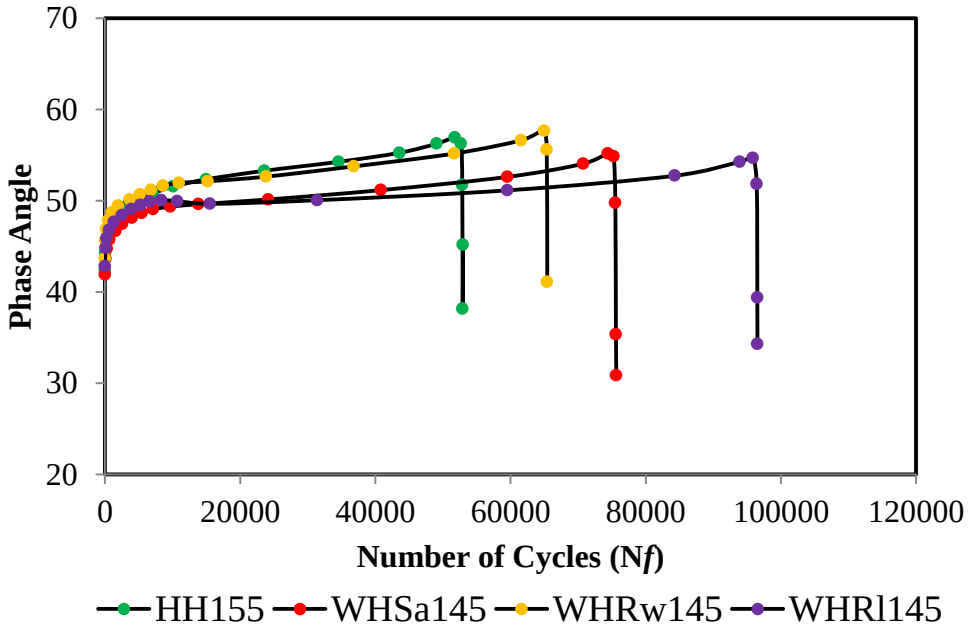

Figure 7.21 Average phase angle against number of cycles for WMAs manufactured at 145°C

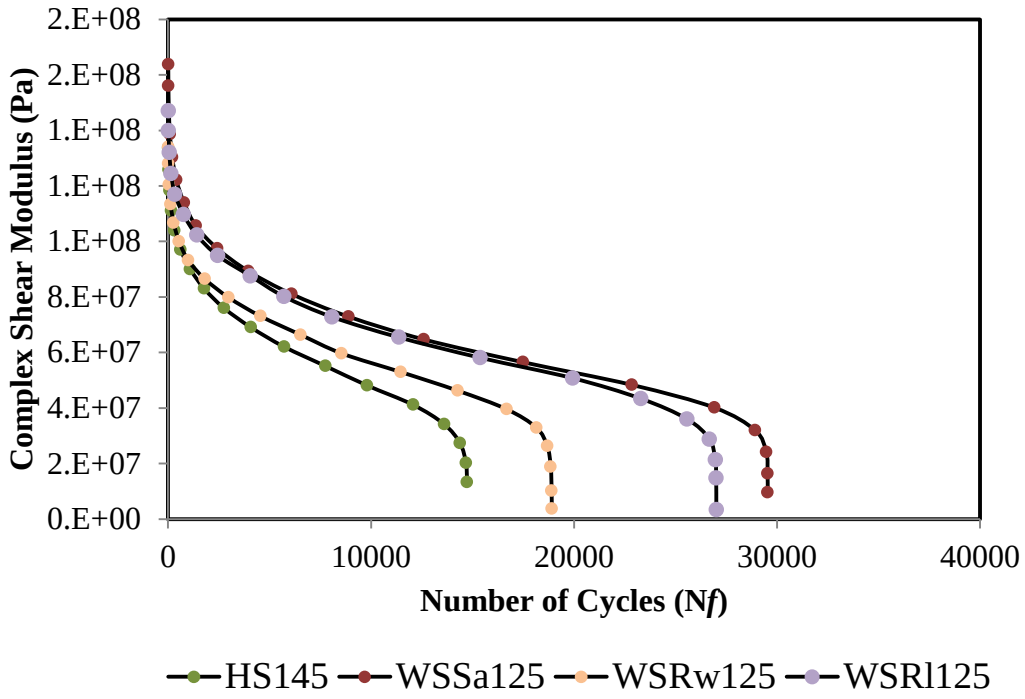

Figure 7.22 Average shear modulus against number of cycles for WMAs manufactured at 125°C

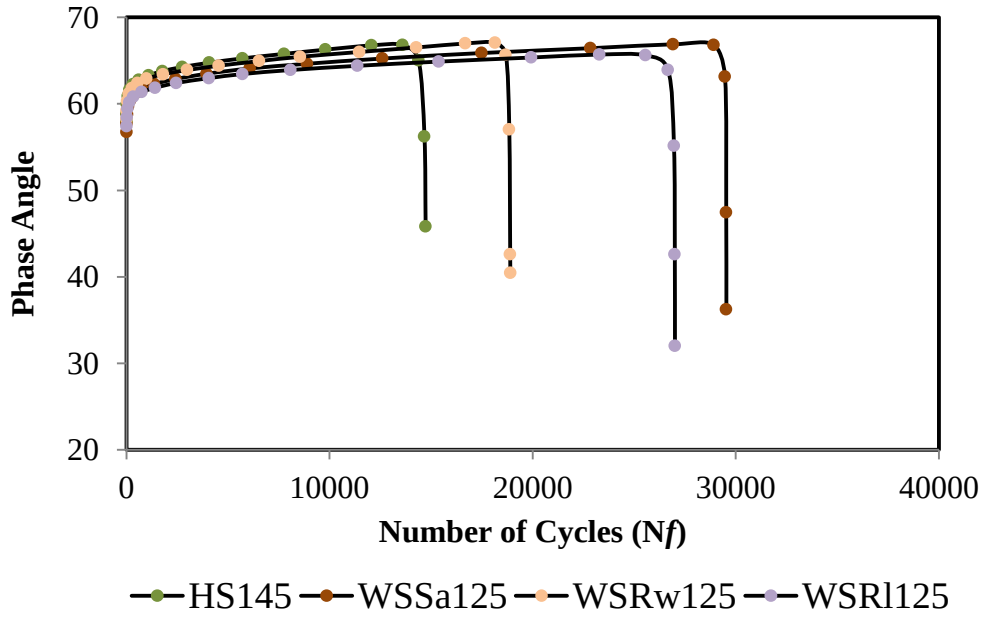

Figure 7.23 Phase angle against number of cycles for WMAs manufactured at 125°C

In order to accurately rank the performance of warm additives in terms of fatigue life, the energy ratio approach was also adopted. As can be seen in Figures 7.24 and 7.25, the WMAs' overall rank is exactly equivalent to their rank when using the traditional approach. The stored energy in the WMAs is higher than that

in the control mixtures. Therefore, the resistance of WMAs to applied repeated load is higher than that of the control mixtures, as the former exhibit more energy until failure.

Moreover, the binder grades play a significant role in the level of reduction in the production temperatures. It has been revealed that the overall performance of WMAs using 40/60 and those using 100/150 binder grades can only be equal if the production temperature is 145°C (lower than control mix HH155 by 10°C) when using a hard binder 40/60 and 125°C (lower than control mix HS145 by 20°C) using a relatively soft binder, 100/150. It can therefore be concluded that the binder grade highly affects the mixing temperature of WMA.

Generally, after taking into account the effect of production temperatures and binder grade, Rediset WMX increased the fatigue life of the asphalt mixture by approximately 32% while Rediset LQ doubled it and Sasobit increased it by approximately 90%. Figure 7.26 shows an example of measuring five samples to estimate the fatigue performance of WSRw125. In order to check the repeatability for the number of DSR samples tested, standard deviation was calculated for each mixture at failure point. The error bars in Figures 7.27 and 7.28 represent standard deviation from the average value.

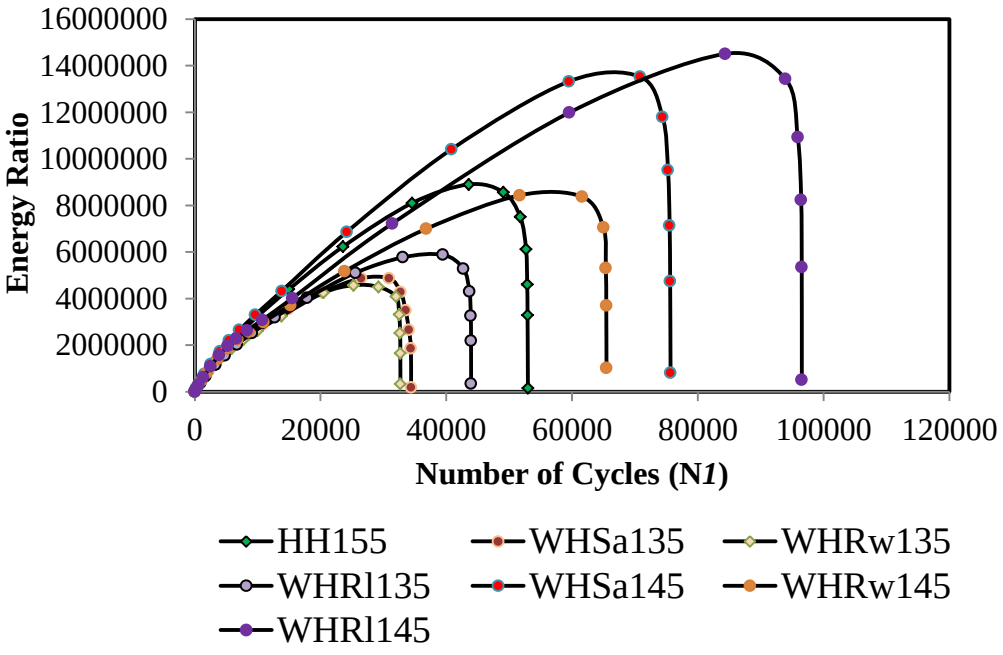

Figure 7.24 Average energy ratio against number of cycles for WMA manufactured using 40/60 binder grade

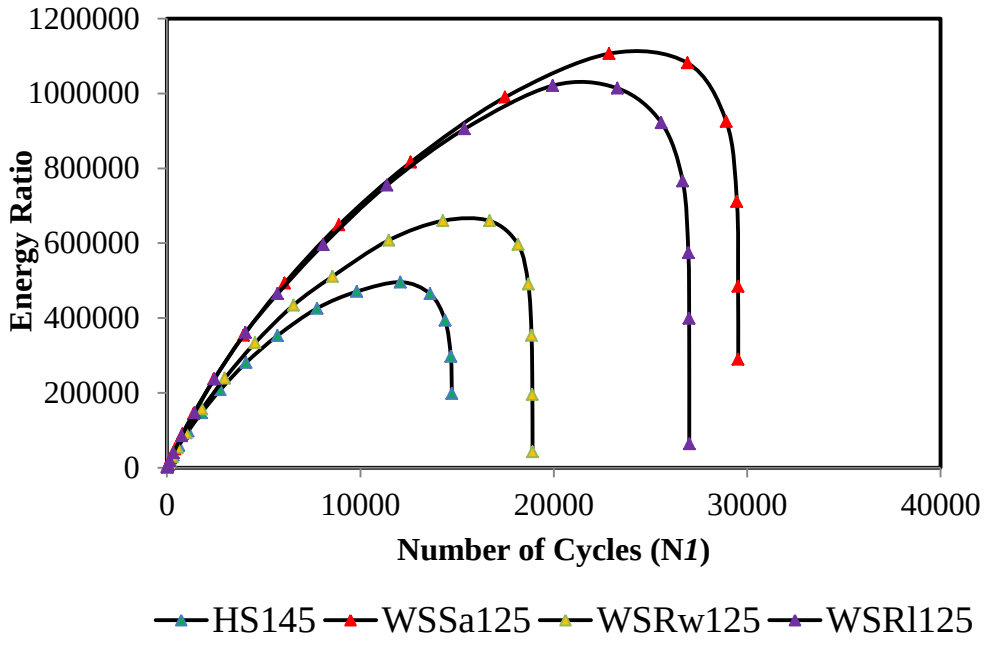

Figure 7.25 Average energy ratio against number of cycles for WMA manufactured using 100/150 binder grade

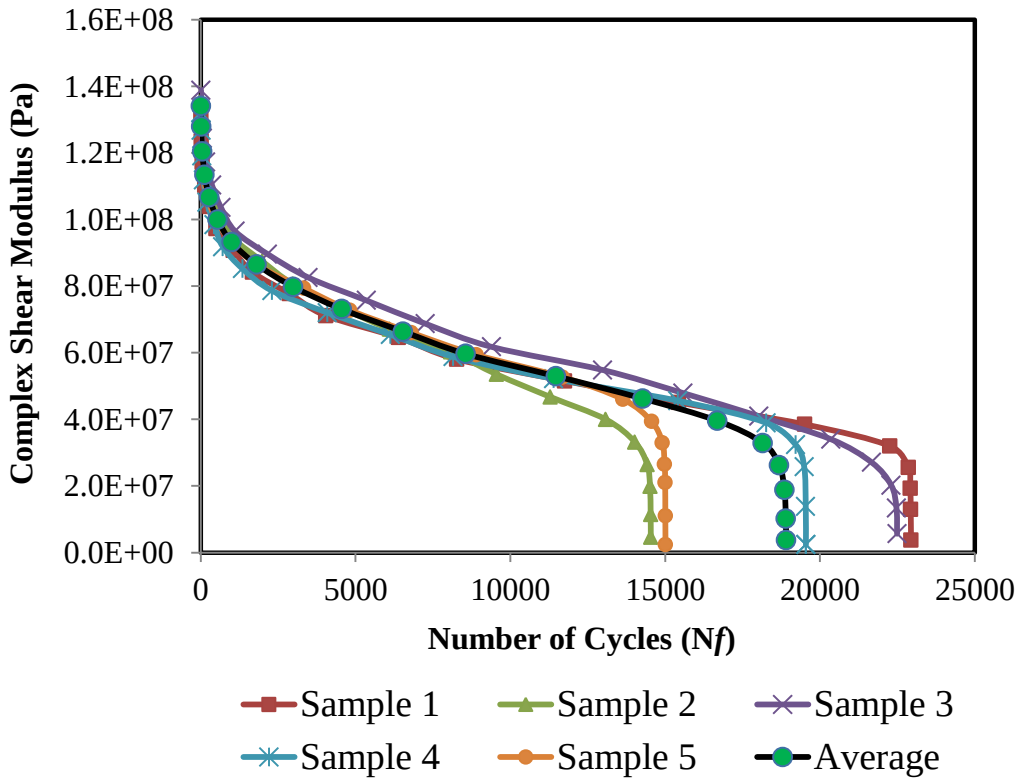

Figure 7.26 Example of measuring five samples to estimate the fatigue performance of WSRw125

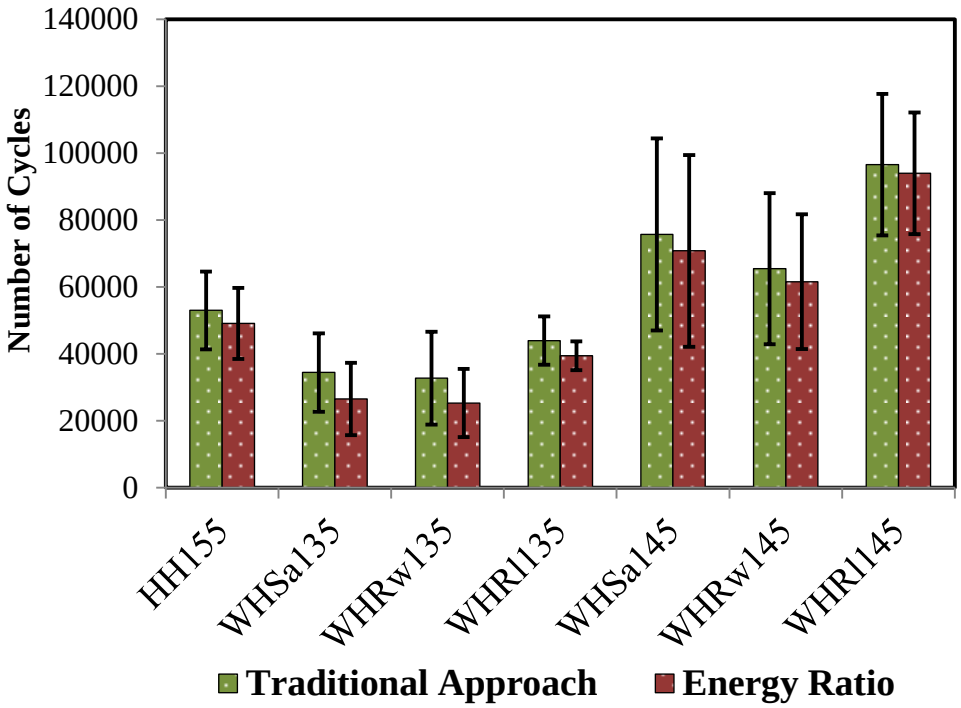

Figure 7.27 Number of cycles at failure point for control HMA and WMAs manufactured using 40/60 binder grade

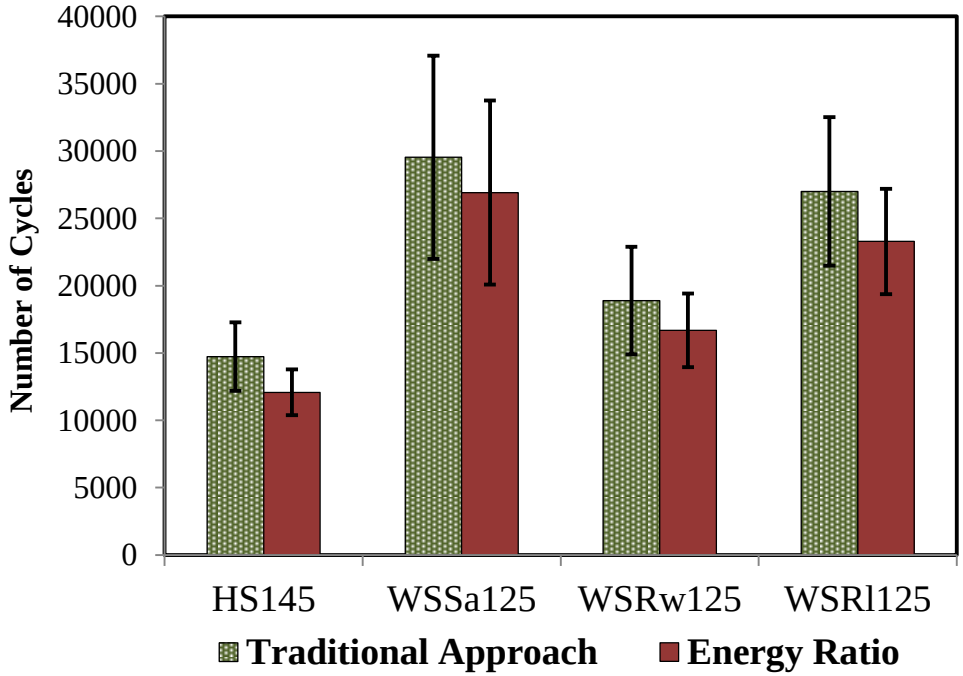

Figure 7.28 Number of cycles at failure point for control HMA and WMAs manufactured using 100/150 binder grade

7.7 Impact of asphalt mixture phases on fatigue performance of WMA

7.7.1 Effect of mechanical properties

Fatigue is one of the main failure modes of pavement materials; it occurs due to the degradation of the bound pavement materials and ultimately results in failure in pavement structure. As mentioned previously, during the degradation of the bound pavement materials' integrity, two phases occur which correspond to fatigue cracking. The first is micro-cracks, which are the result of degradation resulting from damage that is uniformly distributed through the material, and the second is macro-cracks, which propagate within the material. Energy required for the crack to propagate through the bulk of a material is known as cohesive bond energy, while adhesive bond energy is the energy required for a crack to propagate along the interface between binder and aggregate (Howson *et al.* 2012). In asphalt mixtures, the cohesive failure occurs within the mastic while the adhesive failure occurs between aggregate and binder. It is therefore clear that the mechanical properties of mastic and the ITZ play a significant role in determining the fatigue life of asphalt mixtures. In general, the damage represented by the formation of cracks occurs in the matrix of the asphalt mixtures. The matrix components are the fine aggregates passing through a 2.36 mm sieve, filler and bitumen, as highlighted by Song *et al.* (2005), who conducted an X-ray CT study with continuum mechanics to characterise the damage in the DSR samples tested in fatigue. The results showed that the damage in the material developed as cracks which started from the air voids and spread within the matrix. From this concept, it is clear that the stiffness of the matrix in general plays a significant role in evaluating the fatigue life of asphalt mixtures, which significantly depends on the properties of mastic and ITZ.

As presented previously in Chapter 5, the research was successful in measuring the nano-mechanical properties (elastic modulus and hardness) of ITZ and mastic. Therefore, it is time now to explore for the first time the effect of those properties on the overall fatigue life of asphalt mixtures. As presented in Figures 7.29 and 7.30, the elastic modulus and hardness highly correlates with the fatigue life of asphalt mixtures, controlled hot mix asphalt (HMA) and warm mix asphalt (WMAs) by taking into account the effect of warm additives, level of

reduction in the production temperature and binder grade. As presented previously in the current, regardless of the type of warm additives, all WMAs manufactured at 135°C using 40/60 binder grade had a lower fatigue life than the controlled mix HH155, and when the mechanical properties of ITZ and mastic of those mixtures were determined with nanoindentation, it was found that their elastic modulus and hardness were lower than the elastic modulus and hardness of mastic of HH155. However, as WMAs were manufactured at temperature of 10°C lower than that of control mix HH155, the fatigue life of WMA manufactured at 145°C significantly increased because of improving the elastic modulus and hardness of ITZ and mastic, while WMAs manufactured at 125°C using 100/150 binder grade had a better performance than the control mix HS145 in terms of fatigue life and as the nano-mechanical properties of ITZ and mastic were better or equal to that of HS145.

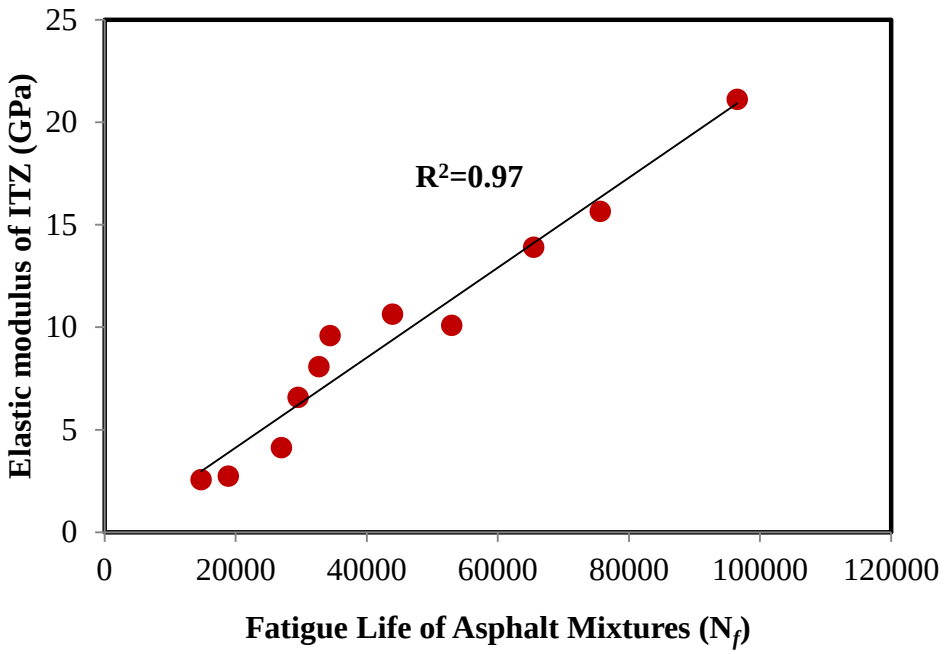

Figure 7.29 Correlation between elastic modulus of ITZ and fatigue life of asphalt mixtures

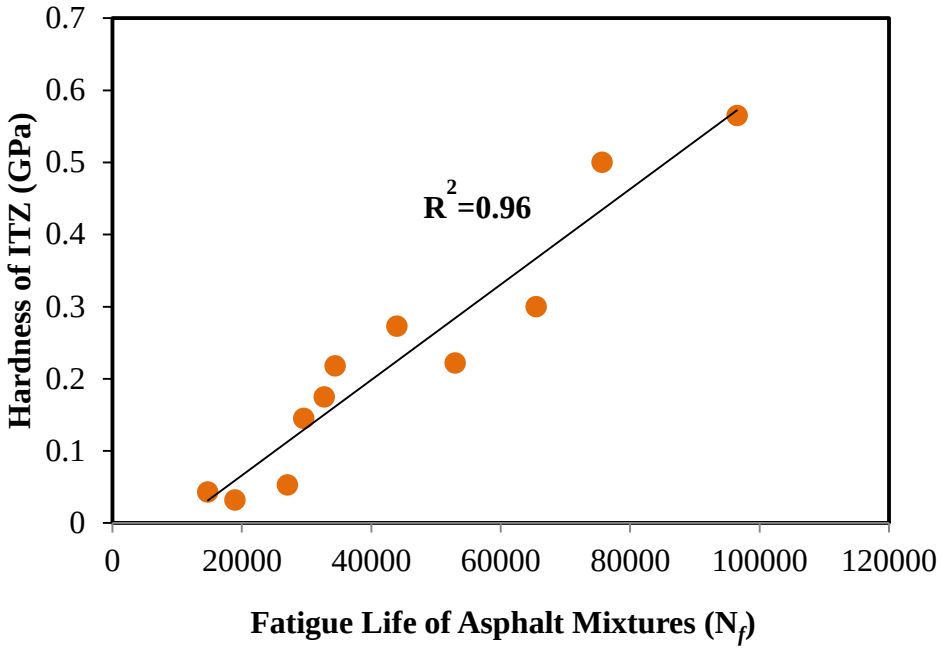

Figure 7.30 Correlation between hardness of ITZ and fatigue life of asphalt mixtures

From this fact, it can be concluded that, if the ITZ is stiff enough or adequate aggregate-binder bonding is available, the degradation in the material's integrity due to repeated loads is delayed. In other words, good bonding between aggregate and binder prevents the formation of cracks and consequently delays the separation of cracks within the matrix. This fact can be clearly seen when adopting Rediset WMX. As presented previously, WHRw145 had slightly lower G* than the control hot mix asphalt HH155 because mechanical properties of mastic were slightly lower than HH155, but its measured fatigue life was longer than HH155 because the elastic modulus and hardness of ITZ were higher than that for HH155. In other words, Rediset WMX improved the aggregate binder adhesion, which was reflected by improvements in the mechanical prophesies of ITZ, as the surfactant part of Rediset WMX acts as a bridge between the binder and the granite surface, so adhesion between aggregate and binder improved. For this reason, in terms of fatigue life, Rediset WMX exhibits longer fatigue life only if the effect of production temperatures is taken into account.

Because of significant improvements in the elastic modulus and hardness of ITZ for warm asphalt mixtures manufactured using Sasobit and Rediset LQ,

their fatigue life was significantly longer than the fatigue life of control mixes HH155 and HS145 as shown previously.

Elastic modulus and hardness of mastic also plays a significant role in affecting the fatigue life of asphalt mixture. As shown in the correlation matrix in Table 7.2, elastic modulus and hardness of mastic have a good correlation with the fatigue life of HMAs and WMAs. It can be seen that, as hardness is highly affected by the level of production temperatures, its effect on fatigue life is more pronounced.

In fact, stiff matrix (mastic and ITZ aggregate and binder) of asphalt mixture exhibits longer fatigue life of that mixture because both improve the aggregate-binder bonds and properties of mastic, which delays the formation and separation of micro-cracks to form within the matrix; therefore, the material exhibited more resistance to applied repeated loads.

Table 7.2 Correlation matrix

	N_f	M_{ITZ}	H_{ITZ}	M_M	H_M
N_f	1.000	0.978	0.961	0.646	0.853
M_{ITZ}	**0.978**	1.000	0.978	0.588	0.802
H_{ITZ}	**0.961**	0.978	1.000	0.657	0.876
M_M	**0.646**	0.588	0.657	1.000	0.892
H_M	**0.853**	0.802	0.876	0.892	1.000

(N_f: Number of cycles to failure, M_{ITZ} and H_{ITZ} elastic modulus and hardness of ITZ (GPa) respectively, M_M and H_M elastic modulus and hardness of mastic (GPa) respectively)

7.7.2 Predicting fatigue life after including nano-mechanical properties

In spite of the complex behaviour of asphalt mixtures, several attempts have been made to develop regression models to predict the fatigue life of HMA. In this regard, the earliest model was introduced during the 1960s, based on the relationship between fatigue life of HMA in terms of number of cycles and horizontal tensile strain and tensile stress at the bottom of the asphalt layer using the basic equations as follows:

$$N_f = a \left(\frac{1}{\varepsilon_t}\right)^b \quad (7.1)$$

$$N_f = a \left(\frac{1}{\sigma_t}\right)^b \quad (7.2)$$

where N_f: is the number of cycles at failure, ε_t and σ_t are the magnitudes of tensile strain and stress repeatedly applied, and *a* and *b* are regression constants. However, later studies continued to take into account mix properties represented by mix stiffness (S_m) to develop the final model as presented in equations 7.3 and 7.4 (Monismith *et al.* 1985).

$$N_f = a \left(\frac{1}{\varepsilon_t}\right)^b \left(\frac{I}{S_m}\right)^c \quad (7.3)$$

$$N_f = a \left(\frac{1}{\sigma_t}\right)^b \left(\frac{I}{S_m}\right)^c \quad (7.4)$$

After that, extensive efforts were made to develop new regression models to predict the fatigue life of asphalt mixtures considering several variables related to the mix properties in order to take into account the variability in the mix properties as well as the test conditions. Bonnaure *et al.* (1980) developed regression models to predict the fatigue life of HMA for strain and stress modes. These models were more comprehensive than the previous models because they also included volumetric binder content (*Vb*) and penetration index (*PI*), as shown in equations 7.5 and 7.6 for stress and strain modes respectively, using an adjustment factor (A_f) to transfer laboratory results to the field. In 1978, the Shell International Petroleum Company also developed a model using the formula in Equation 7.1 for predicting the fatigue life of HMA (Manual and Pavements 1978), but in this case the binder volume (*Vb*) was included in the model, as shown in equation 7.7.

$$N_f = A_f (0.17\text{PI} - 0.0085 PI.V_b + 0.45 V_b - 0.112)^5 \varepsilon_t{}^{-5} S_m{}^{-1.8} \quad (7.5)$$

$$N_f = A_f (0.0252\text{PI} - 0.0012 PI.V_b + 0.006 V_b - 0.0167)^5 \sigma_t{}^{-5} S_m{}^{-1.4} \quad (7.6)$$

$$N_f = \left(\frac{\varepsilon_t}{(0.856V_b + 1.08) S_{mix} \times 0.36}\right)^{-5} \quad (7.7)$$

Furthermore, an energy approach was used in several studies to predict the fatigue performance of HMA This approach is based on the amount of energy dissipated being proportional to the number of cycles during cyclic loading testing (Rowe 1993), as presented in equation 7.8:

$$W = A(N_f)^Z \quad (7.8)$$

where: W is cumulative dissipated energy to failure, and A *and* Z are regression constants.

It can be noticed that, in all the aforementioned models, the predicted number of cycles is based on the overall properties of the mix or the sample of that mix. This research was able to identify the mechanical properties of each phase in the asphalt mixture samples using nanoindentation and assess the effect of those properties on the overall fatigue performance of the asphalt mixture. Therefore, a new regression model obtained using Statistical Package for the Social Sciences (SPSS) is proposed to accurately predict the fatigue life of asphalt mixture, as shown in equation 7.9.

$$N_f = 48836.7(-1611.92A.V - 2.767E\text{-}05G^* - 643.6\,\delta + 4278.16\,M_{ITZ} + 1840.62\,M_M) \quad (7.9)$$

Where: N_f : number of cycles at failure, $A.V$: air voids of sample, $G^*(Pa)$: initial modulus of sample, δ: initial phase angle of sample, $M_{ITZ:}$ elastic modulus of ITZ (GPa) and $M_{M:}$ elastic modulus of mastic (GPa).

As can be seen in Figure 7.31, a high correlation between the measured and predicted values using the determination coefficient (R^2) was found.

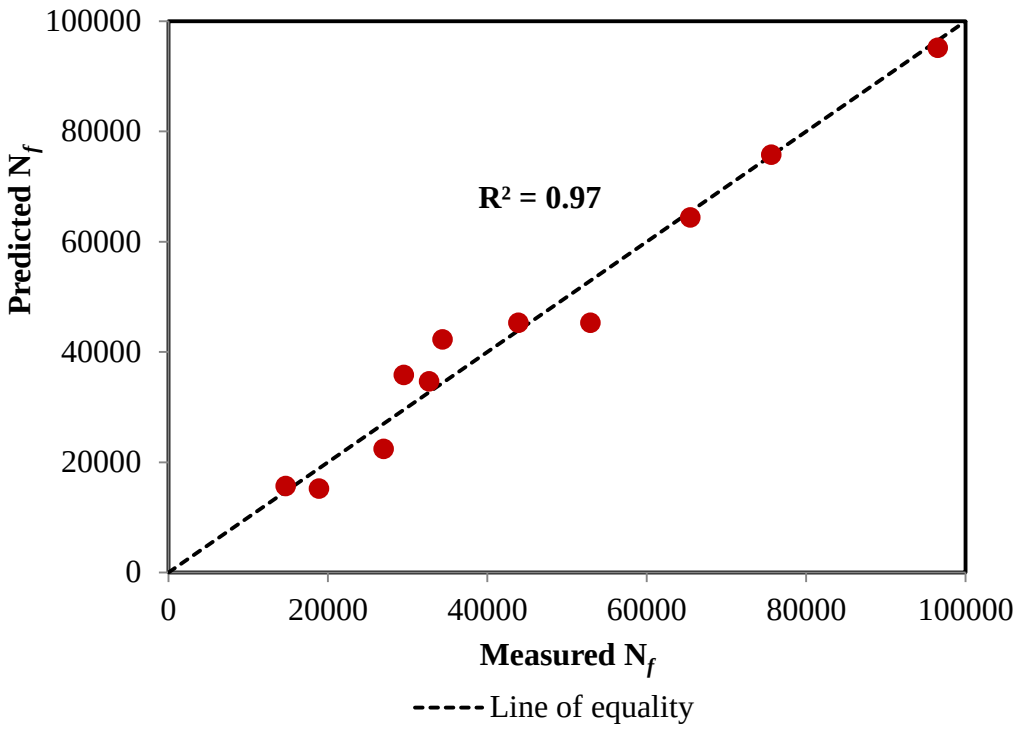

Figure 7. 31 Predicting fatigue life of asphalt mixtures by taking in account nano-mechanical properties of ITZ and mastic

7.8 Conclusion

1. Sasobit increased the stiffness of the asphalt mixtures while Rediset LQ has no negative effect on it if the production temperature is taken into account. In contrast, Rediset WMX slightly decreased the mixtures' stiffness.

2. The production temperature substantially influences the fatigue of the mixture. As a matter of fact, in order to achieve the desired fatigue performance of WMA, there needs to be a difference between the reduction in production temperature for hard and soft binders. This is because this study has found that the performance trend for warm additives on asphalt mixtures produced using 40/60 and 100/150 binder grades was the same if the maximum reduction in the production temperature was limited to 10°C for 40/60 and 20°C for 100/150 binder grades compared to their control mix respectively.

3. After taking the effect of production temperatures in to account, Rediset WMX increased the asphalt mixtures' fatigue life by approximately 32% while Rediset LQ doubled it. Sasobit also increased the fatigue life by approximately 90%.

4. The stiffer the mastic and ITZ of the asphalt mixture are, the longer the fatigue life of that mixture, because improving the aggregate-binder bonds and properties of mastic delays the formation and separation of micro-cracks within the matrix; therefore, the material exhibits more resistance to applied repeated loads.

5. Highway agencies are advised to specify a minimum production temperature for WMA to reach acceptable mixture stability in terms of stiffness and fatigue performance taking into account binder source and grade.

6. All the regression and mechanistic models developed to predict fatigue life of asphalt mixtures are based on the properties of asphalt mixtures in general without taking into account the effect of each asphalt mixture's phase on its overall fatigue. In this chapter, a model was proposed to accurately predict the fatigue life of asphalt mixtures and text the mechanical properties of the ITZ and mastic without separating them from the mixture.

Chapter Eight

Level of Blending Between RAP and Virgin Materials

8.1 Introduction

Reclaimed asphalt pavement (RAP) is one of the most important recycling materials used to produce a sustainable asphalt mixture. The use of RAP is a valuable approach for paving, economic and environmental reasons. It was estimated that in 1999, the UK used of some 26 million tonnes of hot mix asphalt (HMA) which can lead to the assumption that around 20 million tonnes of aggregate were consumed. Such using the amount of aggregate does not seem to be in line with the country's strategy for sustainable construction that requires for minimising the consummation of natural resources (Huang *et al.* 2007). As mentioned in Chapter 2, the reuse of recycled asphalt mixtures decreases the amount of waste produced and significantly helps to resolve the problems associated with disposal of highway construction materials and conserve the natural resources. In UK, the average RAP content increased to approximately 10% in 2015, and it is anticipated to continue rising (Hanson 2016).

However, as the level of blending between RAP and virgin (aggregate and binder) materials is one of the most important factors which directly influence the overall performance of asphalt mixtures and the economic competitiveness of the recycling process (Al-Qadi 2007, Mohajeri *et al*. 2012, Nahar *et al*. 2013a). Based on to what was presented in Chapter 2, Section 2.6.2, the level of interaction between RAP and virgin materials is still ambiguous. To date, this interaction has not been investigated at the nano-scale, which can be of particular importance in reflecting the real level of interaction between materials.

An increasingly popular construction practice is to incorporate and increase the amount of RAP in WMA to produce a more economically and

environmentally friendly asphalt mixture. However, two issues regarding the inclusion RAP materials in asphalt mixtures need to be further investigated: the fatigue behaviour of RAP mixes and the degree of blending between RAP and virgin materials (Nahar *et al.* 2013a). In the current chapter, the effect of warm additives and production temperature on the level of interaction between RAP and virgin material was investigated in detail using the advanced technology of nanoindentation, which can effectively investigate the real interaction between RAP and virgin materials based on nano-mechanical properties of the interfacial transition zone (ITZ) and mastic.

The effect of warm additives (Sasobit and Rediset LQ) and production temperatures on the real interaction was investigated based on elastic modules, hardness and images of ITZ and mastic using nanoindentation. Furthermore, the results were further validated using a scanning electron microscopy (SEM). In order to estimate the overall performance of WMA incorporating RAP materials, stiffness and fatigue life of WMAs were measured in a DSR. In addition a protocol to reach complete blending between RAP and virgin materials has been developed and recommended for use.

8.2 Laboratory testing

8.2.1 Materials

8.2.1.1 Virgin materials

Details about the properties of binders (40/60 and 100/150), warm additives and virgin aggregate were presented in Chapters 3 and 5. However, it should be mentioned that, due to the shortage of virgin aggregate, WMAs incorporating RAP were manufactured using Rediset LQ and Sasobit only. The effect of Rediset WMX on the level of blending is beyond the scope of this chapter. Sasobit and Rediset LQ were also 2% and 0.5% by the weight of binder respectively.

8.2.1.2 RAP materials

Reclaimed asphalt pavement (RAP) was supplied by Hanson Aggregates, UK and binder content and recovered aggregate gradation were determined by Pavement Testing Services Ltd, UK. The penetration and softening points were identified by

the author based on (BS EN 1426 2007,BS EN 1427 2007) respectively. Table 8.1 illustrates the properties of the virgin binders and the recovered RAP binder.

Table 8.1 Properties of virgin and recovered RAP binders

Binder grade	Penetration at 25°C (dmm)	Softening point °C
40/60	45	54.3
100/150	104	43.0
Recovered RAP binder	15	65.5

The RAP aggregate was a combination of sandstone, limestone and gabbro. RAP aggregates were identified by a geologist in the Geology Department, University of Liverpool, UK. Figure 8.1 presents the types of aggregate in RAP. In fact, it is normal to have different types of aggregate in RAP because, in reality, after the reconstruction of roads or highways, all RAP materials are gathered in one stockpile.

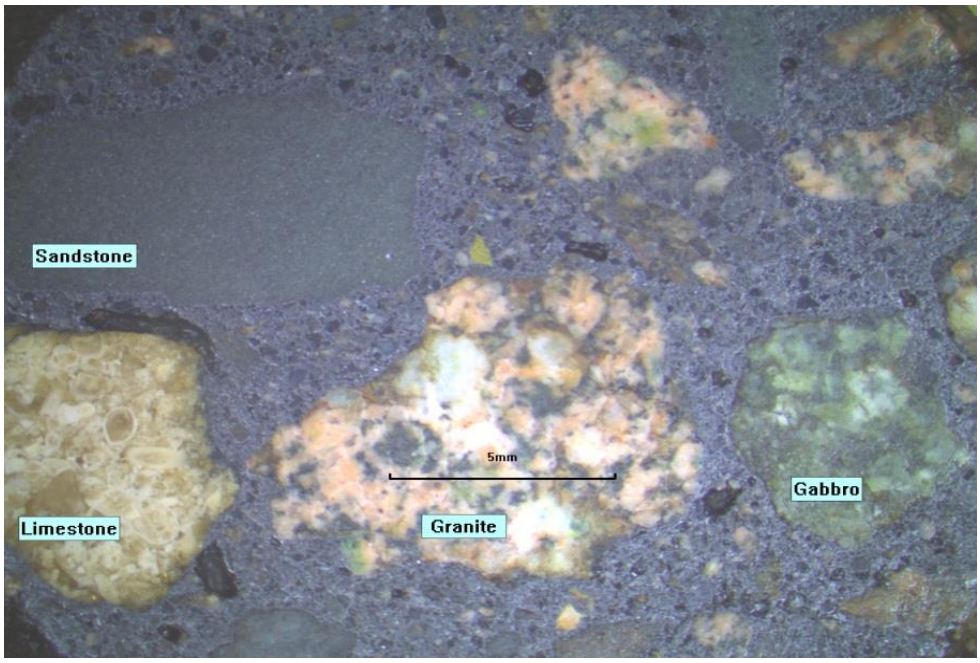

Figure 8.1 Types of aggregate in RAP

8.2.2 Manufacturing asphalt mixtures incorporating RAP

8.2.2.1 Assumptions for including RAP

It was found that, when 40% of recovered RAP binder was mixed with 60% of 100/150 binder grade, the new binder behaved as the 40/60 binder grade. As

presented in Chapter 3, the frequency sweep tests were performed under controlled strain, and frequencies between 0.1 and 10 Hz were adopted over a temperature range between 0°C and 60°C at intervals of 10°C. Figures 8.2 and 8.3 illustrate the master curves of complex shear modulus and phase angle vs. frequency for the control 40/60 binder and the new binder obtained from mixing 40% of the recovered RAP binder and 60% of the 100/150 binder. It is clear that the properties (complex shear modulus and phase angle) of the new binder are exactly same as the virgin 40/60 binder, and its viscoelastic response behaviour during the dynamic test under different loading conditions and testing temperatures is equivalent. Consequently, for all mixtures containing RAP materials, through manufacturing asphalt mixtures, a complete blending was assumed.

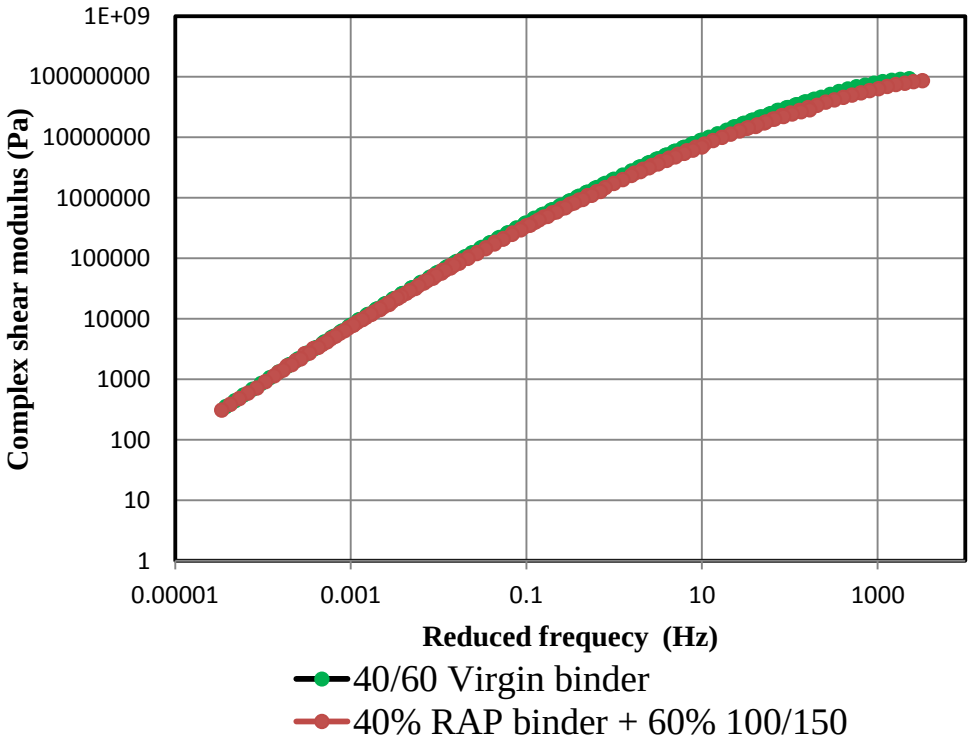

Figure 8.2 Master curves (complex shear modulus vs frequency) of 40/60 virgin binder and binder obtained from mixing 40% of RAP binder and 60% of 100/150 binder

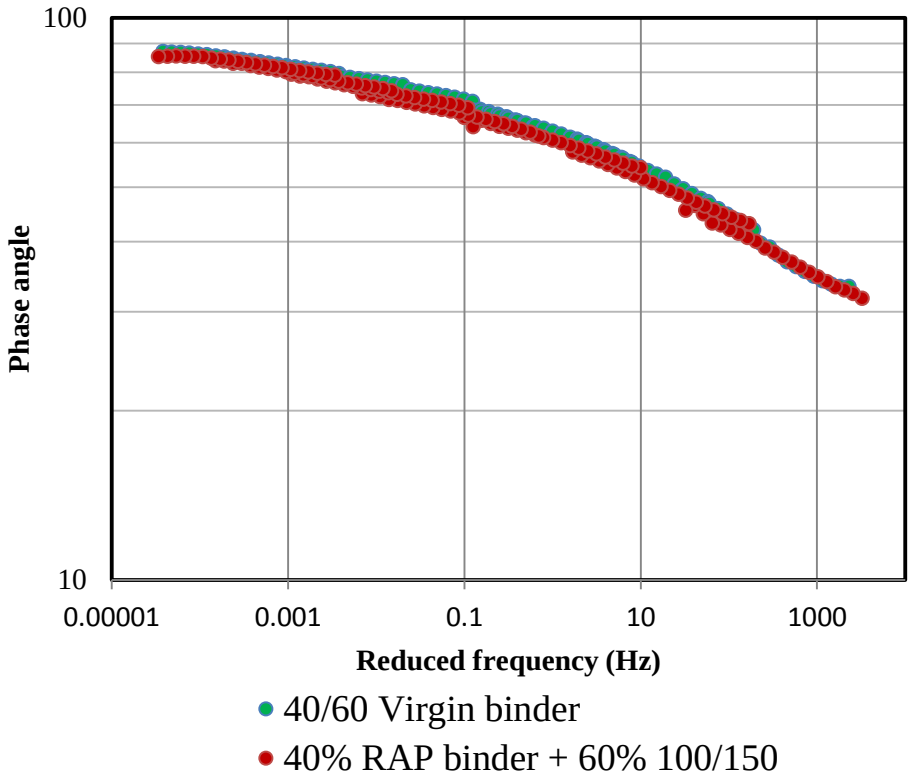

Figure 8.3 Master curves (phase angle vs frequency) of 40/60 virgin binder and binder obtained from mixing 40% of RAP binder and 60% of 100/150 binder

8.2.2.2 Mix design

A gap-graded hot rolled asphalt was also adopted to manufacture HMA-RAP and WMA-RAP. The nominal maximum aggregate size was also 10 mm, which is suitable for surface courses. The recipe specification method was also adopted in the design of the mixes. The HMA-RAP and WMA-RAP were manufactured according to the British Standards recipe (BS 597-1 2005). The same mixture codes as presented in Chapter 5 were also used in the current chapter, but it should be noted that the letter (P) was added when RAP was included in the mixture. The percentage of RAP materials used to manufacture HMA-RAP and WMA-RAP was 40%. Figure 8.4 illustrates the particle size distribution of the virgin aggregate (granite) and 40% of the RAP aggregate mixed with 60% of virgin aggregate.

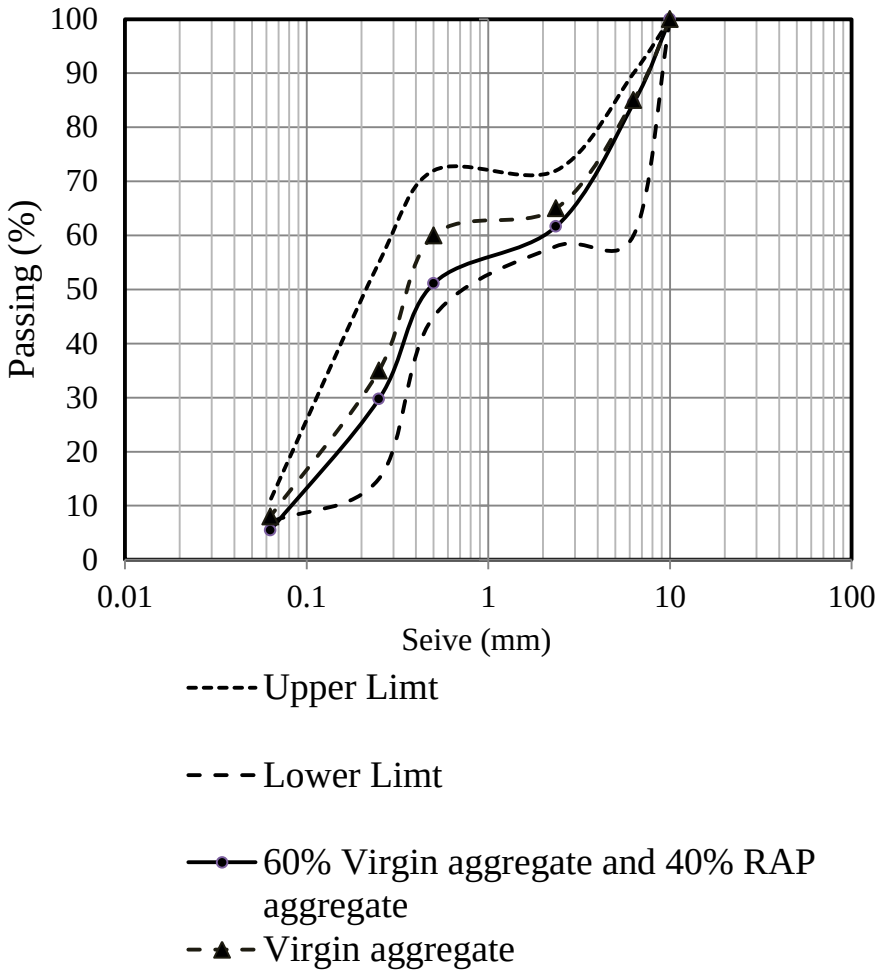

Figure 8.4 Particle size distribution of virgin and 40% of RAP aggregates mixed 60% of virgin aggregate

8.2.2.3 HMA-RAP and WMA-RAP

The procedure for preparing asphalt mixtures incorporating RAP is the same as that reported in Chapter 5, Section 5.4.2. Five mixtures were manufactured incorporating RAP materials: HSP145, WSSaP125, WSSaP155, WSRlP125 and WSRlP155. For example, HSP145 is hot mix asphalt manufactured at 145°C using 60% of virgin materials (100/150 binder grade and virgin granite) with 40% RAP material, while WSSaP125 is a warm mix asphalt manufactured at 125°C using 60% of 100/150 binder and 60% of virgin aggregate with the addition of 2% of Sasobit mixed with 40% of RAP. Table 8.2 illustrate the mixtures' bulk densities and air voids.

Table 8.2 Volumetric properties of for all asphalt mixtures incorporating RAP materials

Mixture	Bulk density (Mg/m3)	Air voids (%)
HSP145	2.31	5.0
WSSaP125	2.304	5.2
WSSaP155	2.323	4.4
WSRlP125	2.313	4.9
WSRlP155	2.317	4.7

8.2.3 Sample preparation

As mentioned previously, the level of blending was investigated based on nano-mechanical properties of mixture phases, overall stiffness and fatigue of asphalt mixture. Preparation and polishing of nanoindentation disc samples (NDSs) were explained in detail in Chapter 5, Section 5.4.4. Stiffness and fatigue were tested using a DSR; therefore, the preparation of DSR samples was exactly the same as presented in Chapter 7 Section 7.5.

8.2.4 Equipment

8.2.4.1 Nanoindentation

Nanoindentation testing was conducted using Keysight Technologies Nanoindenter G200 (USA) with a Berkovich indenter probe. The Hardness-Modulus at depth method was used in the indenter based on Oliver-Pharr method as presented in Chapter 5. The setting for the NDSs incorporating RAP was the same as the setting applied for the control mix (HH155) as presented in Chapter 5, Section 5.5.2. The strain rate target was 0.05 1/s, while peak hold time was 10s and surface approach velocity was 10 nm/s. Calibration was also conducted using standard fused silica before and after testing each batch of samples to ensure that there was no dust on the head of probe, and also to ensure that all obtained results were reliable. Poisson's ratio was also assumed to be 0.3 for all asphalt mixture settings. All tests were conducted at 22°C.

8.2.4.2 Scanning electron microscopy (SEM)

SEM is one of the most widely used techniques for the purpose of identifying and analysing the microstructure of bulk specimens. The scanning electron microscope forms images of bulk specimens by scanning the surface with a finely focused beam of electrons and measuring the intensity of the secondary electrons emitted from each point scanned. The differences in the intensity are used to modulate the intensity of the image shown on the computer screen. In the general concept, as shown in Figure 8.5, electrons from the heated tungsten filament are speeded up towards the anode. Then, the electron beam is created composed through a series of apertures and magnetic lenses, and the focused beam is scanned over the sample and secondary electrons collected at the detectors.

Generally, when the primary electron beam interacts with the scanned sample surface, the electron loses energy and two types of electrons may be produced: secondary electrons and backscattered electrons. Secondary electrons are produced when an incident-excited electron is changed and scattered by the atoms in the sample without or with loss of some of its energy. The secondary electrons have a very short mean-free path and those produced close to the surface will escape and be detected by the secondary electron detector, which is very sensitive to topography, while the backscattered electrons can be deduced from a deeper single position and can undergo large angle scattering. The high energy of the backscattered electrons results in the generation of low-resolution backscattered electrons images as compared to high-resolution secondary electrons images (Suzuki 2002).

During the present investigation, a JSM 6610 SEM, as shown in Figure 8.6, was used to further investigate the level of blending between RAP and virgin materials. The electron beam was focused on spot of 50nm while the accelerating voltage was 20Kv (20000 volts) at working distance of 9-10mm. It should be noted that, for this purpose, samples were coated with a thin layer (20-100nm) of conductive material, chromium, in order to prevent charge build-up. Figure 8.7 shows examples of NDSs after being coated with chromium.

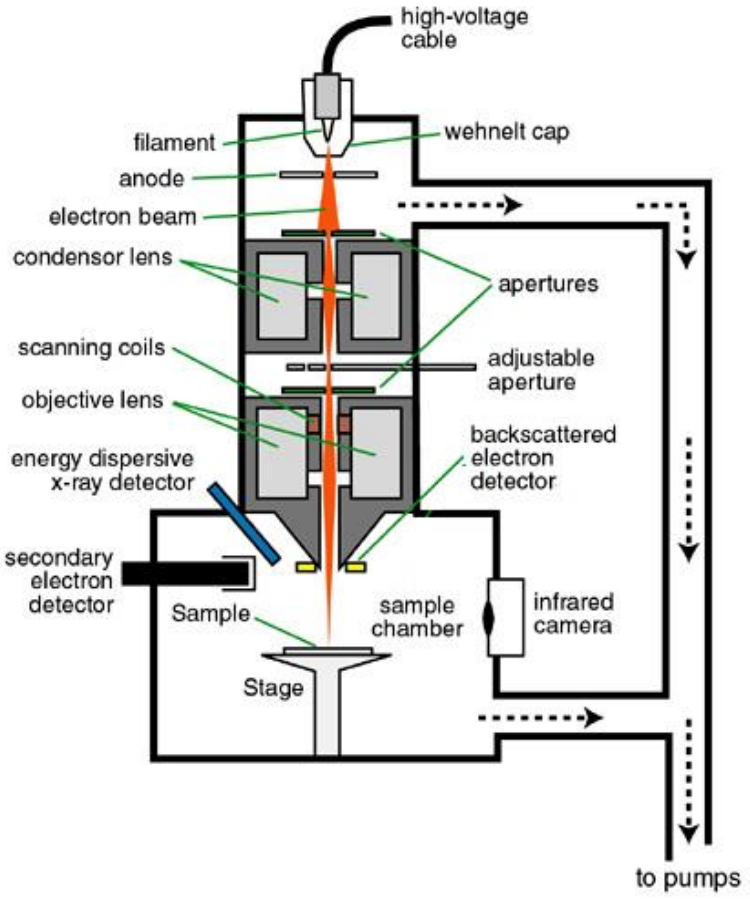

Figure 8.5 Scanning electron microscope schematic diagram (Wittle 2015)

Figure 8.6 JSM 6610 scanning electron microscopy

Figure 8.7 Samples used for SEM investigation (NDSs after being coated with Chromium)

8.2.4.3 Dynamic Shear Rheometer (DSR)

Details about the Kinexus DSR Pro+ were presented in Chapter 3, Section 3.5.1. The DSR was used to investigate stiffness and fatigue life of DSR samples. Setting for the DSR samples and tests was similar to what was reported in Chapter 7.

8.3 Results and discussion

8.3.1 Nano-mechanical properties of mixtures phases

8.3.1.1 Nano-mechanical properties of RAP aggregate

As mentioned previously, the RAP aggregate was a combination of sandstone, limestone and gabbro. RAP aggregates were identified by a geologist (Mr. John Kavanagh) in the Geology Department, University of Liverpool, UK, as presented in Figure 8.1. Elastic modulus and hardness of the RAP aggregate were measured and compared to those of the virgin granite. Figures 8.8 and 8.9 show the elastic modulus and hardness of sandstone, gabbro and limestone. The elastic modulus of all RAP aggregate was equal to or higher than the elastic modulus of the virgin granite. However, it was expected that the hardness of limestone would be less than that of the other types of aggregate, as limestone is considered weaker than granite. The most important consideration in this chapter is that the vast majority of the RAP aggregate was a combination of Sandstone and Gabbro. Therefore, in

the matter of investigating the level of blending between RAP and virgin materials, the effect of the aggregate can be neglected as the properties of the RAP aggregate are approximately equal to the properties of the virgin granite.

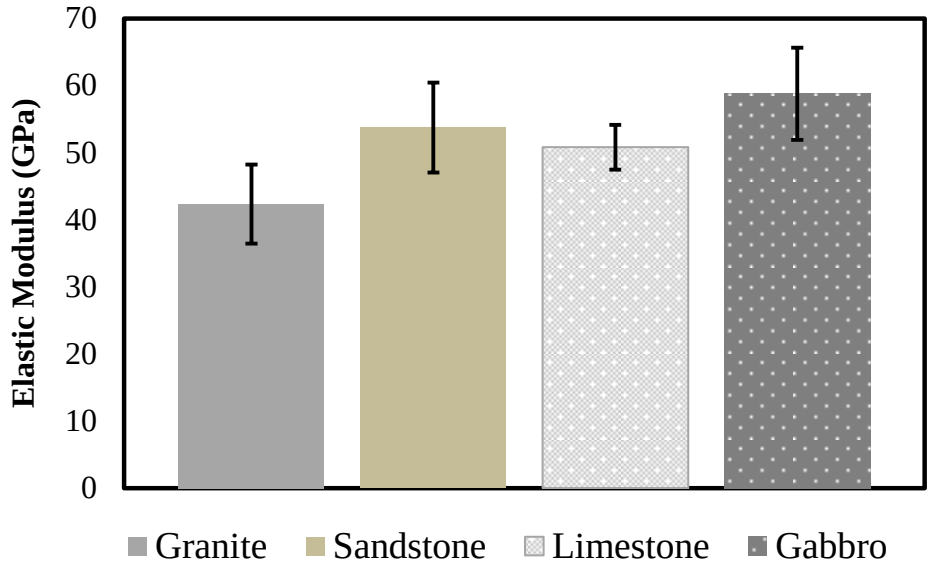

Figure 8.8 Elastic modulus of RAP aggregate compared to virgin granite

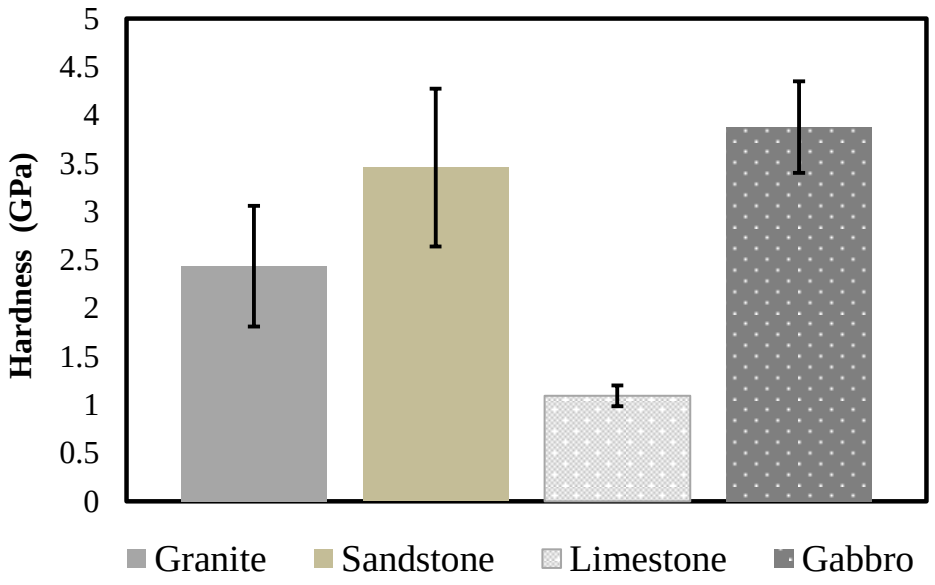

Figure 8.9 Hardness of RAP aggregate compared to virgin granite

8.3.1.2 Nano-mechanical properties of ITZ and mastic

The level of blending between the RAP and the virgin materials was investigated using nanoindentation. Figure 8.10 illustrates the ITZ (interfacial transition zone between virgin aggregate and virgin binder). As can be seen from that figure, there was no gap between the virgin aggregate and the binder/mastic, and so the elastic modulus and hardness of ITZ in this mixtures can be measured directly. However, in the case of incorporating RAP materials, Figure 8.11 explains the ITZ virgin and ITZ RAP (interfacial transition zone between RAP aggregate and RAP binder). It is clear that the binder surrounding the RAP aggregate was not completely affected by the virgin binder. In other words, there was no complete interaction between the old and the virgin binder, as the virgin binder was not completely diffused into the old binder and the old binder did not get way from the RAP aggregate due to the high stiffness of the ITZ RAP. However, in the same mixture, a nice interaction between the virgin binder and virgin aggregate can be observed, as shown in Figure 8.11.

This phenomenon was also noticed in mixtures WSRlP125, WSRlP155 and WSSaP125. Figures 8.12 and 8.13 illustrate the ITZ RAP of mixtures WSRlP125 and WSSaP125 respectively. In those figures, complete blending was not satisfied. However, the effect of Sasobit on the level of blending in mixture WSSaP155 was very considerable. Sasobit has the potential to significantly decrease the viscosity of the binder, which increases diffusion of the virgin binder into the old binder; also, it is expected to decrease the viscosity of the old binder; therefore, the old binder can easily get away from the RAP aggregate, and so a complete blending can occur. This phenomenon was confirmed as presented in Figure 8.14. It is very clear that complete blending occurred and the ITZ RAP disappeared and therefore a complete interaction between the aggregate and the binder/mastic can be noticed.

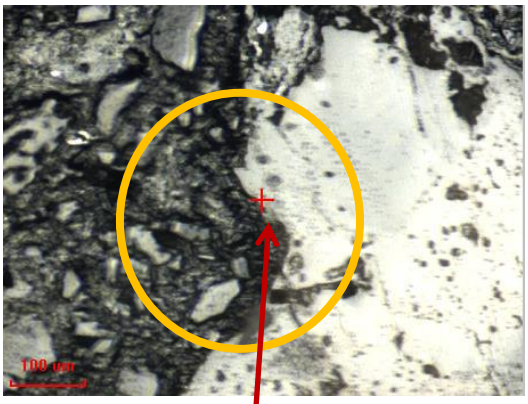

HH155 ITZ virgin

Figure 8.10 ITZ of control mix HH155

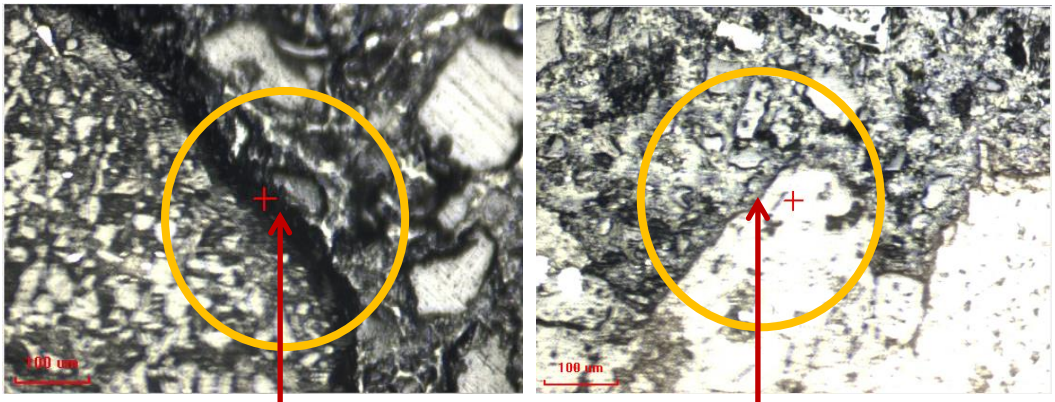

HSP145 ITZ RAP **HSP145 ITZ Virgin**

Figure 8.11 ITZ of RAP and virgin of mixtures HSP145

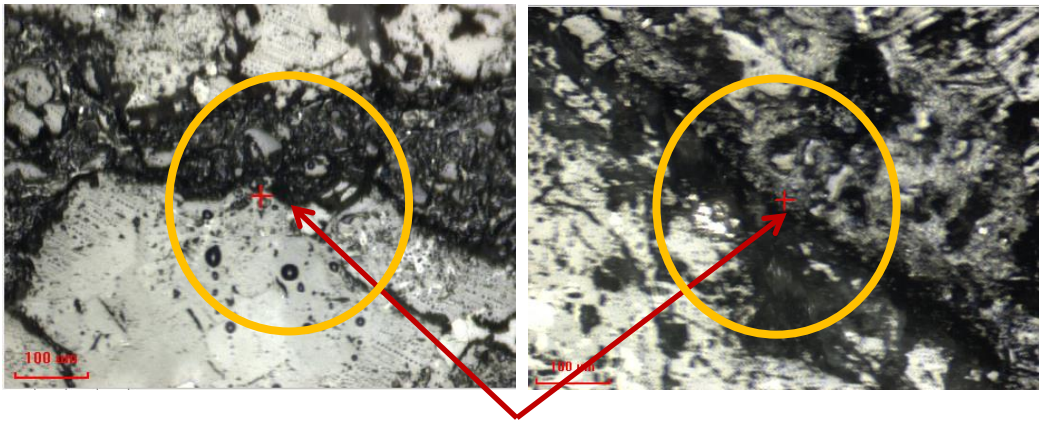

WSRIP125 ITZ RAP

Figure 8.12 ITZ RAP of mixture WSRlP125

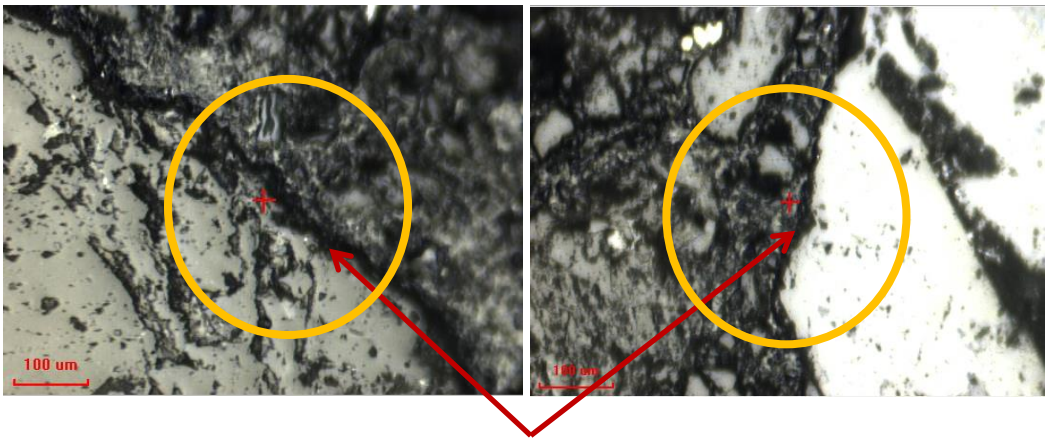

WSSaP125 ITZ RAP

Figure 8.13 ITZ RAP of mixture WSSaP125

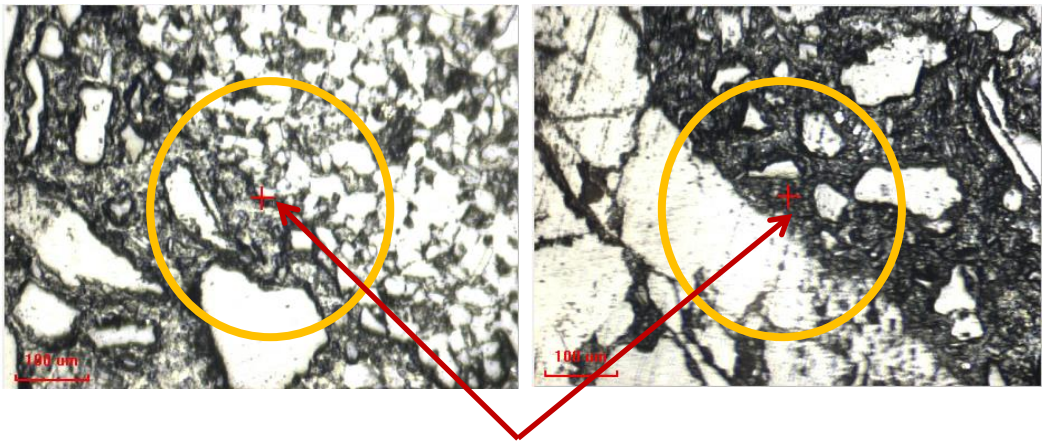

Complete blending WSSaP155

Figure 8.14 Complete blending in mixtures WSSaP155

Confirmation of the aforementioned scenarios can be made based on the mechanical properties of the ITZ RAP, ITZ virgin and mastic. Figures 8.15 and 8.16 show the elastic modulus and hardness of the ITZ RAP compared to the ITZ virgin of the control mix HH155. It is clear that the ITZ RAP of mixtures HSP145, WSSaP125, WSRlP125 and WSRlP155 was statistically stiffer and harder than the ITZ virgin of HH155 ($P < 0.05$) as shown in Table 8.3 This is expected because the binder surrounding the RAP aggregate must be aged for a long time due, perhaps, to some factors such as: oxidation, volatilisation, polymerisation, thixotropy, etc. (Al-Qadi 2007,Roberts *et al.* 1996,Karlsson and Isacsson 2006), as previously mentioned in Chapter 2, Section 2.6.1. However, it can be observed that, at a mixing temperature of 155°C, the mechanical properties of the ITZ RAP of mixture WSSaP155 are a bit higher than those for the ITZ

virgin and lower than those for mixtures HSP145, WSSaP125 and WSSaP125. The reason for that is, at high mixing temperatures, the old binder covering the RAP aggregate starts melting and getting away from the old aggregate. The reduction in the viscosity because of Sasobit has also accelerated this process and the new binder (blending old and virgin binders) with the effect of Sasobit has enhanced the elastic modulus and hardness of the ITZ virgin of mixture WSSaP155, as presented in Figures 8.17and 8.18 respectively. It is therefore clear that the elastic modulus and hardness of the ITZ virgin of WSSaP155 is the same to that of HH155 as there was no significant difference in the mean elastic modulus and hardness between ITZ of WSSaP155 and that of HH155 ($P > 0.05$). Moreover, there was no significant difference in the mean elastic modulus and hardness of mastic for WSSaP155 and HH155 as presented in Figures 8.19 and 8.20 and Table 8.3 which shows the results of ANOVA test for every mixture phase. The reason of that is because the extracted aged binder contributes to increase the elastic modulus and hardness of mastic due to the complete blending between RAP and virgin materials. It can therefore be concluded that complete blending was achieved using Sasobit.

Although at a mixing temperature of 155°C, the ITZ RAP of mixture WSRlP155 seems partially melted, as shown in Figures 8.17 and 8.18, elastic modulus and hardness of ITZ virgin of WSRlP155 were statistically less than those for HH155. The reason for that is because Rediset LQ has no effect on the viscosity of the binder, in which blending between old and virgin binder is unlikely to occur. Furthermore, there was no extracted binder from the old aggregate contributing to improving the properties of the ITZ virgin and mastic as presented in Figures 8.17 to 8.20. Despite the fact that the mastic properties of the HSP145 were statistically the same as the properties of HH155, because of the presence of fine particles of RAP aggregate, the properties of the ITZ virgin of HSP145 were statistically less than those of HH155 due to the same reason mentioned previously in the case of mixture WSRlP155 and the mean elastic modulus and hardness were significant ($P<0.05$). On the other hand, because Sasobit has a superior performance in improving the mixtures stiffness, the ITZ virgin of WSSaP125 is stiffer and harder than that of HSP145 but still statistically

lower than those of HH155 because of the effect of production temperature and incomplete blending between old and virgin binders.

As presented in Table 8.3. It can be noticed that complete blending was only obtained in one scenario in the case of mixture WSSaP155, as there was no statistical difference between the mechanical properties of ITZ and mastic of this mixture and those for control mix HH155 (P>0.05) as mentioned previously. It can therefore be concluded that Sasobit has the potential to help the virgin binder diffuse into the old binder, and also has an effect on the mobilisation of the old binder only if the effect of production temperature is considered.

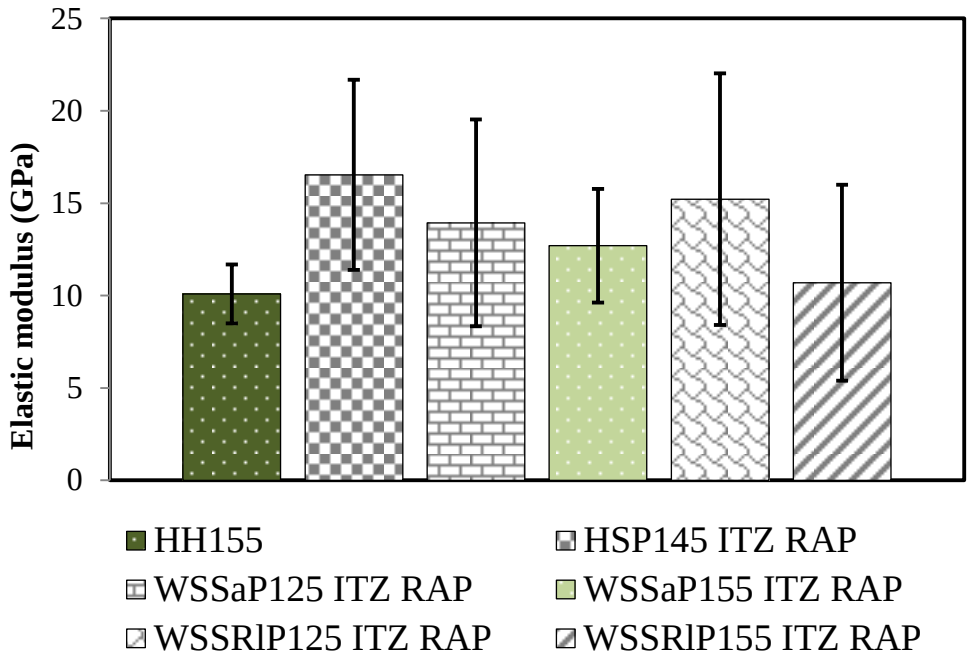

Figure 8.15 Elastic modulus of ITZ RAP compared to elastic modulus of ITZ virgin of control mix HH155

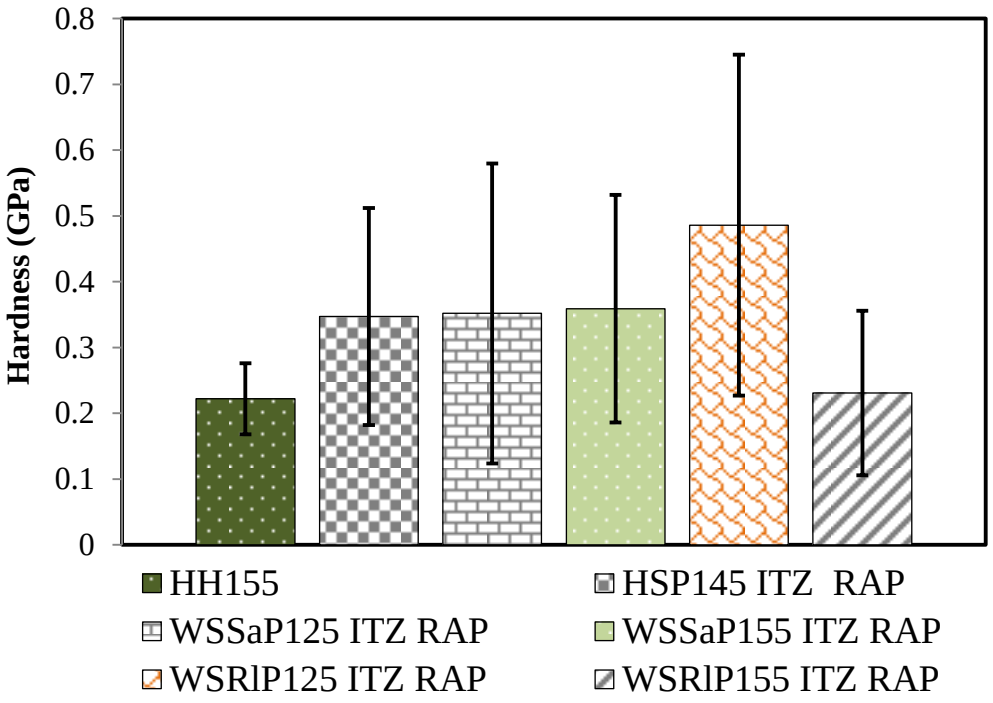

Figure 8.16 Hardness of ITZ RAP compared to hardness of ITZ virgin of control mix HH155

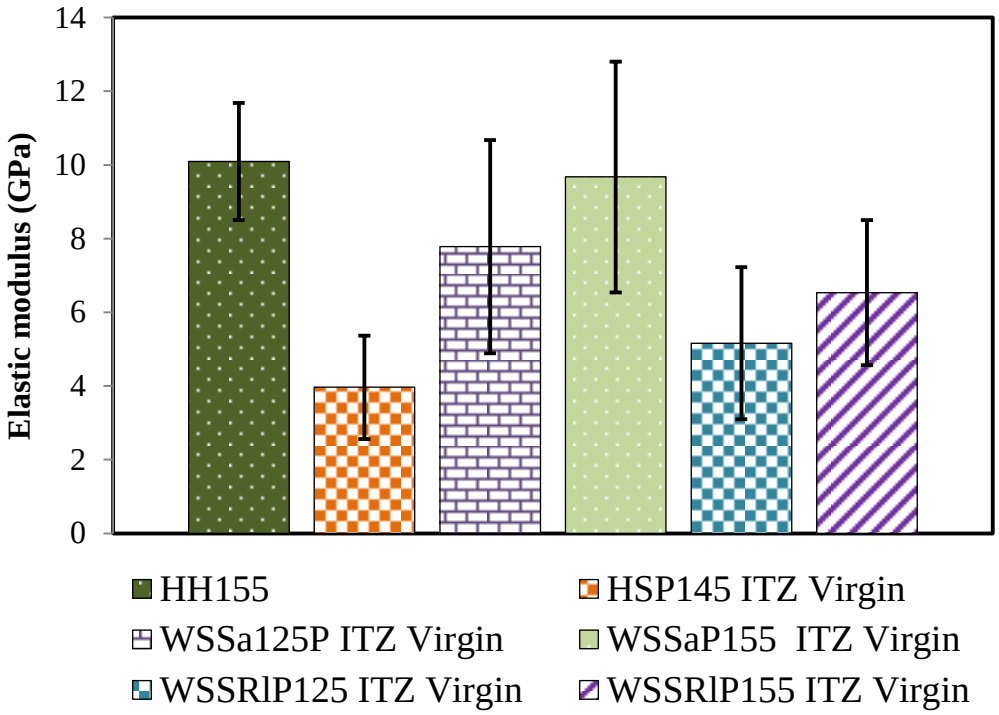

Figure 8.17 Elastic modulus of ITZ virgin of mixtures incorporating RAP materials

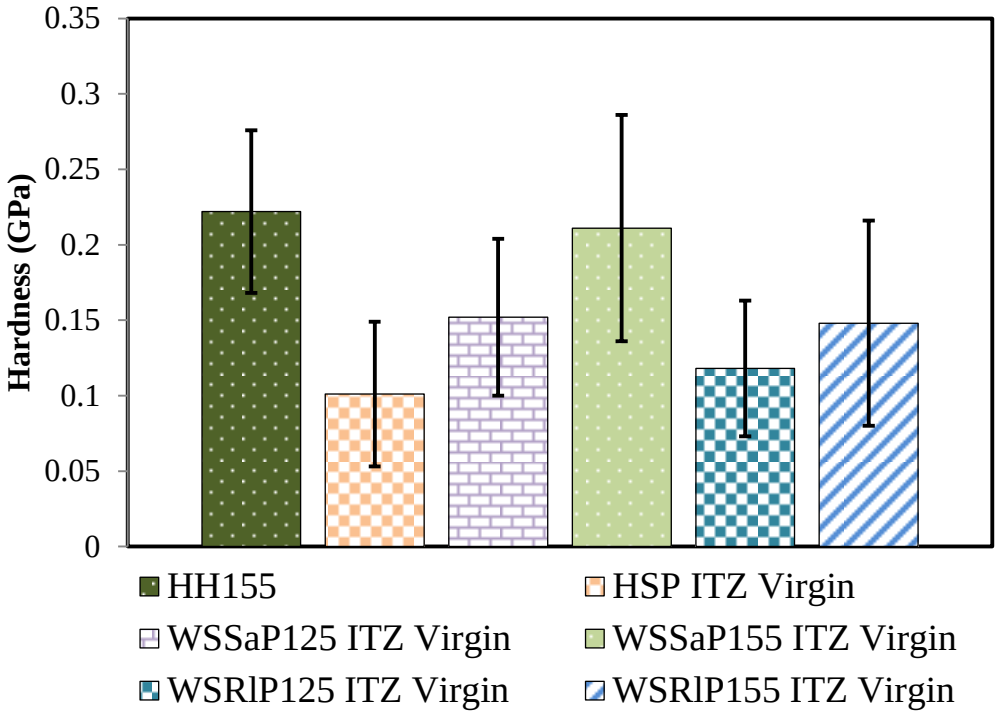

Figure 8.18 Hardness of ITZ virgin of mixtures incorporating RAP materials

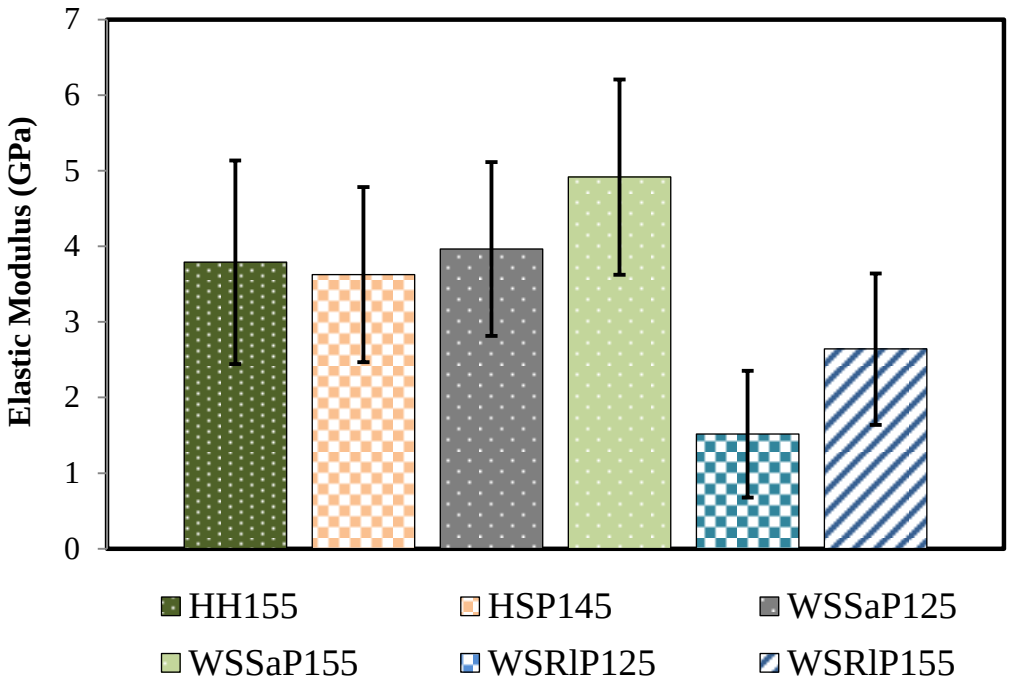

Figure 8.19 Elastic modulus of mastic for mixtures incorporating RAP materials

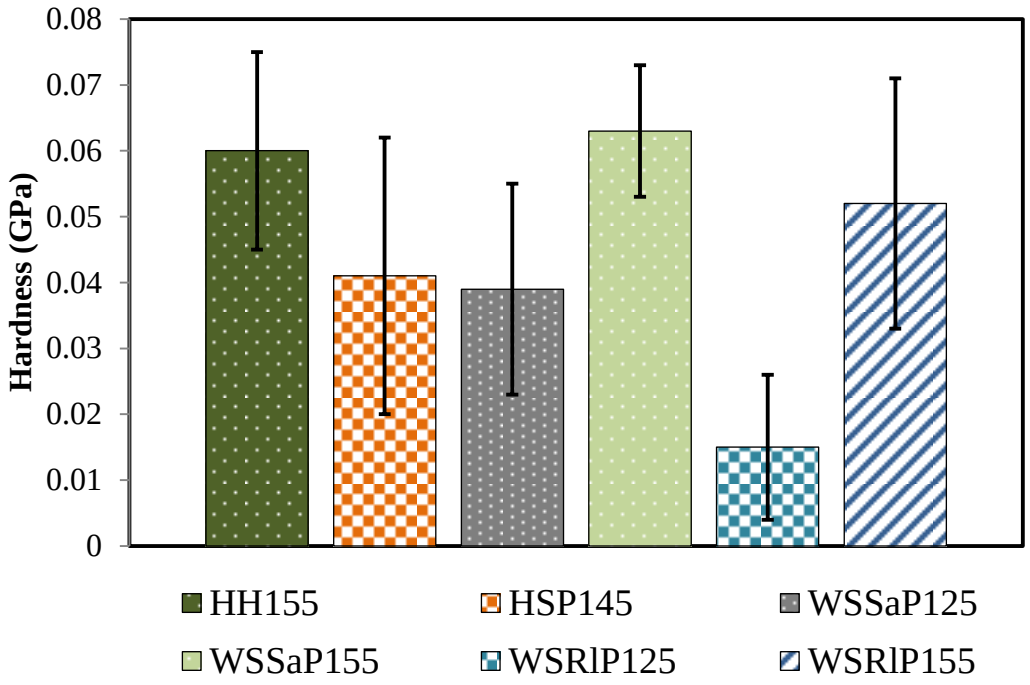

Figure 8.20 Hardness of mastic for mixtures incorporating RAP materials

Table 8.3 Results of ANOVA test for every mixture phase (α=0.05)

Mixtures Between		Elastic modulus			Hardness			Difference
ITZ virgin	*ITZ RAP*	*F*	*P-value*	*F crit*	*F*	*P-value*	*F crit*	
HH155	***HSP145, WSSaP125, WSSaP155, WSRlP125, WSRlP155***	26.05604	9E-06	4.091279	9.532115	0.003709	4.091279	**YES**
ITZ virgin								
HH155	***HSP145***	26.05604	9E-06	4.091279	9.532115	0.003709	4.091279	**YES**
	WSSaP125	8.456838	0.006667	4.159615	14.16602	0.000701	4.159615	**YES**
	WSSaP155	0.275265	0.602516	4.067047	0.270806	0.605461	4.067047	**NO**
	WSRlP125	68.06081	6.58E-10	4.105456	43.10736	1.08E-07	4.105456	**YES**
	WSRlP155	43.34783	2.93E-08	4.038393	15.69861	0.000241	4.038393	**YES**
Mastic								
HH155	***HSP145***	0.064074	0.804128	4.667193	4.323601	0.057944	4.667193	**NO**
	WSSaP125	0.087542	0.771132	4.493998	8.300429	0.01086	4.493998	**YES**
	WSSaP155	3.158423	0.094548	4.493998	0.166487	0.688661	4.493998	**NO**
	WSRlP125	27.6608	1.91E-05	4.241699	75.58687	4.99E-09	4.241699	**YES**
	WSRlP155	4.902428	0.039245	4.38075	0.946548	0.342824	4.38075	**NO**

8.3.2 SEM images

Further investigation on the level of blending between RAP and virgin material was conducted using scanning electron microscopy (SEM). The SEM offers high-resolution images to investigate the degree of blending between RAP and virgin materials. Although the images obtained using optical microscopy integrated in nanoindentation were very clear in showing the interfacial transition zone between the virgin aggregate and virgin binder and also between the aged binder and RAP aggregate, those images can also be validated using a SEM. As can be seen in Figure 8.21, there is complete interaction between the virgin aggregate and virgin binder, as was previously seen in Figure 8.10. However, Figure 8.22 clearly illustrates the ITZ RAP at magnifications of x1000 and x5000. It is obvious that the aged binder still covered the RAP aggregate and there is no blending between virgin and old binders.

As obtained and proved previously, Sasobit has a superior performance in satisfying complete blending between RAP and virgin materials. As presented in Figure 8.23, the region representing the old binder covering the RAP aggregate disappeared and complete interaction between the mastic and RAP aggregate can be seen, as was also noticed under the optical microscope of nanoindentation, as aforementioned and shown in Figure 8.14. Consequently, the overall performance of WSSaP155 is similar to or even better than that for HH155 in term of nano mechanical of ITZ and mastic.

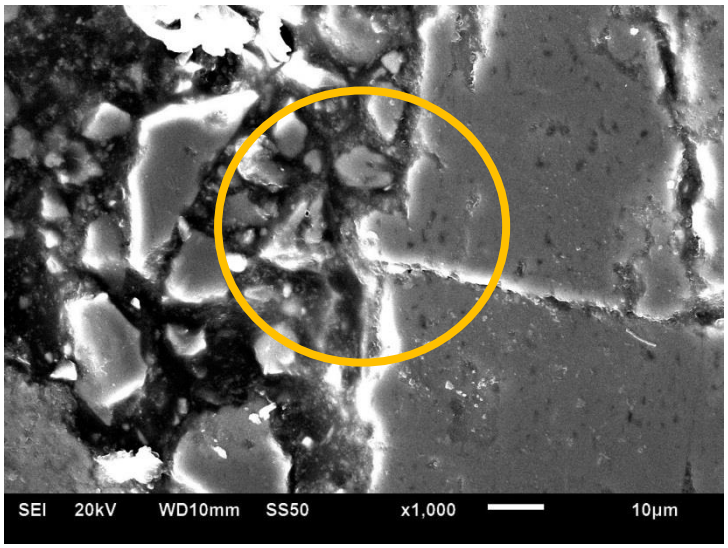

Fig 8.21-A

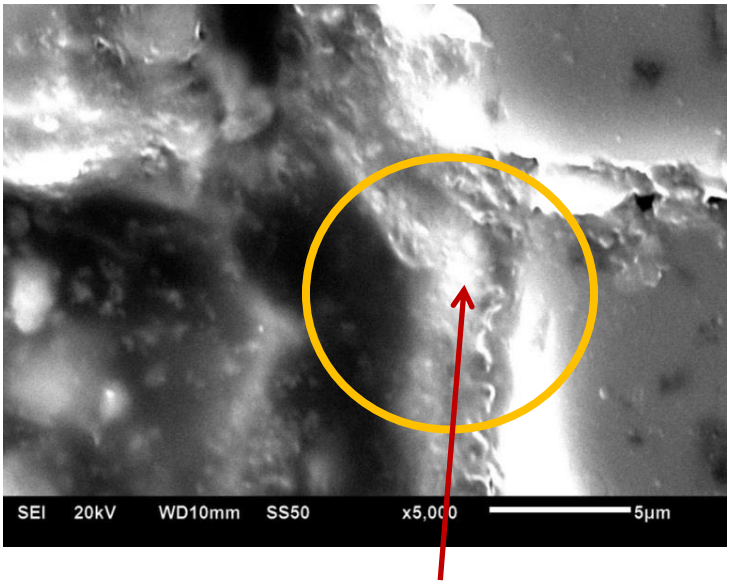

ITZ of virgin mix HH155

Fig 8.21-B

Figure 8.21 ITZ virgin of control mix HH155 A-at x1000 magnification and B-at x5000 magnification

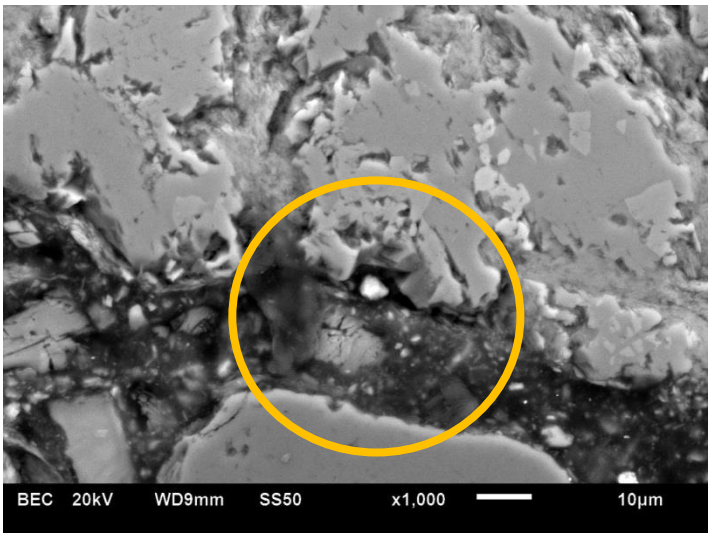

Fig 8.22-A

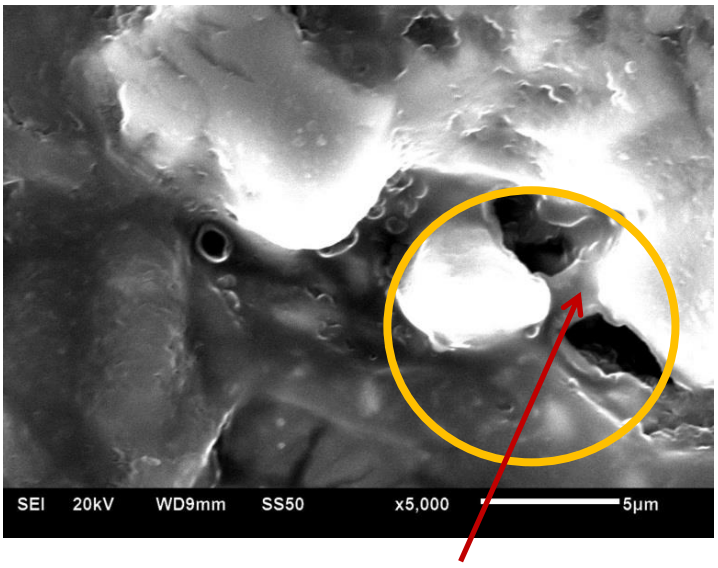

ITZ between RAP and virgin material WSRlP125

Fig 8.22-B

Figure 8.22 ITZ between RAP and virgin materials in mixture WSRlP125 A-at x1000 magnification and B-at x5000 magnification

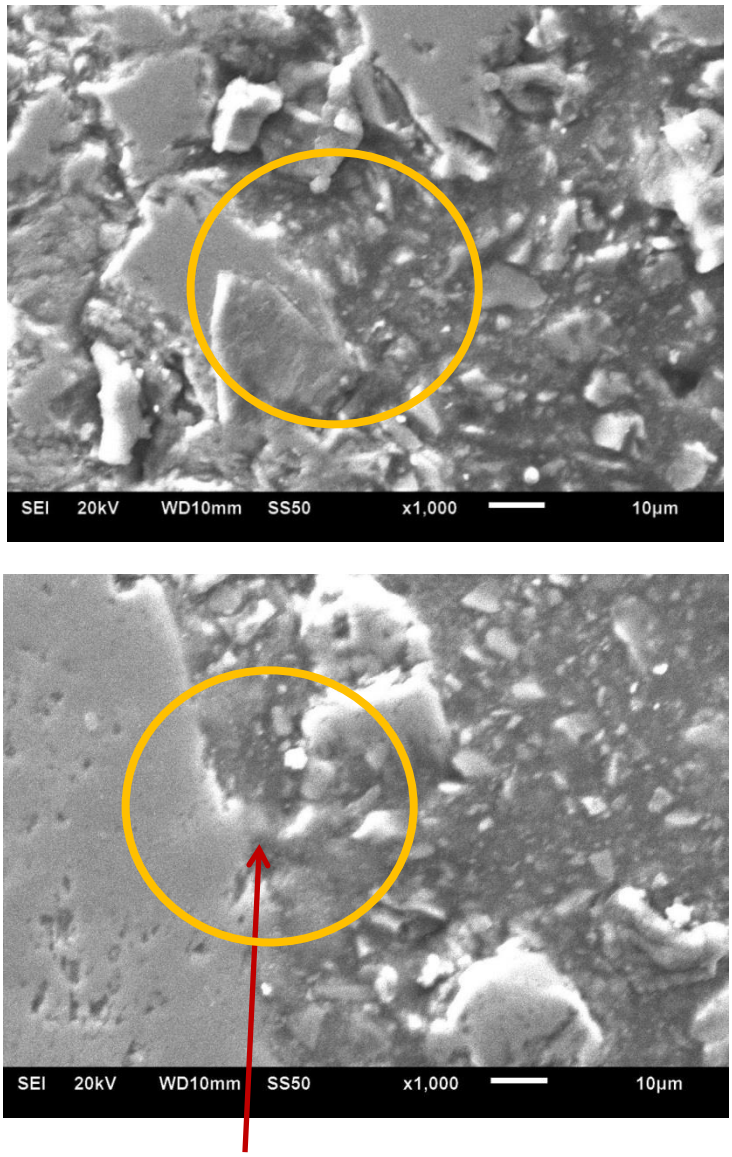

Figure 8.23 Complete blending between RAP and virgin materials at x1000 magnification

8.3.3 Stiffness (DSR samples)

Five samples from each mix were selected to conduct sweep frequency and fatigue tests. Stiffness measurements of HMA-RAP and WMA-RAP were also conducted within linear viscoelastic region of bituminous mixture. The controlled stress value of measurement was 25,000 Pa and the frequency was in the range from 0.1Hz to 10Hz, while the testing temperature was 25°C.

As presented previously, blending 60% of 100/150 binder with 40% of recovered RAP binder produced a binder with exactly the same performance and properties as the 40/60 binder. In terms of asphalt mixture, to obtain a complete blending between RAP and virgin materials two types of scenarios should happen: diffusion of virgin binder into binder surrounding the RAP aggregate and/or the mobilisation of old binder from the RAP aggregate. Those scenarios are governed by certain factors, such as production temperatures, stiffness of virgin binder, and properties of old binder and the effect of including additives. Figures 8.24 and 8.25 illustrate the stiffness and viscoelastic performance of mixtures incorporating RAP materials compared to HH155 and HS145. As can be seen in Figure 8.24, the complex shear modulus of HSP145 is lower than the complex shear modulus of control mix HH155; consequently, regardless of the effect of the RAP aggregate, complete blending between RAP and the virgin materials was not achieved as approved previously using nanoindentation. However, in comparison to control HS145, the stiffness of HSP145 is significantly higher, which definitely means that there is a partial blending between RAP and the virgin materials, or, in other words, partial mobilisation of binder-covered RAP aggregate occurred. Indeed, the following question may arise: is it practical to compare HSP145 with HH155 as the production temperatures are different? An answer to that can be noticed in the performance of WSRlP155. If the effect of Rediset LQ is neglected, the stiffness of WSRlP155 is still less than the stiffness of control HH155. Therefore, there was no need to manufacture another hot mix asphalt with inclusion of RAP materials at 155°C.

The effect of production temperatures and warm additives (Sasobit and Rediset LQ) on the level of blending between RAP and virgin materials is very clear. Al WMA-RAP manufactured at 125°C had lower stiffness than control mix

HH155 but higher stiffness than HS145. However, as the production temperature increased to 155°C, although WSRlP155 exhibited more elastic behaviour than HH155 due to the effect of Rediset LQ, its stiffness is still less than the control HH155 because images and nano-mechanical properties obtain from nanoindentation were shown there was on complete blending between RAP and virgin materials. The reason for that is because the purpose of Rediset is active adhesion, surfactant and compaction aid which are not enough or effective to make the virgin binder diffuses into the old binder and also the old binder cannot completely get away from RAP aggregate. However, the effect of Sasobit on the level of blending of WMA-RAP was very considerable. Sasobit has the potential to significantly decrease the viscosity of the binder which allows diffusing virgin binder into old binder. Also, when Sasobit-modified binder is added to virgin aggregate and RAP, it is expected to also decrease the viscosity of the old binder; therefore, the old binder can easily get away from RAP aggregate, and so complete blending can occur. Consequently, as can be seen in Figures 8.24 and 8.25, WSSaP155 had higher stiffness measurements at different loading times and exhibited higher elastic response compared to control mix HH155.

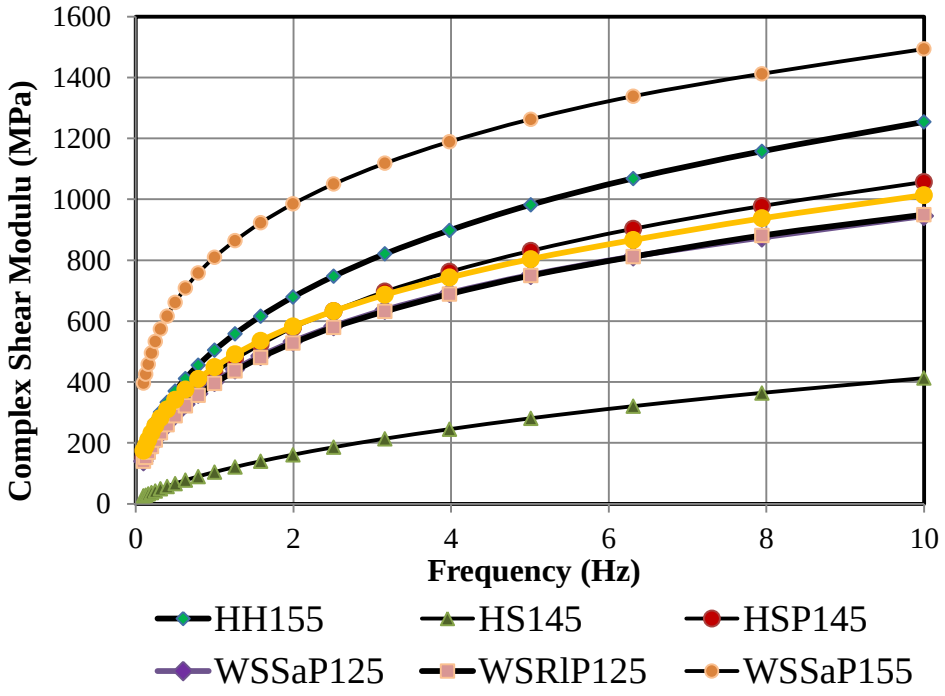

Figure 8.24 Average stiffness of mixtures incorporating RAP materials compared to HH155 and HS145

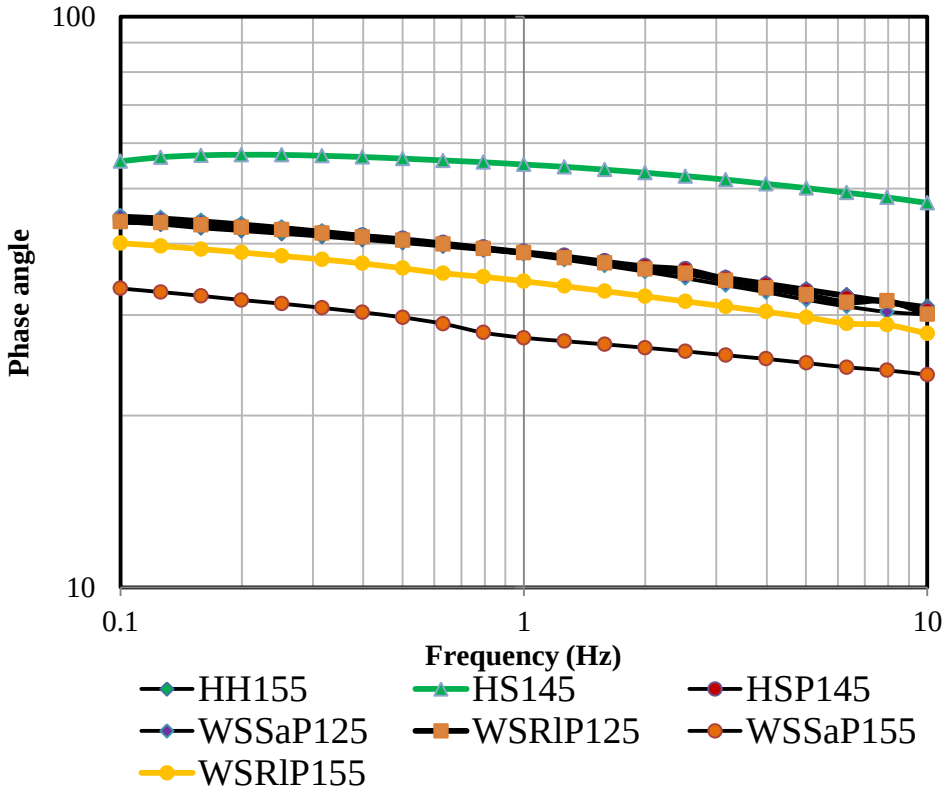

Figure 8.25 Viscoelastic performance of mixtures incorporating RAP materials compared to HH155 and HS145

8.3.4 Fatigue (DSR samples)

More attention should be paid to the fatigue life of asphalt mixtures because the greater the RAP content, the more brittle are the materials included in the mixture. It is therefore important to investigate the level of blending based on the fatigue characterisation of asphalt mixtures. As proved previously, partial blending between RAP and virgin materials was noticed in all HMA-RAP and WMA-RAP apart from WSSaP155, as its stiffness was higher than the control mix HH155, which means complete blending occurred. Fatigue tests were conducted for those mixtures in order to estimate the fatigue life of WMA-RAP. Investigations were carried out under two scenarios, as follows:

- First scenario: fatigue tests were conducted for mixtures HSP145, WSSaP125 and WSRlP125 at controlled stress value of 250KPa and testing temperature of 25°C so a comparison could be made with the control mix HS145.

- Second scenario: fatigue tests were conducted for mixtures HSP145, WSSaP125, WSRlP125, WSRlP155 and WSSaP155 at controlled stress value of 425KPa and testing temperature of 25°C so a comparison could be made with the control mix HH155.

More details about the fatigue test settings for asphalt mixtures (HH155 and HS145) are presented in Chapter 7, Section 7.6.3.1.

In the first scenario, Figure 8.26 shows number of cycles at a reduction of stiffness modulus of the sample to 50% of its initial value, because it was impractical to obtain a complete fracture failure or reduction to 10% of its initial value as the fatigue test took a very long time. It was therefore decided to stop the fatigue test when the complex shear modulus reached 50% reduction from its initial value. As can be seen in that figure, HSP145 exhibited a higher number of cycles until reaching 50% compared to HS145. And, although WSSaP125 and WSRlP125 were manufactured at 125°C, practically, their fatigue lives were longer than that of HS145. This finding agrees with Huang *et al.* (2004a, 2004b). Consequently, the common belief that the more RAP, the more brittle the mixture, thus, the lower the fatigue resistance, is contradicted. It can be therefore confirmed that there was a partial blending between RAP and virgin materials in those mixtures as the fatigue life of HSP145, WSSaP125 and WSRlP125 were longer than that of control mix HS145. However, in order to further investigate whether a complete blending occurred or not, fatigue tests were conducted for those mixtures at 425KPa so that a decision could be made according to their fatigue performance with HH155.

Figures 8.27 and 8.28 present the results of the fatigue tests in the second scenario. It is clear that the number of cycles at the failure point of mixtures HSP145, WSSaP125, WSRlP125 and WSRlP155 was lower than that of HH155, which confirmed the fact that there was no complete blending between RAP and virgin materials. From a fatigue perspective, this region may be considered as a weak region because of the incomplete blending; therefore, under apply higher load, cracks will likely start to initiate and develop over time. Furthermore, the deficiency of mastic to resist the applied higher load accelerates initiating and developing of cracks over time. This assumption is supported by the conclusion

study of Mohajeri *et al.* (2012) who studied the relation between cracking resistance of asphalt mixtures and the degree of blending between RAP and virgin binders. It was reported that the degree of blending between RAP and virgin binders seems to governing the mechanical properties of asphalt mixtures.

Despite the fact that WSRlP155 was manufactured at 155°C with the addition of 0.5% of Rediset LQ, no complete blending was observed, whereas WSSaP155 exhibited approximately the same fatigue life as HH155. The reason for that is because Sasobit is a viscosity reducer and stiffness improver. It can therefore be concluded that a complete blending between RAP and virgin materials occurred in the mixture of WSSaP155.

Fatigue results of all HMA-RAP and WMA-RAP are presented in detail in appendix G, Table G.1.

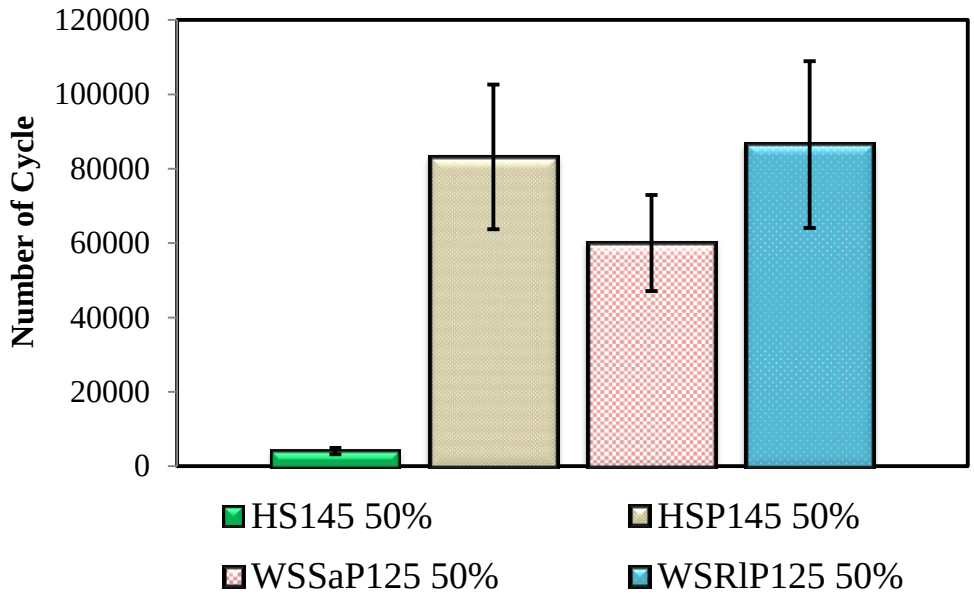

Figure 8.26 Fatigue life of HMA-RAP and WMA-RAP compared to control mix HS145

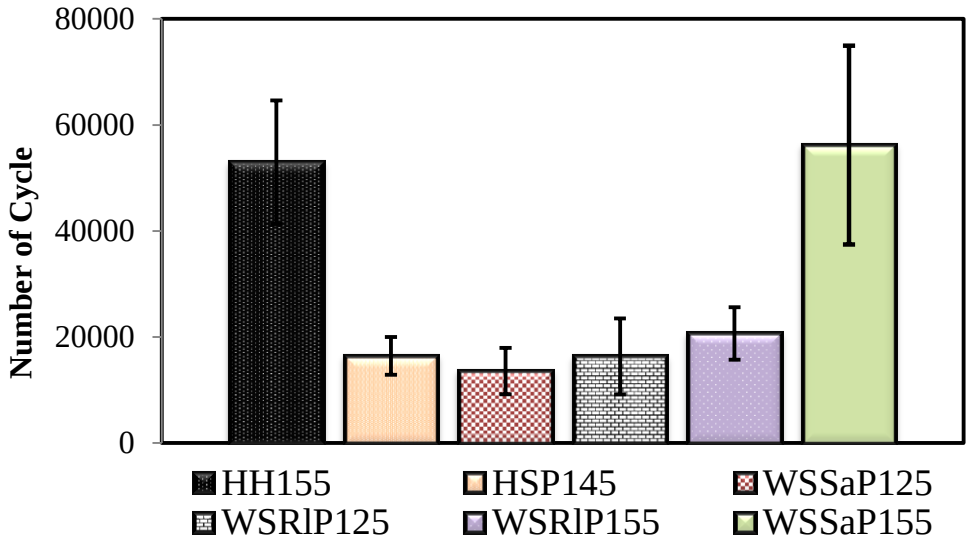

Figure 8.27 Fatigue life of HMA-RAP and WMA-RAP compared to control mix HH155

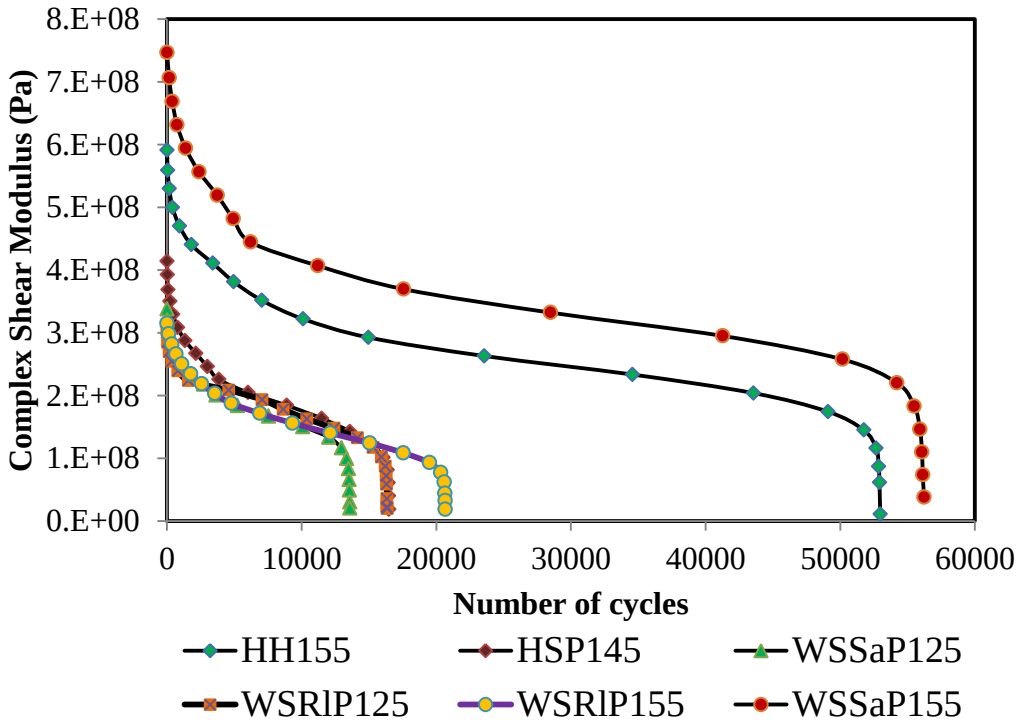

Figure 8.28 Average complex shear modulus vs. number of cycles for HMA-RAP and WMA-RAP tested at 425KPa and 25°C

8.4 Proposed protocol to obtain complete blending

Based on what has been presented in this chapter, a simple protocol is proposed to obtain a complete blending between RAP and virgin binder, which is a key component of suitable practices in the pavement industry. If a complete blending can be reached, natural resources can be significantly conserved and also a more sustainable and cost-effective pavement structure can be constructed. Figure 8.29 illustrates the steps that can be used to reach a complete blending between RAP and virgin materials.

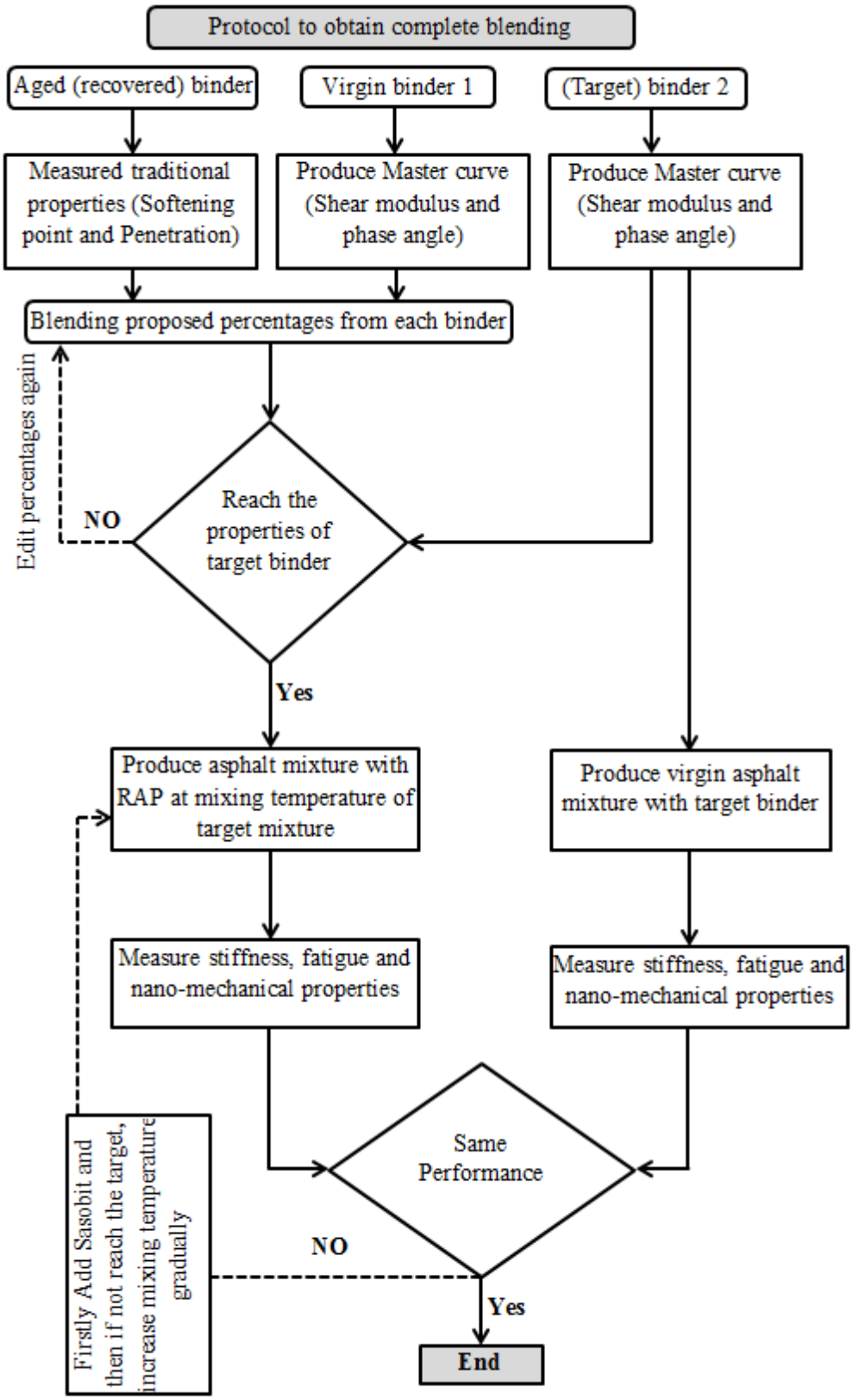

Figure 8.29 Protocol to obtain complete blending between RAP and virgin materials

8.5 Conclusion

Level of blending between RAP and virgin materials is a point of debate among pavement researchers. As aforementioned, to date, this interaction has not been investigated at the nano-scale, which can practically reflect the real level of materials' interactions. In the current chapter, the effect of warm additives of Sasobit and Rediset LQ and production temperatures on the real interaction was investigated using nano-mechanical properties of ITZ and mastic. Results were further validated using scanning electron microscopy, while the overall performance of WMA-RAP was assessed based on overall stiffness and fatigue life. The main findings of this chapter are:

1. It was revealed that, in the incomplete blending scenario, the old binder is still covering the RAP aggregate. However, it was found that the production temperature and Sasobit have a substantial effect on the mobilisation of aged (old) binder and the diffusion of virgin binder into old binder.

2. Once the ITZ RAP disappears, complete blending between RAP and virgin materials can be reached, which can be proved by the mechanical properties of ITZ RAP, ITZ virgin and mastic.

3. Although Rediset LQ can improve the performance of WMA-RAP compared to the control mix, it has no effect on the rejuvenation of aged binder as the purpose of this additives is to decrease the fractional forces at the interfaces of the aggregate and binder without reducing the viscosity of the binder, which is the most important factor that affects the rejuvenation of aged binder and the diffusion of virgin binder.

4. Inclusion of RAP materials in asphalt mixtures increases the stiffness and fatigue life of those mixtures; therefore, the theory of black rocks incorporating RAP is refuted.

5. Inclusion of up to 40% of RAP materials with WMA can produce an asphalt mixture with better performance that the traditional HMA in terms

of stiffness and fatigue life; therefore RAP materials must not be considered as a black rock.

6. A simple protocol has been proposed to reach complete blending between RAP and virgin materials.

Chapter Nine

Overall Performance of Warm Additives

9.1 Introduction

The work presented in this thesis includes five main parts: viscosity, rheological properties and fatigue life of WMBBs, nano-mechanical properties of WMBBs and WMA, methods to evaluate bond strength between aggregate and binder, fatigue life of WMA and the effect of warm additives on the level of blending between RAP and virgin materials. In presenting the aforementioned results and techniques, it is important to bring these different things together and summarise the influence of warm additives on the different properties of binder and asphalt mixtures and at different scales. The current chapter summarises and compares the performance of warm additives investigated in this study.

9.2 Effect of warm additives on the viscosity, rheological properties and fatigue life of binder

The effects of different dosages of Sasobit, Rediset WMA and Rediset LQ on the viscosity of two binder grades, namely 40/60 and 100/150, were investigated. Sasobit and Rediset WMX are expected to decrease the viscosity of binder. However, adding 2% Sasobit or 2% Rediset WMX produced no significant change in binder viscosity. It was therefore expected that the Brookfield viscometer would not be able to predict the necessary reduction in the mixing temperature. In fact, even when increasing the dosage level of those binders up to 6%, which is beyond that recommended by the suppliers, the expected production temperature of WMA was only 10°C for hard binder and 12°C for the soft binder lower than that of control mixtures, whereas Rediset LQ did not affect the viscosity of the virgin binder even when using up to 1.5% of this additive. In fact, Rediset LQ has no effect on the rheological properties of asphalt binder, as shown

in the master curves of binders including different dosages of this additive; therefore, higher than the recommended dosages can be used if required, without having a negative effect on the binder's linear viscoelastic properties. Sasobit significantly increased the complex shear modulus and decreased the phase angle of virgin binder at the recommended dosage. Increasing the dosage of Sasobit resulted in further significant increase in the binder stiffness. Therefore, results of this work suggest to only use the supplier's recommended dosage. However, although the effect of increasing the dosage of Rediset WMX was not as significant as that of Sasobit, an increase in the complex shear modulus and a decrease in the phase angle of the virgin binders was noticed. Therefore, it may be appropriate to use higher than the recommended dosages of Rediset WMX but further investigation on the effect is needed.

Having mentioned there is no clear conclusion about the fatigue life of WMA compared to that of HMA, therefore, there is a need to characterise the fatigue-cracking of WMA. Two questions were addressed in this study. The first is whether the fatigue life improves because of the lower production temperature or because of the effect of warm additives. The second is to what extent the production temperature can be decreased without causing a negative impact on the fatigue-cracking performance of WMA. The study adopted firstly a time sweep test method to evaluate the effect of Sasobit and Rediset WMX and LQ on the fatigue performance of bituminous binders, and study this phenomenon under controlled stress mode using a Dynamic Shear Rheometer. It was found that Sasobit significantly increased the fatigue life of asphalt binder regardless of binder grade. This was confirmed using different criteria to rank the fatigue performance of Sasobit-modified bitumen. This finding does not agree with previous studies that showed that Sasobit increases the tendency towards cracking at low temperature. Improvement in the fatigue life of bituminous binders was also noticed in the case of adding Rediset WMA but its performance was not as remarkable as that of Sasobit. However, Rediset LQ did not affect the fatigue life of bituminous binders because, as found in the viscosity and rheological properties section, Rediset LQ did not alter the bituminous binder properties at either the recommended dosages or at dosages higher than the recommendations.

9.3 Effect of warm additives on the nano-mechanical properties of bituminous binders and mixtures

In order to obtain further understanding about the effect of warm additives and overall asphalt mixtures, there was firstly a need to further understand and evaluate the properties of the mixture phases and link their properties to the overall performance of asphalt mixture. This investigation was conducted using AFM and nanoindentation.

AFM was used to study the effect of warm additives, Sasobit and Rediset WMX and LQ, on the topography, elastic modulus, and adhesion of bituminous binders with the PFQNM modality. PFQNM results show Sasobit and Rediset WMX significantly affected the morphological structure of virgin binders while Rediset LQ has no effect on the morphological structure of bitumen. More importantly, it was found that the presence of the catana phase was associated with the presence of wax. Moreover, the study revealed that Sasobit significantly increased the elastic modulus of the binders at the nano-scale by approximately seven times and five times for 40/60 and 100/150 binder grades respectively. Surprisingly, Sasobit also improved the adhesion properties of the bitumen, with the adhesion force increasing from 17.7 nN to 35.26 nN and from 21.56 nN to 59.01 nN for 40/60 and 100/150 binder grades respectively. Both Rediset WMX and LQ also improved the adhesion characterisations of warm-modified bituminous binders by around 110% and 50% respectively. However, the elastic modulus only increased when using Rediset WMX because Rediset LQ does not alter the binder properties of net bitumen, as found previously in the investigation part relating to viscosity and rheological properties.

Sasobit, Rediset WMX had a significant effect of the elastic modulus and adhesion of bitumen while Rediset LQ only improved the adhesion characterisation of bituminous binders as was also found in the viscosity and rheological properties investigation. Hence, before investigating their overall effect on asphalt mixtures, there was a need to investigate their effect on mixture phases aggregate, ITZ and mastic so that a clear picture regarding their effect on the asphalt mixture performance can be obtained. A novel investigation to evaluate the effect of Sasobit and Rediset WMX and Rediset LQ on the nano-mechanical properties of asphalt mixture phases, aggregate, interfacial transition

zone (ITZ) and mastic was conducted using nanoindentation. It was found that all warm additives improved the nano-mechanical properties of the ITZ only if the production temperature was taken into account. The study revealed that the reduction in the production temperature should not be more than 10°C for an asphalt mixture using such a hard binder as 40/60 and 20°C using 100/150 binder grade compared to control HMAs. The nano-mechanical properties of mastic for all WMAs manufactured at 135°C using 40/60 binder grade were less than the control mix HH155. However, as the production temperature was145°C (only 10°C lower than that of control mix), the elastic modulus and hardness of the mastic and ITZ for all WMAs manufactured at 145°C significantly increased. In contrast, a 20°C reduction in the production temperatures was achieved using 100/150 binder grade with the inclusion of warm additives compared to the production temperature of control mix HS145 and the values of the elastic modulus and hardness of the ITZ and mastic were the same as or even higher than those of control mix HS145.

Results from nanoindentation were further used to introduce a new method called work of indentation as presented in Chapter 6, Section 6.5.1 to evaluate the bond strength between the aggregate and binder/mastic in the mixture and investigate the effect nano- mechanical properties of mixture phases on the overall fatigue life of WMA.

9.4 Effect of warm additives on the bond strength between aggregate and binder

In the present study, the effect of Sasobit, Rediset WMX and Rediset LQ on the adhesive bond strength of an aggregate-binder system was also investigated using the pull-off test. The impact of warm additives, test temperature and binder grade on the work of fracture was investigated. It was found that Sasobit, Rediset WMX and Rediset LQ increased the work of fracture. The contribution of warm additives in improving the work of fracture has been linked to the adhesion force determined using AFM. The performance of warm additives in improving the work of fractures was qualitatively associated with the measured adhesion force determined using PFQNM. The main advantages of using AFM to characterise nano-scale properties were shown to include co-localisation of nano-topography

with adhesion, ease of sample preparation and reduction in experimental time relative to the direct tension pull-off test. It is therefore clear that evaluating the adhesion of bituminous binders using PFQNM can replace the need for evaluating adhesion using the pull-off test.

However, although PFQNM offers great advantages to characterise the adhesion of bituminous binders, there is still a need to directly evaluate the bond strength between aggregate and binder/mastic in the mix. An approach called work of indentation was proposed throughout this study based on the load and displacement on the ITZ. This approach offers great advantages in evaluating the bond strength taking into account the effect of production and compaction temperatures, the effect of aggregate, the effect of ageing that may occur during manufacturing the asphalt mixture, and the effect of any additive that enhances the properties of the mixture. It was also found that the performance of warm additives in improving the work of fractures was qualitatively associated with the work of indentation but, because Rediset LQ is also classified a compaction enhancer, it resulted in considerable amelioration in the bond strength of the WHRl145 compared to the WHRl135.

9.5 Effect of warm additives on the fatigue life of asphalt mixture

An attempt was made to characterise the fatigue-cracking of WMA. The time sweep fatigue test was used to characterise the fatigue cracking of HMAs and WMAs. Although WMA made with hard binder 40/60 was successfully manufactured at a temperature 20°C lower than the traditional HMA and the aggregate was completely coated, its fatigue life was lower than the traditional HMA. However, when WMA modified with hard binder was manufactured at a temperature only 10°C lower than the traditional HMA, its fatigue resistance significantly increased. In addition, successful reduction in the production temperature of up to 20°C was achieved for WMA modified with soft binder compared to control mix. Therefore, there is a need to identify the level of reduction in the production temperature based on the grade of the bitumen in order to produce an asphalt mixture which has a better fatigue life than the traditional HMA.

In fact, if the warm additives have a superior performance in terms of adhesion, why does the fatigue life of WMA manufactured at 135°C have a shorter fatigue life than that for HH155? An answer to this question was obtained using nanoindentation. The elastic modulus and hardness of the ITZ and mastic of the mixture phases were linked to the overall fatigue life of those mixtures. Cracks take place either in mastic or along the interface between aggregate and binder. Basically, the stiffer the mastic and ITZ of the asphalt mixture are, the longer the fatigue life of that mixture, because improving the aggregate-binder bonds and properties of mastic delays the formation and separation of micro-cracks within the matrix; therefore, the material exhibits more resistance to applied repeated loads. It is therefore clear that, when WMA was produced at 135°C, the bond strength between the aggregate and binder and the stiffness of the mastic was not in good level as that for control mix to make WMA exhibit the same or longer fatigue life than that of the control mix. However, as the reduction in the production temperature decreased, the improvements in the elastic modulus and hardness of ITZ and mastic delayed the formation and separation of micro-cracks; therefore, the fatigue life of WMAs were longer than that for control mix HH155. In fact, the contribution of warm additives in improving the bond strength between aggregate and binder in line with improving the hardness and elastic modus of mastic explains the significant improvement in the fatigue life of WMA.

It is believed that there is a minimum production temperature for each binder grade and, under this production temperature, even if the aggregate is fully coated by binder, the lower production temperature will have a negative impact on the bond strength between the aggregate and binder/mastic. Based on this concept, to defend against the development of cracks, it is recommended for highway agencies to specify a minimum production temperature for WMA to reach acceptable mixture stability in terms of fatigue performance taking into account the binder source and grade.

After taking the production temperatures into account, in all scenarios, Rediset WMX increased the fatigue life by approximately 32% while Rediset LQ doubled the fatigue life of the asphalt mixture and Sasobit increased the fatigue life by approximately 90%. It can therefore be concluded that WMA exhibited

better fatigue life than that of HMA, but other considerations should be taken into account such as the production temperature and binder grade.

9.6 Effect of warm additives on the performance of mixtures incorporating RAP materials

The study was also aimed to investigate level of blending between RAP and virgin materials at the nano-scale. The investigation was carried out using nanoindentation, SEM and DSR. There are three scenarios in the case of incorporating RAP materials. The first is if RAP materials incorporated into the mixtures include virgin binder A and it is necessary to make a comparison with a control mix containing 100% of that virgin binder (A). The second is if RAP materials incorporated into the mixtures include virgin binder A and it is necessary to make a comparison with a control mix containing virgin binder (B) (a stiffer binder than A). The third is if RAP materials are considered as black rocks. The results revealed that the RAP materials must not be considered as black rocks because there was always a partial blending between RAP and virgin materials. It was found that Sasobit and Rediset LQ had a superior performance in producing asphalt mixtures incorporating RAP materials that have better performance than the control mix (HS145), even if they were produced at lower temperatures. However, in comparison to HH155, only Sasobit-modified mixture produced at 155°C reached a complete blending between RAP and virgin materials.

In fact, in the case of incorporating RAP materials, the challenge is always how a complete blending can be reached and approved so that pavement designers can be more confident and accurate in estimating the performance of asphalt mixture incorporating RAP materials. The study proposed a procedure to obtain and approve a complete blending in the laboratory.

9.7 Summary of the overall performance of warm additives

In summary, warm additives have a superior performance in producing asphalt mixtures that have an equal or better performance than traditional hot mix asphalt. This fact was reached based on the comprehensive study as presented in this thesis to characterise their performance relative to traditional HMA. In the case of WMA incorporating RAP materials, Sasobit showed a superior performance than Rediset LQ in helping to reach a complete blending with virgin materials. Table 9.1 summarises the performance of Sasobit, Rediset WMX and Rediset LQ at the recommended dosages and their influence on mixture and binder properties.

Table 9.1 Overall effect of warm additives on bituminous binder and mixture properties

Material	Properties	Technique	Sasobit	Rediset WMX	Rediset LQ
Binder	Viscosity	Viscometer	Decreased*	Decreased*	No effect
	Complex Shear Modulus	DSR	Increased**	Increased*	No effect
	Phase angle	DSR	Decreased*	No effect	No effect
	Fatigue	DSR	Increased**	Increased**	No effect
	Topography	AFM	Changed**	Changed**	No effect
	Elastic modulus	AFM	Increased**	Increased**	No effect
	Adhesion force	AFM	Increased**	Increased**	Increased**
	Deformation	AFM	Decreased**	Decreased**	No effect
Aggregate-binder system	Work of fracture	(Pull-off)	Increased**	Increased**	Increased**
Asphalt Mixtures	Hardness (ITZ)	Nanoindentation	Increased**	Increased**	Increased**
	Elastic modulus (ITZ)	Nanoindentation	Increased**	Increased**	Increased**
	Hardness (Mastic)	Nanoindentation	Increased**	Same as control	Same as control
	Elastic modulus (Mastic)	Nanoindentation	Increased**	Same as control	Same as control
	Work of indentation	Nanoindentation	Increased**	Increased*	Increased**
	Stiffness	DSR	Increased**	Decreased*	Same as control
	Fatigue	DSR	Increased**	Increased**	Increased**
	Complete blending between RAP and virgin materials	DSR/ Nanoindentation/ SEM	Yes	-	No

Slightly* (Less than 20%), Significantly ** (Equal or more than 20%)

Chapter Ten

Conclusions and Recommendations for Future Work

10.1 Conclusions

The research aimed to study the effect of warm additives on the mixture properties to produce asphalt mixtures that have the same or better performance than traditional hot mix asphalt. The study focused firstly on understanding the effect of different dosages of Sasobit, Rediset WMX and Rediset LQ on the viscosity and rheological properties of bituminous binders. More attention was paid to the effect of warm additives on the fatigue life of bituminous binders. Further efforts were made to gain a greater understanding of the effect of warm additives on bituminous binder and mixture properties at the nano-scale. AFM was used to investigate nano-scale properties of WMBBs whilst nanoindentation was used to evaluate the effect of warm additives and production temperatures on elastic modulus and hardness of mixture phases with reference to ITZ and mastic. Adhesion properties obtained from AFM and nanoindentation were linked to work of fracture that is required to break the bond between aggregate and binder. The research then focused on the functionality and fatigue behaviour of WMA. The emphasis was on examining the effect of warm additives on the fatigue life of asphalt mixtures considering the influence of production temperatures and binder grade and the effect of the mixture phase's properties on the overall performance of WMA. A nano-mechanical approach was further used to investigate the level of blending between RAP and virgin materials and a protocol was developed to investigate and obtain a complete blending between RAP and virgin materials in the laboratory.

It was found that Rediset LQ has no effect on the viscosity and rheological properties of bituminous virgin binders even when using up to 1.5% of this additive. Consequently, this additive can be used at higher dosages than those

recommended without affecting the binders' viscoelastic properties. Using the recommended dosages of Rediset WMX has a minor effect on the rheological properties of asphalt binder; therefore, dosages higher than the recommended ones can also be used if required, perhaps without having a negative effect on the binder's linear viscoelastic properties. Furthermore, it was also found that the addition of 2% Sasobit had a significant effect on the stiffness and elastic properties of the binder. Using more than 2% of Sasobit further increased the binder stiffness and decreased the phase angle. Thus, increasing the recommend dosages of Sasobit should be avoided, or further investigations into the effect of different dosages of Sasobit on asphalt mixture properties should be conducted.

Furthermore, Sasobit has a positive effect on improving the fatigue life of asphalt binder regardless of binder grade. Previous studies showed that Sasobit increases the tendency towards cracking at low temperatures. However, previously, the effect of Sasobit on the fatigue life of binders was evaluated based on the Superpave fatigue parameter, which has received significant criticism. Rediset WMX also improves the fatigue life of bitumen. However, as Rediset LQ has no effect on the binder properties, it is also not expected to affect the fatigue life of bituminous binders.

In addition, Rediset LQ-modified bituminous binders had the same structure as the control binders, as Rediset LQ did not alter the topography and micro-structure of bitumen phases, matching its effect on the viscosity and rheological properties of binders. Thus, it has no effect on the elastic modulus and deformation of net bitumen, as was also found in terms of viscosity and rheological properties. However, Sasobit significantly increased the modulus of binders at the nano-scale and decreased the deformation of the modified bitumen because it forms a lattice structure and generates a bridge between molecules, which in turn prevents them moving. Interestingly, Sasobit also improved the adhesion characterisation of the bitumen. Perhaps the presence of wax led to this improvement. Both Rediset WMX and LQ have contributed to increasing the adhesion force of warm-modified bituminous binders by around 110% and 50% respectively. However, it should be noted that the deformation and modulus were only improved when using Rediset WMX, compared to Rediset LQ; this is because of the presence of wax in the former.

Nanoindentation has the potential to characterise the properties of mixture phases, aggregate, ITZ and mastic. Improving the mechanical properties of ITZ and mastic can lead to significant improvements in the overall performance of the asphalt mixture. All warm additives improved the nano-mechanical properties of the ITZ only if the production temperature was considered. The production temperature also had a great effect on the mechanical properties of the mastic. The nano-mechanical properties of the mastic for all WMAs manufactured at 20°C lower than the control mix were reduced as compared to the control mix. However, after taking the effect of production temperature into account, the properties of the mastic for all WMAs significantly increased and so the effect of warm additives on the mastic phase was highlighted. In the case of WMAs produced at 125°C using 100/150 binder grade, Sasobit more than doubled the modulus of the ITZ and mastic while Redist WMX and LQ only improved the modulus and hardness of the ITZ, but they raised the elastic modulus and hardness of the mastic to the same levels as the control mix.

Sasobit, Rediset WMX and Rediset LQ have considerable effects on improving the work of fracture. The study revealed that the work of fracture increased by 170, 100 and 143% respectively for the aggregate-binder system produced using a 40/60 binder grade, and 70, 25 and 50% respectively for the aggregate-binder system produced using a 100/150 binder grade. The study also revealed that the contribution of warm additives in improving the work of fracture was qualitatively associated with their effect on the adhesion force determined using AFM-PFQNM. The study also revealed that the contribution of warm additives in improving the work of fracture was qualitatively associated with work of indentation measured using nanoindentation. Nanoindentation therefore has the potential to evaluate the interaction and the adhesive bond strength between aggregate and binder/mastic in the mixture.

The study also revealed that the production temperature has a great influence on the fatigue life of WMA. Stating the finding in another way, in order to achieve the desired fatigue performance of WMA, there needs to be a difference between the reduction in production temperature for hard and soft binders. This suggestion is made because this study revealed that the performance trend for warm additives on asphalt mixtures produced with 40/60 binder grade

and 100/150 binder grade was the same if the production temperature of WMA was limited to a certain degree (10°C for 40/60 grade and 20°C for 100/150 grade) lower than that of the control HMAs. Furthermore, it was highlighted that the mechanical properties of mastic and ITZ play a significant role in the fatigue-cracking behaviour of asphalt mixture. Improving their mechanical properties significantly contributes to extending the asphalt mixture's fatigue life. These improvements delay the formation and separation of micro-cracks within the matrix; therefore, the material exhibits more resistance to applied repeated loads. Generally, Rediset WMX increased the fatigue life of the asphalt mixtures by approximately 32% while Rediset LQ doubled it. Sasobit also increased the fatigue life, by approximately 90%.

The nano-mechanical approach is a novel approach to evaluate the level of blending between RAP and virgin materials. The study found that complete blending between RAP and virgin materials can be reached and proved based on the mechanical properties of ITZ RAP, ITZ virgin and mastic. Once the ITZ RAP disappears, complete blending can be confirmed. Moreover, it was highlighted that the mixture's performance relates directly to the level of blending between RAP and virgin. Once complete blending was reached, WSSaP155 exhibited the same performance as the control mix HH155 in terms of stiffness and fatigue life.

10.2 Recommendations for future works

- Rediset LQ is a relatively new additive and has not been investigated in detail before. In the present thesis, it was revealed that using higher than the recommended dosages of Rediset LQ is appropriate without having a negative impact on binder properties. It is therefore recommended that the effect of higher dosages of Rediset LQ on the mechanical properties of mixture phases and the overall mixture performance should be studied. In line with this, a cost-effective analysis regarding the use of higher dosages is also required before widespread adoption of this additive can be considered.

- The effect of moisture damage in line with the effect of production temperatures on the performance of WMA was beyond the scope of the

thesis. It is recommended that a study is performed that considers the effect of exposure to moisture.

- Nano-mechanical properties of mixture phases have been shown to reflect the real overall performance of asphalt mixtures. It is highly recommended that those mechanical properties are considered with other design parameters to estimate the real performance of asphalt mixtures.

- Fatigue, rutting, healing models, etc., can be re-examined including the mechanical properties of ITZ and mastic in line with monitoring the field performance.

- WMA showed very good fatigue-cracking results in lab-scale tests. It is recommended to use the current conclusions for WMA-fatigue cracking to perform the research in the field, and core samples annually after construction to confirm lab results and monitor the fatigue performance of WMA.

References

Abd, D. & Al-Khalid, H., 2015. Fatigue performance characterization of warm-modified bituminous binders. *Bituminous Mixtures and Pavements VI*, 105.

Abd, D.M., 2011. *Pavement evaluation with particular reference to deflection testing with a falling weight deflectometer*: University of Leeds, Institute for Transport Studies.

Ahmed, T.M., 2016. Fatigue performance of hot mix asphalt tested in controlled stress mode using dynamic shear rheometer. *International Journal of Pavement Engineering*, 1-11.

Ahmed, T.M. & Khalid, H.A., 2015. A new approach in fatigue testing and evaluation of hot mix asphalt using a dynamic shear rheometer. *Bituminous Mixtures and Pavements VI*, 351.

Airey, G.D., 2002. Use of black diagrams to identify inconsistencies in rheological data. *Road Materials and Pavement Design*, 3 (4), 403-424.

Airey, G.D., Rahimzadeh, B. & Collop, A.C., 2003. Viscoelastic linearity limits for bituminous materials. *Materials and Structures*, 36 (10), 643-647.

Akzonobel, 2011. *Https://www.Akzonobel.Com/innovation/our_innovations/more_innovations/rediset* [online]. [Access Date 2014].

Al-Haddad, A. & Al-Khalid, H., 2015. Development of a new aggregate-binder adhesion test method. *Bituminous Mixtures and Pavements VI*, 385.

Al-Khateeb, G. & Shenoy, A., 2004. A distinctive fatigue failure criterion. *Journal of the association of asphalt paving technologists*, 73, 585-622.

Al-Qadi, I.L., Elseifi, Mostafa and Carpenter, Samuel H, 2007. Reclaimed asphalt pavement–a literature review.

Alavi, M., Hajj, E., Hanz, A. & Bahia, H., 2012. Evaluating adhesion properties and moisture damage susceptibility of warm-mix asphalts: Bitumen bond strength and dynamic modulus ratio tests. *Transportation Research Record: Journal of the Transportation Research Board*, (2295), 44-53.

Allen, D.H. & Searcy, C.R., 2001. A micromechanical model for a viscoelastic cohesive zone. *International Journal of Fracture*, 107 (2), 159-176.

Allen, R.G., Little, D.N. & Bhasin, A., 2012. Structural characterization of micromechanical properties in asphalt using atomic force microscopy. *Journal of Materials in Civil Engineering*, 24 (10), 1317-1327.

Anderson, D.A., Christensen, D.W., Bahia, H.U., Dongre, R., Sharma, M., Antle, C.E. & Button, J., 1994. Binder characterization and evaluation, volume 3: Physical characterization. *Strategic Highway Research Program, National Research Council, Washington, DC*.

Apeagyei, A.K., Grenfell, J.R. & Airey, G.D., 2014. Moisture-induced strength degradation of aggregate–asphalt mastic bonds. *Road Materials and Pavement Design*, 15 (sup1), 239-262.

Arabani, M., Roshani, H. & Hamedi, G.H., 2011. Estimating moisture sensitivity of warm mix asphalt modified with zycosoil as an antistrip agent using surface free energy method. *Journal of Materials in Civil Engineering*, 24 (7), 889-897.

Arega, Z., Bhasin, A., Motamed, A. & Turner, F., 2011. Influence of warm-mix additives and reduced aging on the rheology of asphalt binders with

different natural wax contents. *Journal of Materials in Civil Engineering,* 23 (10), 1453-1459.

Artamendi, I., 2003. *A fundamental study into wet process modification of paving binders and mixtures by crumb rubber from used tyres.* PhD Thesis. University of Liverpool

Artamendi, I. & Khalid, H., 2005. Characterization of fatigue damage for paving asphaltic materials*. *Fatigue & fracture of engineering materials & structures,* 28 (12), 1113-1118.

Association, N.a.P., 2009. *Black and green: Sustainable asphalt, now and tomorrow*: National Asphalt Pavement Association.

Banerjee, A., De Fortier Smit, A. & Prozzi, J.A., 2012. The effect of long-term aging on the rheology of warm mix asphalt binders. *Fuel,* 97, 603-611.

Barbati, S., Virgili, A., Pannunzio, V. & Cardone, F., 2009. An evaluation of use of synthetic waxes in warm mix asphalt. *Advanced testing and characterization of bituminous materials, two volume set.* CRC Press.

Barthel, W., Marchand, J. & Von Devivere, M., Year. Warm asphalt mixes by adding a synthetic zeoliteed.^eds. *PROCEEDINGS OF THE 3RD EURASPHALT AND EUROBITUME CONGRESS HELD VIENNA, MAY 2004*.

Bennert, T., Maher, A. & Sauber, R., 2011. Influence of production temperature and aggregate moisture content on the initial performance of warm-mix asphalt. *Transportation Research Record: Journal of the Transportation Research Board,* 2208 (1), 97-107.

Bennert, T., Reinke, G., Mogawer, W. & Mooney, K., 2010. Assessment of workability and compactability of warm-mix asphalt. *Transportation Research Record: Journal of the Transportation Research Board,* 2180 (1), 36-47.

Binnig, G., Quate, C.F. & Gerber, C., 1986. Atomic force microscope. *Physical review letters,* 56 (9), 930.

Binnig, G., Rohrer, H., Gerber, C. & Weibel, E., 1982. Tunneling through a controllable vacuum gap. *Applied Physics Letters,* 40 (2), 178-180.

Bonaquist, R., 2008. Advanced asphalt technologies, llc,(2008).“Mix design practices for warm mix,” interim report nchrp 9-43, national cooperative highway research program. *Transportation Research Board*.

Bonaquist, R.F., 2011. *Mix design practices for warm mix asphalt*: Transportation Research Board.

Bonnaure, F., Gravois, A. & Udron, J., 1980. A new method for predicting the fatigue life of bituminous mixesed.^eds. *Association of Asphalt Paving Technologists Proceedings*.

Bowers, B.F., Moore, J., Huang, B. & Shu, X., 2014. Blending efficiency of reclaimed asphalt pavement: An approach utilizing rheological properties and molecular weight distributions. *Fuel,* 135, 63-68.

Branco, C. & Franco, V.T., 2008. *A unified method for the analysis of nonlinear viscoelasticity and fatigue cracking of asphalt mixtures using the dynamic mechanical analyzer*.

Bs 597-1, 2005. Hot rolled asphalt for roads and other paved areas, in specification for constituent materials and asphalt mixtures. British Standard Institution.

Bs En 1426, 2007. Bitumen and bituminous binders. Determination of needle penetration. British Standards.

Bs En 1427, 2007. Bitumen and bituminous binders. Determination of the softening point. Ring and ball British Standards.

Bs En 12697-6, 2012. Bituminous mixtures-tast methods for hot mix asphalt: Determination of bulk density of bituminous specimens. British Standard Institution.

Bs En 12697-24, 2012. Bituminous mixtures- tests methods for hot mix asphalt: Resistance to fatigue *Resistance to fatigue* British Standard.

Bs En 12697-26, 2012. *Bituminous mixtures-Tests methods for hot mix asphalt. Part 26: Stiffness.* British Standard

Bs En 12697-33, 2003. Specimen prepared by roller compactor, in bituminous mixtures-test methods for hot mix asphalt British Standard Instituation.

Bs En 13302, 2010. Determination of dynamic viscosity of bituminous binder using a rotating spindle apparatus. *Bitumen and bituminous binders.* BRITISH STANDARD INSTITUTION.

Bs En 14770, 2012. Determination of complex shear modulus and phase angle-dynamic shear rheometer (dsr). *Bitumen and bituminpus binders.* British Standaed Institution.

Buddhala, A., Hossain, Z., Wasiuddin, N.M., Zaman, M. & O'rear, E.A., 2012. Effects of an amine anti-stripping agent on moisture susceptibility of sasobit and aspha-min mixes by surface free energy analysis. *Journal of Testing and Evaluation,* 40 (1), 91-99.

Bueche, N., 2009. Warm asphalt bituminous mixtures with regards to energy, emissions and performance. *Young Researchers Seminer (YRS), Torino*.

Button, J.W., Estakhri, C. & Wimsatt, A., 2007. *A synthesis of warm mix asphalt*.

Butz, T., Rahimian, I. & Hildebrand, G., 2001. Modification of road bitumens with the fischer-tropsch paraffin sasobit (r). *Journal of Applied Asphalt Binder Technology,* 1 (2).

Capitão, S., Picado-Santos, L. & Martinho, F., 2012. Pavement engineering materials: Review on the use of warm-mix asphalt. *Construction and Building Materials,* 36, 1016-1024.

Caro, S., Masad, E., Bhasin, A. & Little, D.N., 2008. Moisture susceptibility of asphalt mixtures, part 1: Mechanisms. *International Journal of Pavement Engineering,* 9 (2), 81-98.

Chang, K.-N.G. & Meegoda, J.N., 1997. Micromechanical simulation of hot mix asphalt. *Journal of engineering mechanics,* 123 (5), 495-503.

Cheng, J., Shen, J. & Xiao, F., 2011. Moisture susceptibility of warm-mix asphalt mixtures containing nanosized hydrated lime. *Journal of Materials in Civil Engineering,* 23 (11), 1552-1559.

Chowdhury, A. & Button, J.W., 2008. *A review of warm mix asphalt*.

Chudoba, T. & Richter, F., 2001. Investigation of creep behaviour under load during indentation experiments and its influence on hardness and modulus results. *Surface and Coatings Technology,* 148 (2), 191-198.

Cocurullo, A., Airey, G., Collop, A. & Sangiorgi, C., 2008. Indirect tensile versus two-point bending fatigue testing. *Proceedings of the ICE-Transport,* 161 (4), 207-220.

Copeland, A.R., 2007. *Influence of moisture on bond strength of asphalt-aggregate systems*. Vanderbilt University.

Corrigan, M., 2005. Warm mix asphalt technologyed.^eds. *Presentation to the AASHTO Standing Committee on Highways Technical Meeting, Nashville, TN*.

D'angelo, J.A., Harm, E.E., Bartoszek, J.C., Baumgardner, G.L., Corrigan, M.R., Cowsert, J.E., Harman, T.P., Jamshidi, M., Jones, H.W. & Newcomb, D.E., 2008. *Warm-mix asphalt: European practice*.

Das, P.K., Kringos, N. & Birgisson, B., 2014. Microscale investigation of thin film surface ageing of bitumen. *Journal of microscopy,* 254 (2), 95-107.

Das, P.K., Kringos, N., Wallqvist, V. & Birgisson, B., 2013. Micromechanical investigation of phase separation in bitumen by combining atomic force microscopy with differential scanning calorimetry results. *Road Materials and Pavement Design,* 14 (sup1), 25-37.

Deacon, J., Harvey, J., Tayebali, A. & Monismith, C., 1997. Influence of binder loss modulus on the fatigue performance of asphalt concrete pavements. *Journal of the Association of Asphalt Paving Technologists,* 66, 633-668.

Derjaguin, B.V., Muller, V.M. & Toporov, Y.P., 1975. Effect of contact deformations on the adhesion of particles. *Journal of Colloid and interface science,* 53 (2), 314-326.

Desai, C.S., 2007. Unified dsc constitutive model for pavement materials with numerical implementation. *International Journal of Geomechanics,* 7 (2), 83-101.

Di Benedetto, H., Ashayer Soltani, A. & Chaverot, P., 1996. Fatigue damage for bituminous mixtures: A pertinent approach. *Journal of the Association of Asphalt Paving Technologists,* 65.

Di Benedetto, H., De La Roche, C., Baaj, H., Pronk, A. & Lundström, R., 2004. Fatigue of bituminous mixtures. *Materials and Structures,* 37 (3), 202-216.

Dourado, E., Simao, R. & Leite, L., 2012. Mechanical properties of asphalt binders evaluated by atomic force microscopy. *Journal of microscopy,* 245 (2), 119-128.

Doyle, J.D., Mejias-Santiago, M., Brown, E. & Howard, I.L., 2011. Performance of high rap-wma surface mixtures. *Journal of the Association of Asphalt Paving Technologists,* 80.

Doyle, J.D., Mejías-Santiago, M. & Rushing, J.F., 2013. Binder and mixture testing to assess rutting performance of warm mix asphalt (wma). *Green streets, highways, and development 2013: Advancing the practice.* ASCE Publications, 68-77.

Dunning, R. & Mendenhall, R., 1978. Design of recycled asphalt pavements and selection of modifiers. *Recycling of Bituminous Pavements, ASTM STP,* 662, 35-46.

Eddhahak-Ouni, A., Dony, A., Colin, J., Mendez, S., Navaro, J., Drouadaine, I. & Bruneau, D., 2012. Experimental investigation of the homogeneity of the blended binder of a high rate recycled asphalt. *Road Materials and Pavement Design,* 13 (3), 566-575.

Edwards, Y. & Isacsson, U., 2002. Wax in bitumen. *Evaluation,* 3 (1).

Edwards, Y. & Redelius, P., 2003. Rheological effects of waxes in bitumen. *Energy & Fuels,* 17 (3), 511-520.

Edwards, Y., Tasdemir, Y. & Isacsson, U., 2006. Effects of commercial waxes on asphalt concrete mixtures performance at low and medium temperatures. *Cold regions science and technology,* 45 (1), 31-41.

El Sharkawy, S.A., Wahdan, A.H. & Galal, S.A., 2016. Utilisation of warm-mix asphalt technology to improve bituminous mixtures containing reclaimed asphalt pavement. *Road Materials and Pavement Design,* 1-30.

Equipment, C. & Lounge, M., 2010. The use of warm mix asphalt.

Estakhri, C., Button, J. & Alvarez, A.E., 2010. *Field and laboratory investigation of warm mix asphalt in texas*.

Fischer, H., Stadler, H. & Erina, N., 2013. Quantitative temperature-depending mapping of mechanical properties of bitumen at the nanoscale using the afm operated with peakforce tappingtm mode. *Journal of microscopy*, 250 (3), 210-217.

Gandhi, T., 2008a. *Effects of warm asphalt additives on asphalt binder and mixture properties*. Clemson University.

Gandhi, T., 2008b. *Effects of warm asphalt additives on asphalt binder and mixture properties*. PhD Dissertation. Clemson University.

Gandhi, T., Rogers, W. & Amirkhanian, S., 2010. Laboratory evaluation of warm mix asphalt ageing characteristics. *International Journal of Pavement Engineering*, 11 (2), 133-142.

Gaudefroy, V., Olard, F., Cazacliu, B., De La Roche, C., Beduneau, E. & Antoine, J.P., 2007. Laboratory investigations of mechanical performance of foamed bitumen mixes that use half-warm aggregates. *Transportation Research Record: Journal of the Transportation Research Board*, 1998 (1), 89-95.

Ghabchi, R., Singh, D. & Zaman, M., 2015. Laboratory evaluation of stiffness, low-temperature cracking, rutting, moisture damage, and fatigue performance of wma mixes. *Road Materials and Pavement Design*, 16 (2), 334-357.

Ghabchi, R., Singh, D., Zaman, M. & Tian, Q., 2013. A laboratory study of warm mix asphalt for moisture damage potential using surface free energy method. *Airfield and highway pavement 2013*. American Society of Civil Engineers, 54-63.

Ghuzlan, K.A. & Carpenter, S.H., 2006. Fatigue damage analysis in asphalt concrete mixtures using the dissipated energy approach. *Canadian Journal of Civil Engineering*, 33 (7), 890-901.

Goh, S.W. & You, Z., 2009. Warm mix asphalt using sasobit in cold regioned.^eds. *Proceedings of the 14th Conference on Cold Regions Engineering*, 29-29.

Goh, S.W. & You, Z., 2011a. Evaluation of warm mix asphalt produced at various temperatures through dynamic modulus testing and four point beam fatigue testing. *Pavements and Materials: Recent Advances in Design, Testing and Construction ASCE*, 123-130.

Goh, S.W. & You, Z., 2011b. Evaluation of warm mix asphalt produced at various tempertures through dynamic modulus testing and four beam fatigue testing. *Pavements and Materials: Recent Advances in Design, Testing and Construction ASCE*, 212, 123-130.

Goh, S.W., You, Z. & Van Dam, T.J., 2007. Laboratory evaluation and pavement design for warm mix asphalted.^eds. *Proceedings of the 2007 Mid-Continent transportation research symposium*, 1-11.

Gong, W., Tao, M., Mallick, R.B. & El-Korchi, T., 2012. Investigation of moisture susceptibility of warm-mix asphalt mixes through laboratory mechanical testing. *Transportation Research Record: Journal of the Transportation Research Board*, 2295 (1), 27-34.

Greyling, A.H., 2012. *Development of a standard test method for determining the bitumen bond strength of emulsions-a south african perspective*. Stellenbosch University.

Haggag, M.M., Mogawer, W.S. & Bonaquist, R., 2011. Fatigue evaluation of warm-mix asphalt mixtures. *Transportation Research Record: Journal of the Transportation Research Board,* 2208 (1), 26-32.

Hamzah, M.O., Golchin, B., Jamshidi, A. & Chailleux, E., 2015. Evaluation of rediset for use in warm-mix asphalt: A review of the literatures. *International Journal of Pavement Engineering,* 16 (9), 809-831.

Hamzah, M.O., Golchin, B. & Tye, C.T., 2013. Determination of the optimum binder content of warm mix asphalt incorporating rediset using response surface method. *Construction and Building Materials,* 47, 1328-1336.

Hamzah, M.O., Jamshidi, A., Shahadan, Z., Hasan, M.R.M., Yahaya, A.S., Hamzah, M.O., Jamshidi, A., Shahadan, Z., Mohd Hasan, M.R. & Yahaya, A.S., 2010. Evaluation of engineering properties and economic advantages of wma using local materials. *Journal of applied sciences,* 10 (20), 2433.

Hanson, 2016. *Sustainability summary report. Avaliable on line: Http://www.Hanson-sustainability.Co.Uk/sites/default/files/assets/document/hanson-sustainability-report-2016.Pdf*. [Accssed date 26-08-2016].

Hanz, A., Mahmoud, E. & Bahia, H., 2011. Impacts of wma production temperatures on binder aging and mixture flow number. *Journal of the Association of Asphalt Paving Technologists,* 80.

Harvey, J. & Cebon, D., 2005. Fracture tests on bitumen films. *Journal of materials in civil engineering,* 17 (1), 99-106.

Hearon, A. & Diefenderfer, S., Year. Laboratory evaluation of warm asphalt properties and performanceed.^eds. *Proceedings of the 2008 Conference on Airfield and Highway Pavements, Oct*, 15-18.

Hicks, R., Finn, F., Monismith, C. & Leahy, R., 1993. Validation of shrp binder specification through mix testing (with discussion). *Journal of the Association of Asphalt Paving Technologists,* 62.

Hicks, R.G., 1991. *Moisture damage in asphalt concrete*: Transportation Research Board.

Hill, B., 2011. *Performance evaluation of warm mix asphalt mixtures incorporating reclaimed asphalt pavement*. University of Illinois at Urbana-Champaign.

Hill, B., Behnia, B., Buttlar, W.G. & Reis, H., 2012a. Evaluation of warm mix asphalt mixtures containing reclaimed asphalt pavement through mechanical performance tests and an acoustic emission approach. *Journal of Materials in Civil Engineering,* 25 (12), 1887-1897.

Hill, B., Behnia, B., Hakimzadeh, S., Buttlar, W.G. & Reis, H., 2012b. Evaluation of low-temperature cracking performance of warm-mix asphalt mixtures. *Transportation Research Record: Journal of the Transportation Research Board,* 2294 (1), 81-88.

Hintz, C., Velasquez, R., Johnson, C. & Bahia, H., 2011. Modification and validation of linear amplitude sweep test for binder fatigue specification. *Transportation Research Record: Journal of the Transportation Research Board,* 2207 (1), 99-106.

Hopman, P., Kunst, P. & Pronk, A., Year. A renewed interpretation method for fatigue measurements, verification of miner's ruleed.^eds. *4th Eurobitume Symposium in Madrid*, 5576561.

Hossain, M.I., Faisal, H.M. & Tarefder, R.A., 2016. Determining effects of moisture in mastic materials using nanoindentation. *Materials and Structures*, 49 (3), 1079-1092.

Houeran, G. & Maccarrone, S., 1994. Cold asphalt systems as an alternative to hot mix.

Howson, J., Masad, E., Little, D. & Kassem, E., 2012. Relationship between bond energy and total work of fracture for asphalt binder-aggregate systems. *Road Materials and Pavement Design*, 13 (sup1), 281-303.

Howson, J.E., 2011. *Relationship between surface free energy and total work of fracture of asphalt binder and asphalt binder-aggregate interfaces*. Texas A&M University.

Huang, B., Kingery, W. & Zhang, Z., Year. Laboratory study of fatigue characteristics of hma mixtures containing raped.^eds. *International Symposium on Design and Construction of Long Lasting Asphalt Pavements, 2004, Auburn, Alabama, USA*.

Huang, B., Li, G., Vukosavljevic, D., Shu, X. & Egan, B.K., 2005. Laboratory investigation of mixing hot-mix asphalt with reclaimed asphalt pavement. *Transportation research record: journal of the transportation research board*, 1929 (1), 37-45.

Huang, B., Zhang, Z. & Kinger, W., Year. Fatigue crack characteristics of hma mixtures containing raped.^eds. *Proceedings of the 5th international RILEM conference on reflective cracking in pavements*, 631-638.

Huang, Y., Bird, R.N. & Heidrich, O., 2007. A review of the use of recycled solid waste materials in asphalt pavements. *Resources, Conservation and Recycling*, 52 (1), 58-73.

Hurley, G.C. & Prowell, B.D., 2005a. Evaluation of aspha-min zeolite for use in warm mix asphalt. *NCAT report*, 05-04.

Hurley, G.C. & Prowell, B.D., 2005b. Evaluation of sasobit for use in warm mix asphalt. *NCAT report*, 05-06.

Hurley, G.C. & Prowell, B.D., 2006a. Evaluation of evotherm for use in warm mix asphalt. *NCAT report*, 2, 15-35.

Hurley, G.C. & Prowell, B.D., 2006b. Evaluation of evotherm® for use in warm mix asphalt. *NCAT report*, 2, 15-35.

Igarashi, S., Bentur, A. & Mindess, S., 1996. Microhardness testing of cementitious materials. *Advanced Cement Based Materials*, 4 (2), 48-57.

Jäger, A., Lackner, R., Eisenmenger-Sittner, C. & Blab, R., 2004. Identification of four material phases in bitumen by atomic force microscopy. *Road Materials and Pavement Design*, 5 (sup1), 9-24.

Jamshidi, A., Hamzah, M.O. & You, Z., 2013. Performance of warm mix asphalt containing sasobit®: State-of-the-art. *Construction and Building Materials*, 38, 530-553.

Jenkins, K., De Groot, J., Van De Ven, M. & Molenaar, A., 1999. Half-warm foamed bitumen treatment, a new processed.^eds. *7th Conference on asphalt pavements for Southern Africa (CAPSA 99)*.

Ji, J. & Xu, S., 2010. Study on the impact of sasobit on asphalt's properties and micro-structureed.^eds. *Proceedings of the Pavements and Materials: Characterization and Modeling Symposium*.

Johnson, K.L. & Johnson, K.L., 1987. *Contact mechanics*: Cambridge university press.

Jones, D., Tsai, B.-W. & Signore, J., 2010. Warm-mix asphalt study: Laboratory test results for akzonobel redisettm wmx. *University of California Pavement Research Center (UCPRC).*

Jones, W., 2004. Warm mix asphalt-a state-of-the-art review. *Australian Asphalt Pavement Association Advisory Note,* 17.

Kanitpong, K. & Bahia, H., 2005. Relating adhesion and cohesion of asphalts to the effect of moisture on laboratory performance of asphalt mixtures. *Transportation Research Record: Journal of the Transportation Research Board,* (1901), 33-43.

Kanitpong, K. & Bahia, H.U., Year. Role of adhesion and thin film tackiness of asphalt binders in moisture damage of hmaed.^eds. *Association of Asphalt Paving Technologists Technical Sessions, 2003, Lexington, Kentucky, USA*.

Karlsson, R. & Isacsson, U., 2006. Material-related aspects of asphalt recycling—state-of-the-art. *Journal of materials in civil engineering,* 18 (1), 81-92.

Kheradmand, B., Muniandy, R., Hua, L.T., Yunus, R.B. & Solouki, A., 2014. An overview of the emerging warm mix asphalt technology. *International Journal of Pavement Engineering,* 15 (1), 79-94.

Khodaii, A., Kazemi Tehrani, H. & Haghshenas, H., 2012. Hydrated lime effect on moisture susceptibility of warm mix asphalt. *Construction and Building Materials,* 36, 165-170.

Khorasani, S., Masad, E., Kassem, E. & Abu Al-Rub, R., 2013. Nano-mechanical characterization of mastic, aggregate, and interfacial zone in asphalt composites. *JOURNAL OF TESTING AND EVALUATION,* 41 (6), 924-932.

Kiggundu, B.M. & Roberts, F.L., 1988. *Stripping in hma mixtures: State-of-the-art and critical review of test methods*.

Kim, H., Lee, S.-J. & Amirkhanian, S.N., 2011a. Impact of warm mix additives on rheological properties of polymer modified asphalt binders. *Canadian Journal of Civil Engineering,* 38 (12), 1414-1426.

Kim, H., Lee, S.-J. & Amirkhanian, S.N., 2011b. Rheology of warm mix asphalt binders with aged binders. *Construction and Building Materials,* 25 (1), 183-189.

Kim, H., Lee, S.-J., Amirkhanian, S.N., Kim, H., Lee, S.-J. & Amirkhanian, S.N., 2012. Influence of warm mix additives on pma mixture properties. *Journal of Transportation Engineering,* 138 (8), 991.

Kim, K.W. & Amirkhanian, S., 1991. Evaluation of effectiveness of antistrip additives using fuzzy set procedures. *Transportation Research Record,* (1323).

Kim, Y.-R., Little, D.N., Lytton, R.L., Kim, Y.-R., Little, D.N., Lytton, R.L., Kim, Y.-R., Little, D.N. & Lytton, R.L., 2003. Fatigue and healing characterization of asphalt mixtures. *Journal of Materials in Civil Engineering,* 15 (1), 75.

Koenders, B., Stoker, D., Bowen, C., De Groot, P., Larsen, O., Hardy, D. & Wilms, K., 2000. Innovative process in asphalt production and application to obtain lower operating temperaturesed.^eds. *2nd Eurasphalt & Eurobitumen Congress, Barcelona, Spain*.

Koenders, B., Stoker, D., Robertus, C., Larsen, O. & Johansen, J., 2002. Wam-foam, asphalt production at lower operating temperaturesed.^eds. *Ninth International Conference on Asphalt Pavements*.

Kringos, N., Scarpas, A. & De Bondt, A., 2008. Determination of moisture susceptibility of mastic-stone bond strength and comparison to thermodynamical properties. *Journal of the Association of Asphalt Paving Technologists*, 77.

Kristjansdottir, O., 2006. *Warm mix asphalt for cold weather paving*. Citeseer.

Kristjánsdóttir, Ó., Year. Warm mix asphalt technology adoptioned.^eds. *NVF 33 Annual Meeting*.

Kristjánsdóttir, Ó., Muench, S., Michael, L. & Burke, G., 2007. Assessing potential for warm-mix asphalt technology adoption. *Transportation Research Record: Journal of the Transportation Research Board*, (2040), 91-99.

Kriz, P., Grant, D.L., Veloza, B.A., Gale, M.J., Blahey, A.G., Brownie, J.H., Shirts, R.D. & Maccarrone, S., 2014. Blending and diffusion of reclaimed asphalt pavement and virgin asphalt binders. *Road Materials and Pavement Design*, 15 (sup1), 78-112.

Kutay, M., Gibson, N. & Youtcheff, J., 2008a. *Use of pseudostress and pseudostrain concepts for characterization of asphalt fatigue tests*: CRC Press.

Kutay, M.E., Gibson, N. & Youtcheff, J., 2008b. Conventional and viscoelastic continuum damage (vecd)-based fatigue analysis of polymer modified asphalt pavements (with discussion). *Journal of the Association of Asphalt Paving Technologists*, 77.

Kutay, M.E., Gibson, N., Youtcheff, J. & Dongré, R., 2009. Use of small samples to predict fatigue lives of field cores. *Transportation Research Record: Journal of the Transportation Research Board*, 2127 (1), 90-97.

Larsen, O., Moen, Ø., Robertus, C. & Koenders, B., Year. Wam foam asphalt production at lower operating temperatures as an environmental friendly alternative to hmaed.^eds. *3rd Eurasphalt & Eurobitume Congress, Vienna*.

Lea-Co, C., *Low emission & low energy asphalts for sustainable road construction: The european experience of lea process* [online]. [Accessed Access Date 2014].

Lee, H.-J. & Kim, Y.R., 1998. Viscoelastic constitutive model for asphalt concrete under cyclic loading. *Journal of Engineering Mechanics*, 124 (1), 32-40.

Lee, J.C., Edil, T.B., Tinjum, J.M. & Benson, C.H., 2010. Quantitative assessment of environmental and economic benefits of recycled materials in highway construction. *Transportation Research Record: Journal of the Transportation Research Board*, 2158 (1), 138-142.

Lee, S.-J., Amirkhanian, S.N., Park, N.-W. & Kim, K.W., 2009. Characterization of warm mix asphalt binders containing artificially long-term aged binders. *Construction and Building Materials*, 23 (6), 2371-2379.

Li, G., Li, Y., Metcalf, J. & Pang, S.-S., 1999. Elastic modulus prediction of asphalt concrete. *Journal of Materials in Civil Engineering*, 11 (3), 236-241.

Little, D., Button, J. & Epps, J., 1983. Structural properties of laboratory mixtures containing foamed asphalt and marginal aggregates. *Transportation Research Record*, (911).

Little, D.N., Epps, J.A. & Sebaaly, P., 2001. The benefits of hydrated lime in hot mix asphalt. *National Lime Association*.

Little, D.N. & Jones, D., 2003. Chemical and mechanical processes of moisture damage in hot-mix asphalt pavementsed.^eds. *Transportation Research Board National Seminar, San Diego, CA, USA*, 37-70.

Liu, J., Li, P., Liu, J., Li, P., Liu, J. & Li, P., 2012. Low temperature performance of sasobit-modified warm-mix asphalt. *Journal of Materials in Civil Engineering*, 24 (1), 57.

Loeber, L., Muller, G., Morel, J. & Sutton, O., 1998. Bitumen in colloid science: A chemical, structural and rheological approach. *Fuel*, 77 (13), 1443-1450.

Loeber, L., Sutton, O., Morel, J., Valleton, J.M. & Muller, G., 1996. New direct observations of asphalts and asphalt binders by scanning electron microscopy and atomic force microscopy. *Journal of Microscopy*, 182 (1), 32-39.

Logaraj, S. & Almeida, A., 2009. Surface-active bitumen additive for warm mix asphalt with adhesion promoting properties. *Akzo Nobel Surface Chemistry LLC*.

Lorenz, D., Zeckzer, A., Hilpert, U., Grau, P., Johansen, H. & Leipner, H., 2003. Pop-in effect as homogeneous nucleation of dislocations during nanoindentation. *Physical review B*, 67 (17), 172101.

Losa, M., Bacci, R., Leandri, P. & Collop, A., Year. Experimental characterization of high performance wam-foam trial sectionsed.^eds. *Sixth International Conference on Maintenance and Rehabilitation of Pavements and Technological Control (MAIREPAV6)*.

Luo, X., Luo, R. & L. Lytton, R., 2012. Characterization of fatigue damage in asphalt mixtures using pseudostrain energy. *Journal of Materials in Civil Engineering*, 25 (2), 208-218.

Lyne, Å.L., Wallqvist, V. & Birgisson, B., 2013a. Adhesive surface characteristics of bitumen binders investigated by atomic force microscopy. *Fuel*, 113, 248-256.

Lyne, Å.L., Wallqvist, V., Rutland, M.W., Claesson, P. & Birgisson, B., 2013b. Surface wrinkling: The phenomenon causing bees in bitumen. *Journal of Materials Science*, 48 (20), 6970-6976.

Lytton, R., 2004. Adhesive fracture in asphalt concrete mixtures. *Course Notes*.

Maggiore, C., Di Mino, G., Marsac, P., Di Liberto, M., Collop, A. & Airey, G., 2012. Fatigue resistance: Is it possible having a unique response? *Four Point Bending*, 239.

Mallick, R., Kandhal, P. & Bradbury, R., 2008. Using warm-mix asphalt technology to incorporate high percentage of reclaimed asphalt pavement material in asphalt mixtures. *Transportation Research Record: Journal of the Transportation Research Board*, (2051), 71-79.

Malvern, 2014. *Http://www.Malvern.Com/en/products/product-range/kinexus-range/default.Aspx* [online]. Malvern Instrument Company Available from: [Access Date 2014]

Mamlouk, M., Souliman, M. & Zeiada, W., 2012. Optimum testing conditions to measure hma fatigue and healing using flexural bending tested.^eds. *TRB Annual Meeting 2012*.

Mann, A.B., 2004. Nanomechanical properties of solid surfaces and thin films. Springer handbook of nanotechnology. Springer, 687-716.

Manual, S.P.D. & Pavements, A., 1978. Overlays for road traffic. *Shell International Petroleum, London, UK*.

Masad, E., Castelo Branco, V., Little, D.N. & Lytton, R., 2008a. A unified method for the analysis of controlled-strain and controlled-stress fatigue testing. *International Journal of Pavement Engineering,* 9 (4), 233-246.

Masad, E., Huang, C.-W., Airey, G. & Muliana, A., 2008b. Nonlinear viscoelastic analysis of unaged and aged asphalt binders. *Construction and Building Materials,* 22 (11), 2170-2179.

Masad, E.A., Howson, J.E., Bhasin, A., Caro, S. & Little, D.N., 2010. Relationship of ideal work of fracture to practical work of fracture: Background and experimental results. *Journal of the Association of Asphalt Paving Technologists,* 79.

Masson, J.F., Leblond, V. & Margeson, J., 2006. Bitumen morphologies by phase-detection atomic force microscopy. *Journal of microscopy,* 221 (1), 17-29.

Masson, J.F., Leblond, V., Margeson, J. & Bundalo-Perc, S., 2007. Low-temperature bitumen stiffness and viscous paraffinic nano-and micro-domains by cryogenic afm and pdm. *Journal of microscopy,* 227 (3), 191-202.

Mcdaniel, R.S., Soleymani, H., Anderson, R.M., Turner, P. & Peterson, R., 2000. Recommended use of reclaimed asphalt pavement in the superpave mix design method. *NCHRP Web document,* 30.

Medani, T. & Huurman, M., 2003. Constructing the stiffness master curves for asphaltic mixes. *Delft: TU, Jan*.

Medeiros Jr, M.S., Daniel, J.S., Bolton, H.L. & Meagher, W.C., 2012. Evaluation of moisture and low-temperature cracking susceptibility of warm-mixture asphalt. *International Journal of Pavement Engineering,* 13 (5), 395-400.

Menapace, I., Masad, E., Bhasin, A. & Little, D., 2015. Microstructural properties of warm mix asphalt before and after laboratory-simulated long-term ageing. *Road Materials and Pavement Design,* 16 (sup1), 2-20.

Menapace, I., Masad, E., Little, D., Kassem, E. & Bhasin, A., 2014. Microstructural, chemical and thermal analyses of warm mix asphalt. *Sustainability, Eco-efficiency, and Conservation in Transportation Infrastructure Asset Management,* 157.

Menard, K.P., 2008. *Dynamic mechanical analysis: A practical introduction*: CRC press.

Middleton, B. & Forfylow, R.W., 2009. Evaluation of warm-mix asphalt produced with the double barrel green process. *Transportation Research Record: Journal of the Transportation Research Board,* 2126 (1), 19-26.

Miller, T., Greyling, A., Bahia, H. & Jenkins, K., 2010. Development of a test method for determining emulsion bond strength using the bitumen bond strength (bbs) test: A south african perspectiveed.^eds. *International Sprayed Sealing Conference, 2nd, 2010, Melbourne, Victotria, Australia*.

Mo, L., Li, X., Fang, X., Huurman, M. & Wu, S., 2012. Laboratory investigation of compaction characteristics and performance of warm mix asphalt containing chemical additives. *Construction and Building Materials,* 37, 239-247.

Mogawer, W., Austerman, A., Bahia, H., Mogawer, W.S., Austerman, A.J. & Bahia, H.U., 2011a. Evaluating the effect of warm-mix asphalt technologies on moisture characteristics of asphalt binders and mixtures. *Transportation Research Record Journal of the Transportation Research Board,* 2209 (-1), 52-60.

Mogawer, W.S., Austerman, A.J. & Bahia, H.U., 2011b. Evaluating the effect of warm-mix asphalt technologies on moisture characteristics of asphalt binders and mixtures. *Transportation Research Record: Journal of the Transportation Research Board,* 2209 (1), 52-60.

Mogawer, W.S., Austerman, A.J., Kassem, E. & Masad, E., 2011c. Moisture damage characteristics of warm mix asphalt mixtures. *Journal of the Association of Asphalt Paving Technologists,* 80.

Mohajeri, M., Molenaar, A. & Van De Ven, M., Year. Cracking resistance of recycled asphalt mixtures in relation to blending of ra and virgin bindered.^eds. *7th RILEM International Conference on Cracking in Pavements*Springer, 1311-1321.

Mohammad, L., Saadeh, S. & Cooper, S., 2008. Evaluation of asphalt mixtures containing sasobit warm mix additive. *Geocongress 2008.* American Society of Civil Engineers, 1016-1023.

Mohd Jakami, F., 2012. *Adhesion of asphalt mixtures*. University of Nottingham.

Mondal, P., 2008. *Nanomechanical properties of cementitious materials*: ProQuest.

Monismith, C., Epps, J. & Finn, F., Year. Improved asphalt mix design (with discussion)ed.^eds. *Association of Asphalt Paving Technologists Proc*.

Muller, V., Derjaguin, B. & Toporov, Y.P., 1983. On two methods of calculation of the force of sticking of an elastic sphere to a rigid plane. *Colloids and Surfaces,* 7 (3), 251-259.

Muthen, K., 1998. Foamed asphalt mixes-mix design procedure. *Transportation Research Record,* 898, 290-296.

Nahar, S., Mohajeri, M., Schmets, A.J., Scarpas, A., Van De Ven, M.F. & Schitter, G., 2013a. First observation of blending-zone morphology at interface of reclaimed asphalt binder and virgin bitumen. *Transportation Research Record: Journal of the Transportation Research Board,* 2370 (1), 1-9.

Nahar, S., Schmets, A., Scarpas, A. & Schitter, G., 2013b. Temperature and thermal history dependence of the microstructure in bituminous materials. *European Polymer Journal,* 49 (8), 1964-1974.

Nazzal, M.D. & Abu-Qtaish, L., 2013. *The use of atomic force microscopy to evaluate warm mix asphalt*.

Nguyen, V.H., 2009. *Effects of laboratory mixing methods and rap materials on performance of hot recycled asphalt mixtures*. University of Nottingham.

Oliver, J.W., 2001. The influence of the binder in rap on recycled asphalt properties. *Road Materials and Pavement Design,* 2 (3), 311-325.

Oliver, W.C. & Pharr, G.M., 1992. An improved technique for determining hardness and elastic modulus using load and displacement sensing indentation experiments. *Journal of materials research,* 7 (06), 1564-1583.

Park, S., Kim, Y. & Lee, H., 1999. Fracture toughness for microcracking in a viscoelastic particulate composite. *Journal of engineering mechanics,* 125 (6), 722-725.

Partl, M.N., Bahia, H.U., Canestrari, F., De La Roche, C., Di Benedetto, H., Piber, H. & Sybilski, D., 2013. Advances in interlaboratory testing and evaluation of bituminous materials.

Pauli, A., Branthaver, J., Robertson, R., Grimes, W. & Eggleston, C., 2001. Atomic force microscopy investigation of shrp asphalts: Heavy oil and resid compatibility and stability. *Preprints-American Chemical Society. Division of Petroleum Chemistry,* 46 (2), 104-110.

Perkins, S.W., 2009. *Synthesis of warm mix asphalt paving strategies for use in montana highway construction*.

Petit, C., Millien, A., Canestrari, F., Pannunzio, V. & Virgili, A., 2012. Experimental study on shear fatigue behavior and stiffness performance of warm mix asphalt by adding synthetic wax. *Construction and Building Materials,* 34, 537-544.

Pharr, G., Oliver, W. & Brotzen, F., 1992. On the generality of the relationship among contact stiffness, contact area, and elastic modulus during indentation. *Journal of materials research,* 7 (03), 613-617.

Pittenger, B., Erina, N. & Su, C., 2010. Quantitative mechanical property mapping at the nanoscale with peakforce qnm. *Application Note Veeco Instruments Inc*.

Poulikakos, L.D., Dos Santos, S., Bueno, M., Kuentzel, S., Hugener, M. & Partl, M.N., 2014. Influence of short and long term aging on chemical, microstructural and macro-mechanical properties of recycled asphalt mixtures. *Construction and Building Materials,* 51, 414-423.

Qian, G.-P., Liu, H.-F., Zheng, J.-I. & Jiang, L.-J., 2013. Experiment of tension-compression fatigue and damage for asphalt mixtures. *Journal of Highway and Transportation Research and Development (English Edition),* 7 (2), 15-21.

Qin, Q., Farrar, M.J., Pauli, A.T. & Adams, J.J., 2014. Morphology, thermal analysis and rheology of sasobit modified warm mix asphalt binders. *Fuel,* 115, 416-425.

Rad, F., Sefidmazgi, N. & Bahia, H., 2014. Application of diffusion mechanism: Degree of blending between fresh and recycled asphalt pavement binder in dynamic shear rheometer. *Transportation Research Record: Journal of the Transportation Research Board,* (2444), 71-77.

Rebelo, L., De Sousa, J., Abreu, A., Baroni, M., Alencar, A., Soares, S., Mendes Filho, J. & Soares, J., 2014a. Aging of asphaltic binders investigated with atomic force microscopy. *Fuel,* 117, 15-25.

Rebelo, L.M., De Sousa, J.S., Abreu, A.S., Baroni, M.P.M.A., Alencar, A.E.V., Soares, S.A., Mendes Filho, J., Soares, J.B., Rebelo, L.M., De Sousa, J.S., Abreu, A.S., Baroni, M.P.M.A., Alencar, A.E.V., Soares, S.A., Mendes Filho, J. & Soares, J.B., 2014b. Aging of asphaltic binders investigated with atomic force microscopy. *Fuel,* 117 (1), 15.

Roberts, F.L., Kandhal, P.S., Brown, E.R., Lee, D.-Y. & Kennedy, T.W., 1996. Hot mix asphalt materials, mixture design and construction.

Romier, A., Audeon, M., David, J., Martineau, Y. & Olard, F., 2006. Low-energy asphalt with performance of hot-mix asphalt. *Transportation Research Record: Journal of the Transportation Research Board,* 1962 (1), 101-112.

Rosen, M.J. & Kunjappu, J.T., 2012. *Surfactants and interfacial phenomena*: John Wiley & Sons.

Rowe, G., 1993. Performance of asphalt mixtures in the trapezoidal fatigue test. *Asphalt Paving Technology*, 62, 344-344.

Rowe, G.M. & Bouldin, M.G., Year. Improved techniques to evaluate the fatigue resistance of asphaltic mixturesed.^eds. *2nd Eurasphalt & Eurobitume Congress Barcelona*.

Rubio, M.C., Martínez, G., Baena, L. & Moreno, F., 2012. Warm mix asphalt: An overview. *Journal of Cleaner Production*, 24, 76-84.

Sampath, A., 2010. *Comprehensive evaluation of four warm asphalt mixtures regarding viscosity, tensile strength, moisture sensitivity, dynamic modulus and flow number*. MSc. The University of Iowa.

Sanchez-Alonso, E., Vega-Zamanillo, A., Castro-Fresno, D. & Delrio-Prat, M., 2011. Evaluation of compactability and mechanical properties of bituminous mixes with warm additives. *Construction and Building Materials*, 25 (5), 2304-2311.

Sargand, S., Nazzal, M.D., Al-Rawashdeh, A. & Powers, D., 2011. Field evaluation of warm-mix asphalt technologies. *Journal of Materials in Civil Engineering*, 24 (11), 1343-1349.

Sasolwax, 2014 *Http://www.Sasolwax.Com/en/applications/bitumen+modification/europe/sasobit+technology.Html* [online]. [Access Date 2014].

Sengoz, B. & Oylumluoglu, J., 2013. Utilization of recycled asphalt concrete with different warm mix asphalt additives prepared with different penetration grades bitumen. *Construction and Building Materials*, 45, 173-183.

Sengoz, B., Topal, A. & Gorkem, C., 2013. Evaluation of natural zeolite as warm mix asphalt additive and its comparison with other warm mix additives. *Construction and Building Materials*, 43, 242-252.

Shang, L., Wang, S., Zhang, Y. & Zhang, Y., 2011. Pyrolyzed wax from recycled cross-linked polyethylene as warm mix asphalt (wma) additive for sbs modified asphalt. *Construction and Building Materials*, 25 (2), 886-891.

Shen, J., Huang, B., Shu, X. & Tang, B., 2010. Influence of nano-sized hydrated lime (hl) on selected properties of hot-mix asphalt (hma). *Int J Pavement Res Technol*, 4 (4), 252-257.

Silva, H.M., Oliveira, J.R., Peralta, J. & Zoorob, S.E., 2010. Optimization of warm mix asphalts using different blends of binders and synthetic paraffin wax contents. *Construction and Building Materials*, 24 (9), 1621-1631.

Silva, H.M.R.D.D., Oliveira, J., Ferreira, C. & Peralta, E.J.F., 2009. Evaluation of the rheological behaviour of warm mix asphalt (wma) modified binders.

Sondag, M.S., Chadbourn, B.A. & Drescher, A., 2002. Investigation of recycled asphalt pavement (rap) mixtures.

Song, I., Little, D.N., Masad, E.A. & Lytton, R., 2005. Comprehensive evaluation of damage in asphalt mastics using x-ray ct, continuum mechanics, and micromechanics (with discussion). *Journal of the association of asphalt paving technologists*, 74.

Stangl, K., Jäger, A. & Lackner, R., 2007. The effect of styrene-butadiene-styrene modification on the characteristics and performance of bitumen. *Monatshefte für Chemie-Chemical Monthly*, 138 (4), 301-307.

Stephens, J.E., Mahoney, J. & Dippold, C., 2001. Determination of the pg binder grade to use in a rap mix. *Report No. JHR 00-278, Connecticut Department of Transportation*.

Stilwell, N. & Tabor, D., 1961. Elastic recovery of conical indentations. *Proceedings of the Physical Society,* 78 (2), 169.

Suh, Y., Mun, S. & Yeo, I., 2010. Fatigue life prediction of asphalt concrete pavement using a harmony search algorithm. *KSCE Journal of Civil Engineering,* 14 (5), 725-730.

Suzuki, E., 2002. High-resolution scanning electron microscopy of immunogold-labelled cells by the use of thin plasma coating of osmium. *Journal of Microscopy,* 208 (3), 153-157.

Syroezhko, A., Baranov, M., Ivanov, S. & Maidanova, N., 2011. Influence of natural additives and those synthesized by the fischer-tropsch method on the properties of petroleum bitumen and quality of floated asphalt. *Coke and Chemistry,* 54 (1), 26-31.

Tao, M. & Mallick, R., 2009. Effects of warm-mix asphalt additives on workability and mechanical properties of reclaimed asphalt pavement material. *Transportation Research Record: Journal of the Transportation Research Board,* (2126), 151-160.

Tarefder, R. & Faisal, H., 2013. Nanoindentation characterization of asphalt concrete aging. *Journal of Nanomechanics and Micromechanics*.

Tarefder, R.A. & Zaman, A.M., 2009. Nanoscale evaluation of moisture damage in polymer modified asphalts. *Journal of Materials in Civil Engineering,* 22 (7), 714-725.

Tarefder, R.A., Zaman, A.M. & Uddin, W., 2010. Determining hardness and elastic modulus of asphalt by nanoindentation. *International Journal of Geomechanics,* 10 (3), 106-116.

Terrel, R.L. & Al-Swailmi, S., 1994. *Water sensitivity of asphalt-aggregate mixes: Test selection*.

Thom, N., 2008. *Principles of pavement engineering*.

Timm, D.H., Willis, J.R. & Kvasnak, A., 2011. Full-scale structural evaluation of fatigue characteristics in high reclaimed asphalt pavement and warm-mix asphalt. *Transportation Research Record: Journal of the Transportation Research Board,* 2208 (1), 56-63.

Tsai, B.-W. & Monismith, C., 2005. Influence of asphalt binder properties on the fatigue performance of asphalt concrete pavements (with discussion). *Journal of the Association of Asphalt Paving Technologists,* 74.

Van Dijk, W., 1975. Practical fatigue characterization of bituminous mixes. *Journal of the Association of Asphalt Paving Technologists,* 44, 38-72.

Vargas-Nordcbeck, A. & Timm, D.H., 2012. Rutting characterization of warm mix asphalt and high rap mixtures. *Road Materials and Pavement Design,* 13 (sup1), 1-20.

Wasiuddin, N., Saha, R. & King, W., 2011a. Effects of a wax-based warm mix additive on lower compaction temperaturesed.^eds. *Geo-Frontiers 2011@ sAdvances in Geotechnical Engineering*ASCE, 4614-4623.

Wasiuddin, N., Saltibus, N. & Mohammad, L., 2011b. Effects of a wax-based warm mix additive on cohesive strengths of asphalt bindersed.^eds. *Proc., T&DI Congress 2011: Integrated Transportation and Development for a Better Tomorrow*.

Wasiuddin, N.M., Saltibus, N.E. & Mohammad, L.N., 2011c. Novel moisture-conditioning method for adhesive failure of hot-and warm-mix asphalt binders. *Transportation Research Record: Journal of the Transportation Research Board,* 2208 (1), 108-117.

Wasiuddin, N.M., Selvamohan, S., Zaman, M.M. & Guegan, M.L.T.A., 2007. Comparative laboratory study of sasobit and aspha-min additives in warm-mix asphalt. *Transportation Research Record: Journal of the Transportation Research Board*, 1998 (1), 82-88.

Wasiuddin, N.M., Zaman, M.M. & O'rear, E.A., 2008. Effect of sasobit and aspha-min on wettability and adhesion between asphalt binders and aggregates. *Transportation Research Record: Journal of the Transportation Research Board*, 2051 (1), 80-89.

Williams, D.A., 1998. *Microdamage healing in asphalt concretes: Relating binder composition and surface energy to healing rate*. Texas A&M University.

Wittle, J.H., 2015. *Electron microprobe laboratory, north arizona university*, http://nau.Edu/cefns/labs/electron-microprobe/glg-510-class-notes/instrumentation/#intro. [online]. [Access Date 05/08/2016].

Wu, S.-P., Pang, L., Mo, L.-T., Chen, Y.-C. & Zhu, G.-J., 2009. Influence of aging on the evolution of structure, morphology and rheology of base and sbs modified bitumen. *Construction and Building Materials*, 23 (2), 1005-1010.

Wu, Y., Guo, Y. & Zhang, X., 2011. Performance evaluation of recycled asphalt mixture using warm mix asphalt technologyed.^eds. *Emerging Technologies for Material, Design, Rehabilitation, and Inspection of Roadway Pavements*ASCE, 26-34.

Xiao, F. & Amirkhanian, S.N., 2009. Laboratory investigation of moisture damage in rubberised asphalt mixtures containing reclaimed asphalt pavement. *International Journal of Pavement Engineering*, 10 (5), 319-328.

Xiao, F. & Amirkhanian, S.N., 2010. Effects of liquid antistrip additives on rheology and moisture susceptibility of water bearing warm mixtures. *Construction and Building Materials*, 24 (9), 1649-1655.

Xiao, F., Amirkhanian, S.N. & Putman, B.J., 2010. Evaluation of rutting resistance in warm-mix asphalts containing moist aggregate. *Transportation Research Record: Journal of the Transportation Research Board*, 2180 (1), 75-84.

Xiao, F., Amirkhanian, S.N. & Zhang, R., 2011a. Influence of short-term aging on rheological characteristics of non-foaming wma binders. *Journal of Performance of Constructed Facilities*, 26 (2), 145-152.

Xiao, F., Amirkhanian, S.N. & Zhang, R., 2011b. Rheological investigation of non-foaming wma additives at mid-temperatureed.^eds. *Emerging Technologies for Material, Design, Rehabilitation, and Inspection of Roadway Pavements*ASCE, 1-8.

Xiao, F., Punith, V. & Amirkhanian, S.N., 2012a. Effects of non-foaming wma additives on asphalt binders at high performance temperatures. *Fuel*, 94, 144-155.

Xiao, F., Punith, V., Amirkhanian, S.N. & Putman, B.J., 2013. Rheological and chemical characteristics of warm mix asphalt binders at intermediate and low performance temperatures. *Canadian Journal of Civil Engineering*, 40 (9), 861-868.

Xiao, F., Putman, B. & Amirkhanian, S., 2015. Rheological characteristics investigation of high percentage rap binders with wma technology at various aging states. *Construction and Building Materials*, 98, 315-324.

Xiao, F., Zhao, W., Gandhi, T. & Amirkhanian, S.N., 2012b. Laboratory investigation of moisture susceptibility of long-term saturated warm mix asphalt mixtures. *International Journal of Pavement Engineering,* 13 (5), 401-414.

Yang, Y., Zhang, H. & Wu, Y., Year. Laboratory evaluation of the warm mix asphalt performance in liaoninged.^eds. *ICCTP 2009@ sCritical Issues In Transportation Systems Planning, Development, and Management*ASCE, 1-7.

Young, T., Monclus, M., Burnett, T., Broughton, W., Ogin, S. & Smith, P., 2011. The use of the peakforcetm quantitative nanomechanical mapping afm-based method for high-resolution young's modulus measurement of polymers. *Measurement Science and Technology,* 22 (12), 125703.

Zaumanis, M., 2010. *Warm mix asphalt investigation*. MSc. RIGA TECHNICAL UNIVERSITY.

Zaumanis, M. & Mallick, R.B., 2015. Review of very high-content reclaimed asphalt use in plant-produced pavements: State of the art. *International Journal of Pavement Engineering,* 16 (1), 39-55.

Zaumanis, M., Mallick, R.B. & Frank, R., 2014. 100% recycled hot mix asphalt: A review and analysis. *Resources, Conservation and Recycling,* 92, 230-245.

Zettler, R., 2006. Warm mix stands up to its trials. *Better roads,* 76 (2).

Zhang, H., Wang, H. & Yu, J., 2011. Effect of aging on morphology of organo-montmorillonite modified bitumen by atomic force microscopy. *Journal of Microscopy,* 242 (1), 37-45.

Zhang, H., Yu, J., Feng, Z., Xue, L. & Wu, S., 2012. Effect of aging on the morphology of bitumen by atomic force microscopy. *Journal of microscopy,* 246 (1), 11-19.

Zhao, G.-J. & Guo, P., 2012. Workability of sasobit warm mixture asphalt. *Energy Procedia,* 16, 1230-1236.

Zhao, S., Huang, B., Shu, X., Jia, X. & Woods, M., 2012. Laboratory performance evaluation of warm-mix asphalt containing high percentages of reclaimed asphalt pavement. *Transportation Research Record: Journal of the Transportation Research Board,* 2294 (1), 98-105.

Zhao, S., Huang, B., Shu, X. & Woods, M., 2013. Comparative evaluation of warm mix asphalt containing high percentages of reclaimed asphalt pavement. *Construction and Building Materials,* 44, 92-100.

Zhao, S., Huang, B., Shu, X. & Woods, M.E., 2015a. Quantitative characterization of binder blending: How much recycled binder is mobilized during mixing? *Transportation Research Record: Journal of the Transportation Research Board,* (2506), 72-80.

Zhao, S., Nahar, S.N., Schmets, A.J., Huang, B., Shu, X. & Scarpas, T., 2015b. Investigation on the microstructure of recycled asphalt shingle binder and its blending with virgin bitumen. *Road Materials and Pavement Design,* (ahead-of-print), 1-18.

Zhong, Q., Inniss, D., Kjoller, K. & Elings, V., 1993. Fractured polymer/silica fiber surface studied by tapping mode atomic force microscopy. *Surface Science Letters,* 290 (1-2), L688-L692.

Zhou, F., Mogawer, W., Li, H., Andriescu, A. & Copeland, A., 2012. Evaluation of fatigue tests for characterizing asphalt binders. *Journal of Materials in Civil Engineering,* 25 (5), 610-617.

Appendix A: Fatigue data of WMBBs

Table A.1 Summery of fatigue data for all control and WMBBs

NSM: normalize shear modulus, γ: Strain, G*: Complex shear modulus, $\delta°$: Phase angle, N_f: number of cycles, E_r: energy ratio

H (Control)											H + 2% Sa										
Average						Standard Deviation					Average						Standard Deviation				
NSM	*γ*%	*G* (Pa)*	*δ°*	N_f	*Er*	*γ*(%)	*G**	*δ°*	N_f	*Er*	*NSM*	*γ*%	*G* (Pa)*	*δ°*	N_f	*Er*	*γ*%	*G**	*δ°*	N_f	*Er*
1.00	2.159	8508000	55.38	20	170	0.0007	10607	0.219	0	0.21	1.00	1.30	14040000	49.28	20	281	0.003	21213	0.87	0	0
0.95	2.935	8122000	56.40	60	488	0.0058	14849	0.156	0	0.89	0.95	1.78	13340000	51.17	260	3464	0.003	21213	0.85	57	748
0.90	3.117	7654000	57.48	1340	10268	0.0044	9192	0.205	594	4562.42	0.90	1.88	12630000	52.45	9740	122904	0.001	14142	0.91	2065	25919
0.85	3.302	7228000	57.85	4100	29679	0.0061	12728	0.191	1188	8649.30	0.85	2.00	11930000	53.03	17200	205007	0.002	14142	0.86	2432	28752
0.80	3.510	6808000	58.14	5220	35577	0.0052	9192	0.219	1131	7757.71	0.80	2.12	11230000	53.44	22640	254009	0.002	14142	0.79	1640	18086
0.75	3.746	6379000	58.43	5920	37843	0.0105	16971	0.240	990	6427.23	0.75	2.26	10530000	53.78	26650	280625	0.002	0	0.77	495	5212
0.70	4.018	5962000	58.75	6430	38360	0.0045	4950	0.283	863	5178.09	0.70	2.43	9822000	54.11	29530	289794	0.002	12021	0.77	269	2992
0.65	4.328	5532000	59.09	6830	37879	0.0154	18385	0.318	721	4124.89	0.65	2.62	9119000	54.46	31920	290813	0.003	12021	0.81	905	8630
0.60	4.705	5102000	59.48	7170	36627	0.0094	8485	0.375	608	3167.07	0.60	2.84	8421000	54.82	33800	284301	0.004	14142	0.84	1329	11659
0.55	5.124	4691000	59.87	7440	34960	0.0133	10607	0.424	509	2471.00	0.55	3.10	7719000	55.22	35210	271598	0.002	7778	0.88	1541	12164
0.50	5.650	4265000	60.35	7680	32787	0.0103	5657	0.474	424	1854.63	0.50	3.42	7013000	55.69	36490	255834	0.001	2828	0.94	1853	13092
0.45	6.321	3828000	60.88	7890	30179	0.0032	4243	0.552	354	1318.87	0.45	3.78	6318000	56.20	37500	237825	0.024	35355	0.96	2121	12130
0.40	7.076	3427000	61.44	8050	27575	0.0008	2121	0.615	297	1000.24	0.40	4.29	5611000	56.82	38280	214661	0.000	4950	0.95	2432	13829
0.35	8.194	2991000	62.17	8200	24338	0.0830	31820	0.742	255	494.73	0.35	4.90	4925000	57.55	38960	191822	0.002	2121	1.05	2574	12755
0.30	9.534	2570000	62.92	8310	21289	0.0316	11314	0.799	212	449.47	0.30	5.74	4221000	58.43	39510	166640	0.000	4950	1.09	2673	11468
0.26	11.215	2184000	63.73	8390	18354	0.0437	4950	0.863	184	443.70	0.25	6.94	3510000	59.56	39940	139885	0.014	11314	1.20	2744	10060
0.21	14.170	1773000	64.90	8460	14751	0.3106	41012	1.138	170	51.00	0.20	8.66	2829000	60.87	40240	113686	0.001	5657	1.27	2800	8138
0.15	19.528	1311000	66.31	8510	10872	0.6549	46669	1.414	156	198.34	0.15	11.55	2131000	62.55	40450	86391	0.069	7071	1.40	2843	5786
0.08	31.797	713300	68.55	8540	6854	5.1965	124875	0.721	141	1179.80	0.10	16.73	1449000	64.59	40570	60540	0.835	64347	1.49	2871	1680

H + 2% Rw											H + 0.5% Rl										
Average						Standard Deviation					Average						Standard Deviation				
NSM	*γ%*	*G* (Pa)*	*δ°*	N_f	*Er*	*γ%*	*G**	*δ°*	N_f	*Er*	*NSM*	*γ%*	*G* (Pa)*	*δ°*	N_f	*Er*	*γ%*	*G**	*δ°*	N_f	*Er*
1.00	1.921	9626000	53.0	20	191	0.0204	85560	0.368	0	1.71	1.00	1.772	10790000	52.71	20	236	0.111	1449569	0.31	0	29
0.95	2.621	9171000	54.4	70	638	0.0262	89803	0.057	14	135.09	0.95	2.136	10250000	53.64	3030	36615	0.265	1378858	1.26	3776	46563
0.90	2.775	8659000	55.8	1810	15626	0.0253	77075	0.127	1344	11699.68	0.90	2.257	9706000	54.13	8930	94936	0.279	1303905	1.58	42	12095
0.85	2.940	8178000	56.4	7520	61145	0.0269	72832	0.057	933	8132.82	0.85	2.391	9167000	54.43	11650	116190	0.296	1232487	1.71	1230	2007
0.80	3.126	7698000	56.7	9670	74004	0.0279	67882	0.092	834	7039.47	0.80	2.542	8627000	54.69	13810	129227	0.315	1161776	1.70	2164	4400
0.75	3.338	7215000	57.0	11140	79895	0.0296	64347	0.085	820	6597.56	0.75	2.713	8092000	54.97	15400	134927	0.335	1083288	1.68	2744	7620
0.70	3.578	6739000	57.3	12200	81733	0.0319	58690	0.106	792	6020.17	0.70	2.908	7554000	55.25	16470	134775	0.362	1017527	1.67	2927	7461
0.65	3.857	6258000	57.7	13030	81074	0.0332	53033	0.099	778	5529.43	0.65	3.133	7017000	55.58	17450	132650	0.390	946816	1.65	3125	7502
0.60	4.189	5772000	58.1	13710	78653	0.0385	51619	0.120	750	5006.64	0.60	3.404	6471000	55.92	18280	128102	0.422	868327.1	1.58	3253	7172
0.55	4.567	5305000	58.5	14240	75063	0.0437	49497	0.113	735	4580.35	0.55	3.716	5934000	56.32	18970	121939	0.463	798323.6	1.57	3352	6637
0.50	5.038	4807000	59.0	14690	70332	0.0312	28284	0.099	750	4003.51	0.50	4.089	5399000	56.74	19570	114520	0.512	731148.4	1.51	3437	6022
0.45	5.613	4335000	59.6	15050	64813	0.0556	41719	0.120	750	3854.99	0.45	4.550	4865000	57.24	20100	105927	0.567	653366.7	1.44	3507	5550
0.40	6.336	3859000	60.2	15340	58701	0.0795	47376	0.156	764	3648.19	0.40	5.115	4311000	57.79	20550	96592	0.688	628617.9	1.41	3606	4231
0.35	7.279	3376000	61.0	15570	52046	0.1075	48790	0.156	778	3358.74	0.35	5.890	3786000	58.51	20830	85211	0.719	494974.7	1.24	3804	5424
0.30	8.450	2921000	61.8	15740	45483	0.1362	45962	0.163	792	3011.02	0.30	6.896	3241000	59.37	21140	74145	0.860	432749.4	1.12	3875	4596
0.25	10.402	2381000	63.1	15890	37512	0.1337	29698	0.134	806	2374.31	0.25	8.336	2696000	60.43	21380	62328	1.033	356381.8	0.96	3932	3971
0.20	12.892	1898000	64.3	15980	30607	0.1737	25456	0.028	820	1164.80	0.20	10.401	2209000	61.79	21540	50618	1.032	229102.6	0.62	3960	4454
0.15	17.733	1475000	66.1	16050	22652	1.2130	93338	0.375	806	2633.87	0.15	14.096	1595000	63.59	21650	37948	2.111	256679.8	0.66	4002	1553
0.11	22.737	1073000	67.2	16080	17742	0.9255	44548	0.240	820	189.63	0.10	21.358	1092000	65.97	21710	25378	2.355	125157.9	0.20	4002	2007

S (Control)											S + 2% Sa										
Average						Standard Deviation					Average						Standard Deviation				
NSM	*γ%*	*G*(Pa)*	*δ°*	N_f	*Er*	*γ%*	*G**	*δ°*	N_f	*Er*	*MSM*	*γ%*	*G*(Pa)*	*δ°*	N_f	*Er*	*γ%*	*G**	*δ°*	N_f	*Er*
1.00	3.180	2535000	65.14	20	49	0.19	135765	0.37	0	3	1.00	1.845	4518000	59.38	20	84	0.203	452548	1.22	0	9
0.95	4.497	2407000	66.09	170	402	0.26	129401	0.03	127	317	0.95	2.593	4309000	60.79	60	240	0.292	442649	1.39	0	27
0.90	4.750	2282000	66.38	3200	7071	0.28	123037	0.14	764	2070	0.90	2.743	4064000	61.93	1120	4218	0.300	406586	1.32	57	242
0.85	5.033	2157000	66.48	3910	8157	0.29	115966	0.13	750	2009	0.85	2.907	3839000	62.44	5950	21191	0.319	383959	1.08	184	1629
0.80	5.366	2029000	66.59	4350	8526	0.31	111016	0.13	750	1945	0.80	3.094	3613000	62.74	9560	32308	0.340	362039	0.93	1188	7449
0.75	5.733	1900000	66.71	4660	8564	0.32	99702	0.13	764	1862	0.75	3.305	3387000	62.99	12060	38381	0.362	337997	0.88	2461	11823
0.70	6.144	1775000	66.84	4900	8418	0.34	90510	0.13	764	1750	0.70	3.548	3162000	63.18	13930	41417	0.390	316784	0.87	3097	13512
0.65	6.651	1647000	67.00	5110	8130	0.38	88388	0.12	750	1639	0.65	3.828	2936000	63.40	15350	42395	0.422	293449	0.80	3493	14035
0.60	7.223	1524000	67.16	5280	7759	0.44	85560	0.13	735	1528	0.60	4.158	2713000	63.58	16320	41591	0.464	274357	0.76	3507	13312
0.55	7.870	1397000	67.34	5420	7324	0.43	71418	0.11	735	1377	0.55	4.550	2485000	63.82	17190	40133	0.505	249609	0.74	3606	12616
0.50	8.701	1270000	67.55	5550	6807	0.50	67882	0.11	721	1258	0.50	5.013	2263000	64.11	17890	38019	0.559	227688	0.67	3635	11713
0.45	9.705	1148000	67.79	5660	6250	0.62	67882	0.13	707	1162	0.45	5.598	2034000	64.42	18480	35296	0.621	203647	0.59	3620	10606
0.40	11.063	1007000	68.09	5760	5594	0.66	55579	0.11	707	1004	0.40	6.327	1805000	64.82	18960	32154	0.697	178191	0.49	3592	9410
0.35	12.754	874800	68.42	5840	4932	0.72	46952	0.11	707	869	0.35	7.263	1585000	65.28	19350	28742	0.829	161927	0.42	3550	8353
0.30	14.767	758100	68.76	5900	4307	0.88	43346	0.11	707	770	0.30	8.542	1358000	65.86	19670	24994	0.997	141421	0.30	3521	7212
0.24	17.470	618000	69.15	5950	3643	0.24	8910	0.03	721	494	0.25	10.257	1130000	66.57	19910	21142	1.111	110097	0.16	3521	5897
0.20	22.500	504500	69.58	6000	2824	2.18	52114	0.30	707	643	0.20	13.100	891200	67.55	20110	16800	1.466	90085	0.04	3521	4726
0.15	27.257	374300	70.15	6030	2223	0.45	8627	0.16	721	318	0.15	17.014	679300	68.64	20240	12942	1.725	64347	0.14	3536	3543
0.09	35.898	239100	71.24	6070	1409	0.66	10677	0.23	721	232	0.10	24.014	456600	69.74	20350	8864	1.705	33870	0.35	3550	2225

S+ 2% Rw											S + 0.5% Rl										
Average						Standard Deviation					Average						Standard Deviation				
NSM	γ%	G*(Pa)	δ°.	N.C	ER	γ%	G*	δ°	N.C	ER	NSM	γ%	G*(Pa)	δ°	N.C	ER	γ%	G*	δ°.	N.C	ER
1.00	2.711	2909000	63.24	20	57	0.066	67175	0.01	0	1	1.00	3.180	2547000	64.57	20	48.96	0.183	140007	0.54	0	3
0.95	3.806	2772000	64.31	60	164	0.093	65761	0.31	0	4	0.95	4.476	2424000	65.45	80	186.28	0.268	135057	0.15	0	11
0.90	4.031	2617000	65.15	1750	4514	0.096	60104	0.29	297	870	0.90	4.738	2292000	65.93	1760	3860.29	0.280	126572	0.10	255	338
0.85	4.274	2474000	65.30	3950	9615	0.104	58690	0.27	212	748	0.85	5.024	2164000	66.06	2720	5660.63	0.295	118087	0.08	28	380
0.80	4.550	2327000	65.42	4880	11179	0.108	53033	0.26	226	777	0.80	5.351	2036000	66.17	3190	6249.92	0.315	111016	0.06	99	548
0.75	4.862	2182000	65.55	5490	11793	0.114	49497	0.25	240	788	0.75	5.721	1910000	66.30	3510	6447.6	0.343	106066	0.04	127	606
0.70	5.227	2034000	65.69	5950	11914	0.122	45962	0.23	240	755	0.70	6.133	1784000	66.44	3750	6442.48	0.356	96167	0.02	156	628
0.65	5.644	1890000	65.83	6310	11736	0.136	43841	0.23	240	724	0.65	6.651	1650000	66.59	3960	6290.16	0.392	89803	0.00	170	625
0.60	6.119	1744000	66.00	6600	11350	0.128	35355	0.21	255	671	0.60	7.206	1533000	66.74	4120	6059.96	0.461	90510	0.02	170	622
0.55	6.689	1607000	66.19	6850	10814	0.177	41012	0.22	240	660	0.55	7.910	1397000	66.90	4270	5739.56	0.477	77075	0.04	184	576
0.50	7.393	1458000	66.42	7070	10132	0.188	36062	0.21	240	599	0.50	8.678	1282000	67.06	4390	5397.94	0.562	76368	0.06	184	561
0.45	8.221	1310000	66.68	7250	9377	0.154	24042	0.16	240	485	0.45	9.627	1151000	67.25	4500	5000.74	0.530	57983	0.11	198	481
0.40	9.288	1172000	66.98	7410	8518	0.265	32527	0.17	212	485	0.40	10.842	1029000	67.45	4600	4558.791	0.634	55366	0.13	198	451
0.35	10.728	1009000	67.37	7550	7544	0.149	14142	0.11	212	319	0.35	12.593	890400	67.72	4700	4025.28	0.762	49497	0.17	198	402
0.30	12.491	873300	67.80	7660	6594	0.263	18031	0.09	198	308	0.30	14.676	765100	67.98	4780	3519.602	0.871	41931	0.23	198	346
0.25	15.032	721900	68.34	7760	5553	0.187	9051	0.05	198	212	0.24	17.939	623500	68.37	4860	2918.818	1.022	33375	0.32	198	281
0.20	18.495	575900	68.98	7840	4529	0.065	2475	0.08	198	95	0.20	21.643	510100	68.47	4920	2424.13	1.112	25314	0.42	198	222
0.15	24.205	439500	69.73	7920	3391	0.835	16263	0.18	198	214	0.16	26.969	398100	68.83	4980	1897.838	1.570	24749	0.54	198	199
0.09	32.707	275800	70.96	7990	2226	0.204	3960	0.18	212	27	0.10	35.363	265600	69.94	5050	1250.63	1.924	26163	0.10	212	185

Appendix B: Nano-mechanical properties of all mixtures

Table B.1 Nano-mechanical properties of HMA and WMA

S.D: Standard deviation, COV: coefficient of variance

Mixture code	HH155											
Properties	Modulus			Hardness			Max. Load			Max. Displacement		
Phases	Aggregate	ITZ	Mastic	Aggregate	ITZ	Mastic	Aggregate	ITZ	Mastic	Aggregate	ITZ	Mastic
Mean	42.341	10.093	3.789	2.436	0.222	0.06	228.329	29.361	7.44	2354.411	2514.032	2386.996
S.D	5.883	1.592	1.346	0.625	0.054	0.015	39.189	7.717	2.041	100.014	165.048	110.606
% COV	13.89	15.78	35.52	25.66	24.26	25.06	17.16	26.28	27.43	4.25	6.57	4.63
Mixture code	WHSa135											
Properties	Modulus			Hardness			Max. Load			Max. Displacement		
Phases	Aggregate	ITZ	Mastic	Aggregate	ITZ	Mastic	Aggregate	ITZ	Mastic	Aggregate	ITZ	Mastic
Mean	41.727	9.598	2.489	2.077	0.218	0.031	207.065	33.018	4.097	2389.503	2671.547	2675.164
S.D	6.434	2.091	0.673	0.659	0.074	0.012	46.766	13.846	1.988	92.215	223.121	233.576
% COV	15.42	21.79	27.05	31.73	34.08	38.83	22.59	41.93	48.52	3.86	8.35	8.73
Mixture code	WHSa145											
Properties	Modulus			Hardness			Max. Load			Max. Displacement		
Phases	Aggregate	ITZ	Mastic	Aggregate	ITZ	Mastic	Aggregate	ITZ	Mastic	Aggregate	ITZ	Mastic
Mean	41.111	15.649	5.934	2.14	0.5	0.136	206.714	61.96	14.521	2358.051	2458.438	2235.887
S.D	5.763	3.473	1.233	0.601	0.157	0.036	36.352	27.56	6.128	102.524	480.185	312.695
% COV	14.02	22.19	20.78	28.09	31.46	26.39	17.59	44.48	42.2	4.35	19.53	13.99
Mixture code	WHRw135											
Properties	Modulus			Hardness			Max. Load			Max. Displacement		
Phases	Aggregate	ITZ	Mastic	Aggregate	ITZ	Mastic	Aggregate	ITZ	Mastic	Aggregate	ITZ	Mastic
Mean	42.917	8.085	1.617	2.16	0.175	0.006	234.699	19.616	0.687	2496.586	2351.923	2244.263
S.D	6.063	2.326	0.556	0.681	0.054	0.002	43.415	6.192	0.224	149.889	471.771	112.072
% COV	14.13	28.77	34.37	31.52	30.77	29.86	18.5	31.57	32.61	6	20.06	4.99
Mixture code	WHRw145											
Properties	Modulus			Hardness			Max. Load			Max. Displacement		
Phases	Aggregate	ITZ	Mastic	Aggregate	ITZ	Mastic	Aggregate	ITZ	Mastic	Aggregate	ITZ	Mastic
Mean	44.384	13.9	3.005	2.399	0.3	0.056	217.221	35.065	4.749	2300.338	2346.219	2040.729
S.D	6.968	4.133	1.12	0.817	0.131	0.029	52.865	16.764	2.972	132.469	434.323	426.165
% COV	15.7	29.73	37.29	34.07	43.58	52.71	24.34	47.81	62.58	5.76	18.51	20.88
Mixture code	WHRl135											
Properties	Modulus			Hardness			Max. Load			Max. Displacement		
Phases	Aggregate	ITZ	Mastic	Aggregate	ITZ	Mastic	Aggregate	ITZ	Mastic	Aggregate	ITZ	Mastic
Mean	40.122	10.641	1.255	2.504	0.273	0.036	229.797	40.128	4.297	2348.086	2622.864	2539.229
S.D	4.977	1.567	0.575	0.503	0.076	0.02	34.857	19.161	2.181	73.581	618.313	138.715
% COV	12.4	14.73	45.86	20.08	27.74	55.82	15.17	47.75	50.76	3.13	23.57	5.46
Mixture code	WHRl145											
Properties	Modulus			Hardness			Max. Load			Max. Displacement		
Phases	Aggregate	ITZ	Mastic	Aggregate	ITZ	Mastic	Aggregate	ITZ	Mastic	Aggregate	ITZ	Mastic

Mean	42.06	21.112	4.027	2.083	0.565	0.095	206.449	61.499	10.631	2376.563	2324.029	2349.997
S.D	5.882	5.374	1.104	0.565	0.233	0.035	36.538	27.255	3.244	112.618	340.208	99.632
% COV	13.98	25.46	27.42	27.14	41.23	36.57	17.7	44.32	30.52	4.74	14.64	4.24
Mixture code	**HS145**											
Properties	Modulus			Hardness			Max. Load			Max. Displacement		
Phases	Aggregate	ITZ	Mastic	Aggregate	ITZ	Mastic	Aggregate	ITZ	Mastic	Aggregate	ITZ	Mastic
Mean	42.004	2.562	1.549	2.768	0.043	0.012	225.36	8.78	2.364	2267.594	3116.399	2917.024
S.D	6.521	0.809	0.395	0.789	0.013	0.003	37.339	2.388	0.813	169.775	182.109	184.743
% COV	15.52	31.59	25.52	28.51	29.68	27.47	16.57	27.2	34.39	7.49	5.84	6.33
Mixture code	**WSSa125**											
Properties	Modulus			Hardness			Max. Load			Max. Displacement		
Phases	Aggregate	ITZ	Mastic	Aggregate	ITZ	Mastic	Aggregate	ITZ	Mastic	Aggregate	ITZ	Mastic
Mean	42.123	6.579	4.318	2.839	0.145	0.045	230.456	29.326	8.921	2231.478	3082.482	2996.576
S.D	6.135	1.137	1.174	0.478	0.048	0.013	36.906	12.972	2.229	89.471	507.052	140.68
% COV	14.56	17.27	27.18	16.85	33.47	28.14	16.01	44.23	24.98	4.01	16.45	4.69
Mixture code	**WSRw125**											
Properties	Modulus			Hardness			Max. Load			Max. Displacement		
Phases	Aggregate	ITZ	Mastic	Aggregate	ITZ	Mastic	Aggregate	ITZ	Mastic	Aggregate	ITZ	Mastic
Mean	41.92	2.732	2.163	2.084	0.032	0.018	237.63	8.268	3.531	2534.64	3426.372	2960.034
S.D	8.624	0.767	0.769	0.252	0.01	0.006	28.437	2.592	1.287	112.929	196.437	93.031
% COV	20.57	28.06	35.58	12.08	31.57	33.86	11.97	31.35	36.43	4.46	5.73	3.14
Mixture code	**WSRl125**											
Properties	Modulus			Hardness			Max. Load			Max. Displacement		
Phases	Aggregate	ITZ	Mastic	Aggregate	ITZ	Mastic	Aggregate	ITZ	Mastic	Aggregate	ITZ	Mastic
Mean	47.989	4.136	1.659	2.233	0.053	0.015	228.716	13.747	2.988	2379.996	3420.034	3069.04
S.D	3.945	1.503	0.729	0.441	0.014	0.008	34.115	5.199	1.316	64.917	326.715	543.014
% COV	8.22	36.35	43.98	19.76	26.59	54.26	14.92	37.82	44.06	2.73	9.55	17.69

Appendix C: Summary of all Pull-off test and work of indentation results

Table C.1 Summery of all Pull-off test results

D: displacement, *Tl* : tensile loads and W_f: practical work of fracture

Sample 1			Sample 2			Sample 3			Average			Standard Deviation (S.D)		
D	*Tl*	W_f	***D***	*Tl*	W_f	***D***	*Tl*	W_f	***D***	*Tl*	W_f	***D***	*Tl*	W_f
H (40-60) @20°C														
0.334	186.572	23.391	0.333	190.602	25.381	0.250	155.701	21.761	**0.306**	**177.625**	**23.511**	**0.048**	**19.093**	**1.813**
H + 2% Sa @20°C														
0.417	240.262	57.528	0.333	314.080	62.790	0.542	291.269	65.766	**0.431**	**281.870**	**62.028**	**0.105**	**37.796**	**4.172**
H + 0.5%Rl @20°C														
0.312	433.550	55.213	0.333	221.468	35.438	0.313	378.508	49.673	**0.319**	**344.509**	**46.775**	**0.012**	**110.053**	**10.202**
H + 0.5% Rw @20°C														
0.292	186.572	49.296	0.354	320.801	64.432	0.354	240.262	54.344	**0.333**	**249.212**	**56.024**	**0.036**	**67.561**	**7.706**
S (100-150) @20°C														
0.125	99.320	22.112	0.167	104.689	29.860	0.271	100.659	30.275	**0.187**	**101.556**	**27.416**	**0.075**	**2.795**	**4.598**
S + 2% Sa @20°C														
0.271	99.320	36.407	0.250	96.642	27.297	0.396	153.010	44.021	**0.306**	**116.324**	**35.908**	**0.079**	**31.799**	**8.373**
S + 0.5% Rl @20°C														
0.250	119.461	27.150	0.312	122.139	42.031	0.354	183.889	53.654	**0.306**	**141.830**	**40.945**	**0.053**	**36.449**	**13.285**
S + 2% Rw @20°C														
0.270	100.659	28.277	0.312	106.028	30.051	0.292	106.028	30.079	**0.291**	**104.238**	**29.469**	**0.021**	**3.100**	**1.032**
S (100-150) @10°C														
0.479	218.781	59.959	0.375	251.000	43.051	0.375	165.091	54.532	**0.410**	**211.624**	**52.514**	**0.060**	**43.399**	**8.633**
S + 2% Sa @10°C														
0.542	434.889	88.983	0.583	315.428	85.910	0.562	375.158	87.446	**0.562**	**375.158**	**87.446**	**0.021**	**59.731**	**1.537**
S +0.5% Rl @10°C														
0.479	308.720	64.237	0.562	259.051	61.390	0.562	233.549	66.562	**0.535**	**267.107**	**64.063**	**0.048**	**38.227**	**2.590**
S +2 % Rw @10°C														
0.542	259.051	68.267	0.604	429.520	84.383	0.604	306.029	84.149	**0.583**	**331.533**	**78.933**	**0.036**	**88.050**	**9.238**

Table C-2 Summary of the response load on ITZ, displacement into surface and the work of indentation for all asphalt mixtures

Mix	Max. Load (mN)		Displacement h (nm)		Work of Indentation WI (mN.nm)	
	Average	S.D	Average	S.D	Average	S.D
HH155	29.4	8	2064	139	27550	7894
WHSa135	33.0	14	2179	64	31918	16051
WHSa145	62.0	28	2075	185	60102	28732
WHRl135	40.1	6	2199	205	47203	19866
WHRl145	61.5	27	2046	186	61263	33397
WHRw135	19.6	6	2023	124	17411	7040
WHRw145	35.1	17	2009	260	32218	17321
HS145	8.8	2	2072	121	8562	2357
WSSa125	29.3	13	2175	178	30756	14765
WSRl125	13.7	5	2198	200	14160	6284
WSRw125	8.3	3	2129	85	8296	2676

Appendix D: DSR sequences

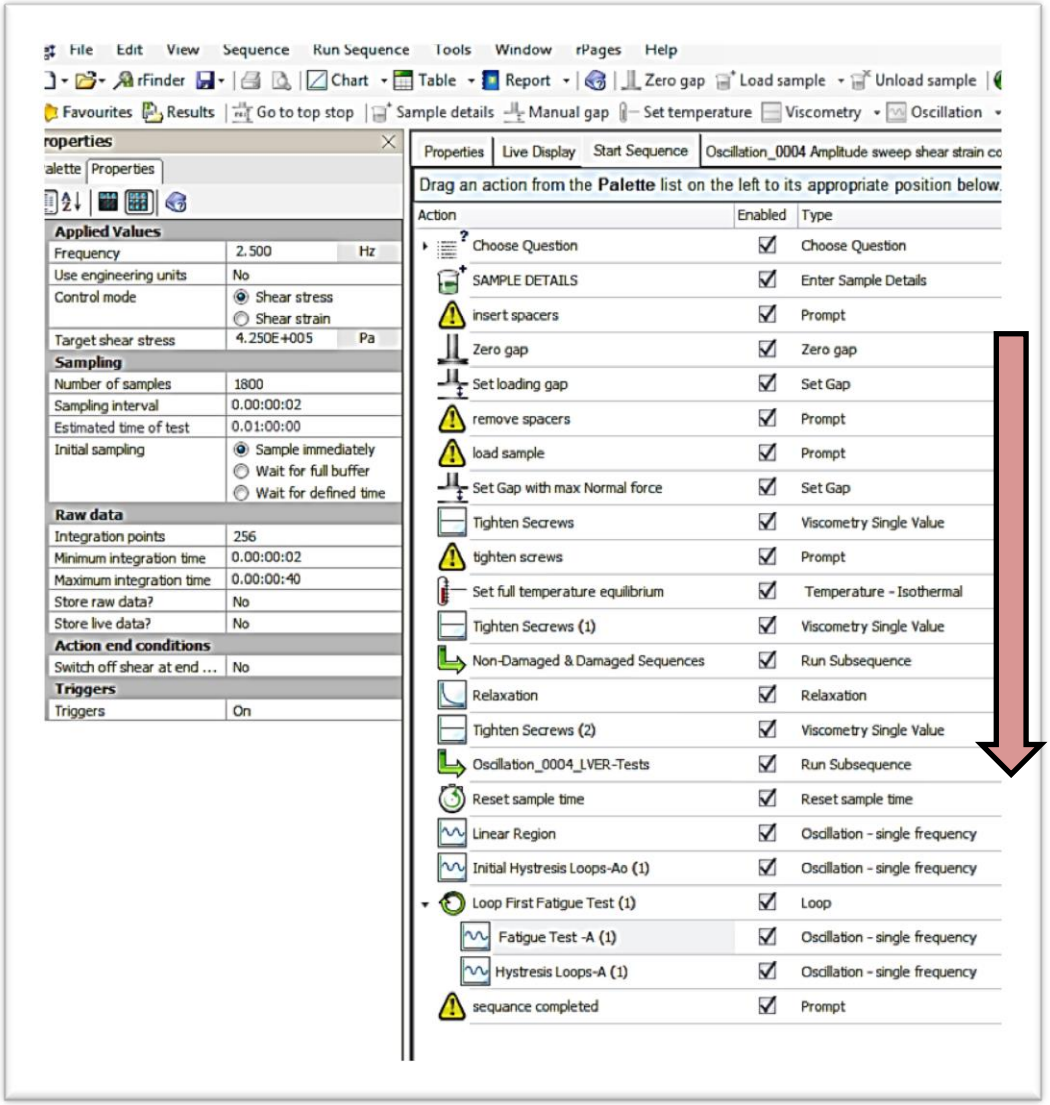

Figure D-1 DSR sequence for measuring fatigue test of asphalt mixture

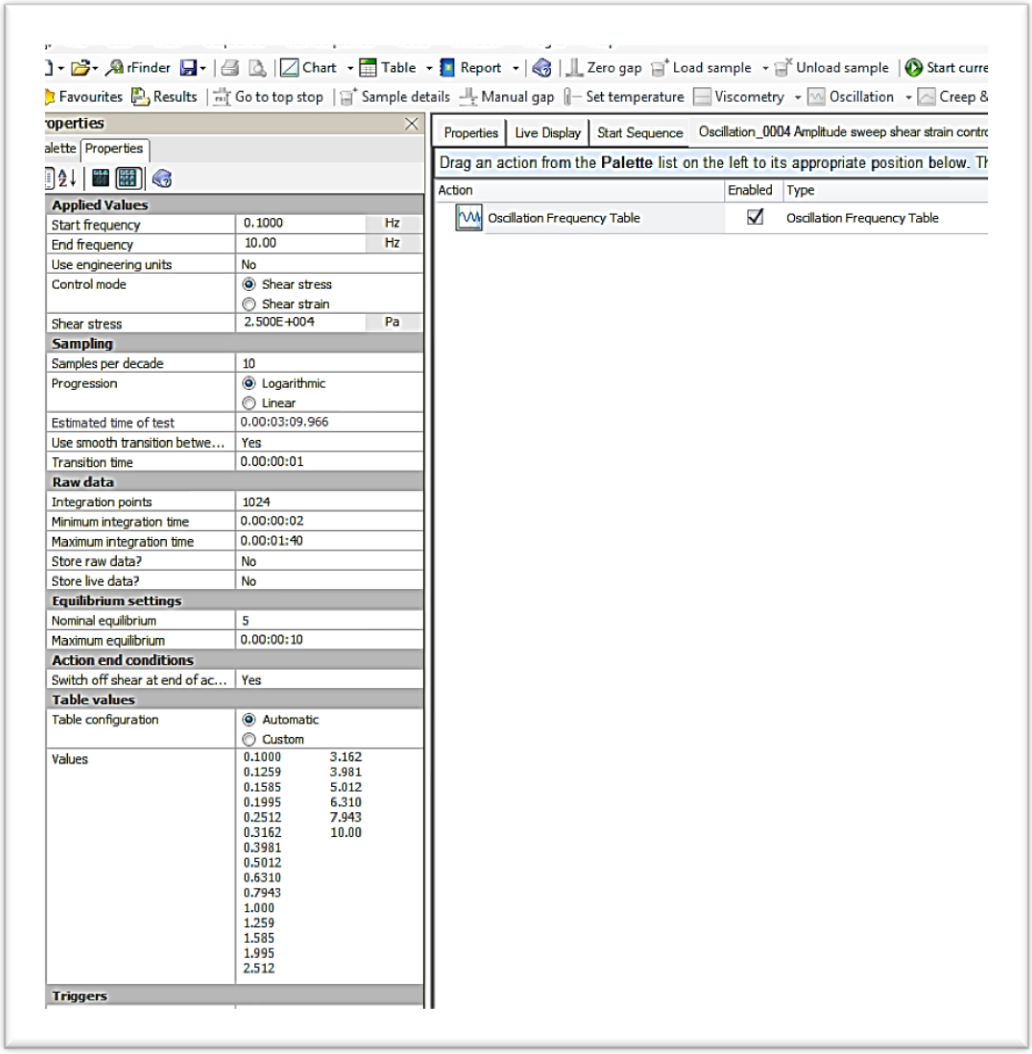

Figure D-2 DSR sequence for conducting frequency sweep for asphalt mixture

Appendix E: Sweep stress data of control mixture

Table E.1 Sweep stress data of control mixtures HH155 and HS145

Stress (pa)	HH155				HS145			
	HH155-S1 dy/dt	HH155-S2 dy/dt	HH155-S3 dy/dt	Average	HS145-S1 dy/dt	HS145-S2 dy/dt	HS145-S3 dy/dt	Average
5000	2.22E-08	1.43423E-07	7.31E-09	5.76E-08	1.72E-07	6.02E-07	2.92E-07	3.55E-07
25000	1.67E-07	4.71526E-07	6.33E-08	2.34E-07	2.41E-05	7.57E-06	9.77E-06	1.38E-05
50000	1.45E-07	1.15294E-06	6.65E-07	6.54E-07	5.93E-05	5.09E-05	3.23E-05	4.75E-05
75000	6.09E-06	1.97174E-06	1.63E-06	3.23E-06	9.51E-05	8.09E-05	6.64E-05	8.08E-05
100000	6.27E-06	4.42666E-06	3.16E-06	4.62E-06	0.000138	0.000115	0.000104	0.000119
125000	7.4E-06	8.85665E-06	4.99E-06	7.08E-06	0.00018	0.000157	0.000146	0.000161
150000	8.73E-06	1.77925E-05	6.87E-06	1.11E-05	0.000232	0.000207	0.000191	0.00021
175000	1.06E-05	1.83885E-05	8.73E-06	1.26E-05	0.000289	0.000266	0.000292	0.000282
200000	1.24E-05	1.95204E-05	1.19E-05	1.46E-05	0.000351	0.00033	0.000401	0.000361
225000	1.42E-05	2.32076E-05	1.36E-05	1.7E-05	0.000423	0.00041	0.000442	0.000425
250000	1.66E-05	2.78156E-05	1.62E-05	2.02E-05	0.000503	0.000493	0.000506	0.000501
275000	1.96E-05	3.06767E-05	2E-05	2.34E-05	0.000598	0.000598	0.00059	0.000595
300000	4.06E-05	3.46593E-05	2.27E-05	3.26E-05	0.000712	0.000716	0.000684	0.000704
325000	4.45E-05	4.06757E-05	2.63E-05	3.72E-05	0.000846	0.000863	0.000803	0.000838
350000	0.000118	0.000109881	7.43E-05	0.000101	0.0024	0.002339	0.002378	0.002372
375000	0.000141	0.000163632	9.34E-05	0.000133	0.003322	0.002998	0.002717	0.003012
400000	0.000159	0.000192511	0.00011	0.000154	0.004044	0.003726	0.003242	0.003671
425000	0.000179	0.000212832	0.000156	0.000183	0.005172	0.005263	0.004037	0.004824
450000	0.000196	0.00023328	0.000167	0.000199	0.00759	0.009713	0.00535	0.007551
475000	0.000217	0.000256533	0.000179	0.000218	-	-	-	-
500000	0.000236	0.000285866	0.000197	0.00024	-	-	-	-
525000	0.000256	0.000314463	0.000217	0.000262	-	-	-	-
550000	0.00032	0.000343934	0.000238	0.000301	-	-	-	-
589000	0.000388	0.000393711	0.000277	0.000353	-	-	-	-

Appendix F: Sweep frequency data

Table F.1 Results of sweep frequency for asphalt mixtures

f: frequency, G*: Complex shear modulus, ***δ***°: Phase angle,

HH155					WHSa135					WHSa145				
f	Average		Standard Deviation		*f*	Average		Standard Deviation		*f*	Average		Standard Deviation	
	*G**	*δ*	*G**	*δ*		*G**	*δ*	*G**	*δ*		*G**	*δ*	*G**	*δ*
0.1	176.3	43.62	29	3.30	0.1	151.9	46.16	14	2.7	0.1	182.0	45.00	25	2.48
0.1259	194.8	43.25	30	3.26	0.1259	168.2	46.03	14	2.8	0.1259	201.7	44.72	27	2.41
0.1585	218.3	42.59	30	2.97	0.1585	188.3	45.69	14	2.7	0.1585	225.2	44.22	30	2.28
0.1995	243.2	42.13	32	2.83	0.1995	212.2	44.89	13	2.4	0.1995	251.7	43.65	33	2.16
0.2512	270.7	41.65	33	2.70	0.2512	237.7	44.44	12	2.5	0.2512	281.5	43.04	36	2.08
0.3162	300.7	41.17	35	2.53	0.3162	265.9	43.99	11	2.8	0.3162	314.3	42.40	38	1.96
0.3981	333.9	40.64	37	2.43	0.3981	298.2	43.26	10	2.5	0.3981	350.4	41.70	41	1.89
0.5012	370.7	40.13	38	2.31	0.5012	334.4	42.76	10	2.8	0.5012	389.9	40.99	43	1.81
0.631	411.2	39.58	39	2.16	0.631	375.1	41.56	9	1.8	0.631	433.3	40.25	45	1.71
0.7943	455.9	39.00	41	2.08	0.7943	418.8	41.05	10	2.0	0.7943	481.0	39.51	47	1.63
1	504.7	38.43	43	1.98	1	467.9	40.35	10	2.1	1	533.3	38.71	49	1.54
1.259	558.1	37.81	45	1.89	1.259	519.6	39.48	10	1.7	1.259	590.4	37.92	50	1.47
1.585	616.3	37.15	49	1.81	1.585	578.3	38.60	11	1.6	1.585	652.5	37.09	50	1.40
1.995	679.3	36.46	52	1.76	1.995	640.6	37.58	12	1.6	1.995	719.8	36.25	51	1.34
2.512	747.5	35.72	56	1.66	2.512	700.0	36.77	16	1.5	2.512	791.9	35.40	51	1.29
3.162	820.7	34.98	62	1.62	3.162	781.6	35.96	18	1.4	3.162	869.0	34.52	51	1.26
3.981	898.1	34.18	66	1.54	3.981	856.7	35.03	21	1.4	3.981	950.6	33.63	50	1.21
5.012	982.2	33.36	74	1.50	5.012	940.0	34.13	27	1.4	5.012	1037.4	32.75	50	1.18
6.31	1068.5	32.57	80	1.46	6.31	1026.0	33.09	34	1.4	6.31	1127.8	31.83	50	1.13
7.943	1157.8	31.77	87	1.33	7.943	1113.7	32.31	40	1.4	7.943	1220.3	31.04	50	1.14
10	1254.3	31.08	94	1.31	10	1211.3	31.33	50	1.3	10	1318.5	30.22	49	0.99

WHRw135					WHRw145					WHRl135				
f	Average		Standard Deviation		*f*	Average		Standard Deviation		*f*	Average		Standard Deviation	
	*G**	*δ*	*G**	*δ*		*G**	*δ*	*G**	*δ*		*G**	*δ*	*G**	*δ*
0.1	132.9	48.27	15	2.04	0.1	151.9	46.38	35	4.51	0.1	112.0	51.83	5	1.47
0.1259	148.3	48.03	16	2.06	0.1259	168.0	46.11	36	4.49	0.1259	125.5	51.64	5	1.34
0.1585	166.8	47.77	19	2.29	0.1585	188.7	45.65	37	4.55	0.1585	143.3	51.09	6	1.34
0.1995	189.1	46.97	21	1.98	0.1995	211.8	45.23	39	4.27	0.1995	163.6	50.48	6	1.38
0.2512	213.0	46.62	23	2.13	0.2512	238.0	44.67	41	4.25	0.2512	186.7	49.92	7	1.37
0.3162	241.2	45.81	24	1.93	0.3162	266.6	44.09	44	4.12	0.3162	212.3	49.15	7	1.37
0.3981	272.5	45.19	26	1.87	0.3981	298.4	43.52	48	3.84	0.3981	242.5	48.44	8	1.22
0.5012	306.9	44.61	28	1.92	0.5012	333.7	42.80	50	3.84	0.5012	275.9	47.78	9	1.21
0.631	344.3	43.89	30	1.91	0.631	373.2	42.11	53	3.70	0.631	312.8	47.00	9	1.14
0.7943	385.8	43.07	32	1.77	0.7943	417.0	41.40	56	3.53	0.7943	353.6	46.26	9	1.20
1	430.8	42.08	34	1.56	1	465.4	40.63	59	3.41	1	398.8	45.24	10	1.09
1.259	480.0	41.34	37	1.58	1.259	517.8	39.87	61	3.22	1.259	447.7	44.36	12	0.92
1.585	530.6	40.49	39	1.58	1.585	574.8	39.09	63	3.00	1.585	500.8	43.32	14	0.91
1.995	588.0	39.41	43	1.41	1.995	637.3	38.23	65	2.93	1.995	560.0	42.43	18	0.85
2.512	652.9	37.60	47	1.86	2.512	708.4	37.28	73	3.00	2.512	617.5	41.00	13	0.97
3.162	712.7	37.59	47	1.47	3.162	777.0	36.46	71	2.72	3.162	692.5	40.32	26	0.79
3.981	781.1	36.52	52	1.34	3.981	854.2	35.61	73	2.46	3.981	772.2	39.75	37	0.47
5.012	858.8	35.57	53	1.38	5.012	936.3	34.67	76	2.40	5.012	849.8	38.28	43	0.69
6.31	936.5	34.56	55	1.40	6.31	1023.4	33.78	79	2.20	6.31	935.3	37.10	52	0.62
7.943	1017.9	33.67	57	1.44	7.943	1113.4	32.96	82	2.05	7.943	1024.6	36.12	62	0.60
10	1104.0	32.43	59	1.48	10	1208.8	32.07	86	2.01	10	1117.4	34.95	67	0.49

WHRw145					WHRl135					WHRl145				
f	Average		Standard Deviation		*f*	Average		Standard Deviation		*f*	Average		Standard Deviation	
	*G**	*δ*	*G**	*δ*		*G**	*δ*	*G**	*δ*		*G**	*δ*	*G**	*δ*
0.1	151.9	46.38	35	4.51	0.1	112.0	51.83	5	1.47	0.1	160.4	45.27	29	3.42
0.1259	168.0	46.11	36	4.49	0.1259	125.5	51.64	5	1.34	0.1259	178.4	44.78	30	3.49
0.1585	188.7	45.65	37	4.55	0.1585	143.3	51.09	6	1.34	0.1585	200.0	44.32	31	3.39
0.1995	211.8	45.23	39	4.27	0.1995	163.6	50.48	6	1.38	0.1995	224.1	43.81	32	3.26
0.2512	238.0	44.67	41	4.25	0.2512	186.7	49.92	7	1.37	0.2512	250.8	43.28	33	3.13
0.3162	266.6	44.09	44	4.12	0.3162	212.3	49.15	7	1.37	0.3162	280.7	42.72	34	2.99
0.3981	298.4	43.52	48	3.84	0.3981	242.5	48.44	8	1.22	0.3981	314.5	42.12	36	2.92
0.5012	333.7	42.80	50	3.84	0.5012	275.9	47.78	9	1.21	0.5012	351.8	41.48	39	2.74
0.631	373.2	42.11	53	3.70	0.631	312.8	47.00	9	1.14	0.631	393.5	40.85	42	2.62
0.7943	417.0	41.40	56	3.53	0.7943	353.6	46.26	9	1.20	0.7943	439.7	40.16	46	2.44
1	465.4	40.63	59	3.41	1	398.8	45.24	10	1.09	1	489.7	39.47	50	2.31
1.259	517.8	39.87	61	3.22	1.259	447.7	44.36	12	0.92	1.259	544.5	38.74	56	2.15
1.585	574.8	39.09	63	3.00	1.585	500.8	43.32	14	0.91	1.585	603.9	37.99	62	2.01
1.995	637.3	38.23	65	2.93	1.995	560.0	42.43	18	0.85	1.995	668.0	37.19	68	1.88
2.512	708.4	37.28	73	3.00	2.512	617.5	41.00	13	0.97	2.512	737.4	36.36	76	1.73
3.162	777.0	36.46	71	2.72	3.162	692.5	40.32	26	0.79	3.162	811.6	35.54	83	1.61
3.981	854.2	35.61	73	2.46	3.981	772.2	39.75	37	0.47	3.981	890.8	34.63	92	1.45
5.012	936.3	34.67	76	2.40	5.012	849.8	38.28	43	0.69	5.012	976.1	33.77	100	1.43
6.31	1023.4	33.78	79	2.20	6.31	935.3	37.10	52	0.62	6.31	1063.0	32.84	110	1.27
7.943	1113.4	32.96	82	2.05	7.943	1024.6	36.12	62	0.60	7.943	1154.8	31.99	121	1.13
10	1208.8	32.07	86	2.01	10	1117.4	34.95	67	0.49	10	1250.3	31.08	132	0.95

HS145					WSSa125					WSRw125				
f	Average		Standard Deviation		f	Average		Standard Deviation		f	Average		Standard Deviation	
	G^*	δ	G^*	δ		G^*	δ	G^*	δ		G^*	δ	G^*	δ
0.1	26.4	55.79	5	2.49	0.1	32.9	54.89	1	0.86	0.1	22.4	58.32	4	5.45
0.1259	28.5	56.72	5	2.75	0.1259	35.8	55.43	1	0.95	0.1259	24.7	59.05	4	5.36
0.1585	32.3	57.16	6	2.85	0.1585	40.6	55.65	2	0.99	0.1585	28.2	59.34	4	5.25
0.1995	37.1	57.28	6	3.03	0.1995	46.5	55.60	2	1.04	0.1995	32.5	59.33	5	5.13
0.2512	42.7	57.26	7	3.12	0.2512	53.5	55.46	2	1.07	0.2512	37.7	59.22	5	5.00
0.3162	49.5	57.05	8	3.19	0.3162	61.7	55.17	2	1.14	0.3162	43.7	58.97	6	4.89
0.3981	57.5	56.77	9	3.23	0.3981	71.4	54.83	2	1.12	0.3981	50.9	58.67	6	4.76
0.5012	66.8	56.40	10	3.25	0.5012	82.7	54.39	3	1.08	0.5012	59.2	58.27	7	4.63
0.631	77.6	55.99	11	3.26	0.631	95.7	53.93	3	1.10	0.631	68.9	57.86	7	4.47
0.7943	90.0	55.58	12	3.24	0.7943	110.6	53.46	4	1.07	0.7943	80.1	57.41	8	4.31
1	104.5	55.07	14	3.22	1	127.8	52.94	4	1.05	1	93.1	56.91	8	4.13
1.259	120.9	54.56	15	3.15	1.259	147.2	52.38	4	0.99	1.259	107.9	56.36	9	3.95
1.585	139.9	53.94	16	3.13	1.585	169.3	51.76	5	0.96	1.585	125.2	55.76	9	3.77
1.995	161.3	53.28	18	3.07	1.995	194.4	51.10	6	0.84	1.995	145.2	55.10	9	3.59
2.512	185.9	52.56	20	3.02	2.512	222.9	50.39	6	0.84	2.512	167.8	54.39	10	3.39
3.162	214.0	51.82	21	2.94	3.162	255.2	49.61	7	0.78	3.162	193.4	53.62	10	3.20
3.981	245.2	50.94	22	2.88	3.981	292.0	48.84	8	0.58	3.981	222.3	52.78	10	3.02
5.012	281.0	50.08	24	2.80	5.012	330.9	47.85	8	0.68	5.012	255.2	51.90	10	2.84
6.31	320.7	49.15	26	2.70	6.31	375.6	46.96	10	0.60	6.31	291.9	50.94	10	2.66
7.943	364.4	48.24	27	2.61	7.943	423.4	46.03	13	0.56	7.943	332.6	50.00	11	2.49
10	412.9	47.16	29	2.45	10	476.7	44.95	17	0.45	10	378.3	48.94	12	2.40

WSRI125					HS145					WSRIP125				
f	Average		Standard Deviation		f	Average		Standard Deviation		f	Average		Standard Deviation	
	G^*	δ	G^*	δ		G^*	δ	G^*	δ		G^*	δ	G^*	δ
0.1	28.3	55.1	3	1.53	0.1	150.9	44.40	31	3.06	0.1	140.0	43.74	17	2.15
0.1259	31.2	55.6	3	1.47	0.1259	165.8	44.05	33	3.13	0.1259	152.6	43.54	18	2.18
0.1585	35.5	55.8	4	1.39	0.1585	184.5	43.62	36	3.12	0.1585	169.4	43.16	20	2.17
0.1995	40.9	55.8	4	1.29	0.1995	205.4	43.08	39	3.13	0.1995	187.9	42.72	21	2.12
0.2512	47.3	55.6	5	1.27	0.2512	229.0	42.48	42	3.15	0.2512	209.5	42.33	23	1.95
0.3162	54.8	55.3	6	1.22	0.3162	254.5	41.93	45	3.11	0.3162	233.1	41.75	25	1.91
0.3981	63.4	55.0	7	1.16	0.3981	283.6	41.42	48	3.02	0.3981	259.5	41.12	27	1.84
0.5012	73.1	54.7	8	1.10	0.5012	315.2	40.88	52	2.95	0.5012	289.3	40.57	30	1.65
0.631	84.3	54.3	8	1.05	0.631	350.2	40.20	56	2.92	0.631	321.9	39.95	34	1.50
0.7943	97.3	53.9	10	1.01	0.7943	388.1	39.48	60	2.87	0.7943	356.9	39.23	37	1.44
1	112.4	53.5	11	0.95	1	429.9	38.81	65	2.79	1	395.4	38.57	42	1.25
1.259	129.6	53.1	13	0.91	1.259	475.2	38.16	70	2.68	1.259	436.2	37.80	46	1.15
1.585	149.4	52.5	14	0.86	1.585	523.3	37.36	75	2.61	1.585	480.8	37.03	52	1.02
1.995	171.8	52.0	16	0.82	1.995	578.4	36.64	79	2.50	1.995	527.9	36.14	57	0.97
2.512	197.2	51.4	18	0.77	2.512	633.0	36.18	88	2.34	2.512	579.9	35.53	65	0.85
3.162	225.8	50.7	21	0.73	3.162	696.7	34.88	91	2.41	3.162	632.0	34.46	69	0.80
3.981	258.4	49.9	24	0.72	3.981	761.9	34.00	98	2.35	3.981	689.0	33.48	77	0.81
5.012	294.5	49.1	27	0.67	5.012	830.8	33.13	106	2.26	5.012	749.6	32.57	85	0.83
6.31	335.5	48.3	31	0.64	6.31	903.1	32.25	113	2.17	6.31	811.6	31.59	93	0.87
7.943	380.4	47.5	34	0.62	7.943	977.9	31.48	122	2.08	7.943	881.0	31.78	110	0.90
10	430.1	46.5	38	0.58	10	1057.0	30.62	131	2.00	10	949.7	30.10	115	1.22

WSRlP155					WSSaP125					WSSaP155				
f	Average		Standard Deviation		*f*	Average		Standard Deviation		*f*	Average		Standard Deviation	
	*G**	*δ*	*G**	*δ*		*G**	*δ*	*G**	*δ*		*G**	*δ*	*G**	*δ*
0.1	163.9	41.11	27.08	2.74	0.1	139.9	44.81	12	1.60	0.1	396.5	33.41	79	3.66
0.1259	179.1	40.70	29.00	2.80	0.1259	153.7	44.48	12	1.63	0.1259	425.7	32.93	79	3.65
0.1585	197.9	40.20	31.25	2.80	0.1585	171.3	43.97	13	1.65	0.1585	459.0	32.42	79	3.73
0.1995	218.6	39.68	33.57	2.80	0.1995	191.1	43.41	15	1.61	0.1995	494.9	31.89	80	3.81
0.2512	241.7	39.13	35.88	2.81	0.2512	213.4	42.79	16	1.59	0.2512	533.2	31.42	81	3.89
0.3162	266.7	38.59	38.01	2.77	0.3162	237.9	42.14	17	1.54	0.3162	573.7	30.89	81	3.95
0.3981	294.0	37.97	39.90	2.76	0.3981	264.9	41.44	19	1.51	0.3981	616.4	30.33	80	4.04
0.5012	324.3	37.26	41.76	2.87	0.5012	294.7	40.71	21	1.45	0.5012	661.4	29.73	80	4.12
0.631	356.9	36.53	43.44	3.02	0.631	327.2	39.96	24	1.41	0.631	708.9	28.97	81	4.19
0.7943	390.9	35.98	44.37	2.86	0.7943	362.3	39.18	26	1.36	0.7943	758.5	27.95	83	4.20
1	428.9	35.32	46.63	2.84	1	400.5	38.37	29	1.33	1	810.1	27.38	87	4.14
1.259	469.4	34.61	49.22	2.87	1.259	441.8	37.52	33	1.32	1.259	863.9	27.01	94	3.91
1.585	512.4	33.90	52.10	2.88	1.585	486.0	36.64	37	1.32	1.585	922.8	26.67	100	3.67
1.995	558.3	33.18	55.91	2.86	1.995	533.2	35.74	42	1.30	1.995	984.7	26.30	106	3.48
2.512	606.7	32.47	60.60	2.77	2.512	583.7	34.82	47	1.32	2.512	1050.2	25.92	114	3.28
3.162	658.5	31.76	66.72	2.63	3.162	636.9	33.84	53	1.35	3.162	1118.2	25.52	123	3.09
3.981	713.0	31.05	73.61	2.46	3.981	692.7	32.91	59	1.36	3.981	1189.0	25.15	133	2.92
5.012	771.3	30.31	82.22	2.32	5.012	751.8	31.92	66	1.38	5.012	1263.0	24.73	144	2.74
6.31	831.3	29.52	91.40	2.20	6.31	812.4	31.07	73	1.13	6.31	1338.5	24.30	156	2.58
7.943	898.5	29.22	106.20	2.25	7.943	874.5	30.39	83	1.68	7.943	1412.3	24.01	169	2.44
10	970.2	28.24	116.52	1.70	10	945.1	30.08	82	1.47	10	1493.5	23.59	181	2.32

Appendix G: Fatigue results of DSR samples

Table G.1 Fatigue results of all asphalt mixtures

NSM: normalize shear modulus, γ: Strain, G*: Complex shear modulus, N_f: number of cycles, E_r: energy ratio

HH155											WHSa135										
Average						Standard Deviation					Average						Standard Deviation				
NSM	*γ%*	*G*(Pa)*	*δ°*	N_f	E_r	*γ*	*G**	*δ*	N_f	E_r	*NSM*	*γ*	*G**	*δ*	N_f	E_r	*γ%*	*G**	*δ*	*Nf*	*Er*
1.00	7.19E-02	5.91E+08	42.37	10	5911.5	0.0043	35533693	1.089	0	355.3369	1.00	0.079	5.38E+08	43.90	25	12961	0.0038	24770211	2.49	30	14950
0.95	7.62E-02	5.59E+08	44.32	59	32761.5	0.0045	33471032	1.047	12	6338.352	0.95	0.084	5.09E+08	45.70	114	56592.25	0.0040	23893706	2.22	98	46170
0.90	8.04E-02	5.3E+08	45.44	175	92128.38	0.0047	31633882	1.048	47	22265.75	0.90	0.088	4.82E+08	46.83	308	146172.8	0.0041	22061184	2.33	197	88192
0.85	8.53E-02	5E+08	46.43	418	208176.3	0.0050	30017814	0.948	126	62241.96	0.85	0.094	4.55E+08	47.77	656	296047.1	0.0044	20955886	2.38	287	120185
0.80	9.06E-02	4.7E+08	47.40	928	434392.3	0.0053	28139000	0.930	148	59306.16	0.80	0.100	4.28E+08	48.65	1303	555306.3	0.0047	19640350	2.28	505	210841
0.75	9.67E-02	4.41E+08	48.36	1804	791903.3	0.0057	26509935	0.758	281	104549.3	0.75	0.106	4.01E+08	50.04	2511	1006137	0.0050	18513306	1.10	907	367102
0.70	1.04E-01	4.11E+08	49.23	3398	1391459	0.0061	24699983	0.702	477	164994.2	0.70	0.114	3.74E+08	50.80	3719	1386413	0.0053	17185144	1.09	892	313697
0.65	1.12E-01	3.82E+08	50.01	4961	1891348	0.0066	22906331	0.690	398	169534.1	0.65	0.123	3.47E+08	51.54	4996	1729997	0.0058	15952638	0.99	702	207837
0.60	1.21E-01	3.52E+08	50.79	7044	2477059	0.0072	21195971	0.746	592	238073.9	0.60	0.133	3.2E+08	52.27	6393	2041084	0.0063	14757230	0.93	805	209916
0.55	1.32E-01	3.22E+08	51.56	10105	3263930	0.0078	19369972	0.938	1338	557350.4	0.55	0.145	2.93E+08	53.02	8274	2418775	0.0069	13547201	0.87	1384	367300
0.50	1.46E-01	2.93E+08	52.36	14970	4394494	0.0086	17587756	1.218	2666	941831.1	0.50	0.160	2.66E+08	53.77	10785	2859462	0.0075	12270968	0.88	2485	605037
0.45	1.62E-01	2.63E+08	53.29	23571	6229328	0.0095	15753412	1.396	6473	1924253	0.45	0.178	2.39E+08	54.57	14860	3540485	0.0083	10988593	0.94	4519	1040656
0.40	1.82E-01	2.34E+08	54.28	34576	8103690	0.0107	13979598	1.459	9707	2506772	0.40	0.200	2.12E+08	55.52	20205	4264011	0.0094	9784810	1.02	7367	1499292
0.35	2.09E-01	2.04E+08	55.26	43563	8901910	0.0123	12225213	1.342	10298	2275747	0.35	0.229	1.86E+08	56.62	26463	4871979	0.0108	8552193	1.06	10831	1927481
0.30	2.44E-01	1.74E+08	56.26	49089	8566995	0.0145	10487572	1.120	10636	1960604	0.30	0.268	1.59E+08	57.73	30919	4861607	0.0126	7290347	0.99	13232	1993931
0.25	2.94E-01	1.45E+08	56.93	51753	7503814	0.0176	8846468	1.139	11370	1701886	0.25	0.323	1.32E+08	58.48	32738	4276822	0.0154	6154131	0.78	13643	1696184
0.20	3.67E-01	1.16E+08	56.29	52671	6118945	0.0239	7774745	2.057	11732	1400417	0.20	0.405	1.05E+08	58.16	33519	3488643	0.0184	4672903	1.55	13074	1286256
0.15	4.89E-01	87252500	51.75	52856	4610716	0.0312	5794983	3.209	11749	1048713	0.15	0.543	78490000	54.59	34053	2651593	0.0263	3722445	5.40	12301	900618
0.10	7.09E-01	61832500	38.17	52911	3288893	0.1315	13128233	2.507	11715	1043237	0.10	0.793	53842500	44.67	34360	1855114	0.0507	3446954	13.57	11779	666669
0.02	1.07E+01	11012000	45.18	52970	148827.5	11.1876	12906113	20.587	11653	192710.5	0.05	2.430	23020000	32.34	34391	182409.7	1.3077	14337087	4.06	11730	229835

WHSa145											WHRw135										
Average						Standard Deviation					Average						Standard Deviation				
NSM	*γ%*	*G*(Pa)*	*δ°.*	N_f	E_r	*γ*	*G**	*δ°*	N_f	*Er*	*NSM*	*γ%*	*G*(Pa)*	*δ°.*	N_f	E_r	*γ%*	*G*(Pa)*	*δ°.*	N_f	E_r
1.00	0.068	6.3E+08	41.92	9	5557	0.007	67863638	1.59	3	1842	1.00	0.080	5.29E+08	44.23	10	5290	0.005	32619881	1.67	0	326
0.95	0.072	5.96E+08	43.64	88	50779	0.007	65130094	1.19	75	40970	0.95	0.085	5.01E+08	46.21	63	31840	0.005	30149903	1.61	32	18009
0.90	0.076	5.64E+08	44.78	274	150261	0.007	60604758	1.06	232	119521	0.90	0.090	4.74E+08	47.35	191	92344	0.006	29189153	1.73	113	59405
0.85	0.080	5.32E+08	45.73	655	339930	0.008	57330467	1.03	544	265129	0.85	0.095	4.47E+08	48.27	413	187546	0.006	27547595	1.88	211	105291
0.80	0.086	5.01E+08	46.70	1541	756515	0.008	53966934	1.06	1222	560825	0.80	0.101	4.21E+08	49.17	1018	434683	0.007	25904440	2.09	407	195823
0.75	0.091	4.69E+08	47.47	2563	1187462	0.009	50529224	1.05	1422	607665	0.75	0.108	3.94E+08	50.14	1970	785713	0.007	24223405	1.71	680	311406
0.70	0.098	4.38E+08	48.12	3999	1737882	0.010	47093975	1.10	1331	527640	0.70	0.116	3.68E+08	50.91	3141	1162999	0.007	22792744	1.66	609	286477
0.65	0.105	4.06E+08	48.64	5440	2199779	0.010	43745133	1.14	1404	533159	0.65	0.125	3.41E+08	51.63	4490	1535040	0.008	21073898	1.49	176	150853
0.60	0.114	3.75E+08	49.08	7089	2648812	0.011	40404321	1.23	1534	566579	0.60	0.135	3.15E+08	52.33	5845	1841119	0.009	19412453	1.24	356	171182
0.55	0.125	3.43E+08	49.35	9643	3306140	0.012	37026612	1.45	2382	833351	0.55	0.148	2.88E+08	52.90	7716	2225601	0.010	17791571	1.01	1036	335427
0.50	0.137	3.12E+08	49.63	13820	4322102	0.013	33599355	1.53	4375	1443370	0.50	0.163	2.62E+08	53.42	9993	2614437	0.010	16163204	0.84	1959	537177
0.45	0.153	2.8E+08	50.15	24174	6861663	0.015	30192866	1.25	11005	3357382	0.45	0.181	2.35E+08	53.93	13798	3244617	0.012	14520417	0.79	4216	1027122
0.40	0.172	2.49E+08	51.17	40819	10412893	0.017	26765650	0.92	19156	5775678	0.40	0.204	2.09E+08	54.60	20458	4247265	0.013	12916495	0.94	7769	1611916
0.35	0.197	2.17E+08	52.62	59511	13327072	0.019	23505531	0.73	26877	7521377	0.35	0.234	1.83E+08	55.63	25259	4572567	0.015	11263917	0.98	10205	1830898
0.30	0.231	1.86E+08	54.07	70778	13532195	0.023	20028709	0.59	28664	7115930	0.30	0.273	1.56E+08	56.38	29206	4501315	0.018	9627911	1.13	11869	1720967
0.25	0.278	1.54E+08	55.18	74383	11802728	0.027	16572769	0.64	28560	5983384	0.25	0.329	1.3E+08	56.66	31991	4080339	0.021	8049172	2.42	13834	1592172
0.20	0.348	1.23E+08	54.86	75245	9514331	0.034	13168998	1.70	28522	4778772	0.20	0.411	1.04E+08	55.33	32500	3315433	0.027	6575135	5.01	13884	1275914
0.15	0.466	91962500	49.79	75504	7134920	0.044	9598022	5.32	28656	3571117	0.15	0.545	78187500	50.45	32643	2520857	0.033	4508158	8.40	13882	988864
0.10	0.705	60920000	35.35	75586	4746273	0.074	7058390	3.04	28698	2439894	0.10	0.823	52102500	39.84	32683	1650827	0.080	5050851	11.03	13905	573958
0.04	1.921	24417500	30.88	75649	808119	0.668	8480642	1.28	28703	1042138	0.03	5.328	14650250	30.67	32696	331183	4.398	11142447	6.91	13912	499985

WHRw145											WHRl135										
Average						Standard Deviation					Average						Standard Deviation				
NSM	*γ%*	*G*(Pa)*	*δ°*	N_f	E_r	*γ%*	*G*(Pa)*	*δ°*	N_f	E_r	*NSM*	*Strain*	*G*(Pa)*	*δ°*	N_f	E_r	*γ%*	*G*(Pa)*	*δ°*	N_f	E_r
1.00	0.077	5.5E+08	43.67	10	5504	0.006	47147888	0.69	0	471	1.00	0.084	5.07E+08	47.08	10	5066	0.034	15555481	0.64	0	156
0.95	0.082	5.21E+08	45.67	51	26904	0.007	44907349	0.61	6	5669	0.95	0.089	4.8E+08	49.02	48	23030	0.036	14771527	0.60	3	1393
0.90	0.087	4.93E+08	46.90	186	92614	0.007	42258047	0.61	35	24638	0.90	0.094	4.54E+08	50.21	170	77011	0.038	13954497	0.64	24	10713
0.85	0.092	4.65E+08	47.84	464	216443	0.008	39750419	0.63	61	40126	0.85	0.099	4.28E+08	51.07	426	182738	0.041	13356534	0.60	94	33876
0.80	0.098	4.38E+08	48.73	1051	465092	0.008	37636906	0.60	182	120513	0.80	0.106	4.03E+08	51.90	929	374557	0.043	12401895	0.56	105	24957
0.75	0.104	4.1E+08	49.46	1949	804519	0.009	35154931	0.61	219	153857	0.75	0.113	3.78E+08	52.63	1733	654509	0.046	11640661	0.55	212	85861
0.70	0.112	3.83E+08	50.12	3645	1398463	0.009	32811418	0.62	179	181328	0.70	0.121	3.52E+08	53.32	3294	1160676	0.049	10792961	0.54	201	64153
0.65	0.120	3.55E+08	50.69	5154	1838086	0.010	30570397	0.67	381	280883	0.65	0.130	3.27E+08	53.97	4778	1560954	0.053	9973615	0.55	288	89906
0.60	0.130	3.28E+08	51.19	6813	2236761	0.011	28091102	0.67	301	278508	0.60	0.141	3.02E+08	54.65	6723	2027312	0.058	9193095	0.59	256	98904
0.55	0.142	3E+08	51.66	8579	2575430	0.012	25682079	0.64	227	253728	0.55	0.154	2.76E+08	55.38	9095	2509982	0.063	8491937	0.63	503	136056
0.50	0.157	2.73E+08	51.97	10961	2987751	0.013	23392449	0.72	330	289016	0.50	0.170	2.51E+08	56.11	12726	3190200	0.069	7689928	0.71	1017	255169
0.45	0.174	2.45E+08	52.13	15198	3719804	0.015	20969979	0.82	535	292215	0.45	0.189	2.26E+08	56.92	17860	4023000	0.077	6863454	0.75	2048	478697
0.40	0.197	2.17E+08	52.65	23826	5167844	0.017	18677705	1.10	2011	447609	0.40	0.212	2E+08	57.83	25531	5101924	0.087	6116780	0.70	3484	709792
0.35	0.225	1.9E+08	53.77	36801	6993263	0.019	16295910	1.26	5958	1296755	0.35	0.243	1.75E+08	58.78	33076	5769204	0.100	5370940	0.61	3821	583436
0.30	0.263	1.62E+08	55.18	51651	8434499	0.022	13922165	1.12	13989	2560902	0.30	0.285	1.5E+08	59.73	39421	5879428	0.116	4580720	0.51	4313	472805
0.25	0.317	1.35E+08	56.63	61561	8376659	0.027	11540364	0.86	20134	3029315	0.25	0.343	1.24E+08	60.45	42688	5282851	0.140	3769217	0.43	6157	604342
0.20	0.398	1.07E+08	57.67	64981	7049566	0.033	9173809	0.52	22668	2701193	0.20	0.430	99004000	60.15	43670	4306377	0.176	3105975	1.17	7135	572113
0.15	0.533	80305000	55.62	65355	5307913	0.046	6962492	0.50	22610	2057677	0.15	0.570	74638000	57.02	43884	3261177	0.233	2522195	3.20	7259	444381
0.10	0.774	55817500	41.12	65428	3702726	0.108	8245736	2.36	22581	1486189	0.10	0.853	50026000	45.35	43924	2190559	0.351	2860914	7.17	7257	349715
0.03	4.898	15627000	63.95	65466	1011603	4.802	10640674	21.08	22568	1070807	0.03	6.735	15075800	42.59	43935	339154	6.923	11656091	17.44	7253	292418

WHRl145											HS145										
Average						Standard Deviation					Average						Standard Deviation				
NSM	*γ%*	*G*(Pa)*	*δ°*	N_f	E_r	*γ%*	*G*(Pa)*	*δ°*	N_f	E_r	*NSM*	*γ%*	*G*(Pa)*	*δ°*	N_f	E_r	*γ%*	*G*(Pa*	*δ°*	N_f	E_r
1.00	0.059	5.8E+08	42.85	10	5803	0.004	35234961	0.84	0	352	1.00	0.144	1.39E+08	58.01	10	1395	0.012	9114275	1.15	0	91
0.95	0.062	5.49E+08	44.83	78	42353	0.005	33610452	0.78	22	11985	0.96	0.150	1.34E+08	58.86	15	2004	0.012	8450789	1.05	0	127
0.90	0.066	5.2E+08	45.90	254	131426	0.005	31463259	0.74	29	29000	0.90	0.160	1.26E+08	59.96	33	4067	0.013	8320407	1.06	6	465
0.85	0.069	4.91E+08	46.79	611	298344	0.005	29788630	0.65	133	76698	0.85	0.170	1.18E+08	60.87	74	8661	0.014	8038397	0.99	14	889
0.80	0.074	4.62E+08	47.67	1336	612554	0.005	27940696	0.52	269	114568	0.80	0.181	1.11E+08	61.61	158	17368	0.015	7355893	0.94	32	2002
0.75	0.079	4.32E+08	48.43	2511	1080078	0.006	26211877	0.39	595	222133	0.75	0.193	1.04E+08	62.25	323	33290	0.016	6780248	0.92	77	5005
0.70	0.085	4.03E+08	49.08	3888	1565961	0.006	24654462	0.22	349	192177	0.70	0.207	96965000	62.79	619	59382	0.017	6310655	0.93	202	12757
0.65	0.091	3.74E+08	49.53	5244	1960182	0.007	22803709	0.16	471	217045	0.65	0.223	90010000	63.30	1095	97583	0.018	5905709	0.95	375	22997
0.60	0.099	3.45E+08	49.91	6616	2281083	0.007	20934242	0.18	673	258219	0.60	0.242	82997500	63.79	1783	146579	0.020	5439108	0.93	575	32636
0.55	0.108	3.16E+08	50.07	8314	2626927	0.008	19158005	0.20	672	288484	0.55	0.264	76020000	64.26	2754	207822	0.022	4981272	0.91	742	38989
0.50	0.119	2.87E+08	49.96	10721	3080085	0.009	17357491	0.38	1147	485210	0.50	0.291	69040000	64.76	4086	280637	0.024	4510188	0.89	896	44767
0.45	0.132	2.58E+08	49.66	15543	4016278	0.010	15670886	0.33	1686	1018355	0.45	0.323	62067500	65.26	5719	353076	0.026	4048525	0.91	1036	38753
0.40	0.149	2.29E+08	50.07	31391	7219693	0.011	13924170	0.70	5903	3500011	0.40	0.364	55110000	65.78	7760	425799	0.030	3590469	0.94	1173	38313
0.35	0.170	2E+08	51.15	59536	11986027	0.012	12126383	1.12	14478	5886337	0.35	0.417	48132500	66.27	9809	470435	0.034	3148718	0.91	1464	47985
0.30	0.199	1.71E+08	52.75	84324	14510894	0.014	10412172	1.20	17735	6253203	0.30	0.488	41152500	66.76	12074	495848	0.040	2698103	0.94	1699	59670
0.25	0.240	1.42E+08	54.28	93918	13431180	0.017	8618730	0.88	18186	5086073	0.25	0.588	34182500	66.80	13603	464623	0.048	2220786	0.85	1953	65653
0.20	0.301	1.13E+08	54.70	95876	10926476	0.022	6822512	1.51	20257	4123489	0.20	0.735	27322500	65.04	14384	393359	0.056	1655866	1.92	2305	67709
0.15	0.401	84997500	51.84	96421	8243745	0.027	4711520	4.11	21066	3109179	0.14	0.996	20222500	56.24	14676	297456	0.088	1419633	11.18	2504	58219
0.10	0.619	55242500	39.39	96508	5349383	0.059	4513479	6.13	21173	1971033	0.10	1.534	13320000	45.81	14733	197714	0.285	1828387	11.60	2544	50650
0.02	3.018	12641750	34.31	96523	507532	1.271	5197722	6.75	21167	630638											

WSSa125											WSRw125										
Average						Standard Deviation					Average						Standard Deviation				
NSM	*γ%*	*G*(Pa)*	*δ°*	N_f	E_r	*γ%*	*G*(Pa)*	*δ°*	N_f	E_r	*NSM*	*γ%*	*G*(Pa)*	*δ°*	N_f	E_r	*Strain*	*G**	*δ°*	N_f	E_r
1.00	0.153	1.64E+08	56.74	10	1638	0.005	5723854	0.34	0	57	1.00	0.186	1.34E+08	58.27	10	1341	0.004	3220714	1.57	0	32
0.95	0.161	1.56E+08	57.72	18	2719	0.007	7115476	0.41	3	361	0.95	0.196	1.28E+08	59.21	18	2304	0.005	3085936	1.64	3	362
0.90	0.170	1.47E+08	58.78	40	5883	0.006	5416641	0.32	10	1448	0.90	0.208	1.2E+08	60.32	48	5796	0.005	2716247	1.53	10	1344
0.85	0.180	1.39E+08	59.69	93	12836	0.006	4827957	0.31	19	2689	0.85	0.221	1.13E+08	61.17	123	13985	0.005	2663081	1.43	28	3427
0.80	0.192	1.3E+08	60.45	203	26413	0.007	4544869	0.28	39	5218	0.80	0.234	1.07E+08	61.83	274	29313	0.006	2528834	1.37	59	6891
0.75	0.205	1.22E+08	61.10	408	49675	0.007	4238710	0.24	81	9479	0.75	0.250	99960000	62.39	544	54535	0.006	2442611	1.35	89	10184
0.70	0.220	1.14E+08	61.71	793	90089	0.008	3914929	0.26	187	20495	0.70	0.268	93204000	62.91	997	93058	0.006	2249084	1.36	160	15973
0.65	0.237	1.06E+08	62.29	1369	144446	0.008	3702589	0.25	201	20100	0.65	0.289	86510000	63.42	1810	157010	0.007	2114781	1.36	311	30222
0.60	0.257	97485000	62.87	2424	236031	0.009	3443191	0.26	341	32004	0.60	0.314	79798000	63.90	2988	238889	0.007	1889992	1.37	458	40537
0.55	0.280	89285000	63.48	3961	353399	0.010	3104733	0.30	389	33102	0.55	0.342	73106000	64.41	4553	333539	0.008	1767181	1.34	544	47536
0.50	0.309	81080000	64.09	6084	492887	0.011	2833525	0.32	627	49086	0.50	0.377	66374000	64.94	6534	434076	0.009	1595707	1.33	491	40494
0.45	0.343	72910000	64.64	8898	649009	0.012	2562538	0.37	942	74500	0.45	0.419	59670000	65.44	8556	510969	0.010	1431852	1.41	569	43652
0.40	0.387	64702500	65.24	12604	816136	0.014	2259386	0.43	1604	112105	0.40	0.473	52962000	66.00	11472	607844	0.011	1271739	1.45	1234	71302
0.35	0.443	56520000	65.88	17489	989776	0.016	1976411	0.52	3186	190030	0.35	0.541	46260000	66.51	14270	659856	0.013	1105351	1.53	1851	85251
0.30	0.518	48332500	66.43	22856	1106125	0.018	1712238	0.64	5117	255899	0.30	0.633	39562000	66.98	16686	659485	0.015	954657	1.65	2727	104033
0.25	0.624	40140000	66.89	26919	1081279	0.022	1412586	0.81	6834	279641	0.25	0.761	32912000	67.06	18152	596761	0.018	788175.1	2.24	3551	113397
0.20	0.784	31960000	66.81	28925	924887	0.028	1136544	1.14	7521	244161	0.20	0.953	26282000	65.65	18682	490388	0.023	625875.4	3.49	3835	97965
0.15	1.040	24105000	63.15	29473	711062	0.041	925869	1.76	7542	186035	0.14	1.361	18870000	57.02	18853	353759	0.260	2898422	11.22	3955	86677
0.10	1.537	16360000	47.44	29534	484772	0.057	590310.7	5.18	7552	133604	0.08	3.796	10236200	42.62	18896	195239	3.841	4476425	9.29	3990	106186
0.06	2.674	9651500	36.23	29541	289302	0.478	1594335	2.13	7552	100958	0.03	7.668	3773200	40.46	18904	42118	2.962	1413489	4.95	3994	52124

WSRl125											HSP145										
Average						Standard Deviation					Average						Standard Deviation				
NSM	*γ%*	*G*(Pa)*	*δ°*	N_f	E_r	*γ%*	*G*(Pa)*	*δ°*	N_f	E_r	*NSM*	*γ%*	*G*(Pa)*	*δ°*	N_f	E_r	*Strain*	*G**	*δ°.*	N_f	E_r
1.00	0.171	1.47E+08	57.42	10	1471	0.016	14460394	0.52	0	145	1.00	0.103	4.14E+08	38.78	10	4140	0.043	34578939	3.31	0	346
0.95	0.180	1.4E+08	58.45	22	3105	0.016	13089614	0.50	3	679	0.95	0.109	3.92E+08	40.14	31	12173	0.045	33177131	3.50	2	1140
0.90	0.191	1.32E+08	59.46	61	8110	0.018	12938238	0.51	7	1650	0.89	0.116	3.69E+08	41.36	83	30865	0.048	32981131	3.78	31	10492
0.85	0.202	1.24E+08	60.18	148	18635	0.019	12197049	0.47	24	4788	0.85	0.122	3.5E+08	41.74	213	74494	0.051	29343705	3.89	53	10260
0.80	0.215	1.17E+08	60.81	337	40074	0.020	11487384	0.47	77	12946	0.80	0.130	3.29E+08	42.63	441	144736	0.054	27599493	3.94	112	21022
0.75	0.230	1.1E+08	61.38	762	85348	0.022	10814250	0.44	220	32925	0.75	0.138	3.09E+08	43.47	793	244467	0.057	25788505	3.94	244	46431
0.70	0.246	1.02E+08	61.86	1419	146868	0.023	10044709	0.39	237	39251	0.70	0.148	2.88E+08	44.50	1335	383795	0.062	24013892	3.74	367	66713
0.65	0.266	94886000	62.41	2452	237238	0.025	9339988	0.35	615	83917	0.65	0.160	2.67E+08	45.13	2152	576691	0.066	22319655	4.41	481	111856
0.60	0.288	87570000	62.97	4061	361245	0.027	8582299	0.35	826	110489	0.60	0.173	2.46E+08	45.20	3005	744811	0.072	20575276	5.27	470	139904
0.55	0.314	80160000	63.45	5717	464344	0.029	7879800	0.35	972	125989	0.55	0.189	2.26E+08	46.05	3851	875080	0.078	18823841	5.24	517	175035
0.50	0.346	72822000	63.91	8077	595760	0.032	7156268	0.35	1335	159457	0.50	0.208	2.05E+08	49.10	6014	1242398	0.086	17103362	3.38	1884	269675
0.45	0.385	65468000	64.40	11372	754816	0.036	6447296	0.34	2014	212566	0.45	0.232	1.84E+08	53.04	8892	1637113	0.096	15412073	1.91	2466	391939
0.40	0.434	58114000	64.88	15383	904941	0.041	5721519	0.30	2545	237194	0.40	0.261	1.64E+08	54.64	11500	1878652	0.108	13646611	1.67	2789	467482
0.35	0.497	50754000	65.36	19940	1020760	0.047	4982633	0.35	3542	254109	0.35	0.299	1.43E+08	55.92	13582	1935823	0.124	11950021	1.27	2903	446377
0.30	0.581	43410000	65.70	23287	1013924	0.055	4272967	0.52	3914	213784	0.30	0.350	1.22E+08	56.80	15240	1857694	0.145	10208575	1.40	3058	412272
0.25	0.699	36058000	65.61	25567	921729	0.066	3537255	1.08	4472	182509	0.25	0.421	1.02E+08	56.83	16048	1624840	0.174	8520039	2.88	3383	365631
0.20	0.876	28794000	63.90	26670	766134	0.084	2905044	2.50	5154	154186	0.20	0.525	81422000	54.50	16369	1328148	0.218	6889787	5.88	3532	301168
0.15	1.182	21334000	55.14	26961	574015	0.099	1845164	7.06	5468	118278	0.15	0.702	60920000	46.15	16432	997105	0.291	5206534	11.78	3561	225602
0.10	1.710	14734000	42.59	27003	398944	0.094	812914.5	9.22	5516	88465	0.10	1.065	40386000	36.22	16456	665629	0.447	4376840	8.97	3567	177318
0.02	9.214	3391200	32.00	27009	63224	3.333	2066242	1.35	5517	75951	0.05	3.464	18907800	30.45	16470	242999	3.150	10600878	1.94	3570	277872

WSRlP125											WSRlP155										
Average						Standard Deviation					Average						Standard Deviation				
NSM	*γ%*	*G*(Pa)*	*δ°*	N_f	E_r	*γ%*	*G*(Pa)*	*δ°*	N_f	E_r	*NSM*	*γ%*	*G*(Pa)*	*δ°.*	N_f	E_r	*Strain*	*G**	*δ°*	N_f	E_r
1.00	0.140	3.05E+08	35.32	5	1523	0.058	23574838	2.08	0	118	1.00	0.136	3.15E+08	37.78	7	2272	0.057	36933697	1.99	3	1125
0.94	0.150	2.85E+08	36.41	53	15280	0.062	19516531	2.38	34	10618	0.95	0.144	2.98E+08	38.66	129	36386	0.061	34998114	1.31	98	30035
0.89	0.158	2.7E+08	36.85	175	47612	0.065	18726906	2.35	88	25986	0.90	0.152	2.82E+08	39.43	372	97814	0.064	33097930	0.73	351	96233
0.84	0.168	2.54E+08	38.23	365	93808	0.069	17664456	2.16	154	42088	0.85	0.161	2.66E+08	40.42	676	168961	0.068	31256999	0.55	557	143579
0.79	0.179	2.39E+08	39.08	821	198865	0.074	16555966	1.99	417	99139	0.80	0.171	2.51E+08	41.39	1111	263887	0.072	29413092	0.76	790	186870
0.74	0.191	2.24E+08	41.32	1611	363524	0.079	15523917	1.17	878	199987	0.75	0.183	2.35E+08	42.94	1756	393139	0.077	27503491	1.43	1095	238502
0.69	0.205	2.09E+08	47.66	4587	987689	0.084	14477638	6.03	3768	857339	0.70	0.196	2.19E+08	44.25	2568	541997	0.082	25711437	1.18	1292	251222
0.64	0.221	1.93E+08	51.02	7078	1402982	0.091	13414433	4.78	4436	861493	0.65	0.211	2.03E+08	45.57	3541	701290	0.089	23847809	1.07	1280	214867
0.59	0.240	1.78E+08	51.99	8647	1575733	0.099	12363373	4.20	4988	885009	0.60	0.229	1.87E+08	46.71	4776	878517	0.096	21975486	1.73	1526	229028
0.54	0.262	1.63E+08	52.57	10402	1734281	0.108	11383321	4.18	5823	975383	0.55	0.250	1.72E+08	49.31	6909	1160493	0.105	20131518	3.66	2414	316099
0.49	0.289	1.48E+08	54.88	12408	1870890	0.119	10431443	1.99	6025	959885	0.50	0.275	1.56E+08	51.90	9335	1423360	0.116	18314120	4.11	3235	422052
0.44	0.323	1.32E+08	56.51	14156	1911595	0.133	9576690	0.89	6159	917336	0.45	0.306	1.4E+08	54.40	12134	1678395	0.129	16444513	3.06	3306	425666
0.39	0.365	1.17E+08	57.09	15316	1828458	0.151	8697988	1.03	6491	870698	0.40	0.345	1.24E+08	56.37	15046	1866212	0.145	14609346	1.81	3129	462508
0.34	0.418	1.02E+08	56.89	15938	1658214	0.173	7824960	1.75	6905	814058	0.35	0.395	1.09E+08	57.50	17563	1916970	0.166	12726448	1.01	3196	538045
0.29	0.492	86910000	55.31	16210	1435426	0.204	7281216	3.12	7087	719101	0.30	0.462	92980000	58.05	19501	1832521	0.194	10853960	1.09	3900	618124
0.24	0.597	71838000	50.11	16297	1192052	0.249	7172260	4.61	7142	612941	0.25	0.555	77406000	57.11	20327	1595044	0.233	8921380	3.18	4587	595940
0.19	0.728	58724000	41.05	16324	978059	0.301	4605077	6.51	7156	478716	0.20	0.691	62156000	53.04	20586	1298539	0.289	6789188	6.23	4896	501799
0.12	1.585	35696000	32.03	16338	607634	1.274	14716871	5.32	7165	497589	0.14	1.030	44366000	44.20	20644	936048	0.528	11053275	8.71	4942	461551
0.09	3.814	22090400	29.78	16349	405183	4.145	13544653	1.66	7170	381140	0.10	1.375	32516000	36.61	20662	684127	0.659	6762040	5.71	4955	305791
0.07	3.935	19590400	29.44	16352	319736	4.092	11276741	1.89	7171	372612	0.06	3.730	18864000	31.64	20667	277611	3.162	11873090	4.23	4957	287300

WSRlP125											WSRlP155										
Average						Standard Deviation					Average						Standard Deviation				
NSM	*γ%*	*G*(Pa)*	*δ°*	*Nf*	*Er*	*γ%*	*G*(Pa)*	*δ°*	*Nf*	*Er*	*NSM*	*γ%*	*G*(Pa)*	*δ°*	*Nf*	*Er*	*γ%*	*G*(Pa)*	*δ°*	*Nf*	*Er*
1.00	0.119	3.38E+08	34.14	5	1689	0.050	33579860	3.78	0	168	1.00	0.058	7.47E+08	35.46	11	8115	0.024	1.09E+08	4.16	2	1290
0.95	0.134	3.2E+08	36.26	32	10087	0.056	32019026	2.79	17	5359	0.95	0.061	7.06E+08	36.46	164	107194	0.026	1.03E+08	2.77	219	149052
0.90	0.141	3.03E+08	37.41	106	31969	0.059	30080392	2.64	45	15864	0.90	0.065	6.69E+08	37.16	395	246803	0.027	97447206	2.51	474	304671
0.85	0.150	2.86E+08	38.50	265	76223	0.063	28346640	2.43	123	42831	0.85	0.068	6.32E+08	38.14	749	442189	0.029	92243905	2.59	866	523872
0.80	0.159	2.69E+08	39.65	537	145375	0.067	26669402	2.22	251	84815	0.80	0.073	5.94E+08	39.09	1388	777626	0.031	86350611	2.97	1383	780679
0.75	0.170	2.52E+08	40.93	1072	273178	0.071	25079115	1.97	521	170141	0.75	0.078	5.57E+08	40.37	2382	1272867	0.033	80869667	2.81	1545	808868
0.70	0.182	2.35E+08	42.60	1817	432448	0.076	23348276	1.68	865	268374	0.70	0.083	5.19E+08	41.96	3737	1895552	0.035	75453184	2.37	1676	839105
0.65	0.196	2.18E+08	44.20	2726	599838	0.082	21653706	1.90	1031	305934	0.65	0.090	4.82E+08	43.13	4920	2323486	0.038	69995393	2.18	1721	782000
0.60	0.213	2.01E+08	45.23	3656	738169	0.089	19974409	1.93	1170	313003	0.60	0.097	4.44E+08	44.20	6213	2724704	0.041	64598274	1.94	2175	980643
0.55	0.233	1.84E+08	47.13	5243	953991	0.097	18357424	3.37	2194	412349	0.55	0.106	4.07E+08	45.18	11193	4446491	0.045	59277441	1.53	6925	2732687
0.50	0.256	1.67E+08	49.95	7533	1257093	0.107	16636316	3.37	3398	635184	0.50	0.117	3.7E+08	46.17	17570	6278243	0.049	53713052	1.63	12848	4589157
0.45	0.285	1.5E+08	52.92	10093	1520996	0.119	14999400	2.92	3936	735197	0.45	0.130	3.32E+08	47.26	28487	9149517	0.055	48308405	1.82	17900	5586529
0.40	0.321	1.34E+08	54.64	12016	1608856	0.134	13277048	2.49	4290	740219	0.40	0.146	2.95E+08	48.52	41284	11860638	0.062	42888285	1.86	21709	5991277
0.35	0.367	1.17E+08	55.51	12952	1517056	0.153	11586932	1.74	4403	675123	0.35	0.167	2.58E+08	49.92	50160	12761278	0.071	37507639	1.52	21258	5163958
0.30	0.429	99864000	55.55	13340	1337520	0.179	9854820	1.11	4427	584882	0.30	0.196	2.2E+08	50.97	54217	11864895	0.083	32020103	0.86	19801	4029864
0.25	0.514	83340000	53.67	13484	1129817	0.214	8094214	1.87	4426	492737	0.25	0.236	1.83E+08	50.78	55501	10106558	0.100	26507301	1.14	19081	3196848
0.20	0.649	66222000	47.55	13541	899804	0.273	7440778	5.87	4414	392724	0.20	0.295	1.46E+08	47.80	55927	8126292	0.125	21236925	3.94	18849	2497425
0.15	0.874	49384000	39.41	13564	673922	0.370	6589346	7.30	4406	312909	0.15	0.391	1.1E+08	40.73	56071	6168653	0.165	15152791	3.08	18792	2003140
0.09	3.460	30498400	33.41	13576	420102	4.723	17923303	5.73	4403	322167	0.10	0.584	74008000	31.23	56131	4116757	0.249	10814923	2.10	18788	1227138
0.06	3.965	20752400	30.12	13583	106103	4.567	12098106	2.22	4403	172657	0.05	1.171	38100000	28.81	56222	1361582	0.545	8829796	3.27	18749	1242652

Appendix H: Nano-mechanical properties of WMA incorporating RAP materials

Table H.1 Nano-mechanical properties of WMA incorporating RAP materials

S.D: Standard deviation, COV: coefficient of variance

Mixture code	HSP145					
Properties	Modulus			Hardness		
Phases	ITZ virgin	ITZ RAP	Mastic	ITZ virgin	ITZ RAP	Mastic
Mean	3.964	16.53	3.625	0.101	0.347	0.041
Std. Dev.	1.403	5.148	1.159	0.048	0.165	0.021
% COV	35.38	31.15	31.97	47.16	47.46	50.25
Mixture code	WSSaP125					
Properties	Modulus			Hardness		
Phases	ITZ Virgin	ITZ RAP	Mastic	ITZ Virgin	ITZ RAP	Mastic
Mean	7.782	13.931	3.964	0.152	0.352	0.039
Std. Dev.	2.892	5.599	1.148	0.052	0.228	0.016
% COV	37.17	40.19	28.95	33.94	64.73	42.21
Mixture code	WSSaP155					
Properties	Modulus			Hardness		
Phases	ITZ virgin	ITZ RAP	Mastic	ITZ Virgin	ITZ RAP	Mastic
Mean	9.672	12.699	4.915	0.211	0.359	0.063
Std. Dev.	3.135	3.081	1.29	0.075	0.173	0.012
% COV	32.41	24.26	26.24	35.32	48.27	19.09
Mixture code	WSRlP125					
Properties	Modulus			Hardness		
Phases	ITZ virgin	ITZ RAP	Mastic	ITZ Virgin	ITZ RAP	Mastic
Mean	5.159	15.222	1.515	0.118	0.486	0.015
Std. Dev.	2.063	6.813	0.839	0.045	0.259	0.011
% COV	39.99	44.76	55.37	38.2	53.23	72.62
Mixture code	WSRlP155					
Properties	Modulus			Hardness		
Phases	ITZ virgin	ITZ RAP	Mastic	ITZ Virgin	ITZ RAP	Mastic
Mean	6.534	10.701	2.639	0.148	0.231	0.052
Std. Dev.	1.966	5.302	1.001	0.068	0.125	0.019
% COV	30.09	49.54	37.95	45.84	54.38	36.81